University of Rhode Island
DigitalCommons@URI

Open Access Dissertations

2015

DESIGN, SYNTHESIS OF A NEW CLASS OF DISSYMMETRIC MACROCYCLES FOR CARCINOGENIC BENZO[*a*]PYRENE DETECTION

Bhasker Radaram
University of Rhode Island, radaram.bhasker08@gmail.com

Follow this and additional works at: https://digitalcommons.uri.edu/oa_diss

Recommended Citation

Radaram, Bhasker, "DESIGN, SYNTHESIS OF A NEW CLASS OF DISSYMMETRIC MACROCYCLES FOR CARCINOGENIC BENZO[*a*]PYRENE DETECTION" (2015). *Open Access Dissertations.* Paper 311.
https://digitalcommons.uri.edu/oa_diss/311

This Dissertation is brought to you for free and open access by DigitalCommons@URI. It has been accepted for inclusion in Open Access Dissertations by an authorized administrator of DigitalCommons@URI. For more information, please contact digitalcommons@etal.uri.edu.

DESIGN, SYNTHESIS OF A NEW CLASS OF DISSYMMETRIC MACROCYCLES FOR CARCINOGENIC BENZO[*a*]PYRENE DETECTION

BY

BHASKER RADARAM

A DISSERTATION SUBMITTED IN PARTIAL FULFILLMENT OF THE

REQUIREMENTS FOR THE DEGREE OF

DOCTOR OF PHILOSOPHY

IN

CHEMISTRY

UNIVERSITY OF RHODE ISLAND

2015

DOCTOR OF PHILOSOPHY DISSERTATION

OF

BHASKER RADARAM

APPROVED:

Thesis Committee:

Major Professor Mindy Levine

Brenton DeBoef

Bongsup Cho

Nasser H. Zawia

DEAN OF THE GRADUATE SCHOOL

UNIVERSITY OF RHODE ISLAND

2015

ABSTRACT

Since 1987, synthetic macrocycles have gained much attention in supramolecular chemistry, especially for their use in the extraction and/or detection of specific guests. The binding of a guest within the host leads to the formation of a host-guest complex. These host-guest complexes are governed by a variety of non-covalent interactions such as π-π stacking, electrostatic interactions, Van der Waals forces, and hydrophobic interactions. Herein we report the rational design and synthesis of a series of macrocycles as hosts for the evaluation of binding and detection of carcinogenic polycyclic aromatic hydrocarbons including benzo[*a*]pyrene. Benzo[*a*]pyrene is one of the most carcinogenic, mutagenic and teratogenic polycyclic aromatic hydrocarbons and persists in the environment ubiquitously.

Current detection methods involve tedious procedures and require multiple instruments for analysis. Hence, there is a need to find more efficient detection methods for this carcinogenic benzo[*a*]pyrene. The synthesized macrocycle hosts were evaluated for the efficient binding of benzo[*a*]pyrene and a high quantum yield fluorophore in the cavity of the macrocycle to generate ternary complexes. Proximity-induced energy transfer from the benzo[*a*]pyrene to a fluorophore resulted in a bright, turn-on fluorescence signal that can be used for benzo[*a*]pyrene detection. These complex systems also provide a key information about the intermolecular interactions that are required for efficient energy transfer to occur, including hydrophobic binding and π-π stacking. While synthesizing these macrocycles, we explored the development of new organic reactions such as green bromination of benzylic alcohols to their benzylic bromides, to optimize and complete the macrocyclization reaction and minimize the generation of environmentally toxic waste products. We have also explored highly efficient and sensitive detection methods for cesium metal ion in aqueous media and for hydrogen peroxide, both in solution and vapor phase.

The first manuscript,"Highly efficient non-covalent energy transfer in all-organic macrocycles," focuses on the use of aromatic organic macrocycles as supramolecular hosts for non-covalent energy transfer. These macrocycles lead to stronger binding and more efficient energy transfer compared to commercially available γ-cyclodextrin. This energy transfer was particularly efficient for the highly toxic benzo[*a*]pyrene with a fluorescent BODIPY acceptor, with up to a 5-fold increase in the fluorophore emission observed.

The second manuscript,**"**A series of dissymmetric macrocycle hosts for the facilitated detection of carcinogenic benzo[*a*]pyrene," describes a series of electronically dissymmetric organic macrocycles that were synthesized and evaluated for the facilitated efficient detection of highly toxic and carcinogenic benzo[*a*]pyrene *via* non-covalent energy transfer. This proximity-induced energy transfer was performed using a fluorescent BODIPY dye as an energy acceptor in combination with benzo[*a*]pyrene as the energy donor. Up to a 300% increase in the resulting fluorophore emission from analyte excitation compared to the emission from direct excitation was observed in the presence of the macrocycle hosts.

The third manuscript**,**"A green bromination method for the synthesis of benzylic dibromides," describes the development of new methodology for the dibromination of benzylic diols. This method proceeds in moderate to good yields for a wide variety of electron-deficient, electron-neutral, and electron-rich aromatic substrates. Moreover, the reagent, 1,3-dibromo-5,5-dimethylhydantoin, and the solvent, tetrahydrofuran, are substantially more environmentally benign than traditional solvents and reagents used for bromination. The utility of this methodology was demonstrated in the high-yielding synthesis of a key intermediate in the synthesis of omeprazole.

The fourth manuscript, "Sensitive and selective detection of cesium via fluorescence quenching," describes the selective detection of cesium metal ion. Herein we report a robust and easy method for detecting cesium metal ion (Cs^{+}) in partially aqueous solutions using the

fluorescence quenching of 2,4-bis[4-(*N*,*N*-dihydroxyethylamino)phenyl]squaraine. This squaraine dye was found to be both highly sensitive (low limits of detection) and selective (limited response to other metals) for cesium ion detection. The detection is likely based on the metal complexing to the dihydroxyethanolamine moieties, which disrupts the donor-acceptor-donor architecture and leads to efficient quenching.

The fifth manuscript, "Highly efficient detection of hydrogen peroxide in solution and in the vapor phase via fluorescence quenching," describes a highly efficient and sensitive detection of hydrogen peroxide in both aqueous solution and in the vapor phase via fluorescence quenching (turn-off mechanism) of the amplified fluorescent conjugated polymer-titanium complex induced by hydrogen peroxide. Inter- and intra-polymer energy migration leads to extremely high sensitivity and substantial improvements compared to current state of the art methods.

ACKNOWLEDGMENTS

First and foremost, I would like to express my sincere gratitude to my thesis advisor and major professor Mindy Levine for her endless patience, constructive guidance, understanding, untiring assistance and support throughout my research. She is an astute and great professor. Her understanding and high level of professional competence have made working with her a privilege.

My dream to obtain the highest degree in the field of chemistry has been challenging for the past six years. My thesis committee members Professor Brenton DeBoef, Professor Bongsup Cho, Professor Matthew Kiesewetter and Professor Ruitang Deng are recognized for their valuable comments and suggestions in the preparation of my thesis. I am also thankful to my collaborator Dr. Igor A Levitsky from Emitech, Inc for his valuable suggestions on one of the manuscripts that I worked on. I would also like to thank my major professor and Department of Chemistry at University of Rhode Island for financial support and valuable teaching and research experience.

My sincere thanks goes to my lab colleagues Nicole Serio, Sauradip Chaudhuri, William Talbert, Joshua Potvin, Justin Gharavi, Patrick Marks, Teresa Mako, Lindsey Prignano, John Roque, Daniel Jones and all the Levine Research Group for their friendship and for their helpful discussions during my research in the lab. I thank all of you for making such a fantastic and encouraging laboratory work environment. I am also thankful to my friends Papireddy Kancharla, Manohar Manikya Prabhu and Shekar Valamoni, Govardhan for their encouragement.

I especially thank my master's research advisor Dr. Edie J Banner for her constant encouragement.

Finally, I would like to dedicate this work to my beloved parents, Mr. Swamy and Mrs. Lakshmi and my wife Malleshwari Radaram for their enormous love and support. I could have not reached this milestone without their encouragement and concurrent support for all these years. I would like to thank my brother Venkatesh and sister Swapna for their support.

In dedication to my beloved Professor Dr. Edie J Banner

and my lovely family.

PREFACE

The dissertation of my research has been presented in manuscript format according to guidelines of the graduate school of the University of Rhode Island. The complete dissertation is divided into five manuscripts.

The first manuscript, "The use of aromatic organic macrocycles as supramolecular hosts for non-covalent energy transfer," is reported herein. These macrocycles lead to stronger binding and more efficient energy transfer compared to commercially available γ-cyclodextrin. This energy transfer was particularly efficient for the highly toxic benzo[*a*]pyrene with a fluorescent BODIPY acceptor, with up to a 5-fold increase in the fluorophore emission observed. This work has been published in *Chem.Commun.* **2013**, *42*, 8259-8261.

The second manuscript,"A series of electronically dissymmetric organic macrocycles were synthesized and evaluated for the facilitated efficient detection of highly toxic and carcinogenic benzo[*a*]pyrene *via* non-covalent energy transfer," is reported herein. This proximity-induced energy transfer was performed using a fluorescent BODIPY dye as an energy acceptor in combination with benzo[*a*]pyrene as the energy donor. Up to a 3-fold increase in the resulting fluorophore emission was observed in the presence of the macrocycle hosts. This manuscript is in preparation for the submission of the journal *Organic and Biomolecular Chemistry*.

The third manuscript reported herein is the identification of new methodology for the dibromination of benzylic diols. This method proceeds in moderate to good yields for a wide variety of electron-deficient, electron-neutral, and electron-rich aromatic substrates. Moreover, the reagent, 1,3-dibromo-5,5-dimethylhydantoin, and the solvent, tetrahydrofuran, are

substantially more environmentally benign than traditional solvents and reagents used for bromination. The utility of this methodology was demonstrated in the high-yielding synthesis of a key intermediate in the synthesis of omeprazole. This work has been published in *Tetrahedron. Lett.* **2014**, *55*, 4905-4908.

The fourth manuscript, "Sensitive and selective detection of cesium via fluorescence quenching," describes the selective detection of cesium metal ion. Herein we report a robust and easy method for detecting cesium metal ion (Cs^+) in partially aqueous solutions using the fluorescence quenching of 2,4-bis[4-(*N*,*N*-dihydroxyethylamino)phenyl]squaraine. This squaraine dye was found to be both highly sensitive (low limits of detection) and selective (limited response to other metals) for cesium ion detection. The detection is likely based on the metal complexing to the dihydroxyethanolamine moieties, which disrupts the donor-acceptor-donor architecture and leads to efficient quenching. This work has been published in *Dalton Trans.* **2013**, *42*, 16726-16728.

The fifth manuscript, "Highly efficient detection of hydrogen peroxide in solution and in the vapor phase via fluorescence quenching," describes a highly efficient and sensitive detection of hydrogen peroxide in both aqueous solution and in the vapor phase via fluorescence quenching (turn-off mechanism) of the amplified fluorescent conjugated polymer-titanium complex induced by hydrogen peroxide. Inter and intra-polymer energy migration leads to extremely high sensitivity. This manuscript has been published in *Chem. Commun.,* **2015**, *51*, 7061-7064.

TABLE OF CONTENTS

LIST OF TABLES

Manuscript 4

Manuscript 5

LIST OF FIGURES

FIGURE PAGE

Manuscript 1:

Manuscript 2:

Manuscript 3:

Manuscript 4:

Manuscript 5

LIST OF SCHEMES

MANUSCRIPT 1

This manuscript is published in *Chem.Commun.*,**2013**, *49*, 8259-8261.

Highly efficient non-covalent energy transfer in all-organic macrocycles

Bhasker Radaram, Joshua Potvin and Mindy Levine*

Corresponding author:

Prof. Mindy Levine

Department of Chemistry

University of Rhode Island

Kingston, Rhode Island 02881

mlevine@chm.uri.edu

MANUSCRIPT 1

Highly efficient non-covalent energy transfer in all-organic macrocycles

Abstract: The use of aromatic organic macrocycles as supramolecular hosts for non-covalent energy transfer is reported herein. These macrocycles lead to stronger binding and more efficient energy transfer compared to commercially available γ-cyclodextrin. This energy transfer was particularly efficient for the highly toxic benzo[*a*]pyrene with a fluorescent BODIPY acceptor, with up to a 5-fold increase in the fluorophore emission observed.

The complexation of small molecules in organic macrocyclesis a highly active area of research, with applications including supramolecular catalysis,[1] small-molecule detection,[2]and macrocycle-promoted energy transfer.[3] We have previously shown that γ-cyclodextrin, a well-known supramolecular host,[4] promotes efficient energy transfer from several polycyclic aromatic hydrocarbons (PAHs) and polychlorinated biphenyls (PCBs) to fluorophore acceptors.[5] This energy transfer occurs with up to 160% efficiency, and has significant potential applications in developing array-based detection schemes.[6]

The use of aromatic macrocycles as supramolecular hosts can lead to even stronger binding of aromatic guests and higher energy transfer efficiencies, as these macrocycles can bind aromatic guests via π-π stacking[7] in addition to hydrophobic binding.[8] Four examples of such macrocycles were synthesized (Figure 1) (synthetic details provided in the ESI). Briefly, a double Williamson etherification reaction[9] followed by a double Suzuki reaction[10] rapidly assembled the linear precursors. The key macrocyclization reactions were accomplished via a double etherification reaction (for compound **1**)[11] or via a double Mitsunobu reaction (for compounds **2-4**).[12]

These macrocycles include three structures that are electronically-dissymmetric (**1-3**), with clearly defined electron-rich and electron-deficient components to the macrocycle, and one that is electronically symmetric. The electronically dissymmetric structures are designed to bind an electron-rich analyte near the electron-deficient component of the macrocycle, and an electron-deficient fluorophore near the electron-rich segment of the macrocycle, to form a stack of four aromatic components with alternating electronic character that will undergo efficient energy transfer. Whether such dissymmetry improves the binding and energy transfer efficiencies was tested by comparison to control macrocycle **4**, which lacks such dissymmetry. Semi-empirical PM3-level calculations of the macrocycles indicate that all of them have internal dimensions analogous to that of γ-cyclodextrin (Table 1),[13] and sufficiently large to promote intra-cavity energy transfer.

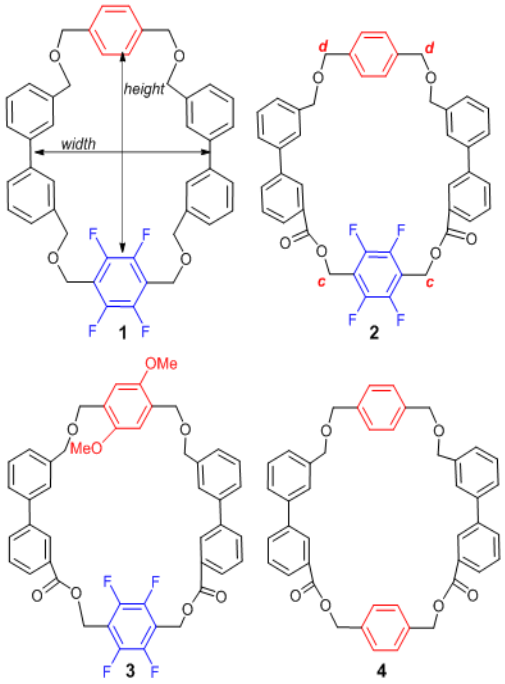

Figure 1: Structures of supramolecular hosts, with electron-rich segments highlighted in red, and electron-deficient segments in blue. Height and width dimensions are shown on macrocycle**1**, and the key protons involved in NMR studies are indicated by letters "c" and "d"

Table 1 Cavity dimensions of compounds **1-4** in the energy-minimized conformations

Compound	Height	Width
1	9.1 Å	11.2 Å
2	5.0 Å	12.6 Å
3	5.7 Å	13.0 Å
4	9.7 Å	8.0 Å

Once synthesized, macrocycles **1-4** were used for two key applications: (a) as supramolecular hosts to bind aromatic PAHs; and (b) as hosts for non-covalent energy transfer from PAHs to fluorophore **7**(Figure 2).[14]

The binding of aromatic PAHs in macrocycles **1-4** was measured by adding concentrated solutions of the macrocycle and PAH in THF to an aqueous solution of phosphate buffered saline. The fluorescence emission spectrum of the PAH was measured in the presence of increasing amounts of the macrocycle. This experimental design resulted in a mostly aqueous solution, which maximized hydrophobic binding of the PAHs.

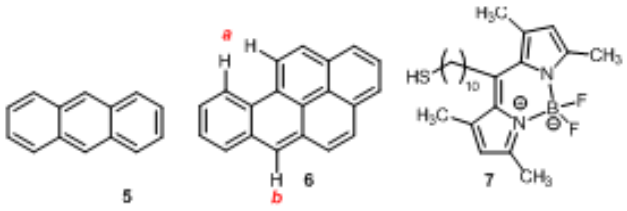

Figure 2: PAH energy donors (**5** and **6**) and fluorophore acceptor (**7**) used in macrocycle-promoted energy transfer

Among all macrocycles tested, macrocycle **2** was the most efficient supramolecular host for binding benzo[*a*]pyrene **6**, with other PAH-macrocycle combinations leading to negligible binding. This binding was quantified by measuring changes in the emission spectra of benzo[*a*]pyrene: the addition of 0.061 mM of macrocycle **2** resulted in a 4-fold increase in the benzo[*a*]pyrene emission (Figure 3a). The sharp increase in the excimer band around 500 nm

with increasing amounts of the macrocycle strongly suggests a 1:2 host: guest complex. Fitting this data to a Benesi-Hildebrand equation for a 1:2 complex revealed an apparent binding constant of 5 x 10^9 M^{-2},[15] which is among the highest binding constants observed for this highly toxic analyte.[16] By comparison, the addition of macrocycle **2** to a solution of anthracene resulted in no significant changes in the anthracene emission beyond spectral broadening (Figure 3b).

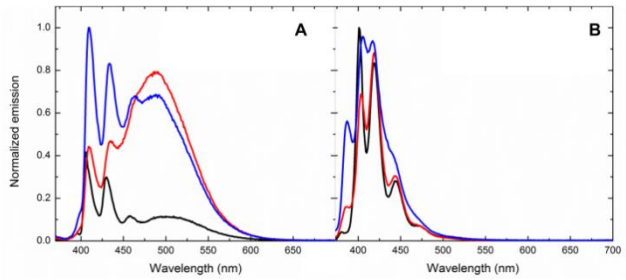

Figure 3: Analyte emission spectra in the presence of increasing amounts of macrocycle **2** for (a) benzo[*a*]pyrene and (b) anthracene. Black line: [**2**] = 0 mM; red line: [**2**] = 0.020 mM; blue line: [**2**] = 0.061 mM.

This binding was further confirmed by ^{1}H NMR titration studies.[17] The titration of benzo[*a*]pyrene into a solution of macrocycle **2** in $CDCl_3$ resulted in a shift of both the benzo[*a*]pyrene peaks and the macrocycle peaks (Table 2; Figure 4). The fact that macrocycle protons C and D shift noticeably indicates that benzo[*a*]pyrene associates with both sides of the macrocycle, although more with the electron-deficient side (as indicated by a larger shift in the C protons). The simultaneous shifts in the host and guest peaks suggest a close association between the host and the guest, and are consistent with the fluorescence data.

Table 2 ^{1}H NMR chemical shifts for **2:6** complex

NMR proton	Initial (ppm)	Final (ppm)	Change in ppm
Peak A	9.005	9.021	+0.016
Peak B	8.471	8.482	+0.021
Peak C	5.542	5.465	-0.077
Peak D	4.571	4.549	-0.022

In addition to their ability to bind PAHs, macrocycles **1-4** were also investigated for their ability to promote energy transfer from analytes **5** and **6** to highly fluorescent BODIPY **7**.[18] The efficiency of such energy transfer was quantified in two ways:

(a) by measuring the decrease in the donor emission from adding an energy acceptor, according to Equation 1:

$$\text{Donor decrease} = F_{DA}/F_{D} \quad (1)$$

where F_{DA} and F_{D} are the integrated emission of the donor in the presence and absence of acceptors, respectively;[19]

and (b) by measuring the increase in the acceptor emission from adding the energy donor, according to Equation 2:

$$\text{Fluorophore increase} = I_{DA}/I_{A} \quad (2)$$

Where I_{DA} is the integrated emission of the fluorophore from analyte excitation, and I_{A} is the integrated emission of the fluorophore (from excitation at the same wavelength) in the absence of the analyte.

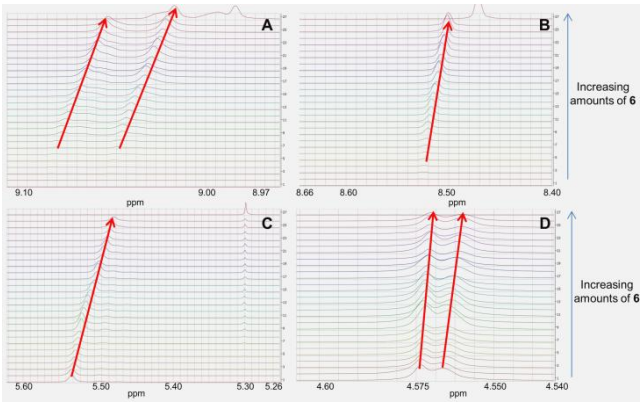

Figure 4: ^{1}H NMR chemical shifts for **2**: **6**complex. (a) Protons A; (b) Protons B; (c) Protons C; (d) Protons D. The designation of protons A-D are shown in Figures 1 and 2.

The results of macrocycle-promoted energy transfer are summarized in Table 3. These experiments were conducted under mostly aqueous conditions to maximize the favourable hydrophobic binding and π-π stacking between the aromatic PAH donor, aromatic fluorophore acceptor, and aromatic macrocycle.

Table 3 Results of macrocycle-promoted energy transfer between compound **6** and compound **7**

Host	Fluorophore Increase	Donor Decrease
Macrocycle**1**	3.3	0.90
Macrocycle**2**	5.3	0.57
Macrocycle**3**	2.4	0.80
Macrocycle**4**	3.6	0.72

a 360 nm excitation in all cases; fluorophore increase calculated according to Equation 2 and donor decrease calculated according to Equation 1

The results clearly indicate that macrocycle **2** was the most efficient host for non-covalent energy transfer, as measured both by the increase in fluorophore emission more than 5-fold and by the decrease in donor emission to 57% of its initial value (Figure 5a and 5b). The minimal amount of excimer emission observed in these spectra strongly suggests that fluorophore **7** displaces one molecule of benzo[*a*]pyrene from the macrocycle's interior.

Interestingly, macrocycle **4** was substantially less efficient than macrocycle **2** at promoting supramolecular energy transfer between benzo[*a*]pyrene **6** and BODIPY **7** (Figure 5c and 5d). The only difference between the two hosts is the replacement of the perfluorophenyl ring in macrocycle **2** with a phenyl ring in macrocycle **4**, which effectively removes the electronic dissymmetry from the structure. This direct comparison indicates that electronic dissymmetry provides a direct benefit for supramolecular energy transfer efficiencies.

Macrocycle **2** was also substantially more efficient at promoting such energy transfer compared to γ-cyclodextrin.[5] Using γ-cyclodextrin as a supramolecular host resulted predominantly in the formation of a benzo[*a*]pyrene excimer, with only weak energy transfer observed. This excimer effectively obscured the fluorophore emission peak, rendering such a system ineffectual for benzo[*a*]pyrene-based energy transfer and detection. In contrast, using macrocycle **2** resulted in a strong BODIPY peak and minimal benzo[*a*]pyrene excimer emission under identical experimental conditions. The ability to use benzo[*a*]pyrene in such energy transfer schemes (and detection schemes based on such energy transfer) is particularly relevant, due to the high toxicity and known carcinogenicity of benzo[*a*]pyrene.[20]

The reasons why macrocycle **2** is substantially more efficient than macrocycles **1**, **3**,and **4** at binding PAHs and promoting energy transfer are currently under investigation, but the following conclusions can already be drawn: (a) Electronic dissymmetry in the host leads to more efficient energy transfer (by comparing macrocycle **2** and **4**); (b) the presence of an ester linkage leads to higher energy transfer efficiencies (by comparing macrocycles**1** and **2**); and (c) the presence of methoxy groups, which increases the electron-donating nature of the top half of the macrocycle, leads to less efficient energy transfer, perhaps by increasing the steric hindrance and limiting cavity accessibility.

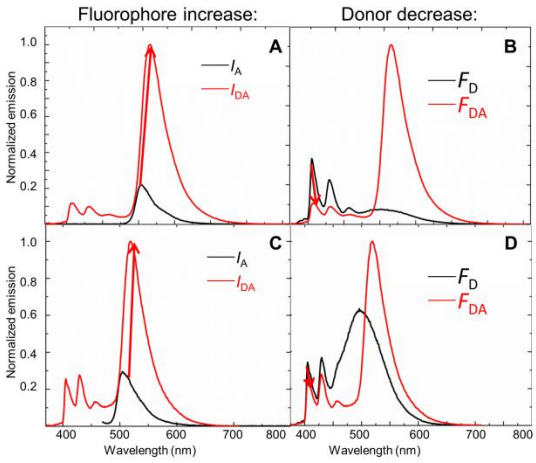

Figure 5: Comparison of the energy transfer in macrocycle **2** (5a and 5b) and macrocycle **4** (5c and 5d).

In summary, reported herein is the use of aromatic organic macrocycles as supramolecular hosts for PAH binding and non-covalent energy transfer. One of the new macrocycles, compound **2**, is substantially more efficient than known macromolecules at binding benzo[*a*]pyrene and promoting energy transfer from this toxicant to a fluorophore. More generally, the ability to modify the supramolecular host for this energy transfer via synthetic organic chemistry provides optimal flexibility in tuning and optimizing such non-covalent energy transfer. The scope of macrocycle-promoted energy transfer and its use in array-based detection scheme is currently under investigation.

Notes and references

1. M. D. Pluth, R. G. Bergman and K. N. Raymond, *Acc. Chem. Res.*, 2009, **42**, 1650; D. Ajami and J. Rebek, *Acc. Chem. Res.*, 2013, **46**, 990.
2. A. T. Wright and E. V. Anslyn, *Chem. Soc. Rev.*, 2006, **36**, 14; B. M. Rambo and J. L. Sessler, *Chem. Eur. J.*, 2011, **17**, 4946.
3. A. Maity, P. Mukherjee, T. Das, P. Ghosh and P. Purkayastha, *Spectrochim. Acta A*, 2012, **92**, 382; D. Sarkar, A. Mahata, P. Das, A. Girigoswami and N. Chattopadhyay,

Chem. Phys. Lett., 2009, **474**, 88; E. J. F. Klotz, T. D. W. Claridge and H. L. Anderson, *J. Am. Chem. Soc.*, 2006, **128**, 15374.

4. S. Hamai, *J. Inclusion Phenom. Macro. Chem.*, 2010, **67**, 471; S. Hamai and H. Satou, *Bull. Chem. Soc. Japan*, 2000, **73**, 2207.
5. N. Serio, K. Miller and M. Levine, *Chem. Commun.*, 2013, **49**, 4821; T. Mako, P. Marks, N. Cook and M. Levine, *Supramol. Chem.*, 2012, **24**, 743.
6. O. R. Miranda, B. Creran and V. M. Rotello, *Curr. Opinion Chem. Biol.*, 2010, **14**, 728.
7. H.-J. Schneider, *Acc. Chem. Res.*, 2013, **46**, 1010.
8. Y. Chen, Y.-M. Zhang and Y. Liu,*Chem. Commun.*, 2010, **46**, 5622.
9. E. Fuhrmann and J. Talbiersky, *Org. Process Res. Dev.*, 2005, **9**, 206.
10. M. Mor, S. Rivara, A. Lodola, P. V. Plazzi, G. Tarzia, A. Duranti, A. Tontini, G. Piersanti, S. Kathuria and D. Piomelli, *J. Med. Chem.*, 2004, **47**, 4998.
11. T. A. Al Hujran, L. N. Dawe and P. E. Georghiou, *Org. Lett.*, 2012, **14**, 3530.
12. T. Y. S. But and P. H. Toy, *J. Am. Chem. Soc.*,2006, **128**, 9636.
13. F. E. Oddy, S.Brovelli, M. T. Stone, E. J. F. Klotz, F. Cacialli and H. L. Anderson, *J. Mater. Chem.*, 2009, **19**, 2846.
14. Experiments done with an unfunctionalized BODIPY indicate essentially identical behavior; see ESI for more details.
15. H. A. Benesi and J. H. Hildebrand, *J. Am. Chem. Soc.*, 1949, **71**, 2703; K. P. Sambasevam, S.Mohamad, N. M. Sarih and N. A. Ismail, *Int. J. Molec. Sci.*, 2013, **14**, 3671.
16. K. Vengatajalabathy Gobi, M. Sasaki, Y.Shoyama and N. Miura, *Sensors Actuators B Chem.*, 2003, **B89**, 137.
17. R. Kumar, T. Guchhait and G. Mani, *Inorg. Chem.*, 2012, **51**, 9029.

18. J. L. Shepherd, A.Kell, E. Chung, C. W. Sinclar, M. S. Workentin and D. Bizzotto, *J. Am. Chem. Soc.*, 2004, **126**, 8329.
19. M. Levine, I. Song, T. L. Andrew, S. E. Kooi and T. M. Swager, *J. Polym. Sci. A Polym.Chem.*, 2010, **48**, 3382.
20. H.-K. Cho and H.-S. Shin, *Food Sci. Biotechnol.*, 2012, **21**, 1329; M. Masiol, A. Hofer, S. Squizzato, R. Piazza, G. Rampazzo and B. Pavoni, *Atmospheric Environ.*, 2012, **60**, 375.

Electronic Supporting Information for

Highly efficient non-covalent energy transfer in all-organic macrocycles

*Bhasker Radaram, Joshua K. Potvin, and Mindy Levine**

Materials and Methods

All reactions were carried out under an atmosphere of dry nitrogen unless otherwise noted. Solvents such as dichloromethane, toluene, tetrahydrofuran were dried using an MBraun dual solvent purification system prior to use. Starting materials, reagents and solvents were purchased from Aldrich Chemical Company, Acros Organics, or Fisher Scientific and were used as received. Reactions were all monitored via analytical thin layer chromatography (TLC) using polyester backed TLC plates. Visualization was accomplished with UV light at 254 nm. Column chromatography was performed with silica gel (230-400 mesh), obtained from Silicycle Incorporated.

^{1}H, ^{13}C and ^{19}F NMR spectra were recorded on a Bruker 300 MHz spectrometer. Multiplicity for ^{1}H NMR data is reported as follows: s = singlet, d = doublet, t = triplet, m = multiplet, br =broad. ^{1}H NMR spectra were referenced to the residual solvent peaks: $CDCl_3$ (7.26 ppm), d_6-DMSO (2.50 ppm), or to tetramethylsilane (TMS) (0.0 ppm). High resolution mass spectra were obtained and analyzed using a Bruker Daltonics APEXIV 4.7 Tesla Fourier Transform Ion Cyclotron Resonance Mass Spectrometer (FT-ICR-MS) at the Massachusetts Institute of Technology, in collaboration with Dr. Li Li. Absorbance measurements were recorded on an Agilent 8453 UV-visible spectrophotometer. Fluorescence measurements were recorded on Shimadzu RF 5301 spectrophotometer.

Synthetic Procedures:

Synthesis of Macrocycle 1:

Overall Scheme 1:

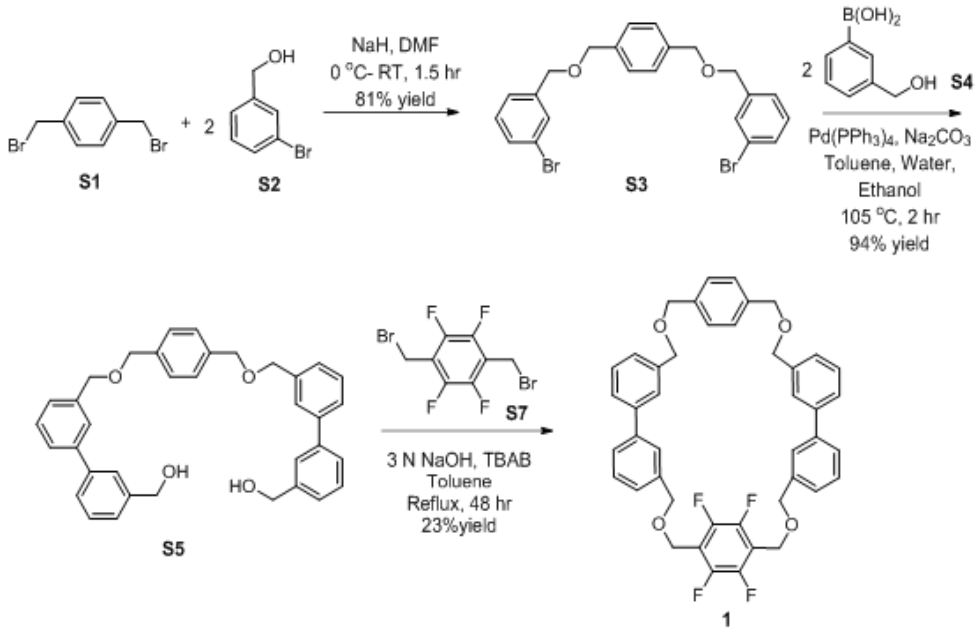

Reaction 1: Synthesis of compound S3:

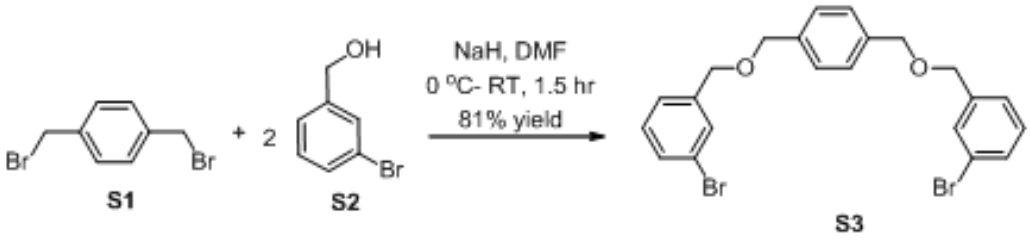

Compound **S1** (1.50 g, 5.68 mmol, 1.0 eq.) and 3-bromobenzyl alcohol **S2** (2.34 g, 12.50 mmol, 2.2 eq.) were dissolved in 20 mL of anhydrous dimethylformamide (DMF). The reaction mixture was stirred for 10 minutes at room temperature and was cooled to 0 °C in an ice bath. Sodium hydride (0.368 g, 15.34 mmol, 2.7 eq.) (60% in mineral oil) was then added to the reaction mixture and the reaction mixture was allowed to warm to room temperature.

The reaction mixture was stirred at room temperature for 2 hours, at which point it was determined to be complete by TLC. Distilled water (10 mL) was added to quench the reaction, and the reaction mixture was then extracted with 3 portions of dichloromethane (20 mL each time). The combined organic extract was washed 9 times with distilled water (20 mL each time), followed by washing with brine. The organic extract was then dried over sodium sulfate, filtered, and concentrated via rotary evaporation to yield the crude product. The product was purified by flash chromatography (9:1 hexanes: ethyl acetate) to afford compound **S3** as a white solid in 81% isolated yield (2.18 grams). R_f: 0.85 (1:1 hexanes: ethyl acetate). ^{1}H NMR ($CDCl_3$, 300 MHz): δ = 7.52 (s, 2 H), 7.43 (d, 6 H, J = 7.8 Hz), 7.31-7.19 (m, 4 H), 4.56 (s, 4 H), 4.52 (s, 4 H); ^{13}C NMR ($CDCl_3$, 75 MHz): δ = 140.6, 137.5, 130.7, 130.6, 130.0, 128.0, 122.6, 72.1, 72.2; HRMS (ESI): Calcd for $[M+NH_4^+$, $C_{22}H_{20}Br_2O_2]^+$ 494.0157, found 494.0178.

Reaction 2: Synthesis of compound S5:

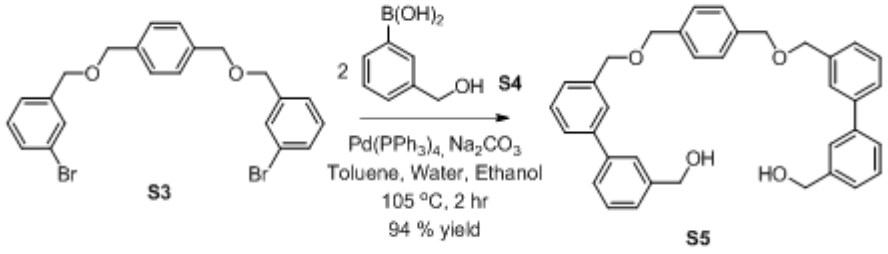

Compound **S3** (496 mg, 1.04 mmol, 1.0 eq.) was dissolved in anhydrous toluene (15 mL), 3-hydroxymethylphenyl boronic acid (compound **S4**) (481 mg, 3.17 mmol, 3.04 eq.) was dissolved in anhydrous ethanol (6.0 mL), and sodium carbonate (1.495 g, 14.11 mmol, 13.5 eq.) was dissolved in water (7.0 mL). The aqueous sodium carbonate solution was degassed under nitrogen for 30-60 minutes. All three solutions were combined in an oven-dried and nitrogen purged round-bottom flask and tetrakis(triphenylphosphine)palladium(0) ($Pd(PPh_3)_4$) (156 mg, 0.14 mmol, 0.13 eq.) was added to the reaction mixture. The reaction mixture was

refluxed at 105 ^{o}C for 3 hours under a nitrogen atmosphere, at which point the reaction was complete by TLC analysis. Water (6.0 mL) was added to quench the reaction and the reaction mixture was extracted with dichloromethane (3 portions of 20 mL each). The combined organic extract was dried over sodium sulfate, filtered, and concentrated via rotary evaporation. The product was further purified by flash chromatography using hexanes: ethyl acetate (4:6) to afford compound **S5** as an off-white solid (517 mg, 94 % yield). ^{1}H NMR ($CDCl_3$, 300 MHz): δ = 7.59 (s, 4 H), 7.52 (d, 4 H, J = 7.8 Hz), 7.43 (d, 4 H, J = 7.5 Hz), 7.41-7.34 (m, 8 H), 4.75 (d, 4 H, J = 5.7 Hz), 4.61 (d, 8 H, J = 5.1 Hz). ^{13}C NMR ($CDCl_3$, 75 MHz): δ = 141.4, 141.3, 141.1, 138.8, 129.0, 128.9, 128.0, 126.8, 126.6, 126.5, 126.4, 125.9, 125.8, 72.1, 72.0, 65.3. HRMS (ESI): Calcd for $[M+H^+, C_{36}H_{34}O_4]^+$ 530.2457, found 530.2454.

Reaction 3: Synthesis of compound S7:

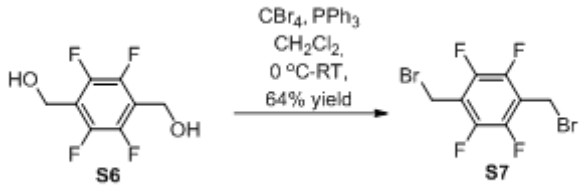

Compound **S6** (1.20 g, 5.71 mmol, 1.0 eq.) was dissolved in dichloromethane (25 mL) and cooled to 0 ^{o}C. Carbon tetrabromide (4.73 g, 14.26 mmol, 2.5 eq.) and triphenylphosphine (3.74 g, 14.26 mmol, 2.5 eq.) were added to the reaction mixture. The reaction mixture was then warmed to room temperature and stirred at room temperature for 16 hours. The solvent was removed using a rotary evaporator, and the crude mixture was purified by flash chromatography (9:1 hexanes: ethyl acetate). The product **S7** was obtained as a white crystalline solid (1.21 g, 64 % yield). R_f: 0.80 (1:1 ethyl acetate: hexanes). ^{1}H NMR ($CDCl_3$, 300 MHz): δ = 4.50 (s, 4 H); ^{13}C NMR ($CDCl_3$, 75 MHz): δ = 146.1, 142.8, 117.5, 16.2; ^{19}F

NMR ($CDCl_3$, 300 MHz): δ = -142.31; HRMS (ESI): Calcd for $[M+H^+, C_8H_4 Br_2F_4]^+$ 333.8616, found 333.8612.

Reaction 4: Synthesis of compound 1:

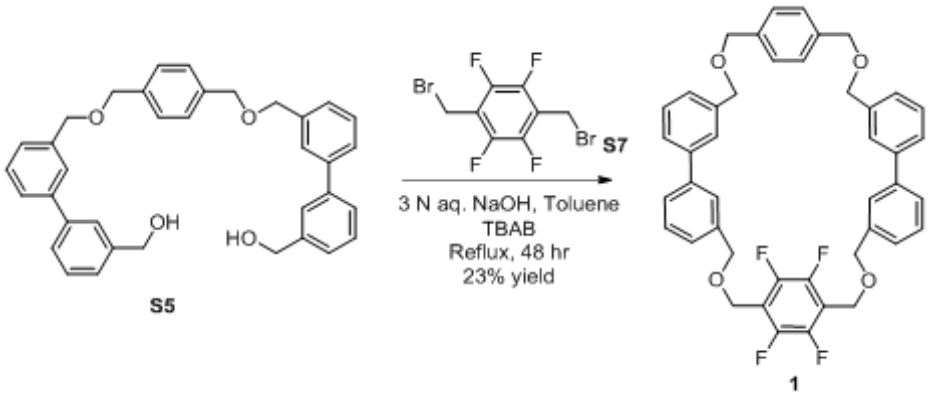

To a mixture of compound **S5** (50. mg, 0.094 mmol, 1.0 eq.), compound **S7** (34 mg, 0.101 mmol, 1.07 eq.) and tetrabutylammonium bromide (TBAB) (60 mg, 0.186 mmol, 1.98 eq.) in anhydrous toluene (50 mL) was added a solution of 3 N aqueous NaOH (8.0 mL). The reaction mixture was refluxed for 48 hours at 120 ^oC. After 48 hours, the reaction mixture was cooled to room temperature and toluene was removed via rotary evaporator. The reaction mixture was extracted with ethyl acetate (3 portions of 5.0 mL), and the combined organic extract was washed with brine solution, dried over anhydrous sodium sulfate, filtered and evaporated to yield the crude product as a yellow liquid. The product was purified via flash chromatography (3:7 ethyl acetate: hexanes) to afford the pale yellow liquid **1** in 23% isolated yield (15 mg). R_f: 0.62 (1: 1 ethyl acetate: hexanes); ^1H NMR ($CDCl_3$, 300 MHz): δ = 7.55 (s, 4 H), 7.49 (d, 4 H, J = 7.8 Hz), 7.42 (d, 2 H, J = 7.5 Hz) 7.40-7.28 (m, 10 H), 4.68 (s, 4 H), 4.61 (s, 4 H), 4.59 (s, 4 H), 4.58 (s, 4 H). ^{13}C NMR ($CDCl_3$, 75 MHz): δ = 140.36, 140.13, 137.77, 136.88, 136.63, 127.78, 126.98, 125.89, 125.75, 125.72, 125.63, 125.46, 70.98, 70.91, 58.36; ^{19}F NMR ($CDCl_3$, 300 MHz): δ = -143.42; HRMS (ESI): Calcd for $[M+Na]^+$, $C_{44}H_{36}F_4O_4]^+$ 727.2447, found 727.2442.

Synthesis of Macrocycle 2:

Overall Scheme 2:

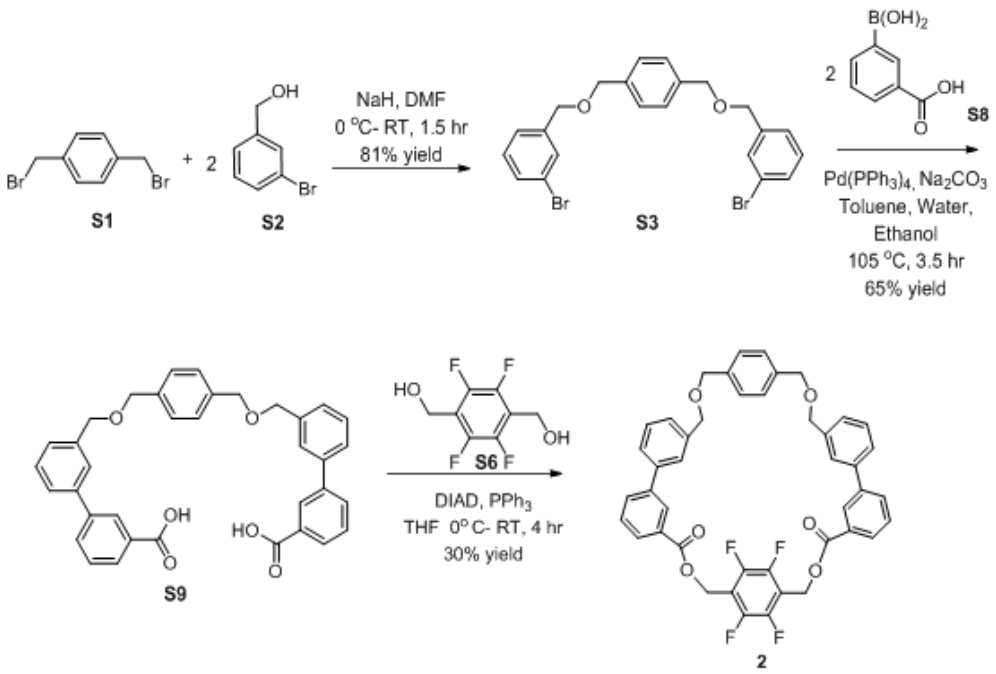

Reaction 5: Synthesis of compound S9:

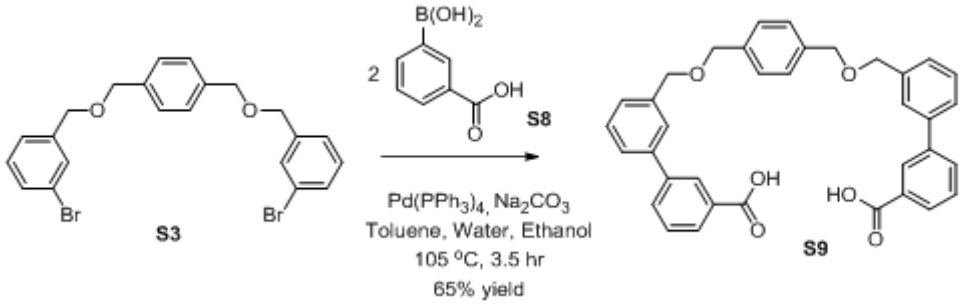

Compound **S3** (500 mg, 1.05 mmol, 1.0 eq.) was dissolved in anhydrous toluene (15.0 mL), 3-carboxyphenyl boronic acid (compound **S8**) (400 mg, 2.41 mmol, 2.3 eq.) was dissolved in anhydrous ethanol (8.0 mL), and sodium carbonate (1.11 g, 10.47 mmol, 9.97 eq.) was dissolved in water (8.0 mL). The aqueous sodium carbonate solution was degassed under nitrogen for 30 minutes. All three solutions were combined in an oven-dried, nitrogen-purged round-bottom flask and tetrakis(triphenylphosphine)palladium(0) ($Pd(PPh_3)_4$) (226 mg, 0.196

mmol, 0.19 eq.) was added to the reaction mixture. The reaction mixture was refluxed at 105 ^{o}C for 3.5 hours under a nitrogen atmosphere, until the reaction was complete by TLC analysis. The reaction mixture was acidified to pH 2 by adding 6N HCl dropwise (approximately 1.5-2 mL) then extracted with 3 portions of ethyl acetate (20 mL each). The combined organic extract was washed with brine and dried over sodium sulfate, filtered, and concentrated via rotary evaporation. The product was further purified by flash chromatography using hexanes: ethyl acetate (6:4) to afford **S9** as a white solid (361 mg, 65% yield). ^{1}H NMR (d_6-DMSO, 300 MHz): δ = 8.17 (s, 2 H), 7.92 (t, 4 H, J = 9 Hz), 7.66-7.56 (m, 6 H), 7.47 (t, 2 H, J = 7.5 Hz), 7.38 (d, 6 H, J = 9.3 Hz), 4.61 (s, 4 H), 4.57 (s, 4 H). ^{13}C NMR (d_6-DMSO, 75 MHz): δ = 167.2, 140.3, 139.3, 139.2, 137.9, 131.5, 131.0, 129.3, 129.1, 128.3, 127.6, 127.2, 127.0, 125.8, 125.8. HRMS (ESI): Calcd for [M-H$^-$, $C_{36}H_{30}O_6$]$^-$ 557.1970, found 557.1978.

Reaction 6: Synthesis of macrocycle 2:

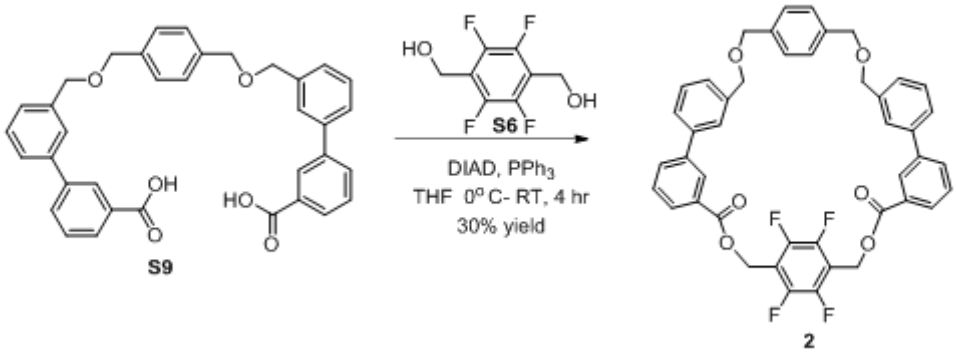

To compound **S9** (130.0 mg, 0.23 mmol, 1.0 eq.), compound **S6**, (54.0 mg, 0.25 mmol, 1.1 eq.) and triphenylphosphine (124.0 mg, 0.47 mmol, 2.04 eq.) in anhydrous THF (50 mL) was added a solution of diisopropylazodicarboxylate (0.096 mL, 0.49 mmol, 2.1 eq.) in anhydrous THF (5.0 mL) slowly at 0 ^{0}C. The reaction mixture was stirred for 15 min at 0 ^{0}C. The reaction mixture was allowed to warm to room temperature, and was stirred for 4 hours at

room temperature. The reaction mixture was diluted with diethyl ether (15 mL), and washed with saturated $NaHCO_3$ (2 x 10 mL portions) and brine (10 mL). The organic layer was dried with sodium sulfate, filtered and evaporated. The residue was purified by column chromatography to afford macrocycle **2** as a white solid (51 mg, 30% yield). ^{1}H NMR ($CDCl_3$, 300 MHz): δ = 8.15 (s, 2 H), 8.03 (d, 2 H, J = 8.1 Hz), 7.77 (d, 2 H, J = 7.8 Hz), 7.50 (d, 4 H, J = 5.1 Hz), 7.45 (t, 4 H, J = 4.8 Hz), 7.39 (d, 2 H, J = 7.2 Hz), 7.33 (d, 2 H, J = 7.5 Hz), 7.31 (s, 4 H), 5.54 (s, 4 H), 4.57 (s, 8 H). ^{13}C NMR ($CDCl_3$, 75 MHz): δ = 165.7, 141.7, 140.4, 139.0, 132.2, 129.8, 128.9, 127.9, 127.1, 126.6, 71.9, 71.7. ^{19}F NMR ($CDCl_3$, 300 MHz): δ = -141.8. HRMS (ESI): Calcd for [M+Na], [$C_{44}H_{32}F_4O_6$] 755.2028, found 755.2047.

Synthesis of Macrocycle 3:

Overall Scheme 3:

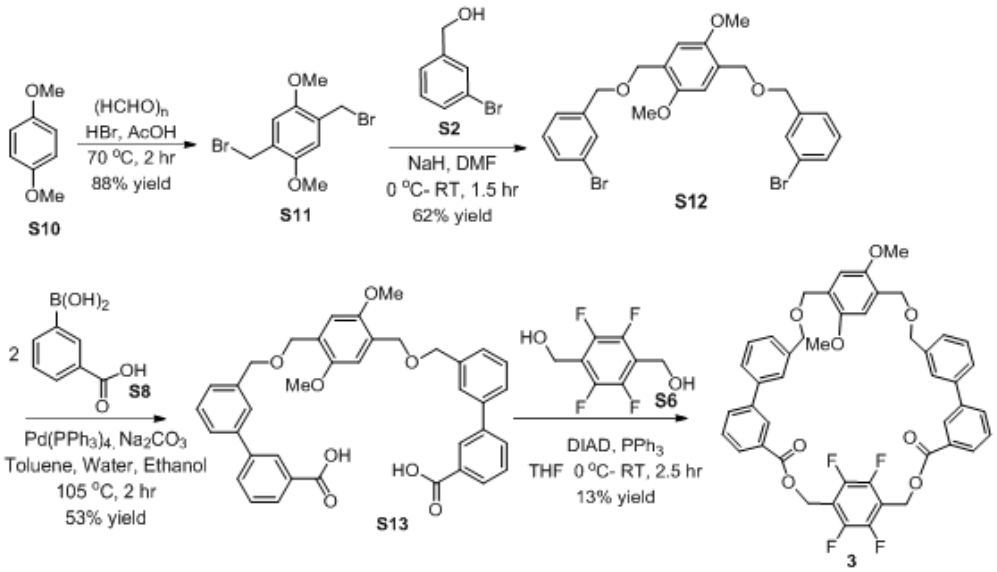

Reaction 7: Synthesis of compound S11:

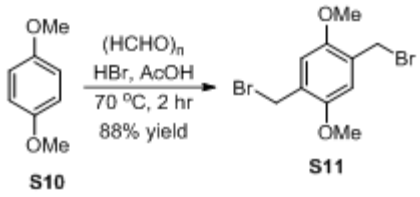

Prepared according to the published procedure: Roviello, A.; Borbone, F.; Carella, A.; Diana, R.; Roviello, G.; Panunzi, B.; Ambrosio, A.; Maddalena, P. *J. Polym. Sci. A Polym. Chem.* **2009**, *47*, 2677-2689.

Reaction 8: Synthesis of compound S12:

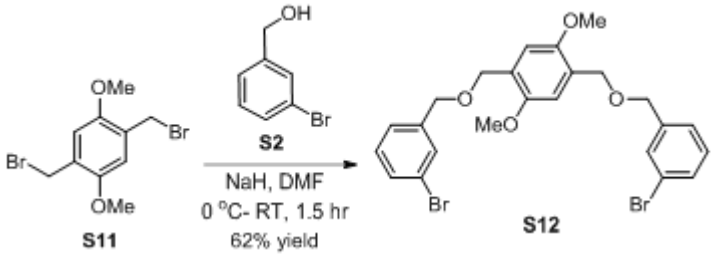

Compound **S11** (1.0 g, 3.09 mmol, 1.0 eq.) and compound **S2** (1.26 g, 6.74 mmol, 2.2 eq.) were dissolved in 10 mL of anhydrous dimethylformamide. The reaction mixture was stirred for 10 minutes at room temperature and was cooled to 0 ^{o}C in an ice bath. Sodium hydride (0.200 g, 8.33 mmol, 2.7 eq.) (60% in mineral oil) was then added to the reaction mixture and the mixture was allowed to warm to room temperature. The reaction mixture was stirred at room temperature for 2 hours, until it was determined to be complete by TLC. Excess distilled water (~15 mL) was added to quench the reaction, and the reaction mixture was then extracted multiple times with dichloromethane (3 x 20 mL). The combined organic extract was washed 10 times with distilled water (10 mL each time), followed by brine. The organic extract was then dried over sodium sulfate, filtered, and concentrated via rotary evaporation to yield the crude product. The crude product was purified by isopropanol (0.5 mL) and hexanes (10 mL) to afford the ether product **S12** as a white solid in 62% isolated yield (1.02 grams) R_f: 0.56 (9:1 hexanes: ethyl acetate). ^{1}H NMR ($CDCl_3$, 300 MHz): δ = 7.49 (s, 2 H), 7.34 (d, 2 H, J =

7.8 Hz), 7.23-7.11 (m, 4 H), 6.90 (s, 2 H), 4.51 (s, 4 H), 4.49 (s, 4 H), 3.74 (s, 6 H); ^{13}C NMR ($CDCl_3$, 75 MHz): δ = 151.1, 140.9, 130.67,129.9, 126.2, 126.1, 122.5, 71.5, 67.0, 56.1; HRMS (ESI): Calcd for $[M+NH_4^+, C_{24}H_{18}Br_2O_4]^+$ 552.0371, found 552.0367.

Reaction 9: Synthesis of compound S13:

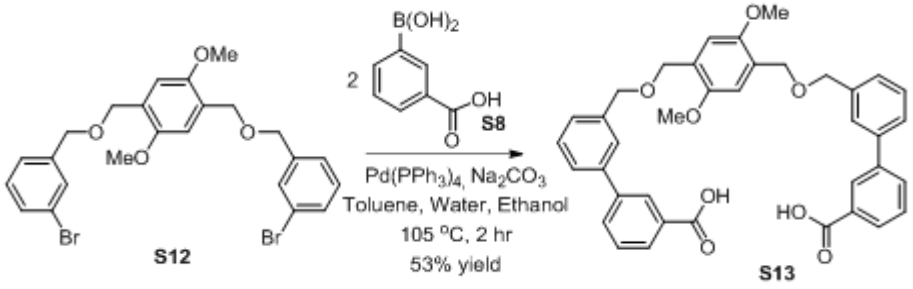

Compound **S12** (0.505 g, 0.94 mmol, 1.0 eq.) was dissolved in anhydrous toluene (15 mL), 3-carboxyphenyl boronic acid (compound **S8**) (0.406 g, 2.45 mmol, 2.6 eq.) was dissolved in anhydrous ethanol (8.0 mL), and sodium carbonate (1.03 g, 9.72 mmol, 10.3 eq.) was dissolved in water (8.0 mL). The aqueous sodium carbonate solution was degassed under nitrogen for 30 minutes. All three solutions were combined in an oven-dried, nitrogen-purged round-bottom flask and tetrakis(triphenylphosphine)palladium(0) ($Pd(PPh_3)_4$) (0.205 g, 0.18 mmol, 0.19 eq.) was added to the reaction mixture. The reaction mixture was refluxed at 105 ^{o}C for 3 hours under a nitrogen atmosphere, until the reaction was complete by TLC analysis. The reaction mixture was cooled to room temperature and acidified to pH 2 by adding 6N HCldropwise (~2 mL), then extracted with ethyl acetate (3 portions of 20 mL each). The combined organic extract was washed with brine solution and dried over sodium sulfate, filtered, and concentrated via rotary evaporation. The product was further purified by flash chromatography using hexanes: ethyl acetate (1:1) to afford **S13** as a white solid (307 mg, 53% yield). ^{1}H NMR (d_6-DMSO, 300 MHz): δ = 13.14 (s, 2 H), 8.19 (s, 2 H), 8.01-7.89 (m, 4 H), 7.70 (s, 2 H), 7.67-7.55 (m, 4 H), 7.49 (t, 2 H, J = 7.5 Hz), 7.41 (d, 2 H, J = 7.5 Hz), 7.04 (s, 2 H), 4.66 (s, 4 H), 4.55 (s, 4 H), 3.72 (s, 6 H). ^{13}C NMR (d_6-DMSO, 75 MHz): δ = 167.1,

150.4, 140.3, 139.4, 131.4, 131.0, 129.3, 129.0, 128.2, 127.2, 126.9, 126.0, 125.7, 111.4, 71.4, 66.3, 55.7. HRMS (ESI): Calcd for $[M\text{-}H^-, C_{36}H_{30}O_6]^-$ 618.6850, found 618.6858.

Reaction 10: Synthesis of macrocycle 3:

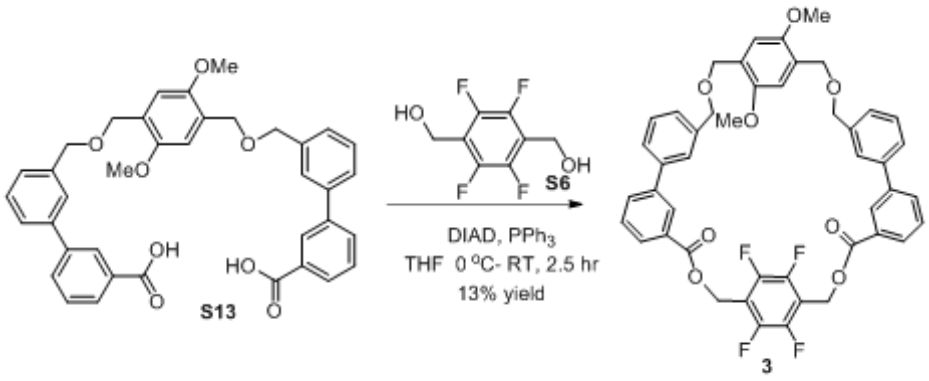

To compound **S13** (100.0 mg, 0.16 mmol, 1.0 eq.), compound **S6** (37.0 mg, 0.18 mmol, 1.1 eq.), and triphenylphosphine (86.0 mg, 0.33 mmol, 2.1 eq.) in anhydrous THF (50 mL) was added a solution of diisopropylazodicarboxylate (DIAD) (0.067 mL, 0.34 mmol, 2.1 eq.) in anhydrous THF (5.0 mL) slowly at 0 ^{0}C. The reaction mixture was stirred for 15 min at 0 ^{0}C. The reaction mixture was stirred for 2.5 hours at room temperature and then the reaction mixture was diluted with diethyl ether (10 mL). The organic phase was washed with saturated $NaHCO_3$ (2x10 mL) and brine (10 mL). The organic layer was dried with sodium sulfate, filtered and the solvent was removed on the rotary evaporator. The residue was purified by column chromatography (45% ethyl acetate: 55% hexanes) to afford macrocycle **3** as a white solid (17 mg, 13% yield). ^{1}H NMR ($CDCl_3$, 300 MHz): δ = 8.14 (s, 2 H), 8.02 (d, 2 H, J = 7.8 Hz), 7.72 (d, 2 H, J = 8.1 Hz), 7.55-7.30 (m, 10 H), 6.88 (s, 2 H), 5.54 (s, 4 H), 4.61 (s, 4 H), 4.56 (s, 4 H), 3.62 (s, 6 H). ^{13}C NMR ($CDCl_3$, 75 MHz): δ = 165.7, 151.1, 141.8, 140.3, 139.3, 132.2, 129.8, 128.9, 128.8, 128.7, 128.4, 127.2, 126.8, 126.3, 111.9, 72.0, 66.8, 55.9, 54.1. ^{19}FNMR ($CDCl_3$, 300 MHz): δ = -141.85. HRMS (ESI): Calcd for $[M+NH_4]^+$, $C_{46}H_{40}F_4O_8N$ 810.2685, found 810.2678.

Synthesis of Macrocycle 4: Overall Scheme 4:

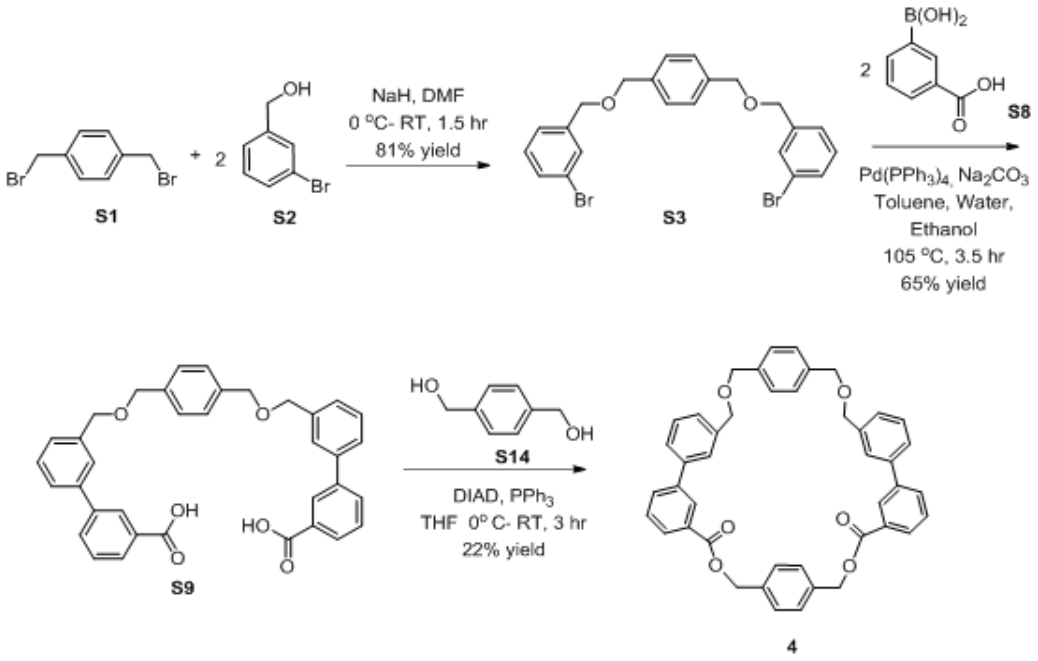

Reaction 11: Synthesis of Macrocycle 4:

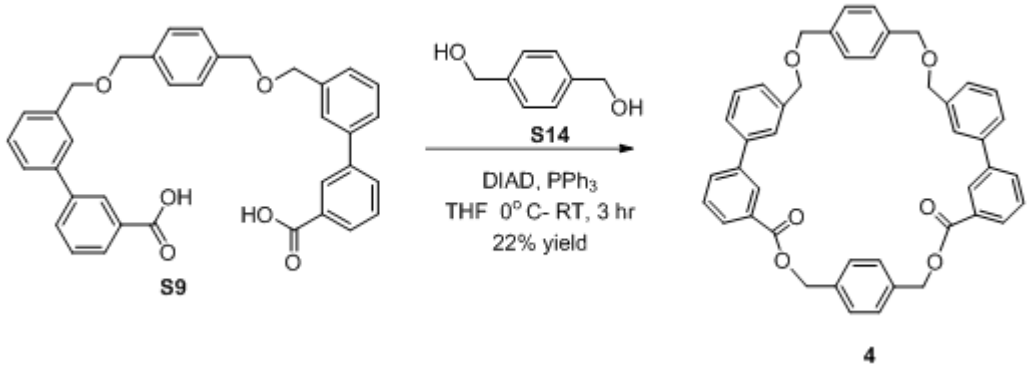

To compound **S9** (140.0 mg, 0.251 mmol, 1.0 eq.), compound **S14**, (58.0 mg, 0.276 mmol, 1.1 eq.) and triphenylphosphine (134.0 mg, 0.512 mmol, 2.04 eq.) in anhydrous THF (25 mL) was added a solution of diisopropylazodicarboxylate (0.096 mL, 0.49 mmol, 2.1 eq.) in anhydrous THF (5.0 mL) slowly at 0 ^{0}C. The reaction mixture was stirred for 15 min at 0 ^{0}C. The reaction mixture was allowed to warm to room temperature, and was stirred for 3 hours at

room temperature. The reaction mixture was diluted with diethyl ether (10 mL), and washed with saturated $NaHCO_3$ (2 x 10 mL portions) and brine (10 mL). The organic layer was dried with sodium sulfate, filtered and evaporated. The residue was purified by column chromatography to afford macrocycle **4** as off-white solid (35 mg, 22% yield). ^{1}H NMR ($CDCl_3$, 300 MHz): δ = 8.29 (t, 1 H), 8.18 (t, 1 H), 8.05 (m, 2 H), 7.78 (d, 2 H, J = 7.8 Hz), 7.70 (m, 4 H), 7.62 (m, 2 H), 7.51 (m, 8 H), 7.39 (s, 2 H), 7.31 (s, 2 H), 5.41 (s, 2 H), 4.62 (d, 4 H, J = 7.5 Hz), 4.57 (s, 4H), 3.95 (s, 2H).

Synthesis of BODIPY 7:

The synthesis of BODIPY 7 was performed according to literature procedures:

Shepherd, J. L.; Kell, A.; Chung, E.; Sinclar, C. W.; Workentin, M. S.; Bizzotto, D. *J. Am. Chem. Soc.* **2004**, *126*, 8329-8335.

Reaction 1:

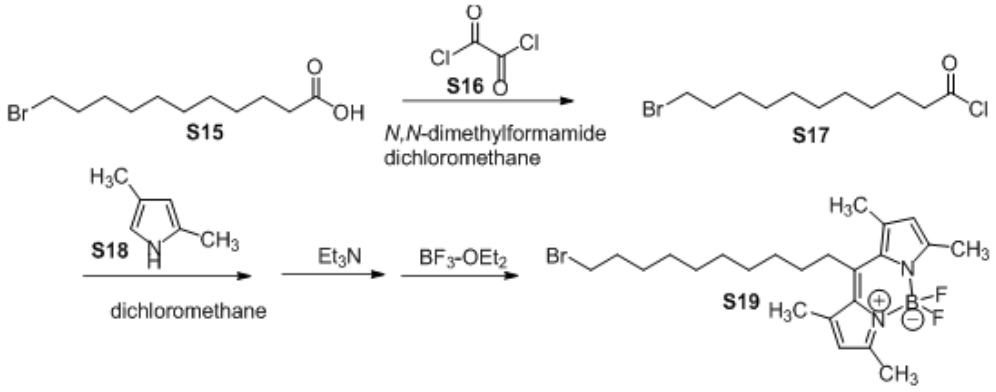

Procedure: 2.0 grams of 11-bromoundecanoic acid **S15** (7.54 mmol, 1.0 eq.) was combined with 2 drops of *N*,*N*-dimethylformamide in 40 mL of dichloromethane. 1.0 gram of oxalyl chloride **S16** (7.88 mmol, 1.05 eq.) was dissolved in 5.0 mL of dichloromethane and added dropwise. The reaction mixture was stirred for one hour, then the crude mixture was concentrated on the rotary evaporator and dried on a vacuum overnight to remove any unreacted oxalyl chloride. The resulting acid chloride **S17** was dissolved in 50 mL of

dichloromethane. 0.772 mL of 2,4-dimethylpyrrole **S18** (7.50 mmol, 0.99 eq.) was dissolved in 5.0 mL of dichloromethane and added to the reaction mixture. The resulting reaction mixture was heated to reflux for 3 hours under a nitrogen atmosphere, during which time the mixture became a dark red color. After three hours, the reaction mixture was cooled to room temperature and solvent was removed on the rotary evaporator until approximately 5.0 mL of the dichloromethane solution remained. 200 mL of *n*-hexanes were added to the flask, and the mixture was cooled overnight in the freezer at -20 ^{o}C. The hexanes were decanted from the insoluble oil and precipitate. The resulting crude product was dissolved in 75 mL of toluene and heated to 80 ^{o}C. 1.0 mL of triethylamine (7.17 mmol, 0.95 eq.) was added and the solution immediately turned light yellow. 1.0 mL of boron trifluoride etherate (8.10 mmol, 1.07 eq.) was then added and the reaction mixture was stirred at 80 ^{o}C for 30 minutes, during which time the color of the mixture darkened and became fluorescent. The reaction mixture was cooled to room temperature, and the product was extracted 3 times with brine (50 mL each time). The organic layer was dried over sodium sulfate, filtered, and concentrated. The crude product was purified by flash chromatography (1:1 dichloromethane: hexanes) to yield the desired product **S19** in 28% yield (comparable to the literature-reported 24% yield).

Reaction 2:

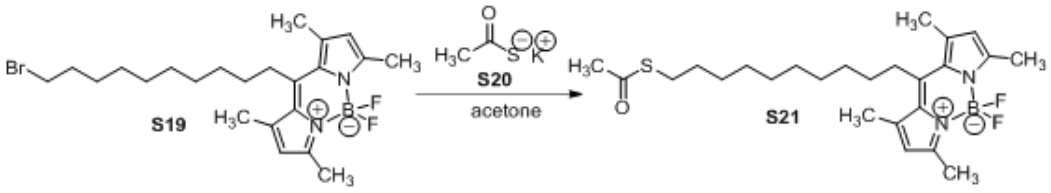

Procedure: Compound **S19** (0.968 g, 2.07 mmol, 1.0 eq.) and compound **S20** (0.27 grams, 2.36 mmol, 1.14 eq.) were dissolved in 50 mL of acetone. The reaction mixture was heated to reflux for two hours. After two hours, the reaction mixture was cooled to room temperature,

acetone was removed, and the crude solid was re-dissolved in dichloromethane and washed with water. The organic extract was dried over sodium sulfate, filtered and concentrated, to yield compound **S21** in 97% yield (0.932 grams).

Reaction 3:

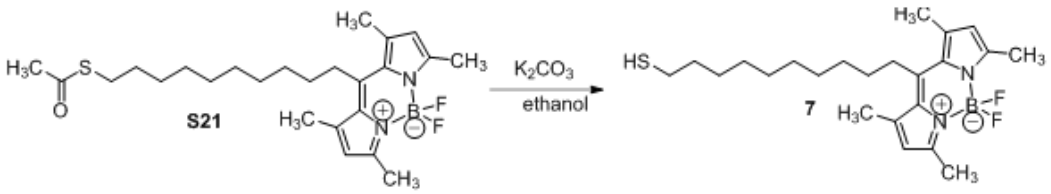

Procedure: Compound **S21** (0.932 grams, 2.01 mmol, 1.0 eq.) was dissolved in 150 mL of anhydrous ethanol that was purged with nitrogen. Potassium carbonate was added, and the reaction mixture was warmed to 30 ^{o}C. The reaction mixture was stirred under nitrogen for 4 hours at 30 ^{o}C. The contents of the flask were poured over 40 mL of aqueous saturated ammonium chloride, at which point the solution turned bright orange. The product was extracted with dichloromethane and washed several times with water. The organic layer was dried over sodium sulfate, filtered, and concentrated. The product was purified via flash chromatography (1:1 dichloromethane: hexanes) to yield compound **7** in 76% yield (674 mg).

Synthesis of control BODIPY (compound S22):

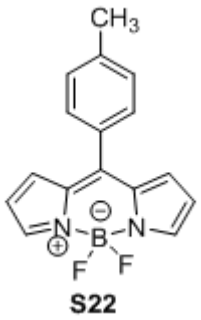

The synthesis of BODIPY **S22** was performed according to literature procedures: Cui, A.; Peng, X.; Fan, J.; Chen, X.; Wu, Y.; Guo. B. *J. Photochem. Photobiol. A. Chem*. **2007**, *186*, 85-92.

Fluorescence Experimental Details:

All fluorescence spectra were recorded on a Shimadzu RF 5301 spectrophotometer. Binding experiments were conducted as follows:

The following stock solutions were made:

3 mg/mL of each macrocycle in THF

1 mg/mL of each PAH analyte in THF

Dilutions of the macrocycle stock solution were made to obtain solutions of 0.1, 0.2, 0.3, 0.4, 0.5, 0.6, 0.7, 0.8, 0.9, 1.0, 2.0 and 3.0 mg/mL solutions of the macrocycle.

20 µL of the PAH stock solution was added to 2.5 mL of phosphate buffered saline (PBS) at pH 7.4. 200 µL of each macrocycle solution was added, and the fluorescence of the solution was recorded with 360 nm excitation (scanned emission 370-710 nm). The fluorescence of the analyte was integrated with respect to wavenumber. The resulting data was plotted using a Benesi-Hildebrand plot, with 1/[macrocycle] (in M) on the X-axis and 1/integrated analyte emission on the Y-axis. Linear fits were obtained using macrocycle **2** as a host and anthracene and benzo[*a*]pyrene as guests (1:1 complex for anthracene and 1:2 complex for benzo[*a*]pyrene). The binding constant was calculated by dividing the y-intercept of the linear fit by the slope of the line.

Energy transfer experiments were conducted as follows:

A 1 mg/mL stock solution of BODIPY**7** in THF was made. 200 µL of the macrocycle host, 20 µL of the PAH analyte, and 20 µL of the BODIPY fluorophore were added to 2.5 mL of PBS. The solution was excited at 360 nm and 460 nm. The fluorescence emission of anthracene and of BODIPY were integrated with respect to wave number, and the efficiency of energy transfer was determined by measuring both the fractional quenching of anthracene emission in the presence of BODIPY, and the percentage of BODIPY emission from analyte excitation compared to direct excitation.

^{1}H NMR titration experiments:

All NMR titrations were carried out by adding aliquots of guest molecules in $CDCl_3$ in an NMR tube containing the host macrocycle. After each addition, spectra were recorded by using Bruker 300 MHz Instrument.

For the titration of macrocycle **2** with anthracene **5**: A $CDCl_3$ solution of macrocycle **2** (3.59 mg, 4.9 x 10^{-3}mmol, 0.5 mL) was titrated by adding an incremental amount (5 µL, 4.9 x 10^{-4} mmol, 0.1 equivalent) of anthracene from a stock solution (0.098 M in $CDCl_3$).

For the titration of macrocycle **2** with benzo[*a*]pyrene as a guest: A $CDCl_3$ solution of macrocycle **2** (3.59 mg, 4.9 x 10^{-3}mmol, 0.5 mL) was titrated by adding an incremental amount (5 µL, 4.9 x 10^{-4}mmol, 0.1 equivalent) of benzo[*a*]pyrene from a stock solution (0.098 M in $CDCl_3$).

Benzo[*a*]pyrene showed clear evidence of binding in macrocycle **2** (see paper for details). Anthracene showed no shift in the ^{1}H NMR peaks, as shown below:

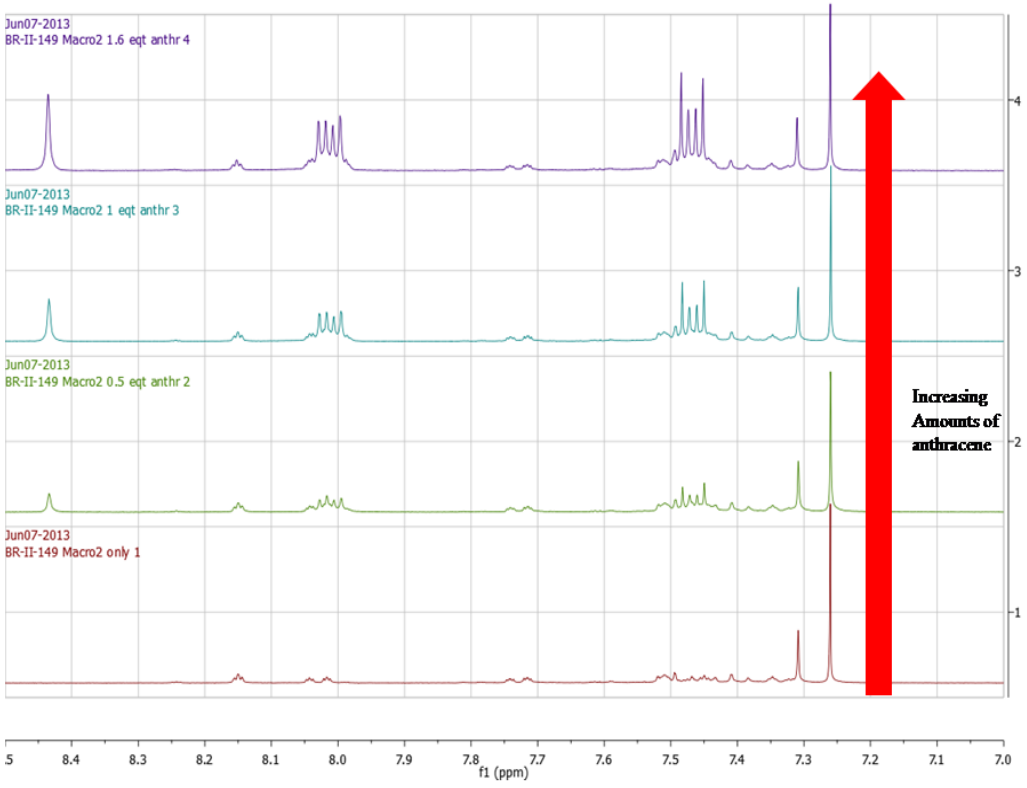

Spectral Copies:

^{1}H NMR of Compound S3:

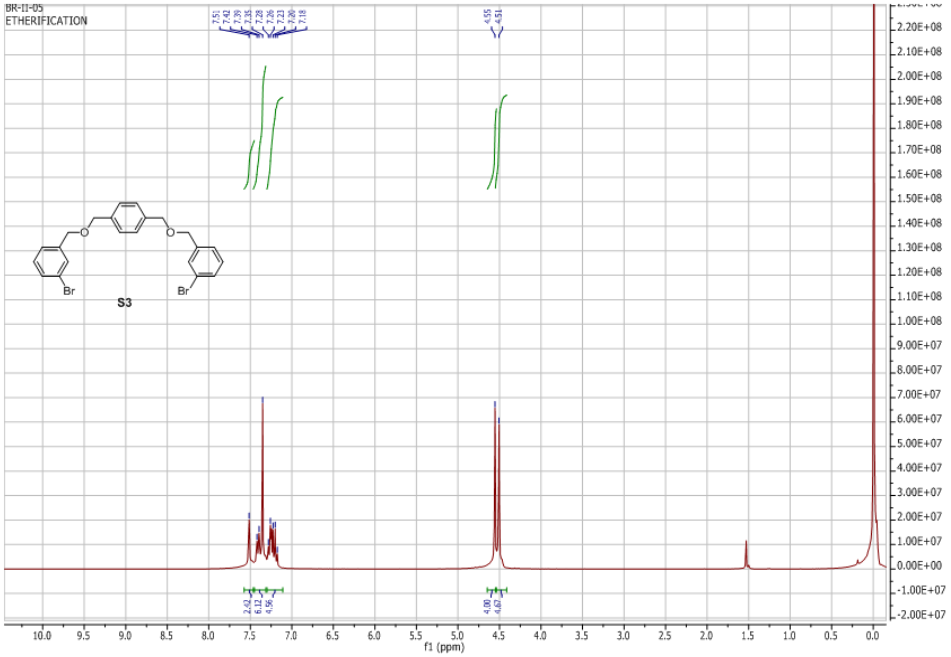

^{13}C NMR of Compound S3:

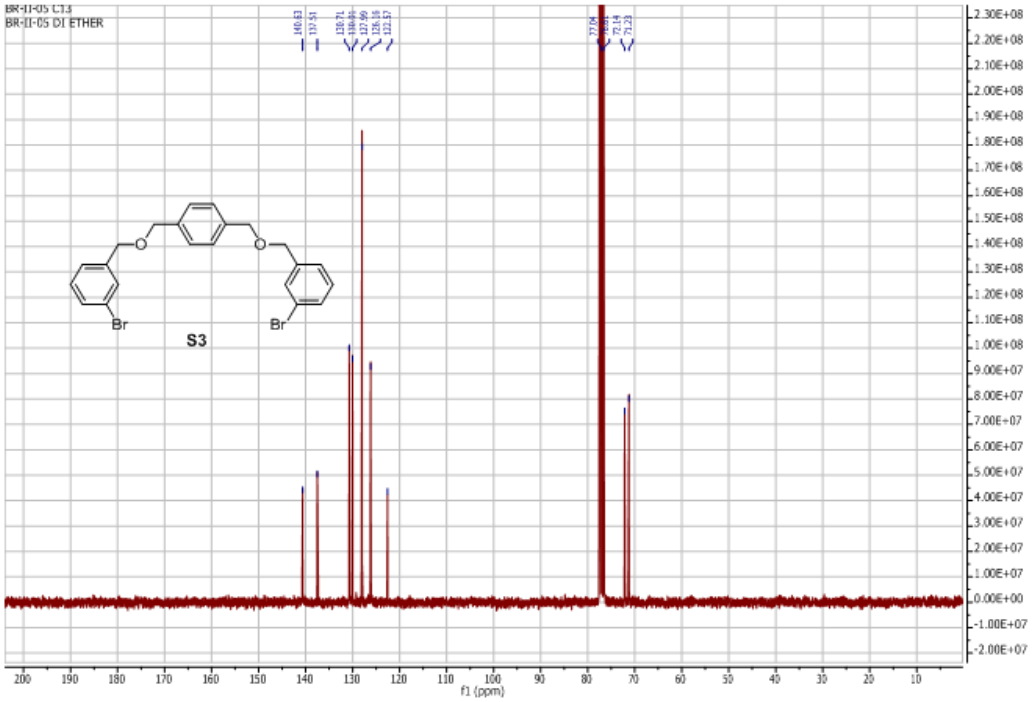

^{1}H NMR of Compound S5:

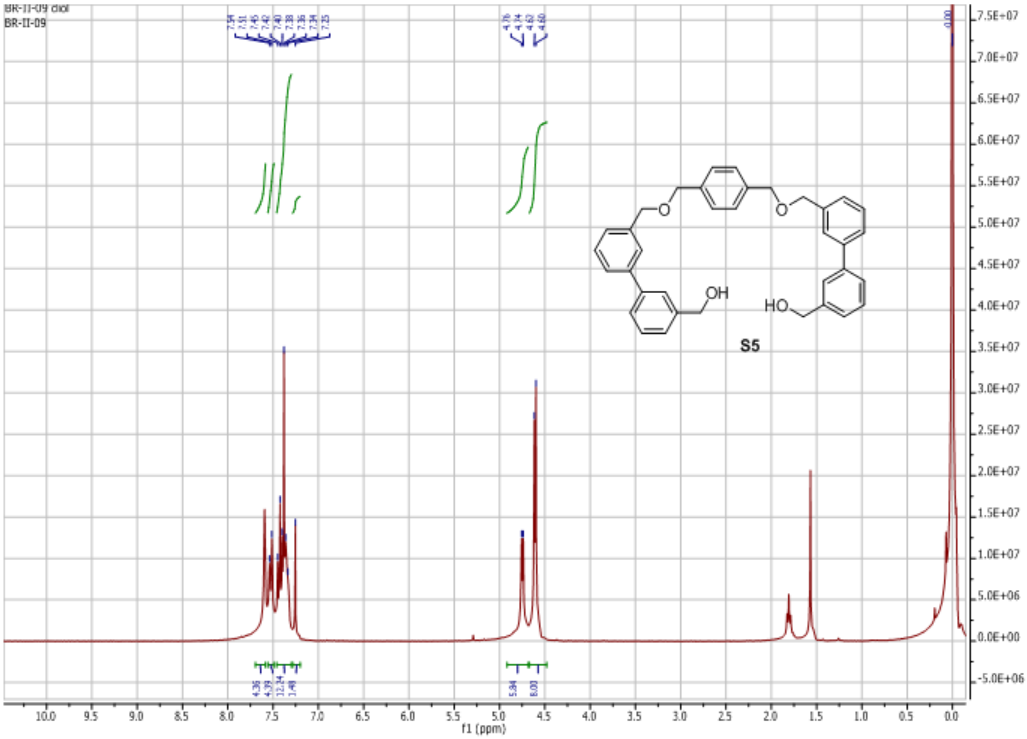

^{13}C NMR of Compound S5:

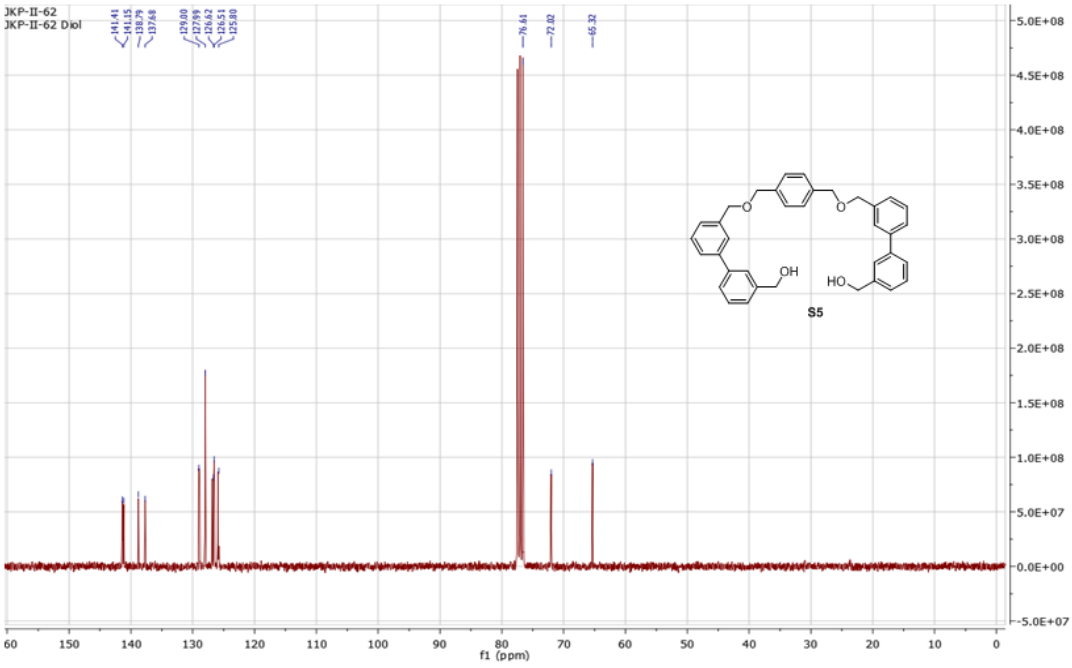

^{1}H NMR of Compound S7:

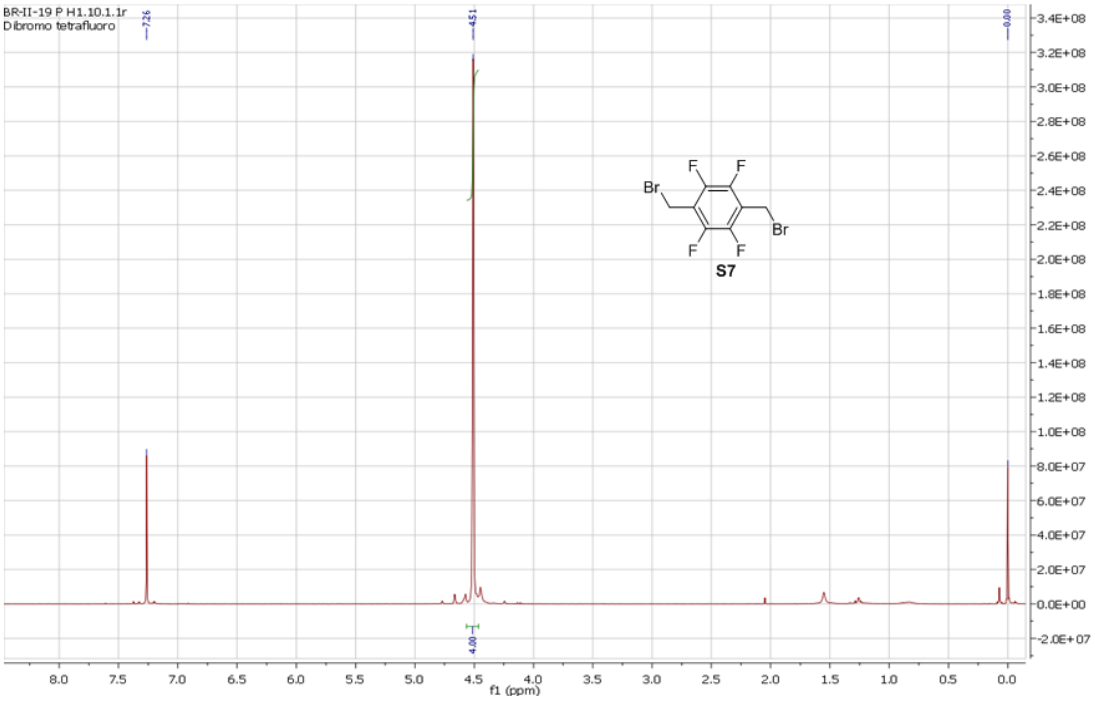

^{13}C NMR of Compound S7:

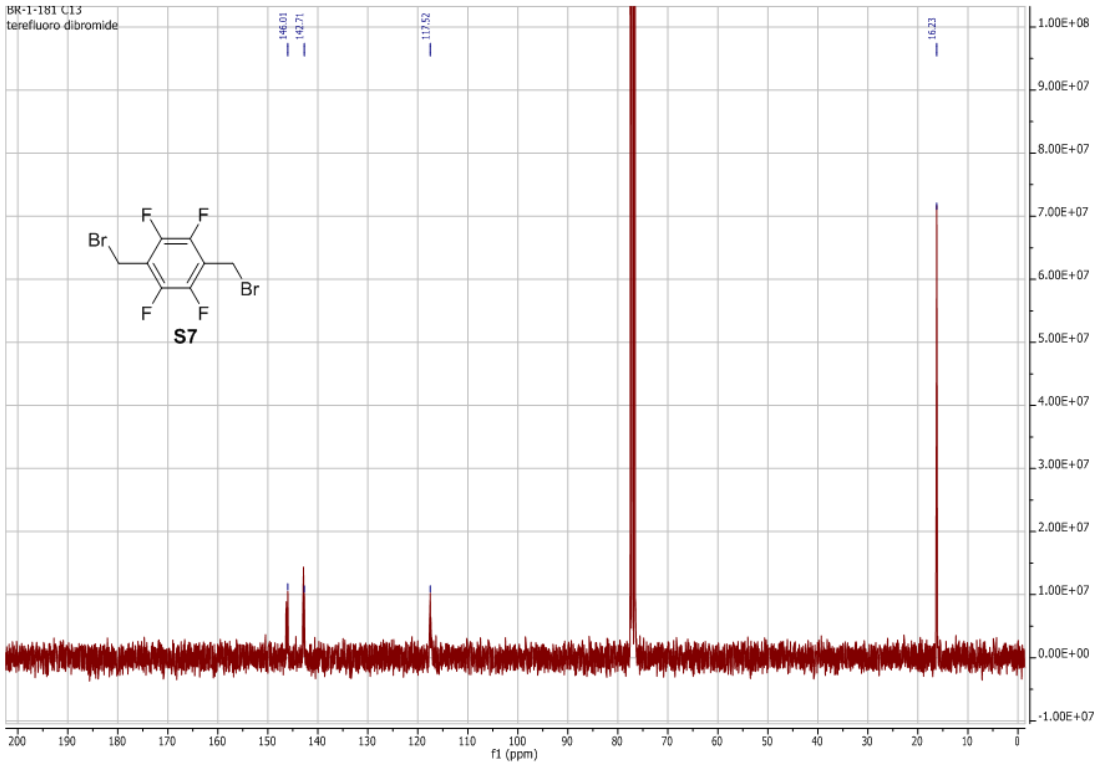

^{19}F NMR of Compound S7:

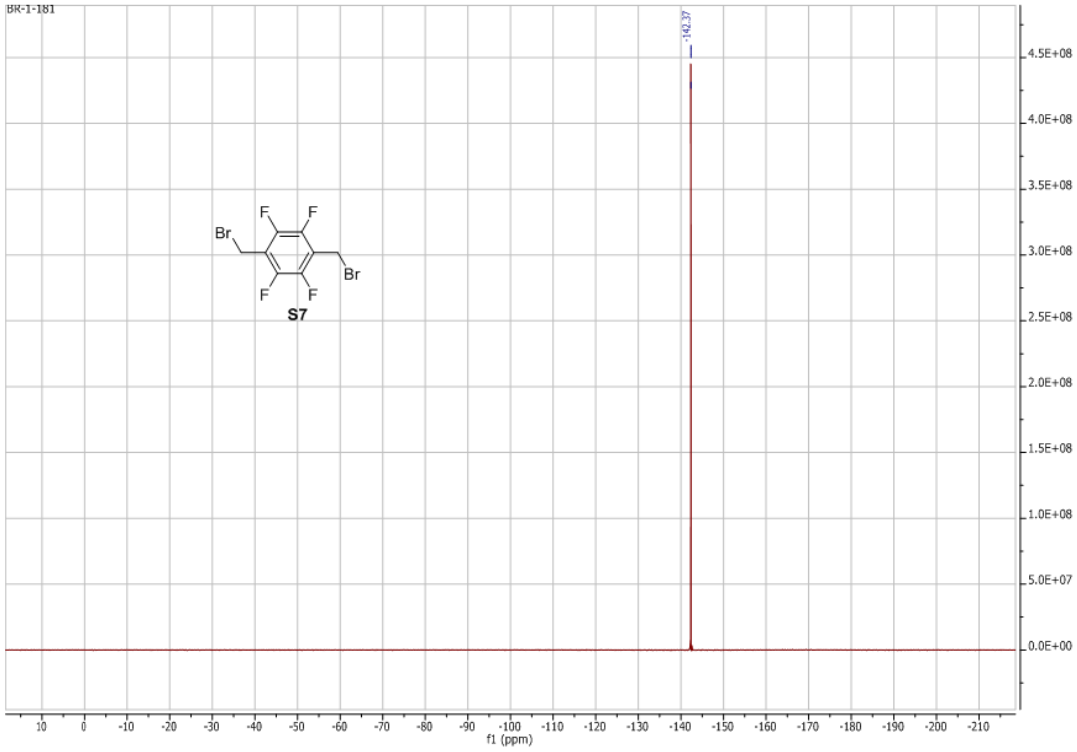

^{1}H NMR of Macrocycle 1:

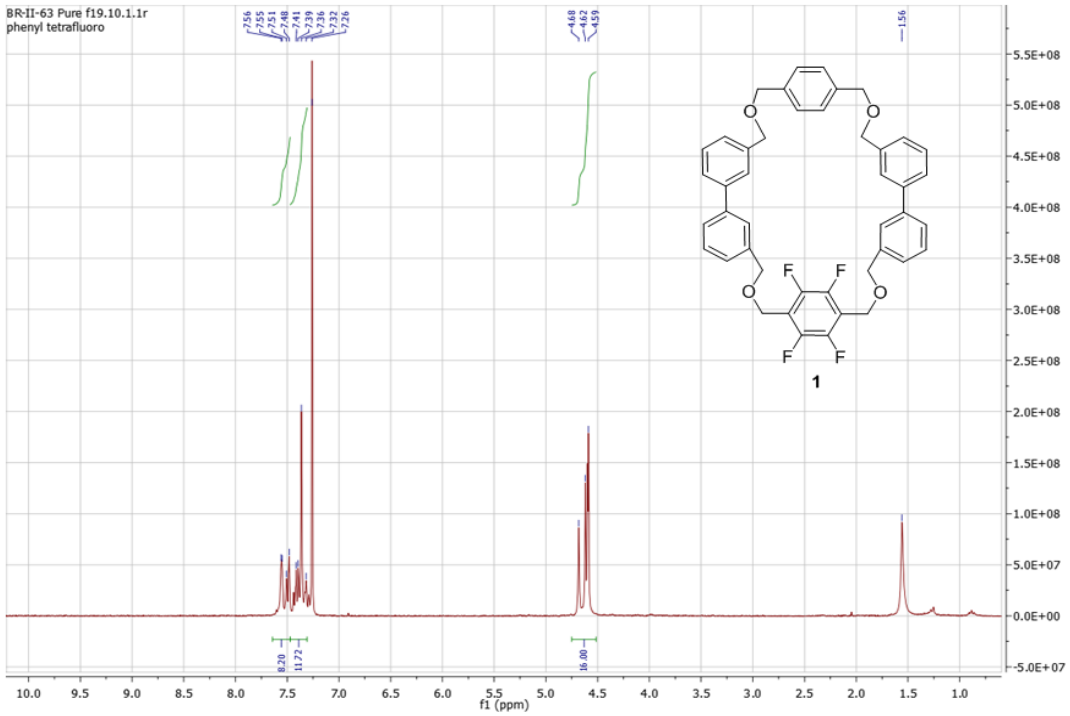

^{13}C NMR of Macrocycle 1:

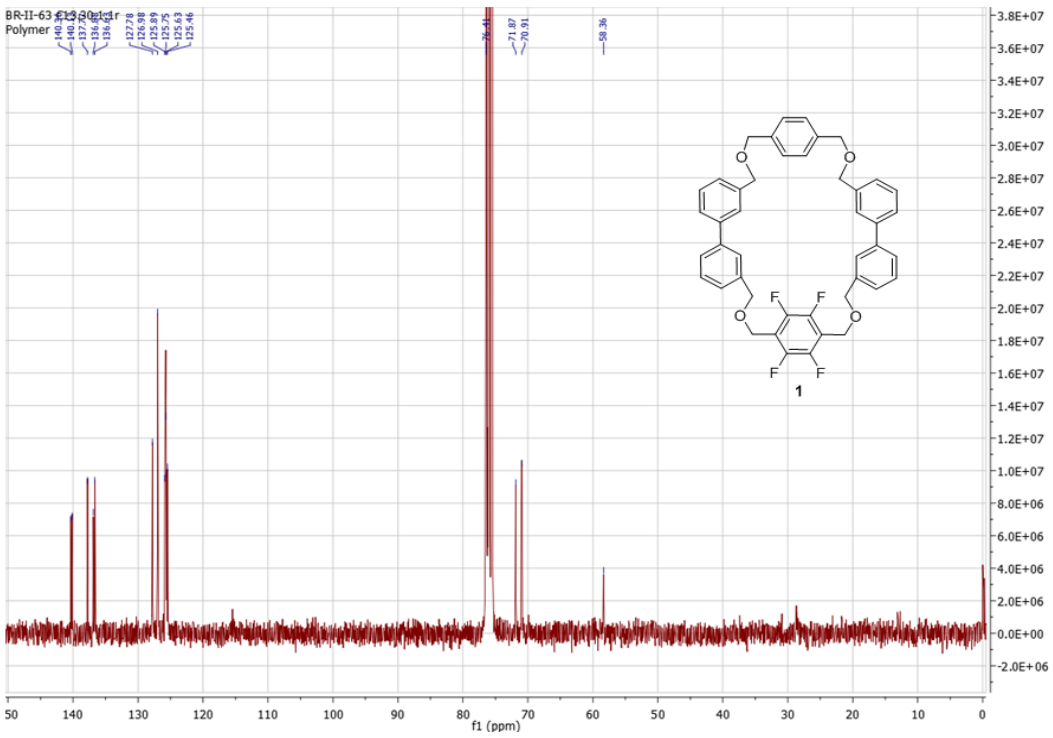

^{19}F NMR of Macrocycle 1:

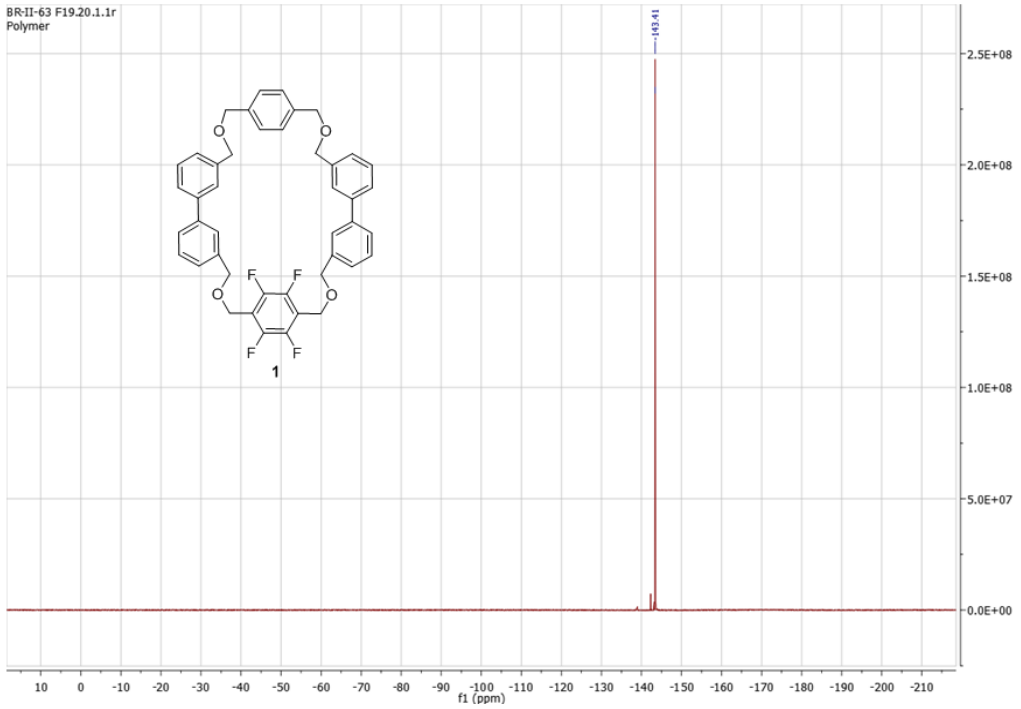

^{1}H NMR of Compound S9:

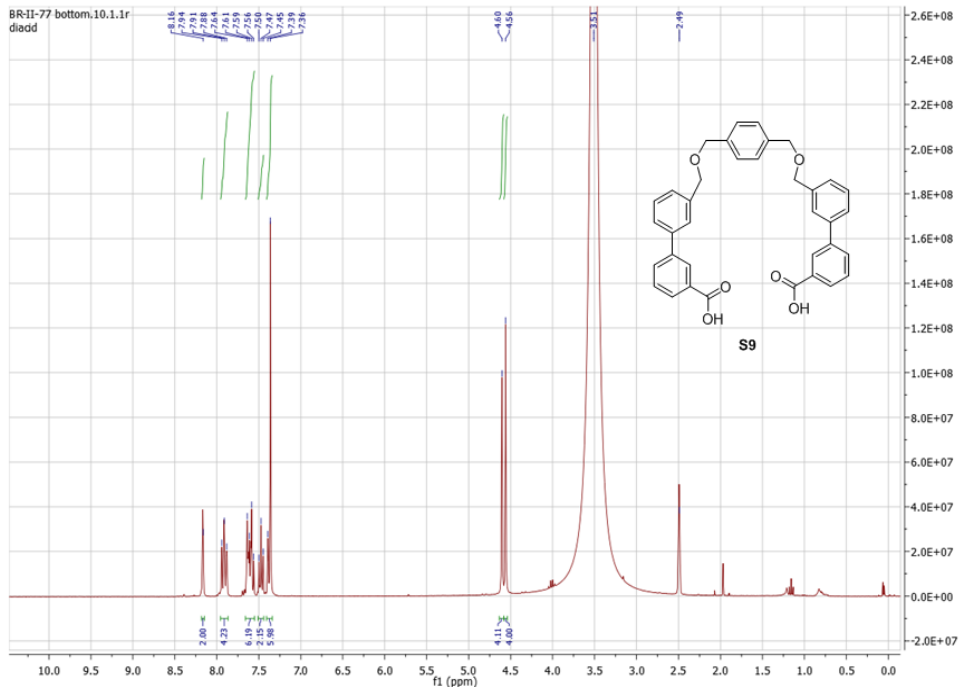

^{13}C NMR of Compound S9:

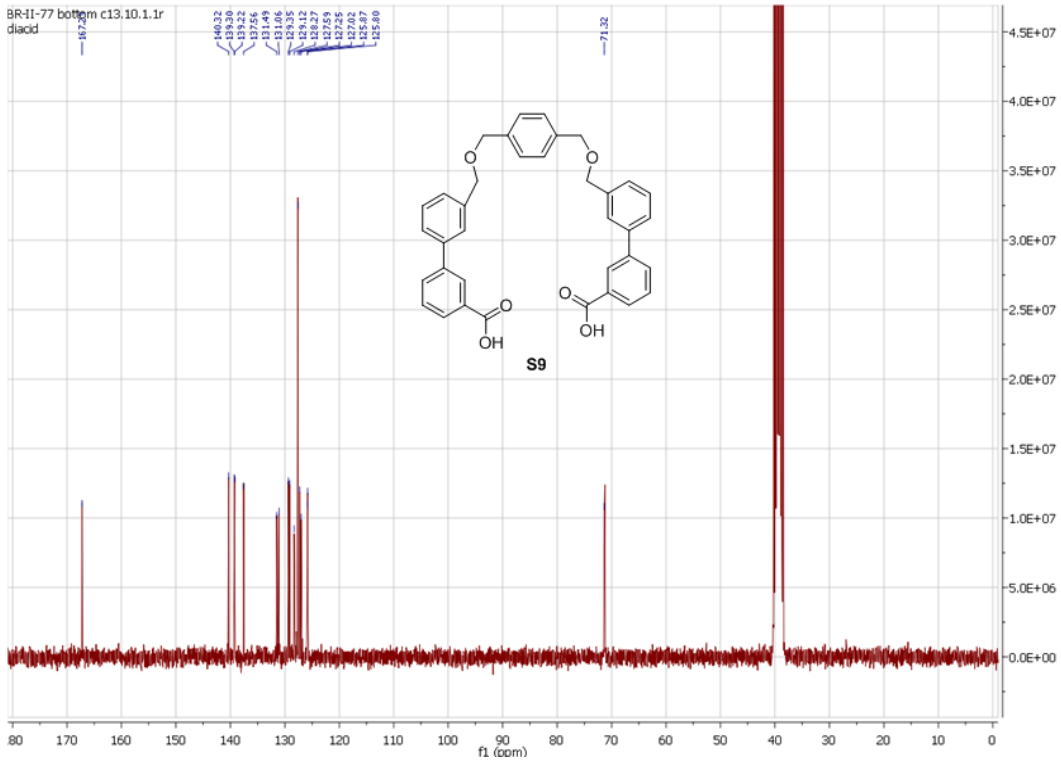

^{1}H NMR of Macrocycle 2:

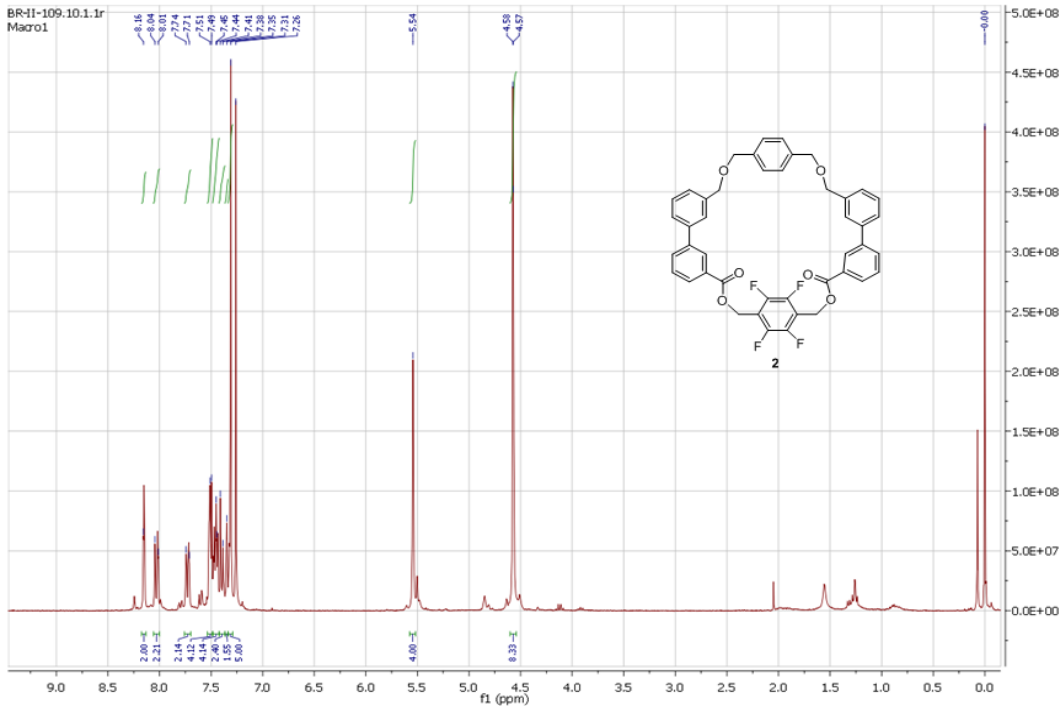

^{13}C NMR of Macrocycle 2:

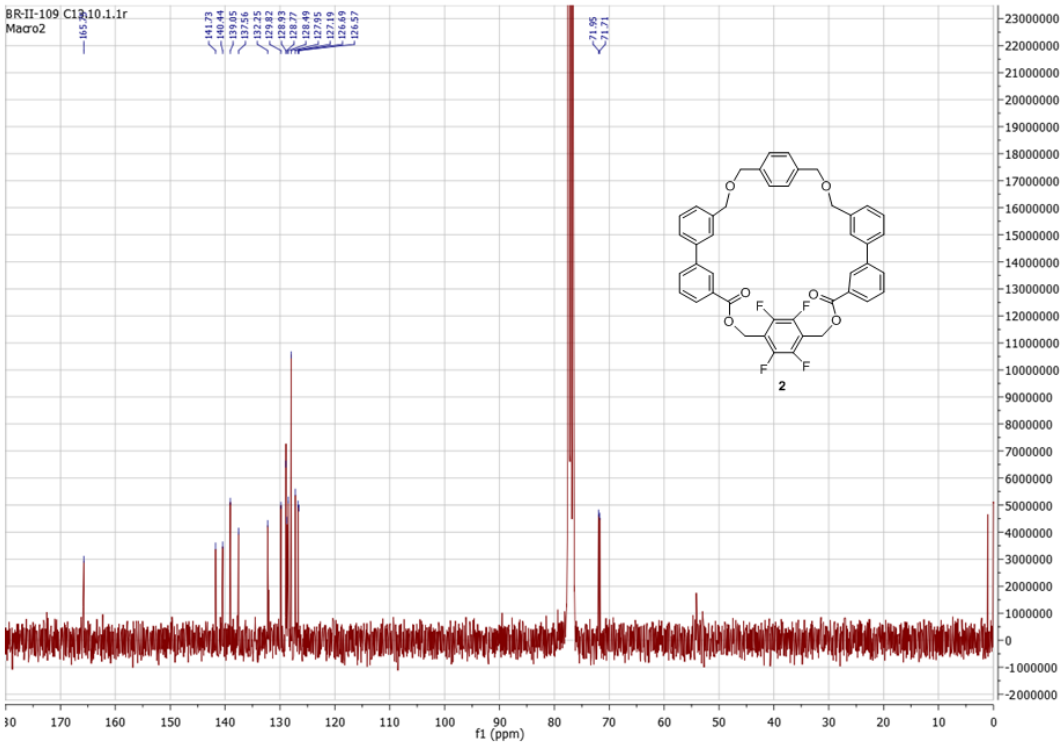

^{19}F NMR of Macrocycle 2:

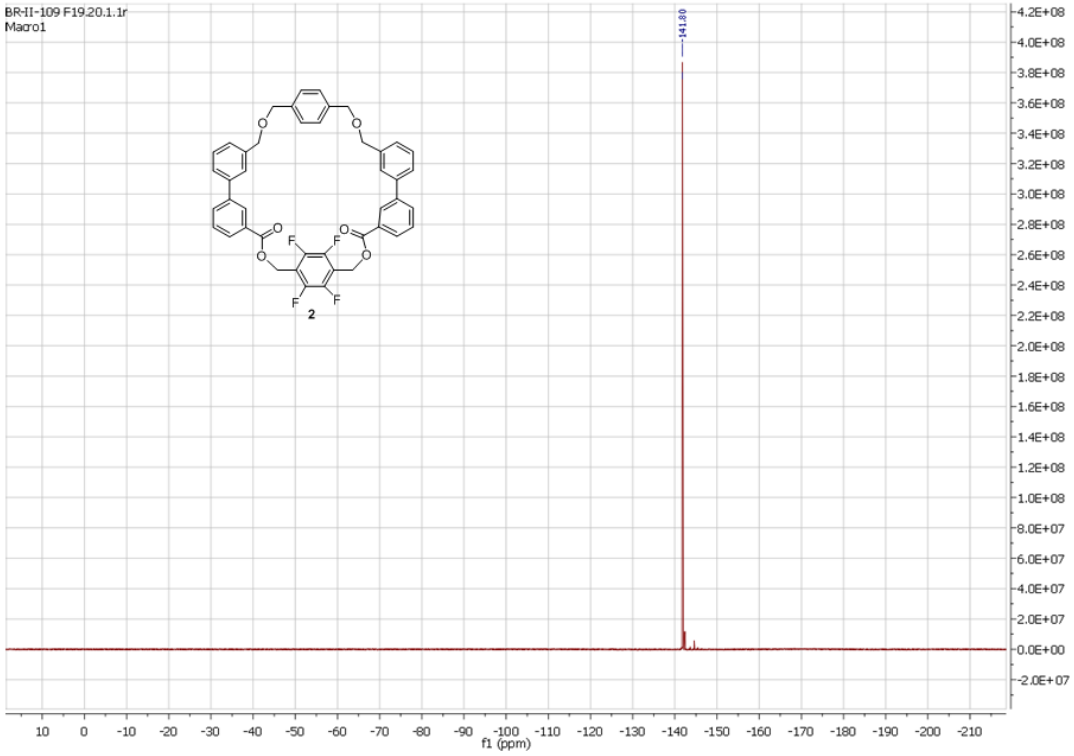

^{1}H NMR of Compound S12:

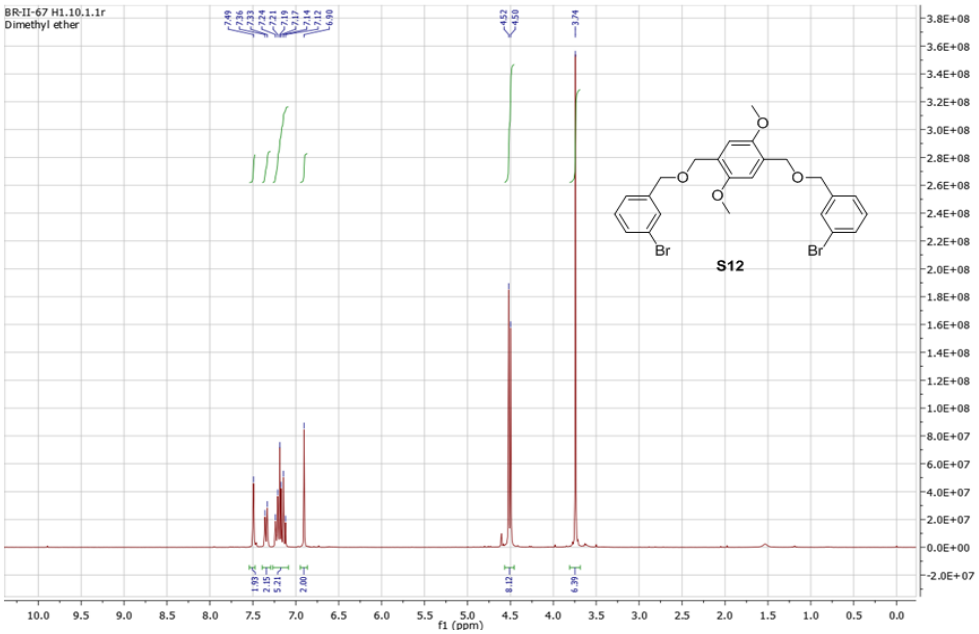

^{13}C NMR of Compound S12:

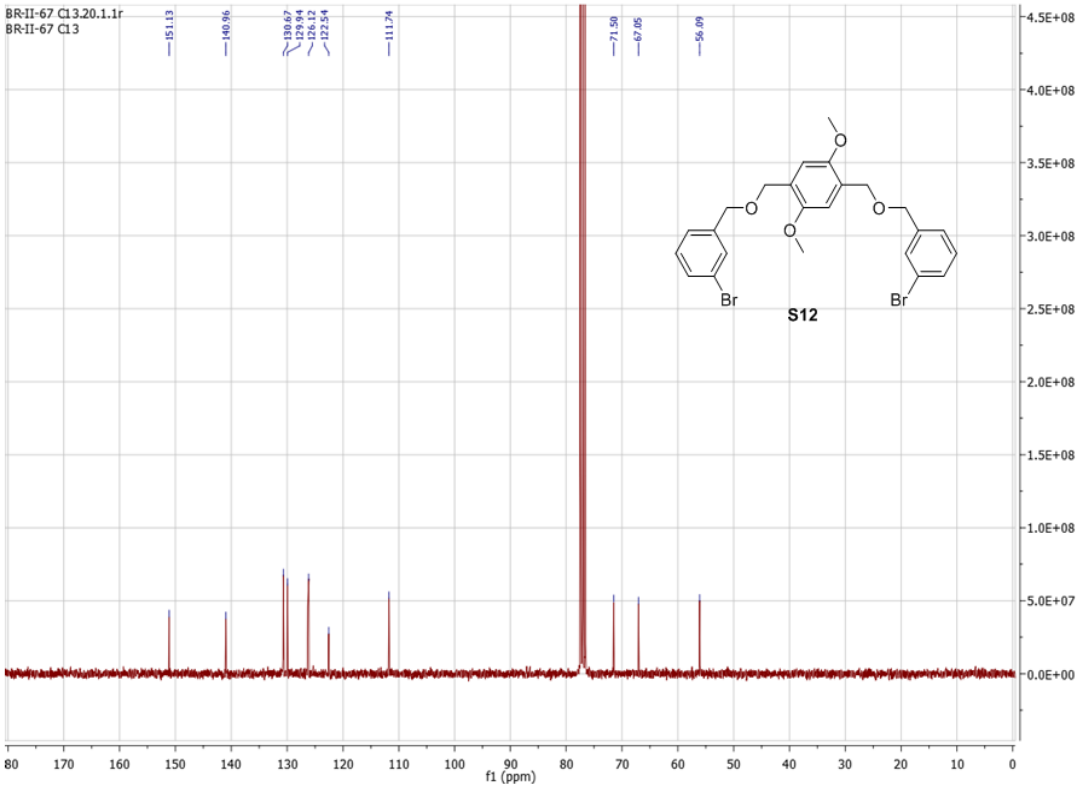

^{1}H NMR of Compound S13:

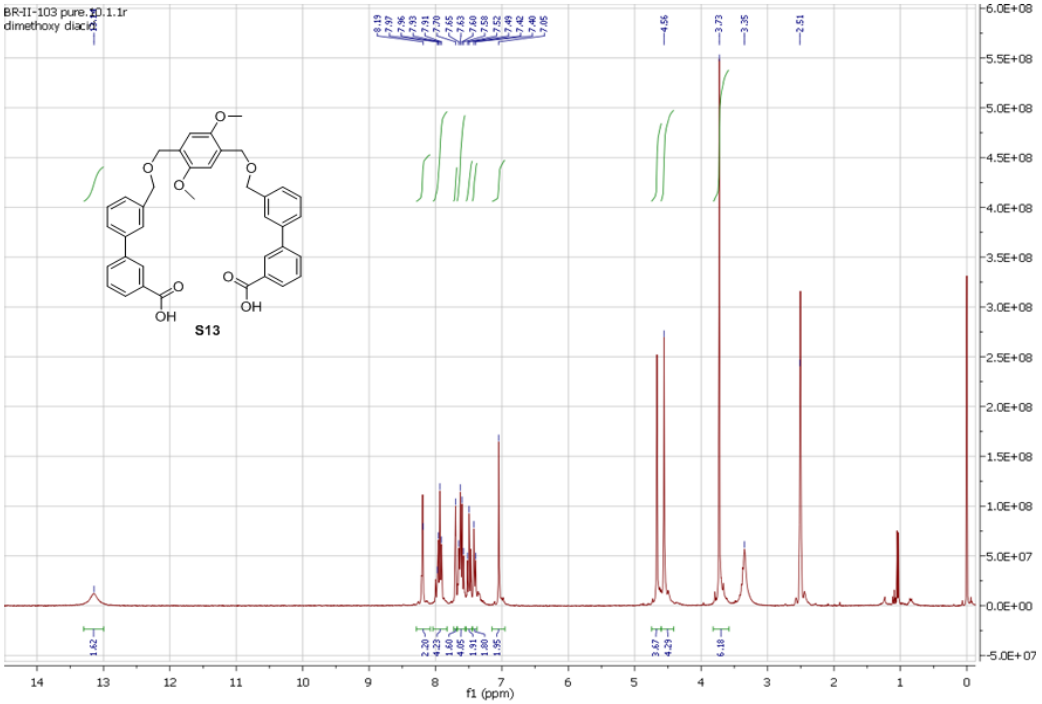

^{13}C NMR of Compound S13:

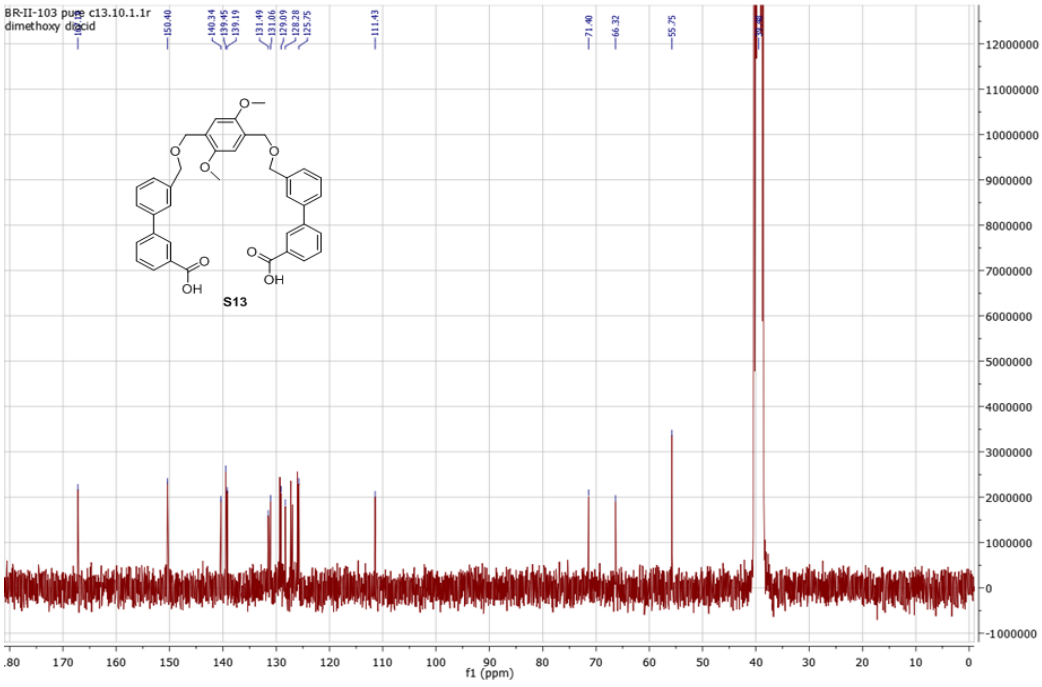

^{1}H NMR of Macrocycle 3:

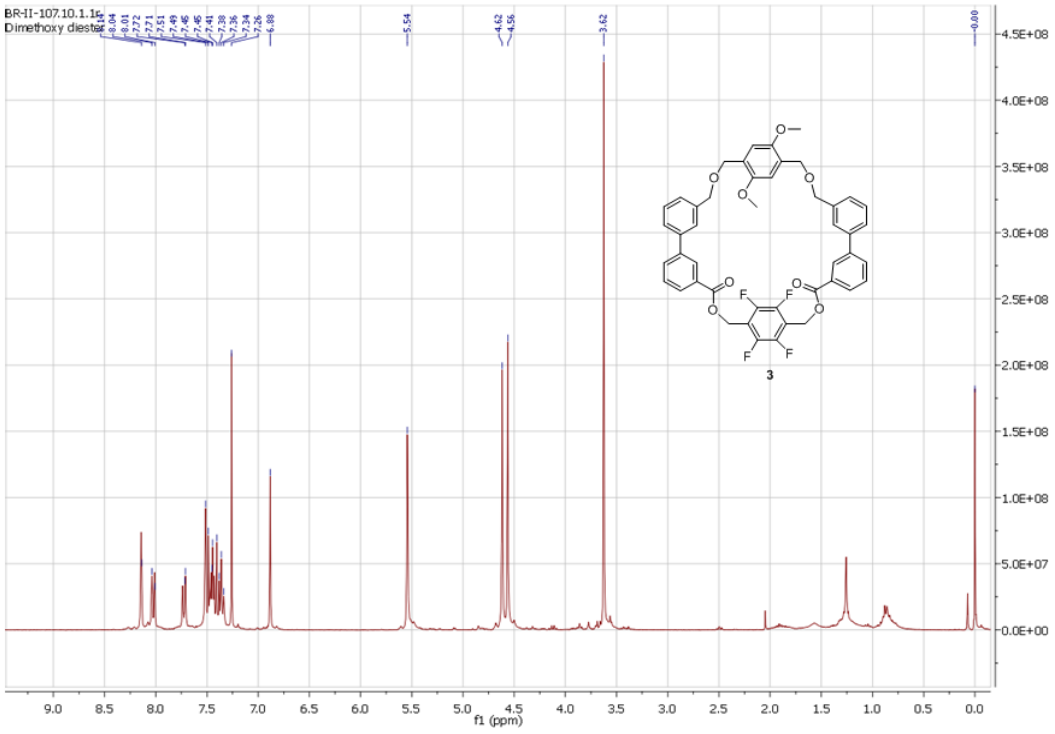

^{13}C NMR of Macrocycle 3:

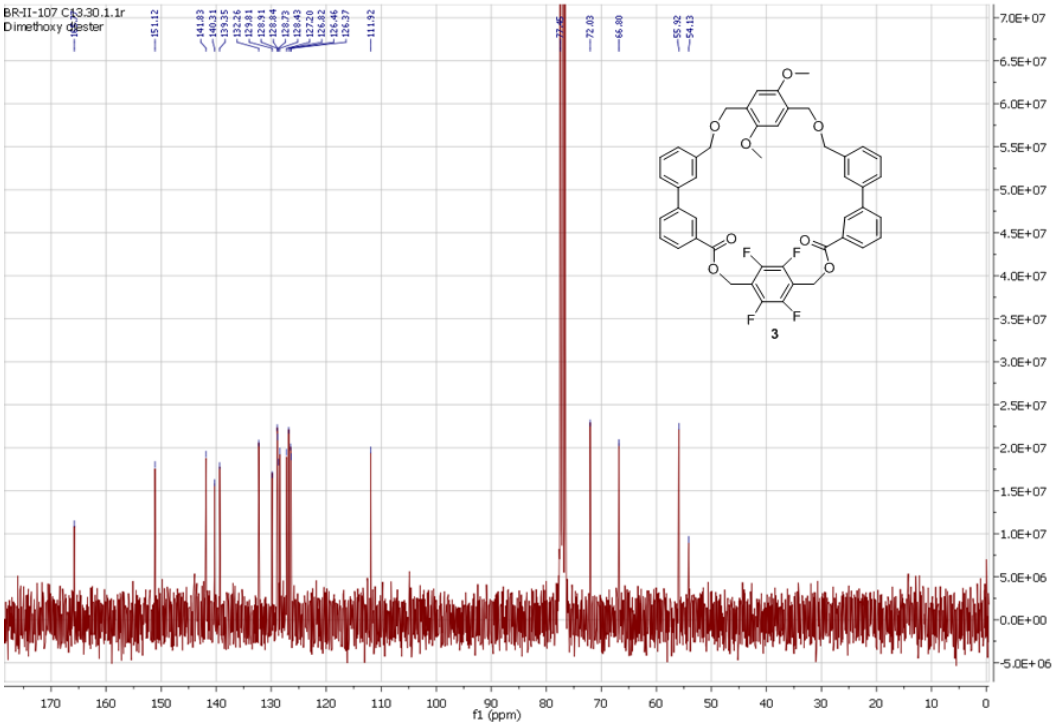

^{19}F NMR of Macrocycle 3:

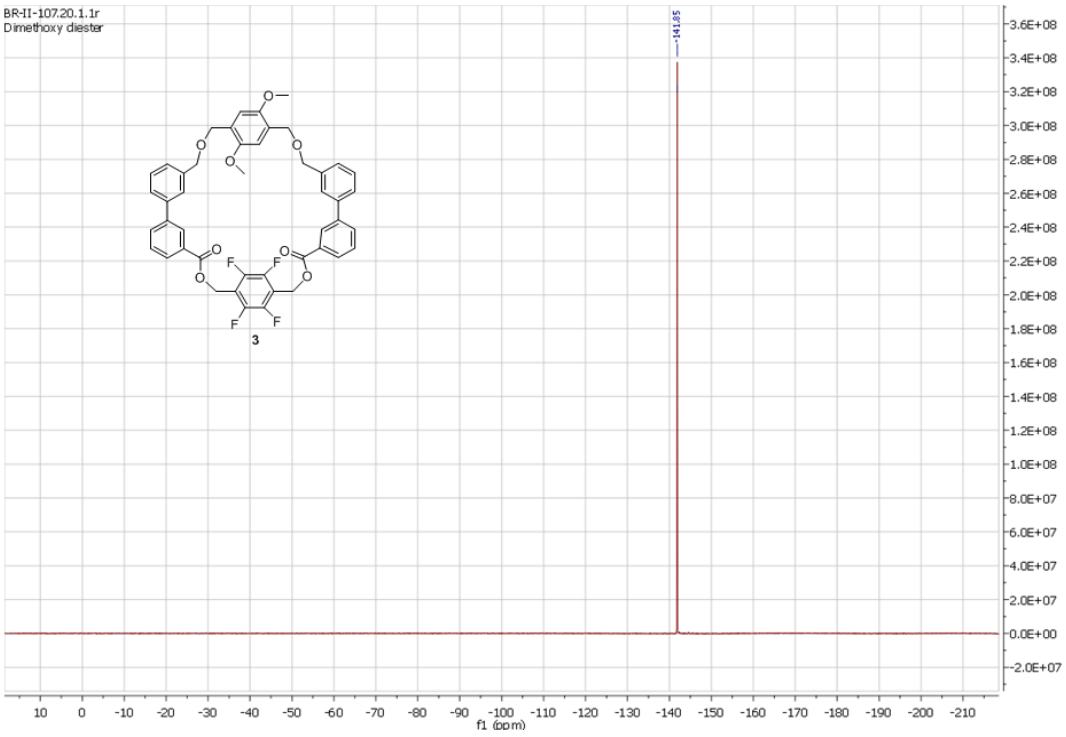

^{1}H NMR of Macrocycle 4:

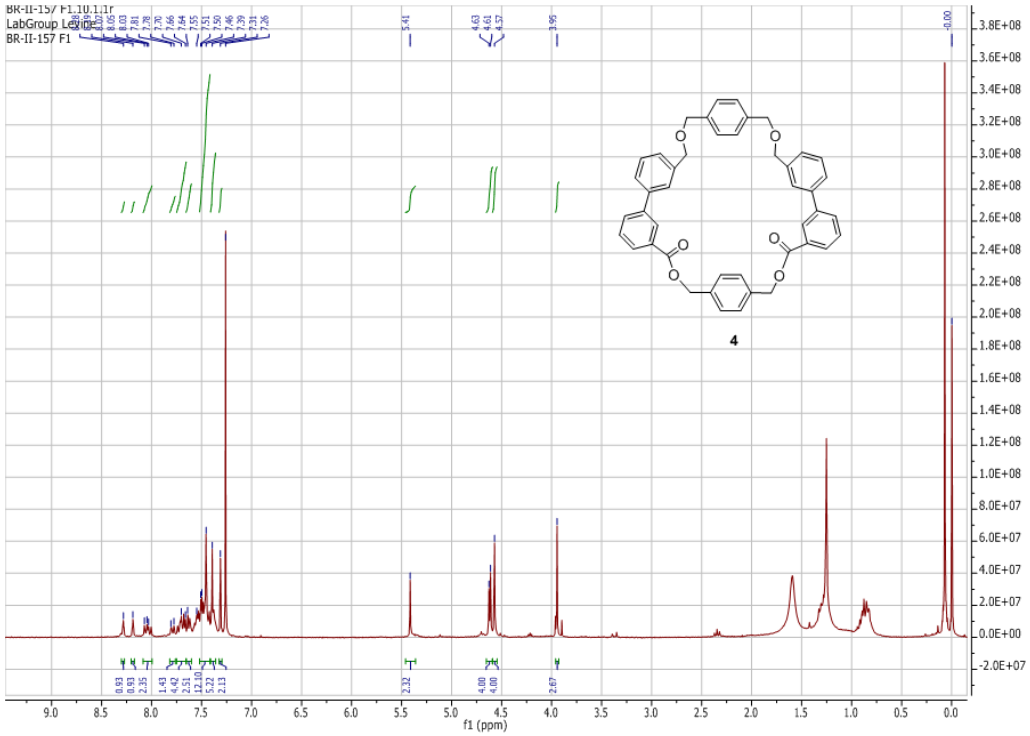

MANUSCRIPT 2

Manuscript is in preparation to *Organic and Biomolecular Chemistry*

A Series of Dissymmetric Macrocycle Hosts for the Facilitated Detection of Carcinogenic Benzo[*a*]pyrene

*Bhasker Radaram, Lindsey Prignano, Mindy Levine**

Corresponding author:

Prof. Mindy Levine

Department of Chemistry

University of Rhode Island

Kingston, Rhode Island 02881

mlevine@chm.uri.edu

MANUSCRIPT 2

A Series of Dissymmetric Macrocycle Hosts for the Facilitated Detection of Carcinogenic Benzo[*a*]pyrene

Abstract: A series of electronically dissymmetric organic macrocycles were synthesized and evaluated for the facilitated efficient detection of highly toxic and carcinogenic benzo[*a*]pyrene *via* non-covalent energy transfer. This proximity-induced energy transfer was performed using a fluorescent BODIPY dye as an energy acceptor in combination with benzo[*a*]pyrene as the energy donor. Up to a 3-fold increase in the resulting fluorophore emission was observed in the presence of the macrocycle hosts.

Since 1987, synthetic macrocycles have gained much attention in supramolecular chemistry, especially for their use in the extraction and/or detection of specific guests.[1,2] The binding of a guest within the host leads to the formation of a host-guest complex. If the guest is embedded inside the cavity of the host, the phenomenon is termed "encapsulation." These host-guest complexes are governed by a variety of non-covalent interactions such as π-π stacking, electrostatic, Van der Waals forces, and hydrophobic interactions.[3-5]

Supramolecular hosts including cyclodextrins,[6-9] calix[n]arenes,[10] Exbox,[11] and metallomacrocycles,[12, 13] have been used in a variety of applications, including the extraction and detection of carcinogenic and highly toxic polycyclic aromatic hydrocarbons (PAHs). PAHs represent an important group of ubiquitous environmental pollutants.[14,15] They are formed as byproducts from the incomplete combustion of fuel or organic materials, and have been found in the environment following oil spills.[16] Among all the PAHs, benzo[*a*]pyrene **8** was found to be one of the most carcinogenic, mutagenic and teratogenic.[17, 18] Although there

are methods to detect benzo[*a*]pyrene that have been reported in the literature,[19] these methods are very tedious and requires multiple instruments to analyze. Hence, there is a need to develop an efficient detection method to this highly carcinogenic molecule. Recently, we have reported the use of dissymmetric organic macrocycles as well as multiple cyclodextrin derivatives as supramolecular hosts for the efficient detection of benzo[*a*]pyrene *via* non-covalent energy transfer.[7-9, 20,21, 22]

Herein we report a substantial extension of this work, to include the synthesis of a series of dissymmetric organic macrocycles (Figure 1, compounds **1-6**), including those with heteroaromatic moieties embedded in the macrocycle framework, and the use of these macrocycles for the binding and detection of benzo[*a*]pyrene. This detection occurs via non-covalent energy transfer between the benzo[*a*]pyrene donor **8** and fluorescent BODIPY acceptor (compound **7**). Computational studies were carried out to measure the dimensions of each cavity, to gain insight into how the guest molecules fit inside the cavity of these newly synthesized electronically-dissymmetric macrocycles.

Dissymmetric organic macrocycles **1-6** were designed to include electron-rich aromatic moiety (shown in red) and an electron-deficient aromatic moiety (shown in blue), connected via biphenyl linkers to make an electronically dissymmetric organic macrocycle (Figure 1).These types of macrocycles will allow PAH analytes to bind to the electron-deficient portion of the macrocycle, and the electron-deficient fluorophore to bind to the electron-rich portion of the macrocycle. The proximity of the PAH donor and fluorophore acceptor facilitates efficient energy transfer from the PAH to the fluorophore, resulting in selective fluorophore emission via PAH excitation. We have previously demonstrated that the electronic dissymmetry leads to noticeable benefits in the observed energy transfer efficiency.[20]

Macrocycles **1-6** (Figure 1) were synthesized following our previously developed synthetic route, using a double etherification reaction followed by a double Suzuki reaction to rapidly assemble a linear precursor. Mitsunobu reaction conditions or phase transfer etherification conditions were used to effect the desired macrocyclization[20] (see ESI for more details).

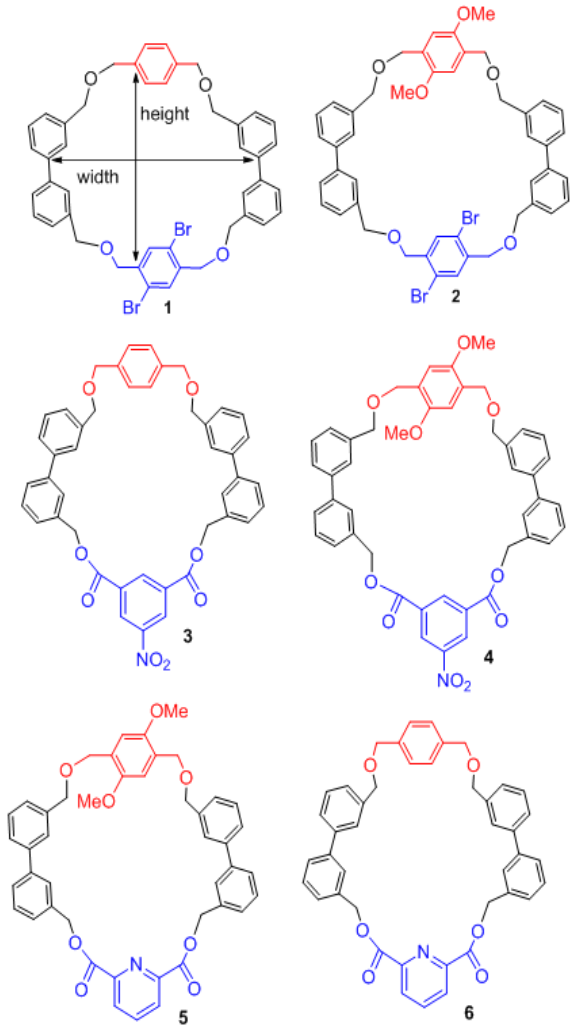

Fig. 1 Structures of dissymmetric macrocycles (electron rich segments highlighted in red, and electron deficient segments in blue. Height and width dimensions are shown on macrocycle **1**).

Computational studies using semi-empirical PM3 level calculations were performed to determine the dimensions of macrocycles **1-6**. The calculated dimensions are analogous to the

reported cavity dimensions of γ-cyclodextrin (Table 1),[23] which has been used previously for PAH isolation and detection.[7-9, 21, 22]

Table 1 Cavity dimensions of macrocycle **1**-**6** in the energy-minimized conformations

Macrocycle	Height (Å)	Width (Å)
1	5.44	12.12
2	8.23	9.16
3	8.23	11.38
4	11.90	5.38
5	7.35	9.88
6	8.58	7.72
γ-cyclodextrin	7.80	9.50

Macrocycles **1**-**6** were then examined to determine their capabilities as supramolecular hosts. First, their binding affinities with highly carcinogenic benzo[*a*]pyrene **8** to form binary complexes were measured via ^{1}H NMR and fluorescence spectroscopy. Second, their abilities to facilitate efficient energy transfer between benzo[*a*]pyrene **8** and fluorescent BODIPY **7** (Fig. 2) were evaluated via fluorescence spectroscopy.

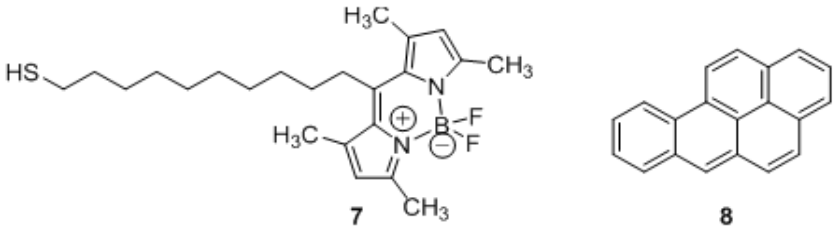

Fig. 2 Structures of the benzo[*a*]pyrene energy donor (**8**) and BODIPY energy acceptor (**7**).

The ability of dissymmetric organic macrocycles **1-6** to bind benzo[*a*]pyrene was evaluated by both fluorescence and ^{1}H NMR titrations. Increases in the fluorescence emission of benzo[*a*]pyrene **8** in the presence of increasing concentrations of the macrocycle demonstrated efficient binding.[20]

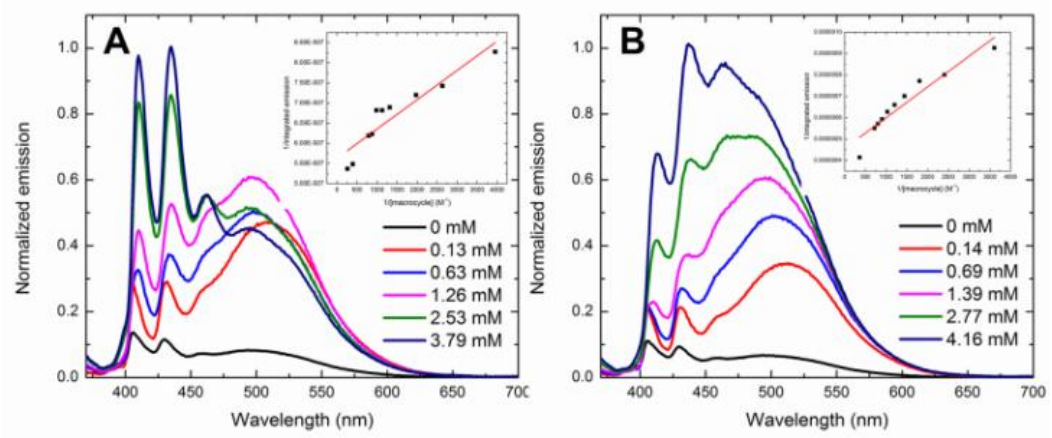

Fig. 3 Emission spectra of 0.031 mM benzo[*a*]pyrene in the presence of increasing concentrations of (A) macrocycle **1** and (B) macrocycle **5** at the excitation wavelength of 360 nm.

Of all the macrocycles tested, macrocycles **1** and **5** were found to be the most efficient hosts for benzo[*a*]pyrene **8**. As shown in Figure 3A, an increase in the benzo[*a*]pyrene monomer emission (below 450 nm) was observed in the presence of increasing concentrations of macrocycle **1**. The benzo[*a*]pyrene excimer emission (measured above 450 nm), by contrast, demonstrated less consistent trends. Fitting the fluorescence intensity data to a Benesi-

Hildebrand plot for a 1:1 complex yielded a good linear fit, with a calculated association constant of 8.6 x 10^3 M^{-1}(see ESI for details)[24,25] showing strong binding with the highly toxic PAH analyte.

Similarly, the binding affinity of macrocycle **5** with benzo[*a*]pyrene **8** was observed by monitoring the fluorescence changes in the benzo[*a*]pyrene emission (Figure 3B). A 3-fold increase in the emission of benzo[*a*]pyrene was observed upon adding increasing amounts of up to 1.39 mM of macrocycle **5**. Fitting the data to a Benesi-Hildebrand plot for a 1:1 complex yielded a binding constant of 5.0 x 10^3 M^{-1} using the Benesi-Hildebrand plot.

To confirm the binding of benzo[*a*]pyrene in the macrocycle cavities, ^{1}H NMR titration experiments[26] were carried out (Figure 4). Upon the addition of up to 1 equivalent of benzo[*a*]pyrene **8** to macrocycle **5**, the H_a and H_b protons of benzo[*a*]pyrene (Figure 2) shifted from 9.076 ppm and 9.046 ppm to 9.083 ppm and 9.054 ppm, respectively. Similarly, the H_c proton was also shifted downfield from 8.519 ppm to 8.525 ppm. Additionally, downfield shifts of H_d, H_e, and H_j, H_k were observed (Figure 4).

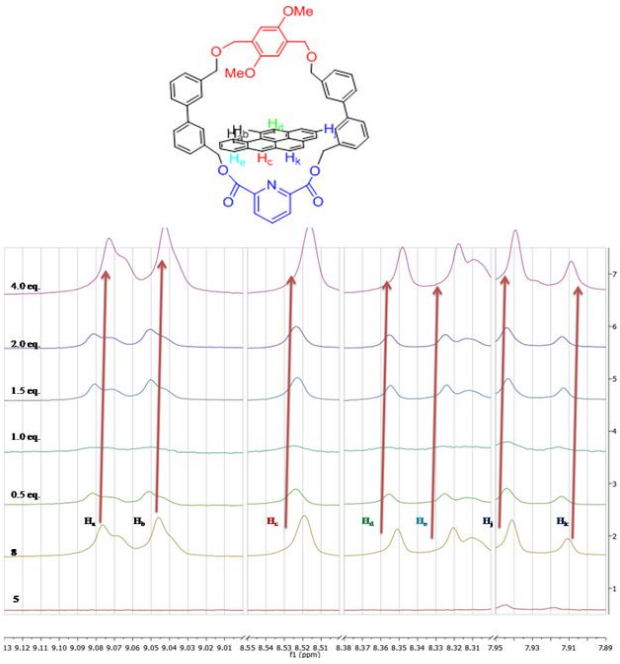

Fig. 4 Sections of ^{1}H NMR spectra of the complex of host **5** with increasing amounts of benzo[*a*]pyrene **8**.

These shifts indicate that benzo[*a*]pyrene associates strongly with macrocycle **5**. Further addition (beyond 1 equivalent) of guest **8** to macrocycle **5** resulted in no further downfield shift of the protons, which confirms the formation of a 1:1 host: guest complex. A Job plot analysis of this NMR data gave a maximum mole fraction of 0.5, clearly indicating the formation of 1:1 host: guest binding stoichiometry (Fig. 5).

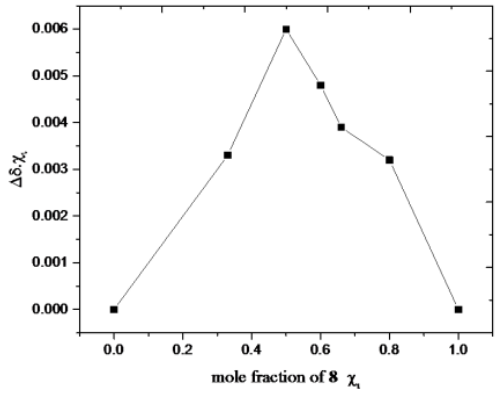

Fig. 5 Job plot of H_c proton of **8** with **5** in $CDCl_3$ showing a maximum at 0.5 mole fraction of **8**.

Macrocycles **1** and **5** were further investigated for their ability to promote energy transfer from analyte **8** to highly fluorescent BODIPY **7**.[27] Energy transfer efficiencies from the analyte to the fluorophore were measured by adding concentrated solutions of compounds **7**, **8**, and the macrocycle in tetrahydrofuran (THF) to an aqueous solution of phosphate buffered saline. This solvent composition was designed to maximize hydrophobic binding while ensuring full dissolution of all organic compounds. The solution was excited near the absorbance maximum of benzo[*a*]pyrene **8** and near the maximum of fluorophore **7**, and energy transfer efficiencies were calculated (see ESI for details). This energy transfer was measured both by the decrease in the donor emission (E_{exp}, Equation 1)

$$E_{exp} = 1 - F_{DA}/F_D \qquad \text{(Eq. 1)}$$

where F_{DA} and F_D are the integrated emission of the donor in the presence and absence of acceptors, respectively, and the increase in the fluorophore emission (E.T.%, Equation 2).

$$\text{E.T.\%} = I_{DA}/I_A \times 100\% \qquad \text{(Eq. 2)}$$

Where I_{DA} is the integration of the fluorophore from analyte excitation and I_A is the integrated fluorophore emission from direct excitation.

Table 2 Results of host macrocycle-promoted energy transfer between compound **8** and compound **7**

Macrocycle	ET%
1	322
2	162
3	53
4	32
5	345
6	118

The energy transfer efficiency results of both macrocycles **1** and **5** are 322% and 345%, respectively and clearly indicate that they are the most efficient supramolecular hosts for facilitating non-covalent energy transfer (Table 2).

Macrocycles **1** and **5** are most efficient in promoting energy transfer between benzo[*a*]pyrene **8** and BODIPY **7**.

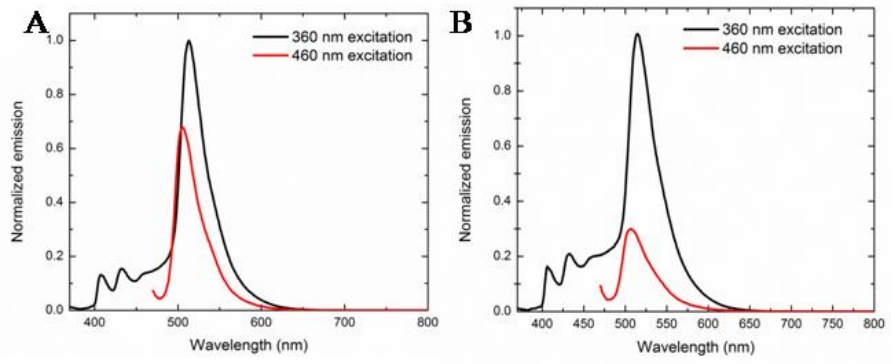

Fig. 6 Energy transfer efficiencies in the presence of (A) macrocycle **1** and (B) macrocycle **5**. (In both cases, black line is the excitation of benzo[*a*]pyrene and red line is the excitation of BODIPY)

This energy transfer occurs due to strong non-covalent interactions, including hydrophobic interactions and π-π stacking, between the macrocycle, benzo[*a*]pyrene **8**, and BODIPY **7**.

However, no significant energy transfer was observed in the presence of macrocycle **3** and **4,** likely because of their inability to bindbenzo[*a*]pyrene **8** efficiently because of the smaller cavity size (see Fig.S11 in the ESI). Substantially less energy transfer occurred in the presence

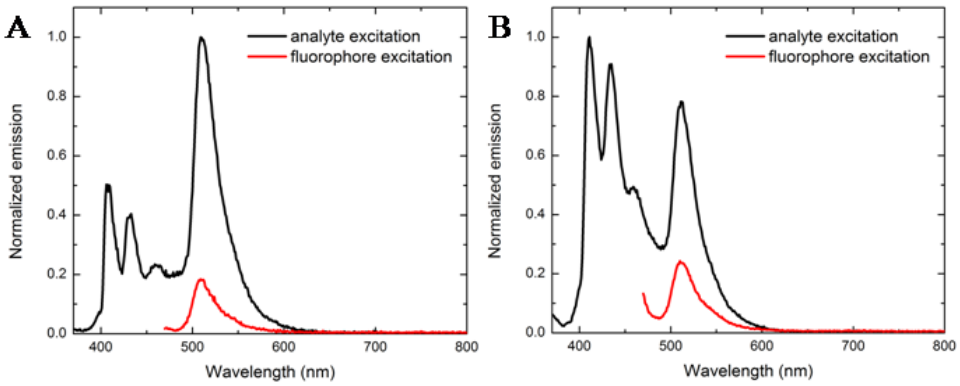

Fig. 7 Energy transfer efficiencies in the presence of (A) efficient macrocycle **2** of our previous paper (ref. 20) and (B) macrocycle **5** of this work.

of macrocycle **2** (Fig. 8B) when compared to macrocycle **1** (Fig. 8A). Similarly, macrocycle **6** (Fig. 8D) was not able to bind electron rich benzo[*a*]pyrene **8** efficiently due to smaller cavity size when compared to macrcoycle **5** (Fig. 8C), in which led to substantially less energy transfer. Moreover, structural conformations plays an important role in associating the guest molecules in an orientation that facilitates efficient energy transfer.

To truly assess the energy transfer efficiency, we compared the energy transfer efficiency of macrocycle **5** with one of the most efficient macrocycle **2** of our previous paper.[20] We observed that slightly less efficient energy transfer occurred in macrocycle **5**. This could be due to less proximity between benzo[*a*]pyrene and BODIPY; current efforts are focused on elucidating the reasons for this difference. We have also calculated the limit of detection for benzo[*a*]pyrene using benzo[*a*]pyrene to BODIPY energy transfer in the presence of macrocycle **5**, and found it to be 1.00 mM (see ESI for details).

Macrocycle **1** and **5** both have shown their efficiency in promoting energy transfer compared to our previously reported work with γ-cyclodextrin.[7, 8] The reason macrocycles **2**, **3**, **4** and **6** are not efficient in promoting the energy transfer is most likely due to their inability to bind benzo[*a*]pyrene **8** efficiently, which in turn limits their ability to promote efficient energy transfer.

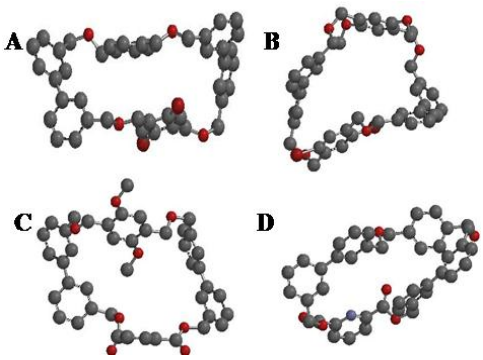

Fig.8 Energy-minimized conformations of (A) macrocycle **1**, (B) macrocycle **2**, and (C) macrocycle **5**, (D) macrocycle **6** using semi empirical PM3 level calculations (hydrogen atoms omitted for clarity).

Computational work also highlights the extent to which small structural changes in the macrocycles lead to significant changes in their cavity dimensions and their ability to form host-guest complexes with small molecule guests. Macrocycles **1** (Figure 8A) and **5** (Figure 8C) looks like rectangular in their cavity sizes whereas the introduction of methoxy substituents in the macrocycle **2** changed it's conformation (Figure 8B) in such a way not to bind the analyte effectively and removal of methoxy groups in the macrocycle **6** (Figure 8D) leads to changes its conformation not to bind the analyte efficiently.

In summary, reported herein is the design, synthesis, and evaluation of a series of electronically dissymmetric macrocycles as hosts for binding highly toxic benzo[*a*]pyrene and as promoters for non-covalent fluorescence energy transfer. Among the macrocycles reported herein, we have identified two that are both more efficient at binding benzo[*a*]pyrene and

better at or comparable to promoting non-covalent energy transfer compared to our previously reported macrocycles. More generally, the results reported herein underscore the complex relationship between macrocycle structure, supramolecular conformation, and application performance. Our demonstrated ability to synthetically tune the structures of these hosts can enable both a more detailed understanding of this relationship as well as significant advances in the performance of the hosts in crucial fluorescence-based detection applications. Efforts towards these research goals are currently underway in our laboratory.

Notes and references

1. Y. W. Yang, Y. L. Sun and N. Song, *Acc. Chem. Res.*, 2014, **47**, 1950.
2. D. J. Cram, *Angew. Chem. Int. Ed.*, 1988, **27**, 1009.
3. S. E. Wheeler, *Acc. Chem. Res.*, 2013, **46**, 1029.
4. K. Muller-Dethlefs and P. Hobza, *Chem. Rev.*, 2000, **100**, 143.
5. L. Liu and Q.-H. Guo, *J. Inclusion. Phenom. Macrocyclic Chem.*, 2002, **42**, 1.
6. L. A. Blyshak, K. Y. Dodson, G. Patonay, I. M. Warner and W. E. May, *Anal. Chem.*, 1989, **61**, 955.
7. N. Serio, C. Chanthalyma, L. Prignano and M. Levine, *Supramol. Chem.*, 2014, **26**, 714.
8. N. Serio, K. Miller and M. Levine, *Chem. Commun.*, 2013, **49**, 4821.
9. N. Serio, L. Prignano, S. Peters and M. Levine, *Poly. Arom. Compds.*, 2014, **34**, 561.
10. A. Bandela, J. P. Chinta, V. K. Hinge, A. G. Dikundwar, T. N. G. Row and C. P. Rao, *J. Org. Chem.*, 2011, **76**, 1742.
11. J. C. Barnes, M. Juricek, N. L. Strutt, M. Frasconi, S. Sampath, M. A. Giesener, P. L. McGrier, C. J. Bruns, C. L. Stern, A. A. Sarjeant and J. F. Stoddart, *J. Am. Chem. Soc.*, 2013, **135**, 183.

12. V. Blanco, M. D. Garcia, A. Terenzi, E. Pia, A. Fernandez-Mato, C. Peinador and J. M. Quintela, *Chem. -Eur. J.*, 2010, **16**, 12373.

13. C. Peinador, E. Pia, V. Blanco, M. D. Garcia and J. M. Quintela, *Org. Lett.*, 2010, **12**, 1380.

14. K. Srogi, *Environ. Chem. Lett.*, 2007, **5**, 169.

15. Y. Guo, K. Wu, X. Huo and X. Xu, *J. Environ. Health.*, 2011, **73**, 22.

16. R. J. Law, C. Kelly, K. Baker, J. Jones, A. D. McIntosh and C. F. Moffat, *J. Environ. Monit.*, 2002, **4**, 383.

17. C. L. Copper and M. J. Sepanlak, *Anal. Chem.*, 1994, **66**, 147.

18. H. Cernohorska, S. Klimesova, L. Lepsa, P. Jinoch, A. Milcova, J. Schmuczerova, J. Topinka and J. Labaj, *Mutat. Res.*, 2012, **742**, 2.

19. M. S. G. Falcon, S. G. Amigo, M. A. L. Yusty, M. J. Lopez de Alda Villaizan and J. S. Lozano, *J. Chromatogr. A.*, 1996, **753**, 207.

20. B. Radaram, J. Potvin and M. Levine, *Chem. Commun.*, 2013, **49**, 8259.

21. N. Serio, C. Chanthalyma, L. Prignano and M. Levine, *ACS Appl. Mater. Interfaces.*, 2013, **5**, 11951.

22. T. Mako, P. Marks, N. Cook and M. Levine, *Supramol. Chem.*, 2012, **24**, 743.

23. Y. Chen, Y. M. Zhang and Y. Liu, *Chem. Commun.*, 2010, **46**, 5622.

24. H. A. Benesi and J. H. Hildebrand, *J. Am. Chem. Soc.*, 1949, **71**, 2703.

25. K. C. Tayade, A. S. Kuwar, U. A. Fegade, H. Sharma, N. Singh, U. D. Patil and S. B. Attarde, *J. Fluoresc.*, 2013, **24**, 19.

26. O. Altintas, D. S. Suenninghausen, B. Luy and C. B. Kowollik, *ACS Macro. Lett.*, 2013, **2**, 211.

27. J. L. Shepherd, A. Kell, E. Chung, C. W. Sinclar, M. S. Workentin and D. Bizzotto, *J. Am. Chem. Soc.*, 2004, **126**, 8329.

Electronic Supporting Information for

A Series of Dissymmetric Macrocycle Hosts for the Facilitated Detection of Carcinogenic Benzo[*a*]pyrene

*Bhasker Radaram, Lindsey Prignano, Mindy Levine**

Materials and Methods

All the starting materials, reagents, and solvents were purchased from Sigma Aldrich, Acros Organics, TCI chemicals, Alfa Aesar, or Fisher Scientific and were used as received. All reactions were carried out under an inert atmosphere. Solvents were dried using an MBraun dual solvent purification system prior to use. Reactions were all monitored via analytical thin layer chromatography (TLC) using polyester backed TLC plates. Visualization was accomplished with UV light at 254 nm and/or with a $KMnO_4$ TLC stain. Product isolation was performed by using preparative TLC plates or silica gel chromatography. Both analytical TLC plates and preparative TLC plates were purchased from Sorbent Technologies, GA. Column chromatography was performed with SiliaFlash F60 (230-400 mesh) silica gel, obtained from Silicycle Inc. Canada.

^{1}H NMR and^{13}C NMR spectra were taken on a Bruker 300 MHz spectrometer and were recorded in $CDCl_3$ at ambient temperature. Chemical shifts (δ) are in parts per million relative to chloroform at 7.26 ppm, dimethylsulfoxide at 2.50 ppm, or to tetramethylsilane (TMS) at 0.00 ppm for ^{1}HNMR and relative to $CDCl_3$ at 77.16 ppm or DMSO at 40.76 ppm for ^{13}C NMR spectra. Multiplicity for ^{1}H NMR data is reported as follows: s = singlet, d = doublet, t = triplet, m = multiplet, br = broad. High resolution mass spectra were obtained and analyzed using a Bruker Daltonics APEX 4.7 Tesla Fourier Transform Ion Cyclotron Resonance Mass

Spectrometer at the Massachusetts Institute of Technology, in collaboration with Dr. Li Li. Binding and fluorescence energy transfer experiments were recorded on Shimadzu RF 5301 spectrophotometer with 1.5 nm excitation and 1.5 nm emission slit widths. Absorbance measurements were recorded on an Agilent 8453 UV-visible spectrophotometer.

Computational work was performed with Spartan software (Spartan 10, version 1.1.0), obtained from Wavefunction, Inc. CA. All calculations were performed using equilibrium geometry at the ground state, semi-empirical PM3 level. All the conformations shown were energy-minimized.

Synthetic Procedures for all Macrocycles and Intermediates:

Synthesis of Compound S5:

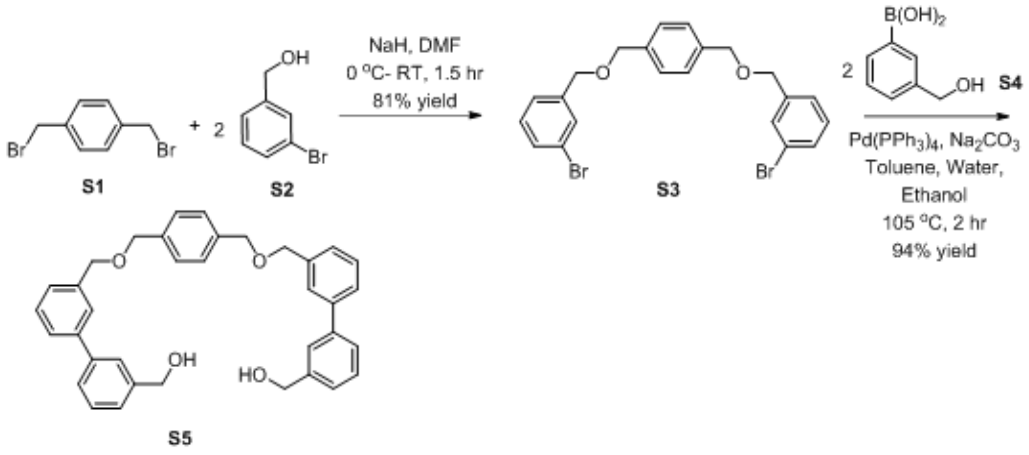

Compound **S5** was prepared according to the reported literature procedure: Radaram, B.; Potvin, J.: Levine, M. *Chem. Commun*.**2013**, *49*, 8259-8261.

Synthesis of Compound S8:

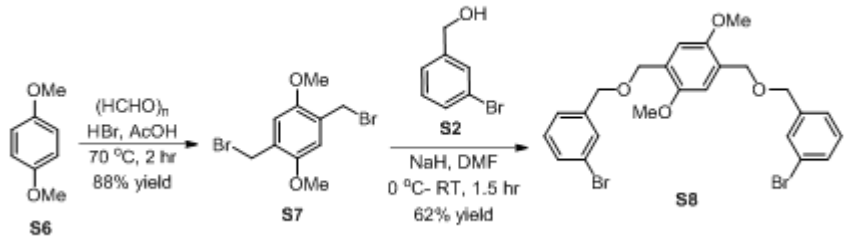

Compound **S8** was prepared according to the reported literature procedure: Radaram, B.; Potvin, J.; Levine, M. *Chem. Commun*.**2013**, *49*, 8259-8261.

Synthesis of Compound S10:

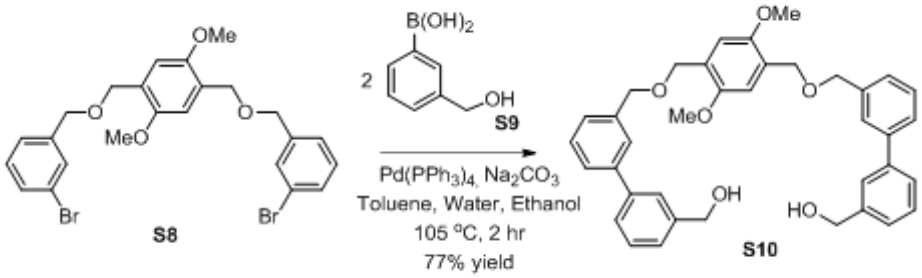

Compound **S8** (1.00 g, 1.872 mmol, 1.0 eq.) was dissolved in anhydrous toluene (30 mL), 3-hydroxymethylphenyl boronic acid (compound **S9**) (654 mg, 4.307 mmol, 2.3 eq.) was dissolved in anhydrous ethanol (16 mL), and sodium carbonate (1.984 g, 18.726 mmol, 10 eq.) was dissolved in water (16 mL). The aqueous sodium carbonate solution was degassed under nitrogen for 30-60 minutes. All three solutions were combined in an oven-dried and nitrogen-purged round-bottom flask and tetrakis(triphenylphosphine)palladium(0) ($Pd(PPh_3)_4$) (281 mg, 0.243 mmol, 0.13 eq.) was added to the reaction mixture. The reaction mixture was refluxed at 105 ^oC for 2 hours under a nitrogen atmosphere, at which point the reaction was complete by TLC analysis. Water (14 mL) was added to quench the reaction mixture and the reaction mixture was extracted with ethyl acetate (3 portions of 30 mL each). The combined organic

extract was dried over sodium sulfate, filtered, and concentrated via rotary evaporation. The product was further purified by flash chromatography using hexanes: ethyl acetate (4:6) to afford compound **S10** as pale yellow solid (850 mg, 77 % yield). ^{1}H NMR ($CDCl_3$, 300 MHz): δ = 7.61 (d, 4 H, J = 8.4 Hz), 7.53 (d, 4 H, J = 7.5 Hz), 7.42 (t, 4 H, J = 7.5 Hz), 7.35(t, 4 H, J = 7.5 Hz), 7.00 (s, 2H), 4.75 (s, 4 H), 4.67 (s, 4H), 4.63 (s, 4H), 3.76 (s, 6H). ^{13}C NMR ($CDCl_3$, 75 MHz): δ = 151.19, 141.56, 141.40, 139.11, 129.03, 126.45, 125.79, 111.87, 72.47, 67.04, 65.24, 56.16; HRMS (ESI): Calcd for [M+Na^+, $C_{38}H_{38}O_6Na]^+$ 613.2561, found 613.2550.

Synthesis of Macrocycle 1:

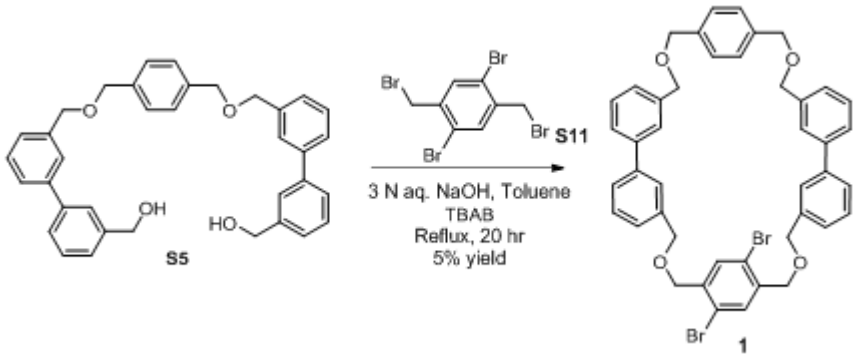

2,5-dibromo-1,4-bis(bromomethyl)benzene (compound **S11)** was prepared according to the published procedure: Bonifacio, M.C.; Robertson, C.R.; Jung, J-Y.; King, B.T. *J.Org. Chem.* **2005,** *70,* 8522-8526.

To a mixture of compound **S5** (200 mg, 0.376 mmol, 1.0 eq.), compound **S11** (174 mg, 0.413 mmol, 1.1 eq.) and tetrabutylammonium bromide (TBAB) (243 mg, 0.753 mmol, 2.0 eq.) in anhydrous toluene (12 mL) was added a solution of 3N aqueous NaOH (6.0 mL). The reaction mixture was refluxed for 20 hours at 100 ^{o}C. After 20 hours, the reaction mixture was cooled to room temperature and toluene was removed via rotary evaporator. The reaction mixture was

extracted with ethyl acetate (3 portions of 10 mL), and the combined organic extract was washed with brine solution, dried over anhydrous sodium sulfate, filtered and evaporated to yield the crude product. The crude product was purified via flash chromatography (1.5:8.5 ethyl acetate: hexanes) to afford macrocycle **1** as an off-white solid (15 mg, 5% yield). R_f: 0.85 (1:1 ethyl acetate: hexanes);^{1}H NMR ($CDCl_3$, 300 MHz): δ = 7.69 (d, 2H, J = 8.1 Hz),7.65 (s, 1H), 7.57 (d, 4 H, J = 8.4 Hz), 7.52 (s, 3 H), 7.45-7.33 (m, 12 H), 4.67 (d, 4 H, J = 6.3 Hz), 4.59 (d, 12 H, J = 4.8 Hz);^{13}C NMR ($CDCl_3$, 75 MHz): δ = 141.58, 141.36, 138.95, 138.63, 138.32, 137.77, 132.90, 129.01, 128.96, 128.10, 127.07, 127.01, 126.93,126.70, 121.66, 72.98, 72.25, 72.10, 70.84;HRMS (ESI): Calcd for $[M+Na]^+$, $[C_{44}H_{38}Br_2O_4Na]^+$ 811.1035, found 811.1024.

Synthesis of Macrocycle 2:

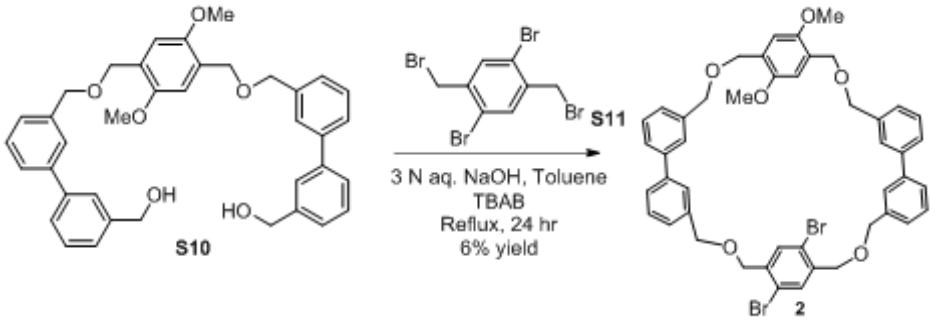

To a mixture of compound **S10** (300 mg, 0.508 mmol, 1.0 eq.), compound **S11** (278 mg, 0.659 mmol, 1.3 eq.) and tetrabutylammonium bromide (TBAB) (327 mg, 1.01 mmol, 2.0 eq.) in anhydrous toluene (20 mL) was added a solution of 3N aqueous NaOH (10 mL). The reaction mixture was refluxed for 24 hours. After 24 hours, the reaction mixture was cooled to room temperature and toluene was removed via rotary evaporator. The reaction mixture was extracted with ethyl acetate (3 portions of 10 mL), and the combined organic extract was washed with brine solution, dried over anhydrous sodium sulfate, filtered and evaporated to

yield the crude product. The crude product was purified by preparative TLC, eluted with 30% ethyl acetate: 70% hexanes to afford the macrocycle **2** as pale yellow solid (25 mg, 6% yield). R_f: 0.85 (1: 1 ethyl acetate: hexanes); ^{1}H NMR ($CDCl_3$, 300 MHz): δ = 7.70-7.61 (m, 6 H), 7.52 (t, 4 H, J = 6.9 Hz), 7.42 (t, 4 H, J = 7.5 Hz), 7.35 (t, 4 H, J = 6.3 Hz), 6.94 (d, 2 H, J = 6.3 Hz), 4.65 (d, 8 H, J = 5.1 Hz), 4.57 (d, 8 H, J = 6.3 Hz), 3.67 (s, 6 H); ^{13}C NMR ($CDCl_3$, 75 MHz): δ =151.24, 141.64, 141.24, 139.24, 138.61, 138.30, 132.88, 129.00, 128.91, 127.06, 126.92, 126.56, 121.62, 111.97, 73.03, 72.52, 70.85, 66.97, 56.14; HRMS (ESI): Calcd for $[M+Na]^+$, $[C_{46}H_{42}Br_2O_6Na]^+$ 871.1246, found 871.1267.

Synthesis of Macrocycle 3:

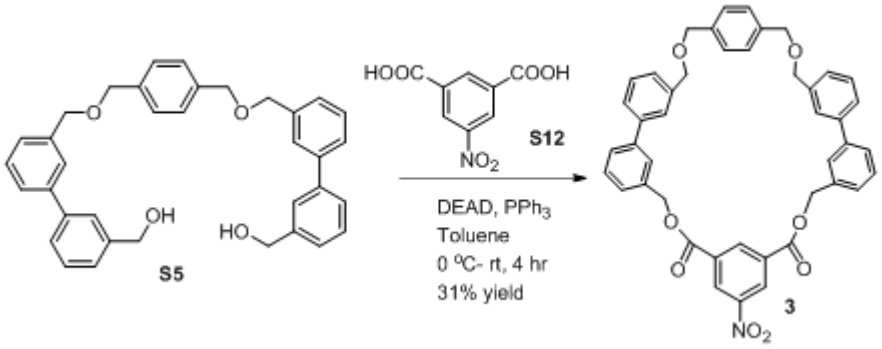

To compound **S5** (50.0 mg, 0.094 mmol, 1.0 eq.), 5-nitroisophthalic acid **S12** (22.0 mg, 0.104 mmol, 1.1 eq.) and triphenylphosphine (51.0 mg, 0.194 mmol, 2.1 eq.) in anhydrous toluene (30 mL) was added a 40 wt% solution of diethylazodicarboxylate (0.140 mL, 0.358 mmol, 3.8 eq.) in anhydrous toluene slowly at 0 ^{o}C. The reaction mixture was stirred for 15 min at 0 ^{o}C. The reaction mixture was allowed to warm to room temperature, and was stirred for 4 hours at room temperature. The reaction mixture was diluted with ethyl acetate (15 mL), and washed with saturated $NaHCO_3$ (2 x 10 mL portions) and brine (10 mL). The organic layer was dried with sodium sulfate, filtered and evaporated under reduced pressure. The crude product was purified by column chromatography, eluted with 15% ethyl acetate: 85% hexanes to afford

macrocycle **3** as an off-white solid (21 mg, 31% yield). R_f: 0.80 (1:1 ethyl acetate: hexanes); ^{1}H NMR ($CDCl_3$, 300 MHz): δ = 9.04 (s, 2 H), 8.93 (s, 1 H), 7.59-7.33 (m, 20 H), 5.46 (s, 4 H), 4.58 (s, 8 H);^{13}C NMR ($CDCl_3$, 75 MHz): δ = 163.78, 148.57, 141.99, 141.03, 139.01, 137.76, 136.14, 135.63, 132.66, 129.30, 129.01, 128.56, 128.06, 127.91, 127.84, 126.74, 72.14, 68.15. HRMS (ESI): Calcd for $[M+NH_4]^+$, $[C_{44}H_{39}N_2O_8]$ 723.2706, found 723.2720.

Synthesis of Macrocycle 4:

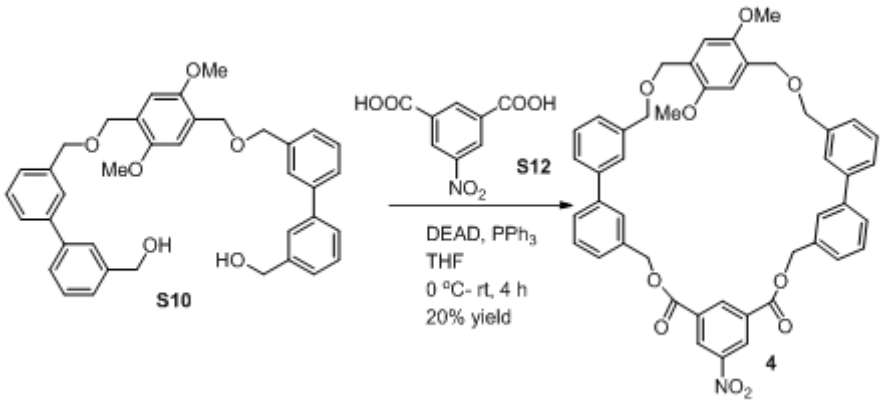

To compound **S10** (150.0 mg, 0.254 mmol, 1.0 eq.), 5-nitroisophthalic acid **S12** (80.4 mg, 0.381 mmol, 1.5 eq.), and triphenylphosphine (273 mg, 1.041 mmol, 4.1 eq.) in anhydrous tetrahydrofuran (75 mL) was added a 40% wt. solution of diethylazodicarboxylate (0.410 mL, 1.041mmol, 3.8 eq.) in anhydrous toluene slowly at 0 ^{o}C. The reaction mixture was stirred for 15 min at 0 ^{o}C. The reaction mixture was allowed to warm to room temperature, and was stirred for 4 hours at room temperature. Most of the tetrahydrofuran was evaporated and the residue was diluted with ethyl acetate (20 mL), and washed with saturated $NaHCO_3$ (2 x 10 mL portions) and brine (10 mL). The organic layer was dried with sodium sulfate, filtered and evaporated under reduced pressure. The crude product was purified by column chromatography, eluted with 30% ethyl acetate: 70% hexanes to afford macrocycle **4** as an off-white solid (40 mg, 21% yield). R_f: 0.85 (1:1 ethyl acetate: hexanes); ^{1}H NMR ($CDCl_3$,

300 MHz): δ = 9.04 (s, 2 H), 8.94 (s, 1 H), 7.59 (d, 6 H, J = 8.1 Hz), 7.50-7.29 (m, 12 H), 6.95 (s, 2H), 5.45 (s, 4 H), 4.64 (s, 4 H), 4.59 (s, 4 H), 3.69 (s, 6 H); ^{13}C NMR ($CDCl_3$, 75 MHz): δ = 163.70, 151.21, 142.01, 140.86, 139.28, 135.61, 132.62, 129.27, 128.76, 128.52, 127.96, 127.73, 127.16, 126.81, 126.56, 111.97, 72.36, 68.11, 66.97, 56.12. HRMS (ESI): Calcd for $[M+NH_4]^+$, $[C_{46}H_{43}N_2O_{10}]$ 783.2917, found 783.2896.

Synthesis of Macrocycle 5:

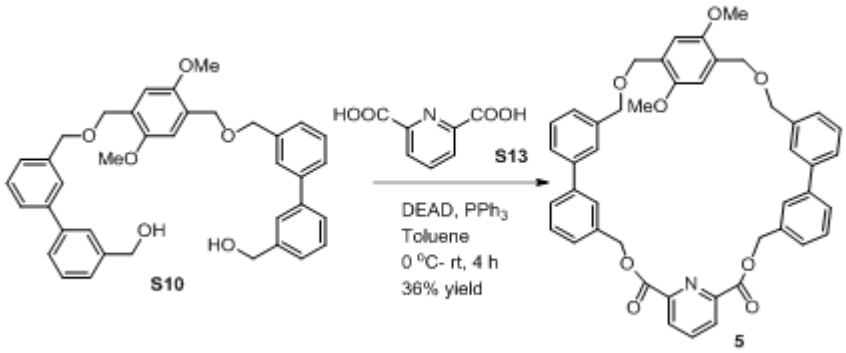

To compound **S10** (100 mg, 0.169 mmol, 1.0 eq.), 2,6-pyridinedicarboxylic acid **S13** (31 mg, 0.186 mmol, 1.1 eq.) and triphenylphosphine (93.0 mg, 0.354 mmol, 2.1 eq.) in anhydrous toluene (50 mL) was added a 40% wt. solution of diethylazodicarboxylate (0.240 mL, 0.643 mmol, 3.8 eq.) in anhydrous toluene dropwise slowly at 0 °C. The reaction mixture was stirred for 15 min at 0 °C. The reaction mixture was allowed to warm to room temperature, and was stirred for 4 hours at room temperature. After 4 hours, the reaction mixture was diluted with ethyl acetate (10 mL), and washed with saturated $NaHCO_3$ (2 x 15 mL portions) and brine (10 mL). The organic layer was dried with sodium sulfate, filtered and evaporated under reduced pressure. The crude product was purified by column chromatography, eluted with 45% ethyl acetate: 55% hexanes to afford macrocycle **5** as an off-white solid (45 mg, 37% yield). R_f: 0.80 (1:1 ethyl acetate: hexanes); ^{1}H NMR ($CDCl_3$, 300 MHz): δ = 8.26 (d, 2 H, J = 7.8 Hz), 7.94 (t, 1 H, J = 7.8 Hz), 7.65 (s, 2H), 7.58 (s, 2 H), 7.50 (m, 4 H), 7.37 (m, 8 H), 6.94 (s, 2 H),

5.48 (s, 4 H), 4.64 (s, 4 H), 4.60 (s, 4 H), 3.68 (s, 6 H); ^{13}C NMR ($CDCl_3$, 75 MHz): δ = 164.56, 151.29, 148.60, 141.79, 140.97, 139.32, 138.34, 136.05, 129.12, 128.91, 128.19, 127.70, 127.45, 127.04, 126.91, 126.61, 126.49, 112.08, 72.31, 67.83, 66.99, 56.16; HRMS (ESI): Calcd for $[M+H]^+$, $[C_{45}H_{40}NO_8]$ 722.2754, found 722.2762.

Synthesis of Macrocycle 6:

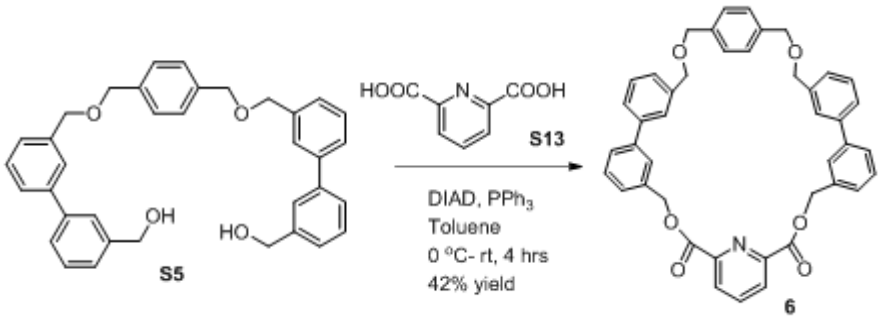

To compound **S5** (200 mg, 0.377 mmol, 1.0 eq.), 2,6-pyridinedicarboxylic acid **S13** (75.6 mg, 0.452 mmol, 1.2eq.) and triphenylphosphine (217 mg, 0.827 mmol, 2.2 eq.) in anhydrous toluene (70 mL) was added a solution of diisopropylazodicarboxylate (0.163 mL, 0.829 mmol, 2.2 eq.) in anhydrous toluene (3 mL) slowly at 0 ^{o}C. The reaction mixture was stirred for 15 min at 0 ^{o}C. The reaction mixture was allowed to warm to room temperature, and was stirred for 4 hours at room temperature. Most of the toluene was evaporated under reduced pressure. The residue was diluted with chloroform (25 mL), and washed with saturated $NaHCO_3$ (2 x 10 mL portions) and brine (10 mL). The organic layer was dried with sodium sulfate, filtered and evaporated under reduced pressure. The crude product was purified by column chromatography, eluted with 45% ethyl acetate: 55% hexanes to afford macrocycle **6** as an off-white solid (105 mg, 42% yield). R_f: 0.85 (1:1 ethyl acetate: hexanes); ^{1}H NMR ($CDCl_3$, 300 MHz): δ = 8.26 (d, 2 H, J = 7.8 Hz), 7.95 (t, 1 H, J = 7.5 Hz), 7.65 (s, 2H), 7.52 (d, 5 H, J = 6.0 Hz), 7.46 (m, 4 H), 7.40 (d, 3 H, J = 7.2 Hz), 7.33 (s, 6 H), 5.50 (s, 4 H), 4.58 (s, 8 H);

^{13}C NMR ($CDCl_3$, 75 MHz): δ = 164.58, 148.63, 141.76, 141.15, 138.99, 138.32, 137.75, 136.00, 129.13, 128.94, 128.18, 128.13, 127.96, 127.82, 127.57, 127.09, 126.67, 72.03, 67.91; HRMS (ESI): Calcd for $[M+H]^+$, $[C_{43}H_{36}NO_6]$ 662.2543, found 662.2550.

Synthesis of BODIPY 7 fluorophore:

The synthesis of BODIPY **7** was performed according to literature procedures:

Shepherd, J. L.; Kell, A.; Chung, E.; Sinclar, C. W.; Workentin, M. S.; Bizzotto, D. *J. Am. Chem. Soc.***2004**, *126*, 8329-8335.

Reaction 1:

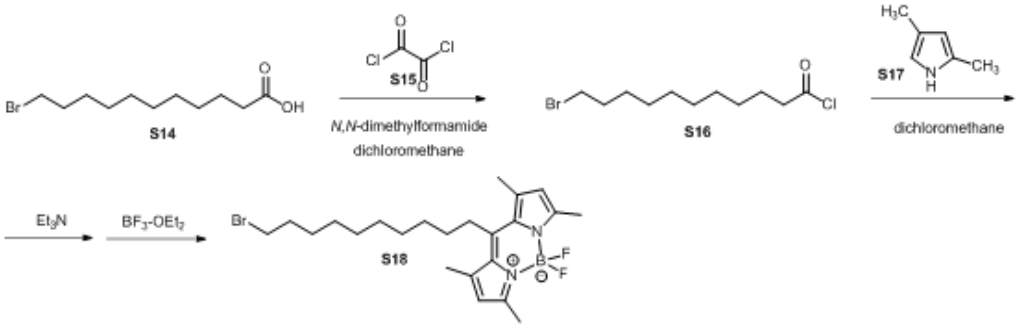

Procedure: 2.0 grams of 11-bromoundecanoic acid **S14** (7.54 mmol, 1.0 eq.) was combined with 2 drops of *N,N*-dimethylformamide in 40 mL of dichloromethane. 1.0 gram of oxalyl chloride **S15** (7.88 mmol, 1.05 eq.) was dissolved in 5.0 mL of dichloromethane and added dropwise. The reaction mixture was stirred for one hour, then the crude mixture was concentrated on the rotary evaporator and dried on a vacuum overnight to remove any unreacted oxalyl chloride. The resulting acid chloride **S16** was dissolved in 50 mL of dichloromethane. 0.772 mL of 2,4-dimethylpyrrole **S17** (7.50 mmol, 0.99 eq.) was dissolved in 5.0 mL of dichloromethane and added to the reaction mixture. The resulting reaction mixture was heated to reflux for 3 hours under a nitrogen atmosphere, during which time the mixture became a dark red color. After three hours, the reaction mixture was cooled to room

temperature and solvent was removed on the rotary evaporator until approximately 5.0 mL of the dichloromethane solution remained. 200 mL of *n*-hexanes were added to the flask, and the mixture was cooled overnight in the freezer at -20 ^{o}C. The hexanes were decanted from the insoluble oil and precipitate. The resulting crude product was dissolved in 75 mL of toluene and heated to 80 ^{o}C. 1.0 mL of triethylamine (7.17 mmol, 0.95 eq.) was added and the solution immediately turned light yellow. 1.0 mL of boron trifluorideetherate (8.10 mmol, 1.07 eq.) was then added and the reaction mixture was stirred at 80 ^{o}C for 30 minutes, during which time the color of the mixture darkened and became fluorescent. The reaction mixture was cooled to room temperature, and the product was extracted 3 times with brine (50 mL each time). The organic layer was dried over sodium sulfate, filtered, and concentrated. The crude product was purified by flash chromatography (1:1 dichloromethane: hexanes) to yield the desired product **S18** in 28% yield (comparable to the literature-reported 24% yield).

Reaction 2:

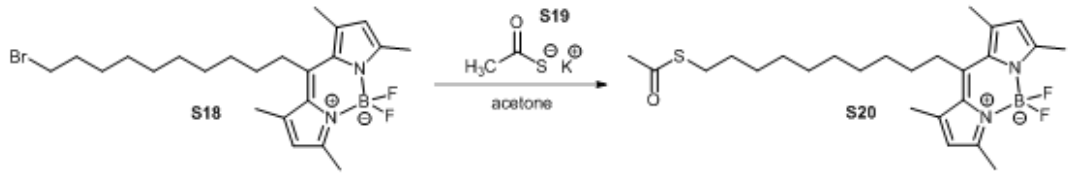

Procedure: Compound **S18** (0.968 g, 2.07 mmol, 1.0 eq.) and compound **S19** (0.27 grams, 2.36 mmol, 1.14 eq.) were dissolved in 50 mL of acetone. The reaction mixture was heated to reflux for two hours. After two hours, the reaction mixture was cooled to room temperature, acetone was removed, and the crude solid was re-dissolved in dichloromethane and washed with water. The organic extract was dried over sodium sulfate, filtered and concentrated, to yield compound **S20** in 97% yield (0.932 grams).

Reaction 3:

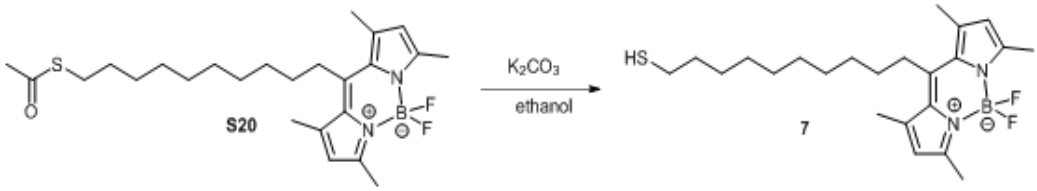

Procedure: Compound **S20** (0.932 grams, 2.01 mmol, 1.0 eq.) was dissolved in 150 mL of anhydrous ethanol that was purged with nitrogen. Potassium carbonate was added, and the reaction mixture was warmed to 30 ^{o}C. The reaction mixture was stirred under nitrogen for 4 hours at 30 ^{o}C. The contents of the flask were poured over 40 mL of aqueous saturated ammonium chloride, at which point the solution turned bright orange. The product was extracted with dichloromethane and washed several times with water. The organic layer was dried over sodium sulfate, filtered, and concentrated. The product was purified via flash chromatography (1:1 dichloromethane: hexanes) to yield compound **7** in 76% yield (674 mg)

Fluorescence Experimental Procedures:

All fluorescence spectra were recorded on a Shimadzu RF 5301 spectrophotometer. Binding experiments were conducted as follows:

The following stock solutions were made:

3 mg/mL of each macrocycle in THF

1 mg/mL of each PAH analyte in THF

Dilutions of the macrocycle stock solution were made to obtain solutions of 0.1, 0.2, 0.3, 0.4, 0.5, 0.6, 0.7, 0.8, 0.9, 1.0, 2.0 and 3.0 mg/mL solutions of each macrocycle.

20 μL of the PAH stock solution was added to 2.5 mL of phosphate buffered saline (PBS) at pH 7.4. 200 μL of each macrocycle solution was added, and the fluorescence of the solution was recorded with 360 nm excitation (scanned emission 370-710 nm). The fluorescence of the analyte was integrated with respect to wave number on the X-axis. The resulting data was

plotted using a Benesi-Hildebrand plot, with 1/[macrocycle] (in M) on the X-axis and 1/integrated analyte emission on the Y-axis. Linear fits were obtained using macrocycles **1** and **5** as hosts and benzo[*a*]pyrene **8** as a guest. The binding constants were calculated by dividing the y-intercept of the linear equation by the slope of the line.

Energy transfer experiments were conducted as follows:

A 1 mg/mL stock solution of BODIPY **7** in THF was made. 200 μL of the macrocycle host, 20 μL of the PAH analyte, and 20 μL of the BODIPY **7** fluorophore were added to 2.5 mL of PBS. The solution was excited at 360 nm and 460 nm (scanned emission 370-710 nm and 470-800 nm, respectively). The fluorescence emission of benzo[*a*]pyrene **8** and of BODIPY **7** were integrated with respect to wavenumber, and the efficiency of energy transfer was determined by measuring both the fractional quenching of benzo[*a*]pyrene **8** emission in the presence of BODIPY **7** (Equation 1), and the percentage of BODIPY emission from analyte excitation compared to direct excitation (Equation 2, see the main text for equations).

Summary Tables for all Binding and Energy Transfer Experiments:

Table S1: Summary Table of Binding Experiments:

BH association constant: The binding constant measured via Benesi-Hildebrand plots

% Fluorescence change: The change in the fluorescence emission of benzo[*a*]pyrene **8** on going from the lowest macrocycle concentration to the highest macrocycle concentration.

Macrocycle	B H association constant (M^{-1})	% fluorescence change
1	8571.43	166
2	20000	158
3	*a*	53
4	*a*	52
5	5000	305
6	*a*	83

a: negative values were obtained for the Benesi Hildebrand plots resembles poor binding.

Benesi-Hildebrand Plots for all Macrocycle-Benzo[*a*]pyrene Combinations:

Benesi-Hildebrand plots for Macrocycle **1** and **5** are included in the main text.

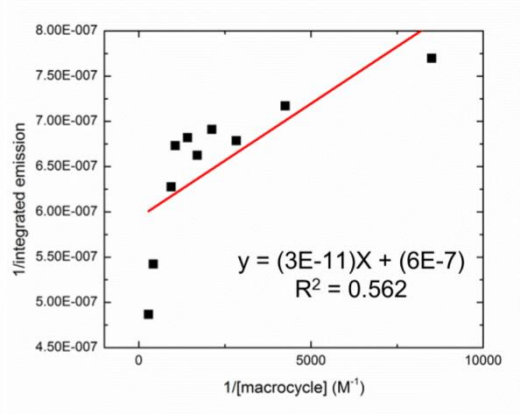

Fig. S1: Benesi-Hildebrand plot for Macrocycle **2**

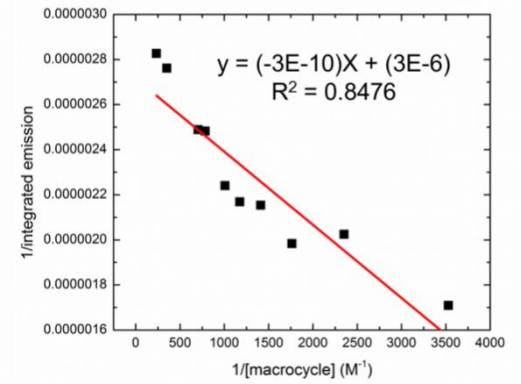

Fig. S2: Benesi-Hildebrand plot for Macrocycle **3**

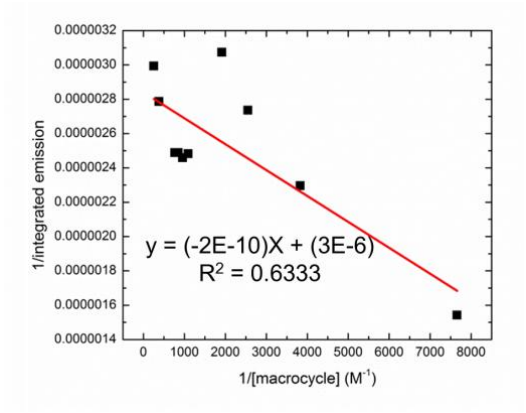

Fig. S3: Benesi-Hildebrand plot for Macrocycle **4**

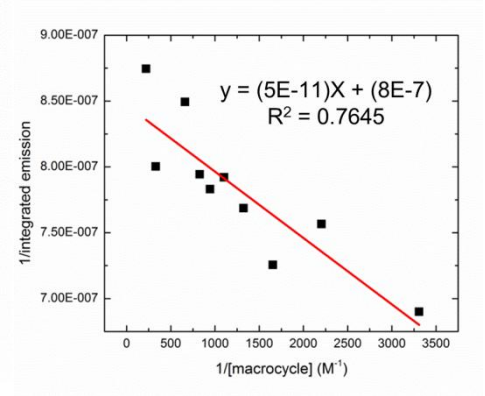

Fig. S4: Benesi-Hildebrand plot for Macrocycle **6**

^{1}H NMR Titration Experiments:

All ^{1}H NMR titrations were carried out by adding aliquots of benzo[*a*]pyrene in $CDCl_3$ to an NMR tube containing the host macrocycle already dissolved in $CDCl_3$. After each addition, the spectrum was recorded by using Bruker 300 MHz Instrument.

For the titration of macrocycle **5** with benzo[*a*]pyrene **8**: A $CDCl_3$ solution of macrocycle **5** (5.35 mg, 14.8 mM, 0.5 mL) was titrated by adding increasing amounts of benzo[*a*]pyrene **8** (0.5, 1.0, 1.5, 2.0 and 4.0 equivalents) from a $CDCl_3$ stock solution (18.70 mg, 29.6 mM, 2.5 mL) and showed a 1:1 ratio of binding in macrocycle **5**.

Table S2: ^{1}H NMR chemical shifts of **5:8** complex at 1:1 stoichiometry

Proton of **8**	Initial (ppm)	Final (ppm)	Change in Chemical Shift (ppm)
H_a	9.076	9.083	+ 0.007
H_b	9.046	9.054	+ 0.008
H_c	8.514	8.526	+ 0.012

Table S3: Data associated with the Job plot of **5:8** host:guest complex performed *via* ^{1}H NMR titration in $CDCl_3$ at ambient temperature.

[5] (mg)	[**8**] (mg)	[**5**] (mM)	[**8**] (mM)	[**8**]/([**5**]+ [**8**])	**δ** (ppm)	**δΔ** (ppm)	**(δΔ)** [**8**]/([**5**]+ [**8**])
5.35	0.0	7.4	0.0	0.00	8.514	0.000	0.000
5.35	0.935	7.4	3.70	0.33	8.524	0.010	0.0033
5.35	1.87	7.4	7.40	0.50	8.526	0.012	0.0060
5.35	2.80	7.4	11.10	0.60	8.522	0.008	0.0048
5.35	3.74	7.4	14.80	0.66	8.520	0.006	0.0039
5.35	7.48	7.4	29.60	0.80	8.510	0.004	0.0032
0.0	7.48	0.0	29.60	1.00	8.514	0.000	0.000

[**8**]/([**5**]+ [**8**]) is represented as χ_i (mole fraction of **8**)

δ is measured with respect to H_c proton of benzo[*a*]pyrene **8**

Energy Transfer Figures for all Macrocycle-Benzo[*a*]pyrene Combinations:

E_{exp}: The black line represents the fluorescence emission of the energy donor from excitation at 360 nm, and the red line represents the fluorescence emission of the energy donor in the presence of the fluorophore acceptor from excitation at 360 nm.

E.T. %: The black line represents the fluorescence emission from excitation of the energy donor at 360 nm in the presence of the acceptor, and the red line represents the fluorescence emission from direct excitation of the fluorophore acceptor at 460 nm.

Energy transfer efficiencies in the presence of macrocycles **1** and **5** were shown in the main text.

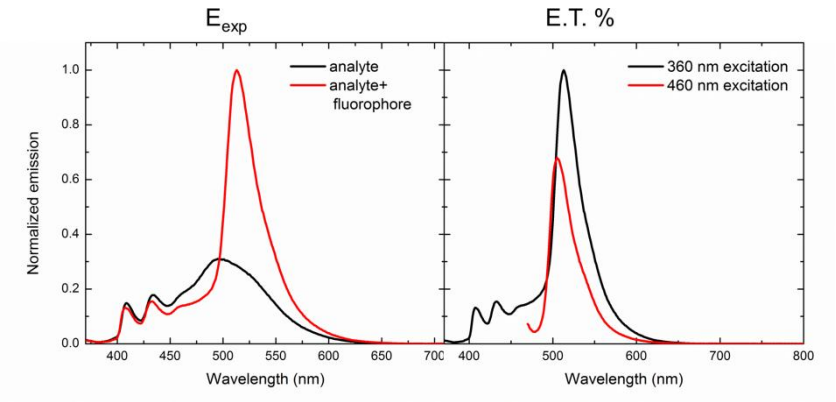

Fig. S5: Energy transfer efficiency in the presence of macrocycle **2**

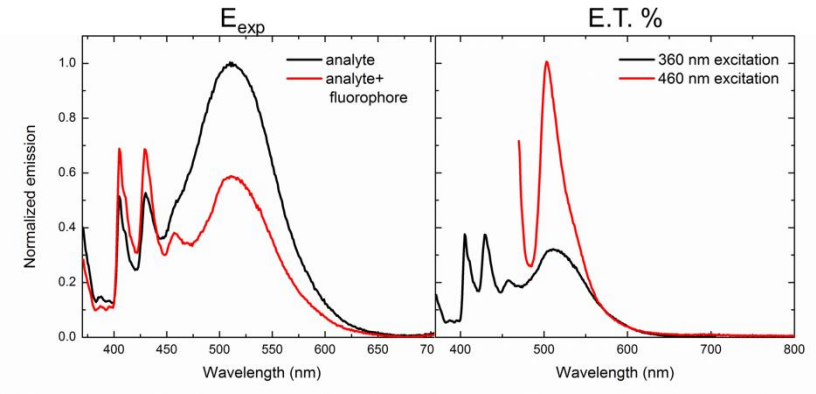

Fig. S6: Energy transfer efficiency in the presence of macrocycle **3**

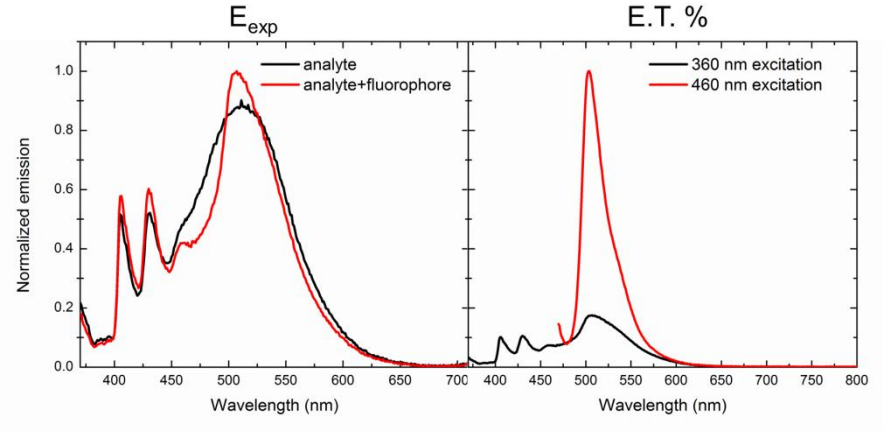

Fig. S7: Energy transfer efficiency in the presence of macrocycle **4**

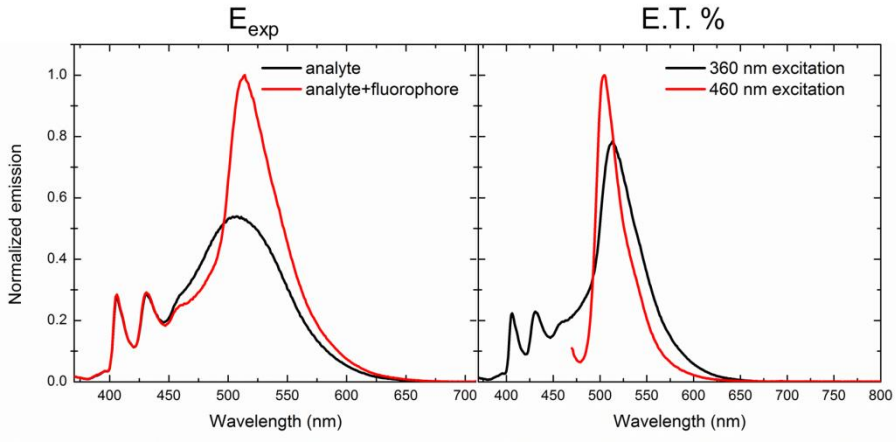

Fig. S8: Energy transfer efficiency in the presence of macrocycle **6**

EXPERIMENTAL DETAILS FOR LIMIT OF DETECTION

The limit of detection (LOD) is defined as the lowest concentration of analyte at which a signal can be detected. The lowest concentration of analyte that can be accurately quantified is called limit of quantification (LOQ). Herein we compared the LOD of macrocycle **5** with the most efficient macrocycle **2** in our previous paper (Radaram, B.; Potvin, J.: Levine, M. *Chem. Commun.* **2013**, *49*, 8259-8261).

The following procedure was used to determine the limit of detection and limit of quantification for each fluorophore-analyte combination.

We prepared the following solutions:

3 mg/mL of most efficient macrocycle **2** of previous paper & **5** in THF

1 mg/mL of benzo[*a*]pyrene in THF

0.1 mg/mL of BODIPY in THF

To determine the limit of detection, each fluorophore-benzo[*a*]pyrene combination was examined in the following manner:

1. To a 2.5 mL of PBS into a cuvette was added 200 µL of the macrocycle and 20 µL of BODIPY solution in THF. The solution was excited at the benzo[*a*]pyrene's excitation

wavelength (360 nm) and the fluorescence emission spectrum was recorded. Six repeat measurements were made for the fluorescence emission spectra.

2. 20 μL of benzo[*a*]pyrene solution in THF was added to the cuvette and the solution was again excited at the analyte excitation wavelength (360 nm). Six repeat measurements were taken.

3. Step 2 was repeated for 40 μL, 60 μL, 80 μL, 100 μL of benzo[*a*]pyrene. In each case, the solution was excited at the benzo[*a*]pyrene excitation wavelength (360 nm) and the fluorescence emission spectrum was recorded six times.

4. All the fluorescence emission spectra were integrated vs. wave number, and we generated calibration curves with the analyte concentration on the X-axis (in mM) and the integrated fluorophore emission on the Y-axis. The curve was then fitted to a straight line and an equation for the line was determined.

5. For each case, the fluorophore with macrocycle (before any analyte was added), was also excited at the excitation wavelength for the analyte, and the fluorescence emission spectrum was recorded (as per step 1). These measurements are referred as the "blank."

6. The limit of the blank is defined according to the following equation:

$$LoB_{LOD} = m_{blank} + 3(SD_{blank})$$

Where m is the mean of the blank integrations and SD is the standard deviation.

7. The limit of the blank was then entered into the equation determined in step 4 (for the y value), and the corresponding X value was determined. This value provided the LOD in mM

8. The limit of quantification (LOQ) was calculated in a similar way to the limit of detection. First, the limit of the blank for quantification was determined according to the following equation:

$$LoB_{LOQ} = m_{blank} + 10(SD_{blank})$$

This value was then entered into the equation determined in step 4 (for the y value), and the corresponding X value was determined. This value provided the LOQ in mM.

Table S4: Summary Table for LOD experiments:

Macrocycle	Fluorophore	Analyte	Equation	R^2	LOD (mM)	LOQ (mM)
2	**7**	**8**	y =(1518)X +(3008)	0.832	8.03	8.00
5	**7**	**8**	y = (2991)X +(4331)	0.788	9.99	1.00

Summary Graphs for LOD experiments:

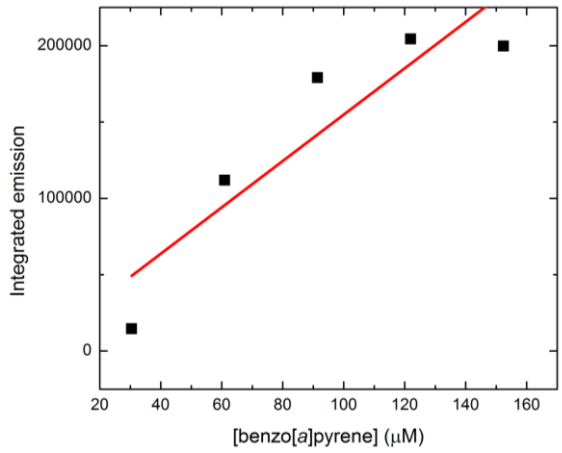

Fig S9: LOD graph for Benzo[*a*]pyrene **8** in the presence of macrocycle **2**.

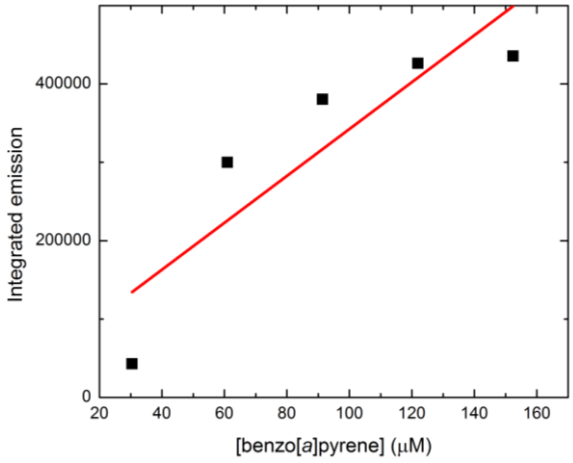

Fig S10: LOD graph for Benzo[*a*]pyrene **8** in the presence of macrocycle **5**.

Computational Structures:

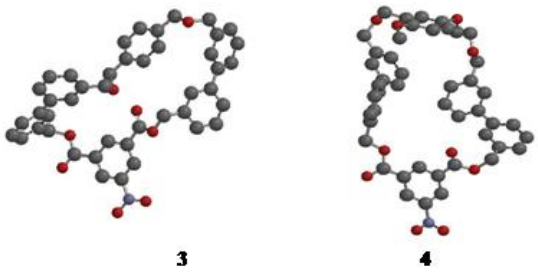

Fig. S11: Energy-minimized conformations of macrocycles **3** and **4 (**hydrogen atoms omitted for clarity).

Copies of all NMR Spectra:

^{1}H NMR of compound **S10** in $CDCl_3$ (300 MHz):

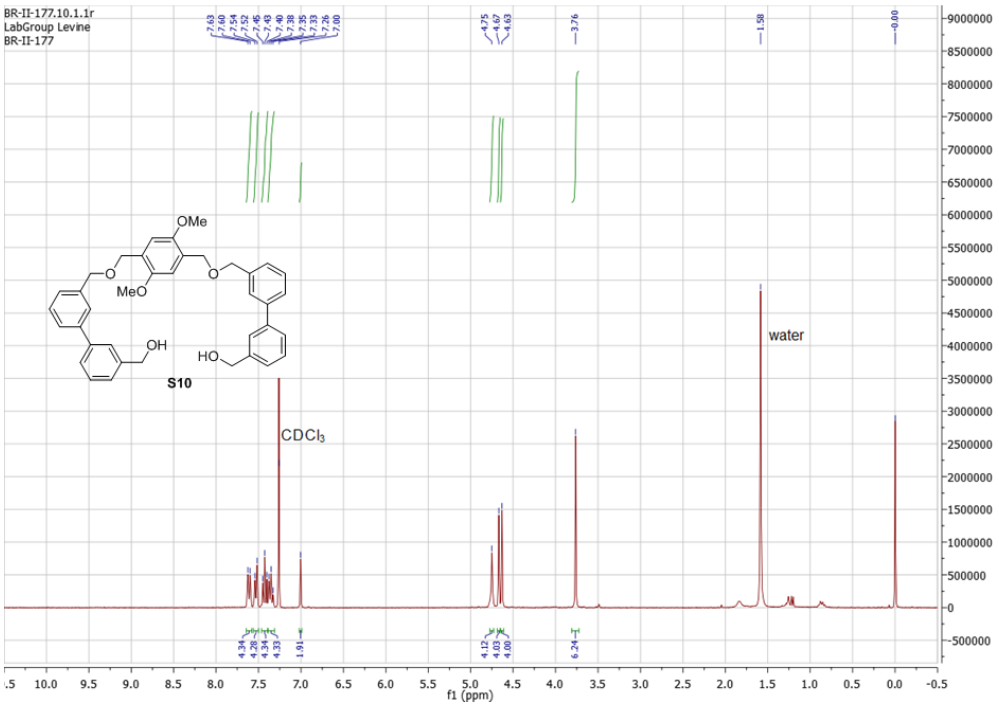

^{13}C NMR of compound **S10** in $CDCl_3$ (75 MHz):

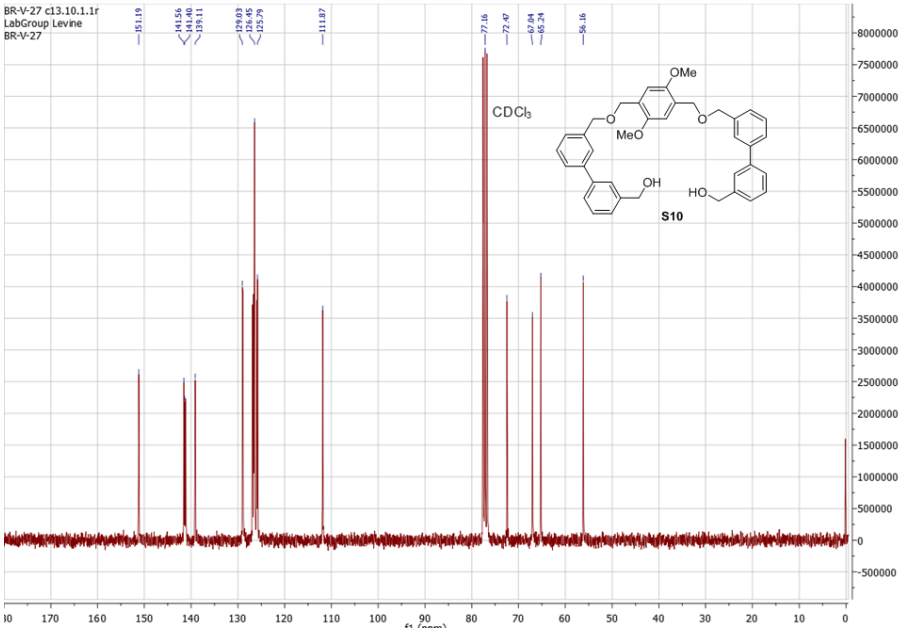

^{1}H NMR of macrocycle **1** in $CDCl_3$ (300 MHz):

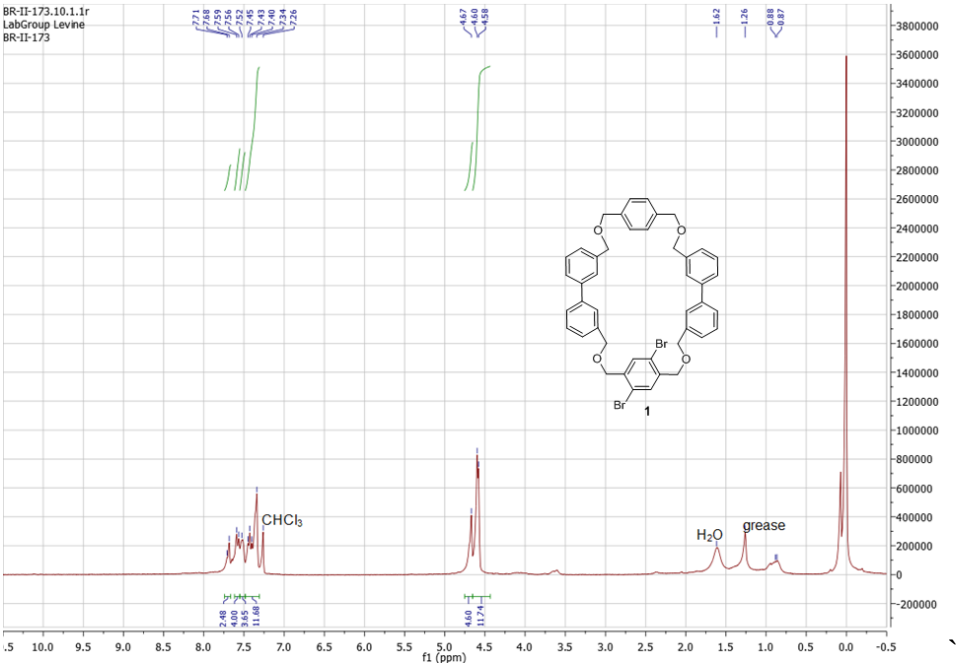

^{13}C NMR of macrocycle **1** in $CDCl_3$ (75 MHz):

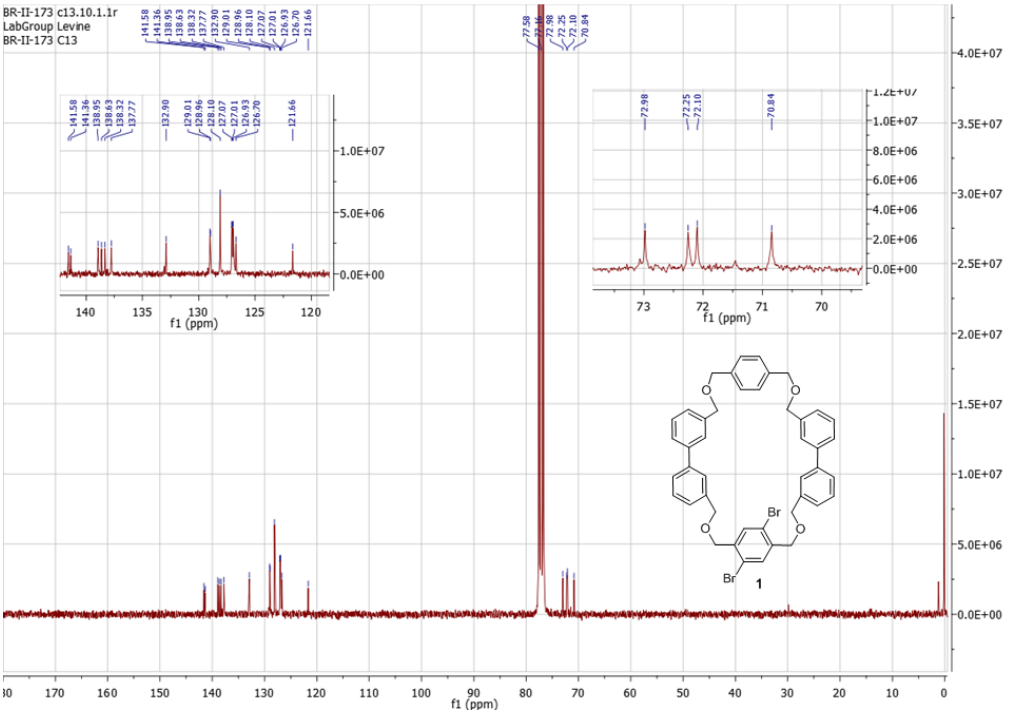

^{1}H NMR of macrocycle **2** in $CDCl_3$ (300 MHz):

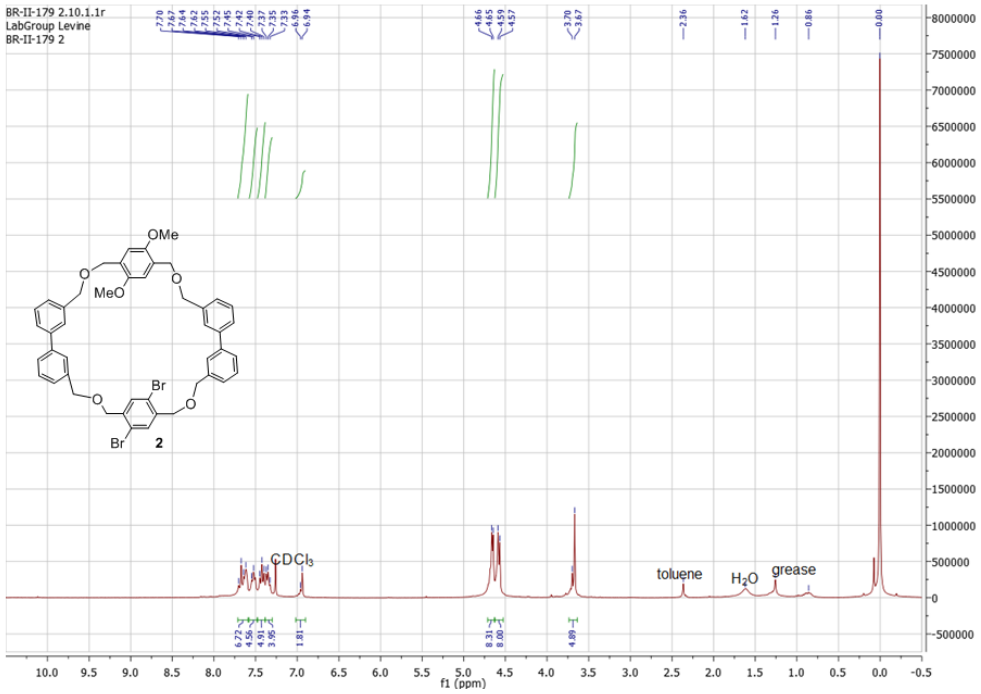

^{13}C NMR of macrocycle **2** in $CDCl_3$ (75 MHz):

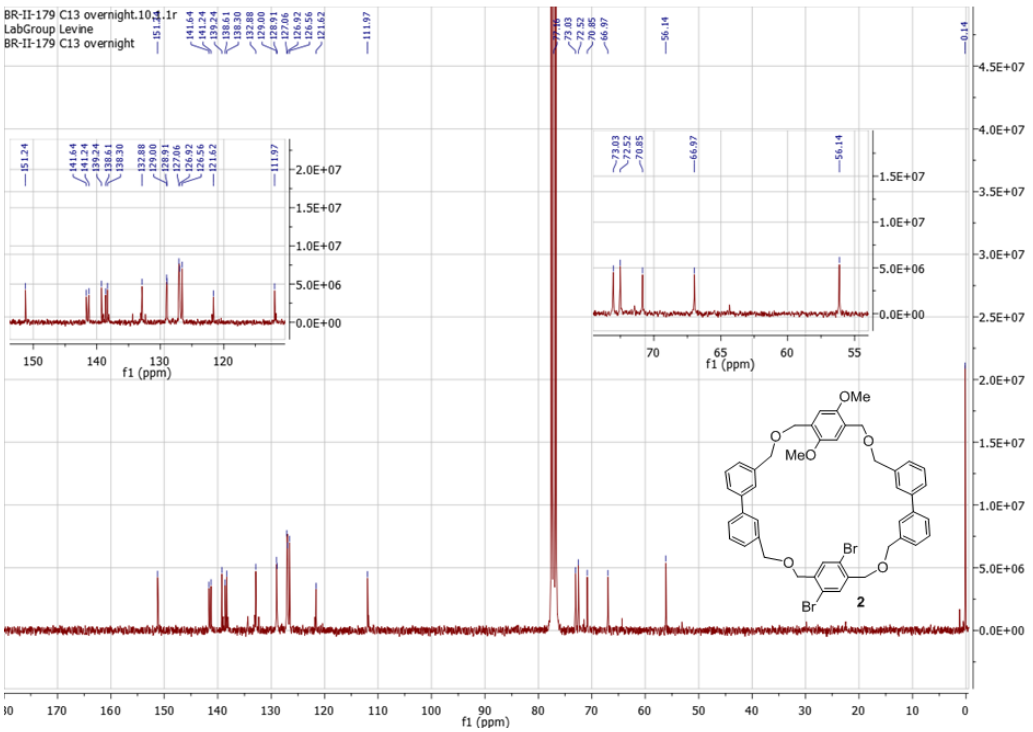

^{1}H NMR of macrocycle **3** in $CDCl_3$ (300 MHz):

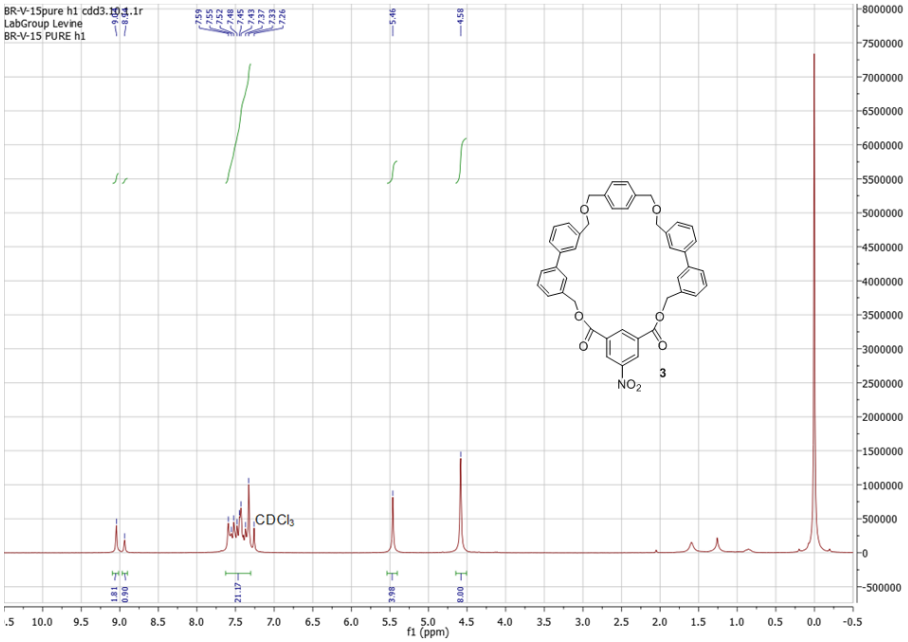

^{13}C NMR of macrocycle **3** in $CDCl_3$ (75 MHz):

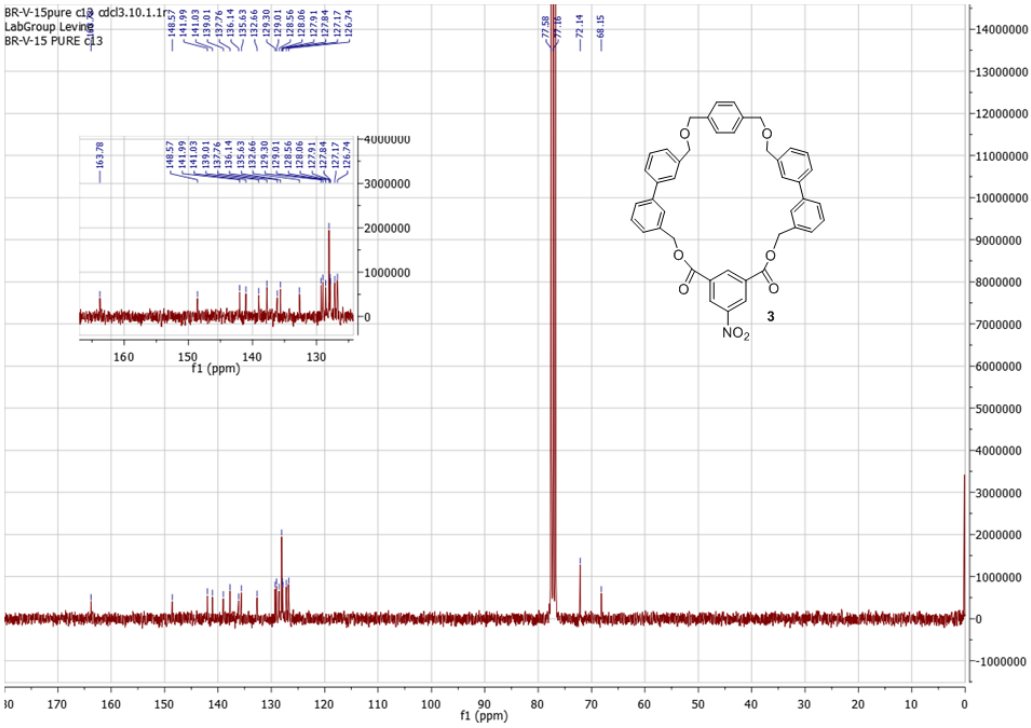

^{1}H NMR of macrocycle **4** in $CDCl_3$ (300 MHz):

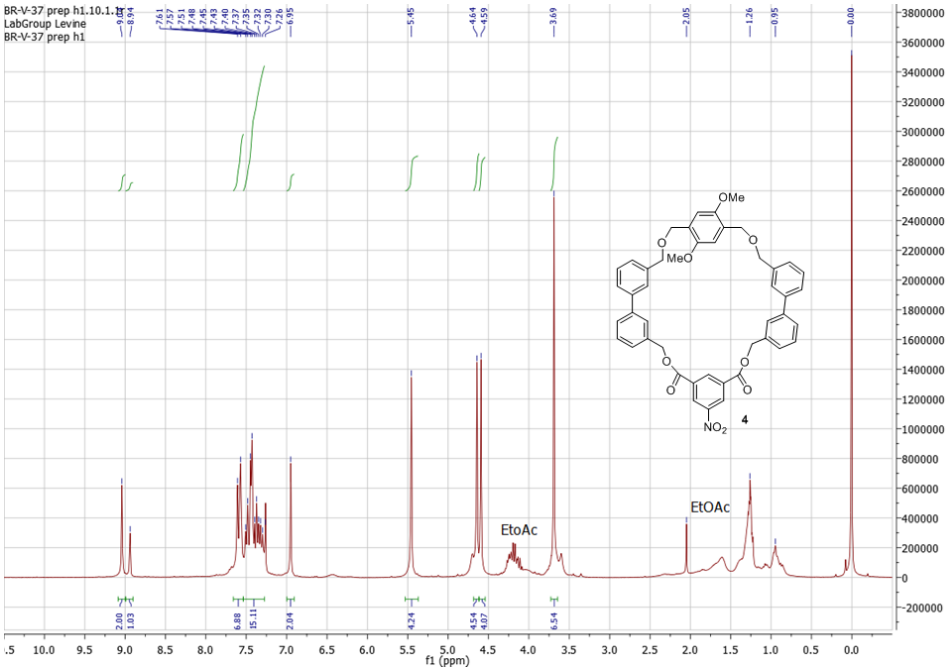

^{13}C NMR of macrocycle **4** in $CDCl_3$ (75 MHz):

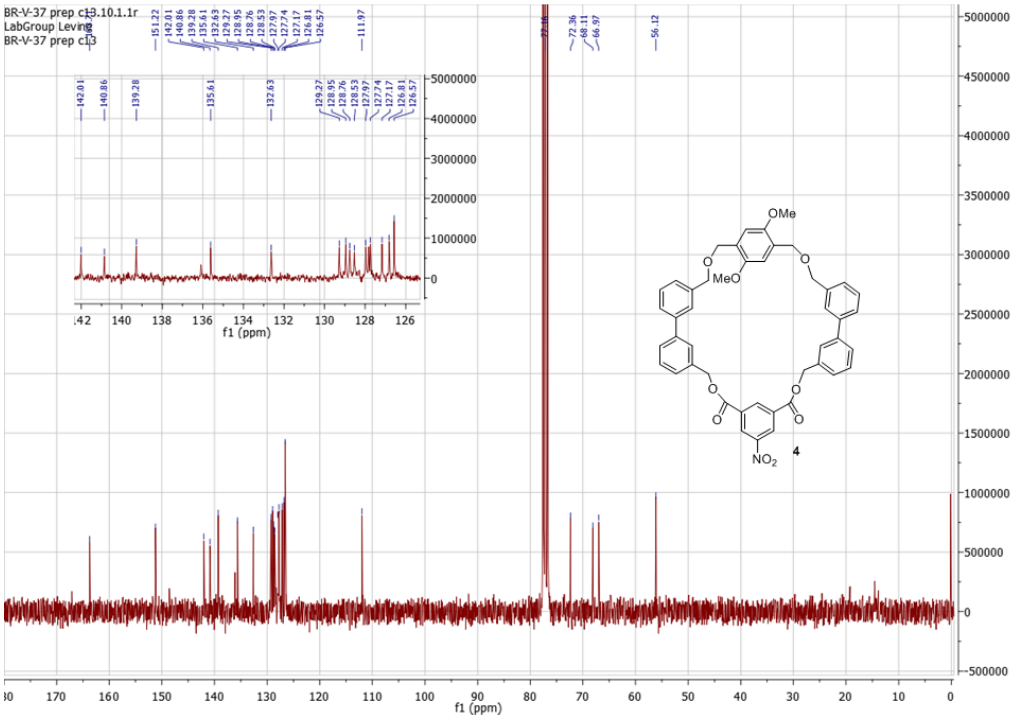

^{1}H NMR of macrocycle **5** in $CDCl_3$ (300 MHz):

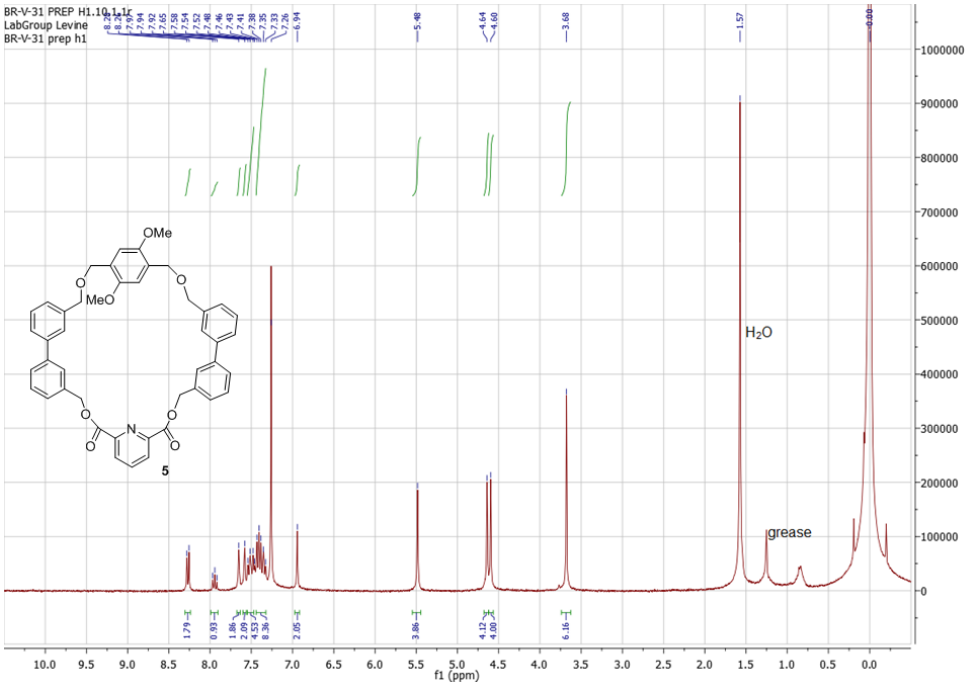

^{13}C NMR of macrocycle **5** in $CDCl_3$ (75 MHz):

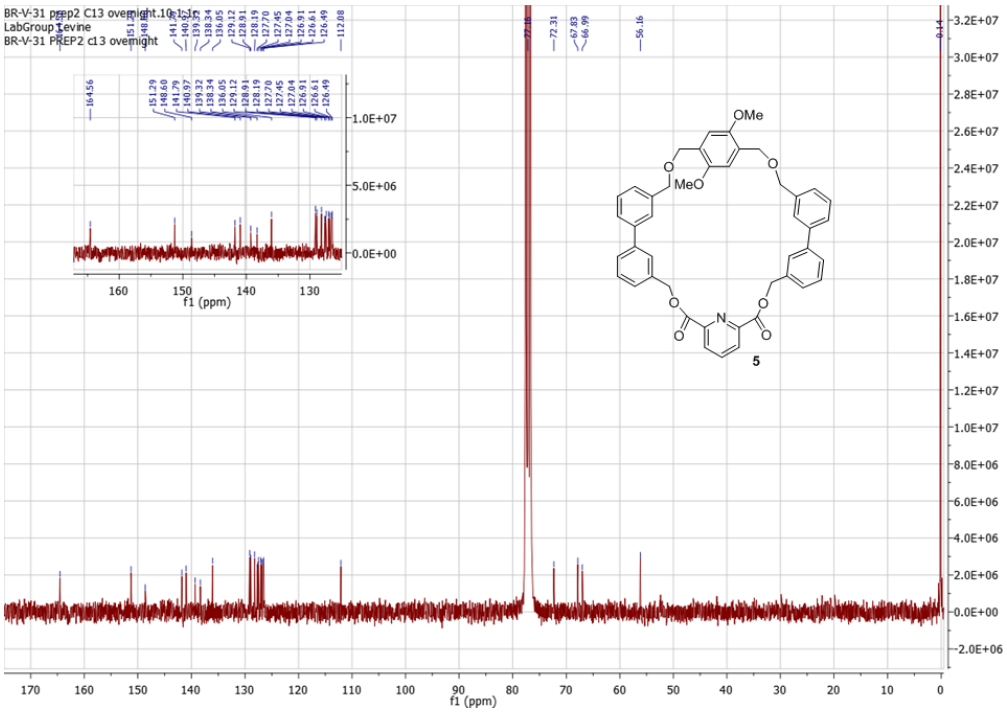

^{1}H NMR of macrocycle **6** in $CDCl_3$ (300 MHz):

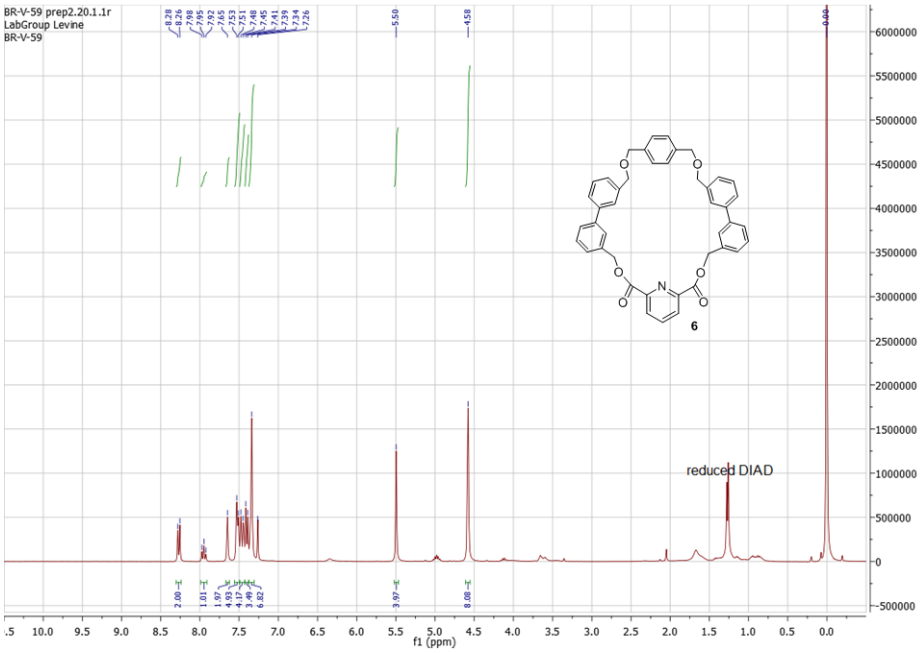

^{13}C NMR of macrocycle **6** in $CDCl_3$ (75 MHz):

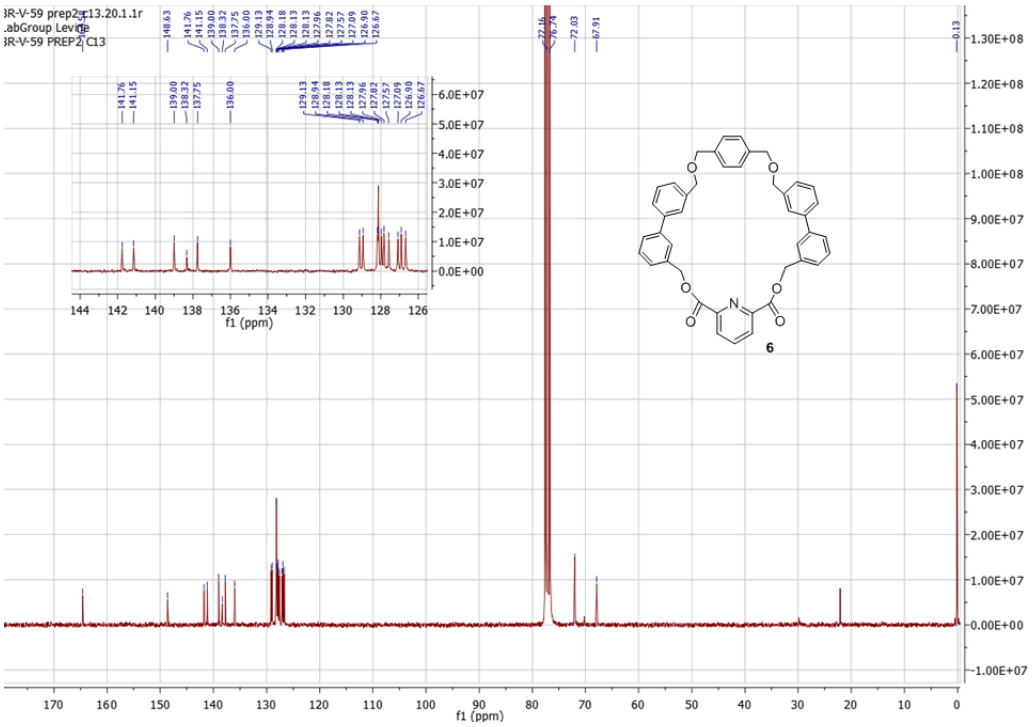

MANUSCRIPT 3

This manuscript is published in *Tetrahedron Lett.*, **2014**, *55*, 4905-4908.

A Green Bromination Method for the Synthesis of BenzylicDibromides

Bhasker Radaram, and Mindy Levine*

Corresponding author:

Prof. Mindy Levine

Department of Chemistry

University of Rhode Island

Kingston, Rhode Island 02881

mlevine@chm.uri.edu

MANUSCRIPT 3

A green bromination method for the synthesis of benzylic dibromides

Abstract

Reported herein is the identification of new methodology for the dibromination of benzylic diols. This method proceeds in moderate to good yields for a wide variety of electron-deficient, electron-neutral, and electron-rich aromatic substrates. Moreover, the reagent, 1,3-dibromo-5,5-dimethylhydantoin, and the solvent, tetrahydrofuran, are substantially more environmentally benign than traditional solvents and reagents used for bromination. The utility of this methodology was demonstrated in the high-yielding synthesis of a key intermediate in the synthesis of omeprazole.

Introduction

The bromination of benzylic alcohols to yield benzylic bromides is a widely used transformation in synthetic organic chemistry,[1] with applications in the synthesis of key drug intermediates,[2] natural products,[3] highly functionalized materials,[4] and multiple dyes and pigments.[5] Conventional reagents for the bromination of benzylic alcohols include molecular bromine,[6] hydrobromic acid,[7] carbon tetrabromide,[8] and *N*-bromosuccinimide (NBS).[9] Conventional solvents for this transformation include chloroform, dichloromethane, and carbon tetrachloride.

All of the brominating reagents and solvents listed above have been shown to be harmful to the environment,[10] toxic to a wide variety of organisms,[11] and expensive to use and dispose of safely.[12] More environmentally benign reagents and solvents that efficiently brominate a wide variety of substrates would provide significant operational advantages in accomplishing such synthetic transformations while limiting the potential environmental damage.

Some examples of environmentally benign bromination methods include the use of solvent-free conditions,[13] ionic liquids,[14] and aqueous solvents[15] to promote the reactions of organic substrates with bromine-containing salts. The substrates for these reactions include both alkenes and aromatic compounds; however, bromination of benzylic alcohols using environmentally benign reagents has not been reported to date.

1,3-dibromo-5,5-dimethylhydantoin (DBDMH, compound **2**) has been well-studied in the literature as a catalyst,[16] oxidant,[17] and commercial disinfectant.[18]It has also been used as a bromination reagent for aromatic C-H bonds,[19] alkenes,[20] and alkynes.[21] These literature precedents prompted our investigation into the use of this reagent as a less toxic bromination reagent to achieve efficient benzylic bromination.

Results

Initial investigations focused on the synthesis of dibromide **3a**, driven by ongoing research in the synthesis of electronically-differentiated macrocycles (Scheme 1).[22] A screen of various reaction conditions quickly led to the identification of optimal conditions (Table 1, entry 6): tetrahydrofuran (THF) solvent, 2.2 equivalents of DBDMH and triphenylphosphine, 2 hour reaction time, and a reaction temperature of 0 ^{o}C to room temperature. Under these optimized conditions, compound **1a** was converted to its dibrominated product **3a** in 54% yield (with no detectable amounts of monobrominated compound **3aa**), compared to the 64% yield observed when the same substrate was treated with carbon tetrabromide in dichloromethane. Both the DBDMH reagent and THF solvent are substantially less environmentally harmful than the previously used bromination reagent and solvent,[23] and led to only a mild reduction in the product yield.

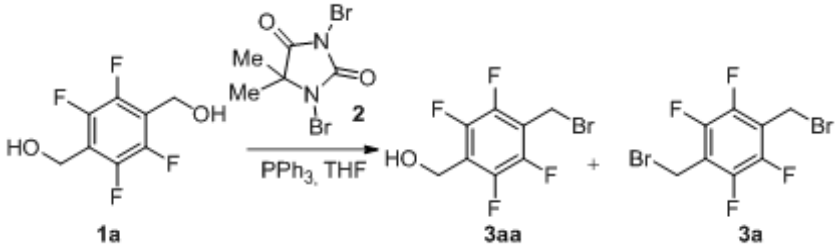

Scheme 1. Synthesis of **3a**

Under these optimized conditions, a wide variety of electron-deficient benzylic diols were converted to their corresponding dibromides in moderate to good yields (Scheme 2, compounds **3a**-**3g**). Multiple substitution patterns were well-tolerated (both 1,4-diols and 1,3-diols worked well), as were a wide variety of electron-deficient substituents. Interestingly, whereas one bromine substituent was well-tolerated (compound **3c**), the introduction of two bromine substituents completely shut down the bromination to form compound **3f**. Rather, a mixture of mono- and dialdehydes was formed under these conditions. DBDMH is a well-known oxidant;[17] however, it is interesting that this is the only substrate for which such reactivity was observed.

Table 1. Optimization of Reaction Conditions

	solvent	eq. **2**	time	temp.	yield **3aa**	yield **3a**
1	CH_3CN	1.1	1 hr	0 ^oC	30%	15%
2	CH_3CN	1.5	1.5 hr	RT	39%	19%
3	CH_3CN	2.5	3 hr	0 ^oC-RT	0%	53%
4	EtOAc	2.2	2 hr	RT	0%	17%
5	THF	2.2	2 hr	0 ^oC	0%	50%
6	THF	2.2	2 hr	0 ^oC-RT	0%	54%

These reaction conditions also worked well for a variety of electron-neutral and electron-rich benzylic diols (compounds **3h**-**3n**), which formed the benzylic dibromide products. Again, multiple substitution patterns were well-tolerated, with 1,2-, 1,3- and 1,4-diol substrates proceeding in high yields. The only limitation observed for these substrates is that the presence of a hydroxyl group or methoxy group at the meta position led to a 0% yield of compounds **3j** and **3k**. Instead, substrates **1j** and **1k** underwent both benzylic bromination as well as aromatic bromination to form compounds **3jj** and **3kk**, in accordance with the literature precedent (see ESI for a detailed structural elucidation).[24] The strongly activating nature of the hydroxyl group, combined with its small steric size, leads to the bromination of all available ortho- and para- positions to form **3jj**.The methoxy substituent, by contrast, directs para- bromination to form **3kk**, but has sufficient steric bulk to shut down the ortho-bromination pathway. The bromination reaction also proceeded well for a heteroaromatic diol to yield the desired dibromide in moderate yield (compound **3n**).

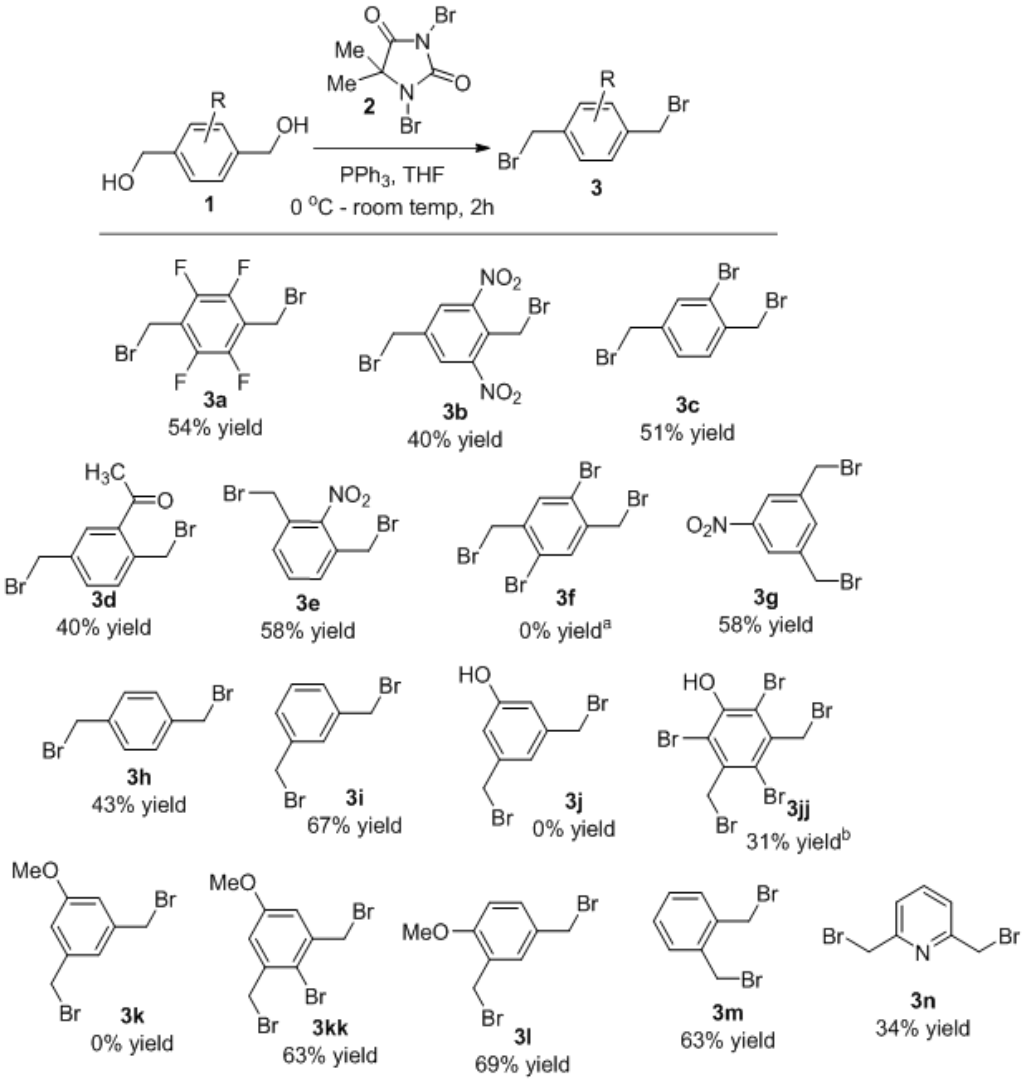

a The reaction of diol **1f** led to the formation of a mixture of aldehydes rather than the desired dibromide **3f**.

b The reactions of **1j** and **1k** led to the formation of **3jj** and **3kk** rather than **3j** and **3k**.

Scheme 2. Synthesis of Benzylic Dibromides

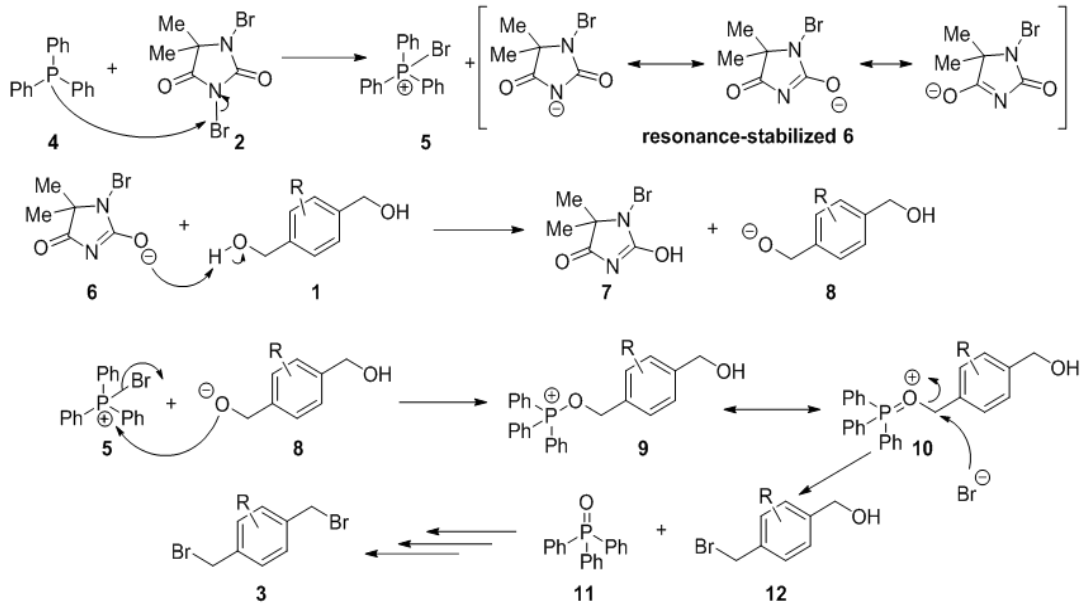

Scheme 3. Proposed Mechanism for the Dibromination of Benzylic Diols with DBDMH

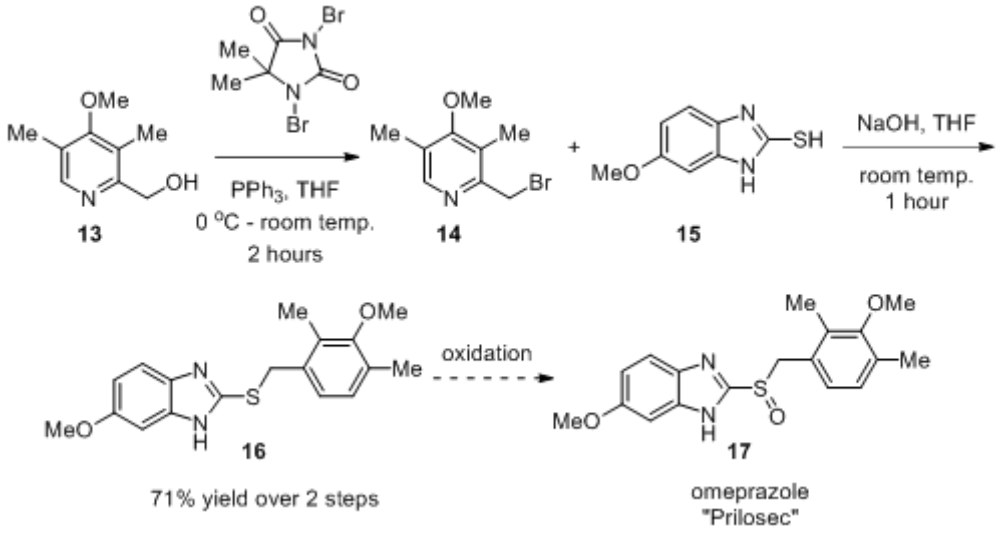

Scheme 4. Application of DBDMH Bromination in the Synthesis of an Omeprazole Precursor

A direct comparison of the yields obtained using DBDMH and CBr_4 in THF are shown in Table 2, and indicate that the DBDMH bromination yields were equal to or higher than yields obtained using CBr_4 for all substrates investigated. Whereas CBr_4 worked well for electron-deficient substrates **1a-e**, it was much less efficient for electron-rich substrates. DBDMH, by contrast, led to moderate to good bromination yields in all cases, and has the added advantage of being substantially less toxic to both the environment and to human health. Although higher yields for DBDMH-promoted reactions could likely be found in chlorinated solvents, our focus on green chemistry led us away from pursuing that direction of research.

Discussion

The proposed mechanism of this reaction is shown in Scheme 3, and involves the initial formation of a phosphonium bromide salt **5** and highly resonance-stabilized anion **6**, which deprotonates one of the benzylic diols to form anion **8**. Nucleophilic attack of compound **8** on phosphonium **5** leads to the formation of intermediate **9**, which undergoes nucleophilic attack by a bromide ion to form the monobrominated product. Repeating this mechanistic sequence then leads to the formation of the desired dibromide product. In support of this mechanistic proposal, both DBDMH and triphenylphosphine were shown to be essential for achieving the desired reactivity.

Table 2. Percent Yield Comparison Using DBDMH and CBr_4 as Brominating Agents

substrate	DBDMH[a]	CBr_4[b]
1a	53%	55%
1b	40%	40%
1c	51%	20%
1d	40%	35%
1e	58%	25%
1g	58%	33%
1h	43%	11%
1i	67%	14%
1m	63%	28%

a DBDMH, PPh_3, THF, 0 ^oC to room temp., 2 hours

b CBr_4, PPh_3, THF, 0 ^oC to room temp., 16 hours

Finally, the practical utility of this benzylic bromination methodology was demonstrated through a one-pot synthesis of a key precursor for omeprazole **17**, a commercially available antacid (Prilosec) (Scheme 4). The monobromination of compound **13** occurred using DBDMH in THF, and was followed by removal of the solvent and introduction of sulfide**15** under basic conditions to generate compound **16** in 71% yield over two steps. Compound **16** is remarkably close to the structure of Prilosec (compound **17**), requiring only an oxidation of the sulfur to complete the synthetic sequence.

A direct comparison of several common brominating reagents (DBDMH, CBr_4, N-Bromosuccinimide, and bromine in acetic acid) indicates that DBDMH has several operational advantages. It is substantially cheaper than both CBr_4 and bromine in acetic acid,[25] it is stable at room temperature (unlike both N-bromosuccinimide and bromine in acetic acid, which require cold temperature storage), and it is purchased as an easy-to-handle white solid. Additional advantages were found when the reactions of substrate **1h** and **1l** were scaled to 4 and 8 times the standard scale. Under theses scaled-up conditions, compound **3h** was formed in 70% yield for both 2.9 mmol and 5.8 mmol scale reactions, compared to the 43% yield observed under standard conditions. Compound **3l** was formed in 65% isolated yield on 2.4 mmol and 4.8 mmol scales, highlighting the practical utility of this methodology for larger scale reactions.

Conclusion

In conclusion, a new methodology for benzylic bromination using an environmentally friendly solvent and reagent is reported herein. This methodology has a number of advantages compared with traditional bromination reactions, including the ability to achieve good yields for a wide range of electron-rich, electron-deficient, and electron-neutral substrates, the substantially reduced reagent toxicity, and the ability to conduct these reactions in environmentally benign tetrahydrofuran rather than more toxic chlorinated solvents. The applications of this methodology in the synthesis of more complex molecules, as well as detailed mechanistic investigations, are currently underway in our group, and results will be reported in due course.

References

1. (a) Shibatomi, K.; Zhang, Y.; Yamamoto, H. *Chem. Asian. J.* **2008**, *3*, 1581-1584; (b) Joseph, K. M.; Larraza-Sanchez, I. *Tetrahedron Lett.* **2011**, *52*, 13-16.
2. (a) Mistry, S. N.; Valant, C.; Sexton, P. M.; Capuano, B.; Christopoulos, A.; Scammells, P. J. *J. Med. Chem.* **2013**, *56*, 5151-5172; (b) Abbasi, M. A.; Aziz-Ur-Rehman; Muhmood, T.; Khan, K. M.; Ashraf, M.; Ejaz, S. A.; Arshad, S. *J. Chem. Soc. Pakistan* **2013**, *35*, 405-411.
3. (a) Qiu, Y.; Ma, D.; Fu, C.; Ma, S. *Org. Biomol. Chem.* **2013**, *11*, 1666-1671; (b) Mascall, K. C.; Jacobi, P. A. *Heterocycles* **2014**, *88*, 1527-1538.
4. (a) Wagner, M.; Nuyken, O. *Macromolecules* **2003**, *36*, 6716-6721; (b) Zhao, C. H.; Gong, Y.; Liu, Q. L.; Zhang, Q. G.; Zhu, A. M. *Int. J. Hydrogen Energy* **2012**, *37*, 11383-11393
5. (a) Pedersen, M. *Phytochem.* **1978**, *17*, 291-298; (b) Rath, P. C.; Jesthi, P. K.; Mishra, P. K.; Rout, M. K. *Indian J. Chem.***1966**, *4*, 24-26.
6. Stefely, J. A.; Palchaudhuri, R.; Miller, P. A.; Peterson, R. J.; Moraski, G. C.; Hergenrother, P. J.; Miller, M. J. *J. Med. Chem.* **2010**, *53*, 3389-3395.
7. Moghaddam, F. M.; Farimani, M. M. *Tetrahedron Lett.* **2010**, *51*, 540-542.
8. Hawker, C. J.; Frechet, J. M. J. *Macromolecules* **1990**, *23*, 4726-4729.
9. Lee, J. C.; Hwang, E. Y. *Synth. Commun.* **2004**, *34*, 2959-2963.
10. (a) Sturchio, E.; Boccia, P.; Zanellato, M.; Beni, C.; Bagni, G.; Mascini, M.; Pezzella, M. *Int. J. Environ. Health* **2007**, *1*, 563-579; (b) McCulloch, A. *Chemosphere* **2003**, *50*, 1291-1308; (c) Kim, K.-H.; Shon, Z.-H.; Nguyen, H. T.; Jeon, E.-C. *Atmospheric Environ.* **2011**, *45*, 1369-1382.

11. (a) Roldan-Arjona, T.; Pueyo, C. *Mutagenesis* **1993**, *8*, 127-131; (b) Rogers, J. V.; Price, J. A. *Target Organ Toxicol. Series* **2010**, *29*, 375-387.
12. Pekelney, D. *J. Hazard. Mater.* **1990**, *23*, 293-315.
13. (a) Kumar, A.; Alimenla, B.; Jamir, L.; Sinha, D.; Sinha, U. B. *Organic Commun*. **2012**, *5*, 64-69; (b) Sinha, U. B. *J. Applicable Chem.* **2012**, *1*, 137-142.
14. (a) Wang, H.; Wen, K.; Nurahmat, N.; Shao, Y.; Zhang, H.; Wei, C.; Li, Y.; Shen, Y.; Sun, Z. *Beilstein J. Org. Chem*. **2012**, *8*, 744-748; (b) Primerano, P.; Cordaro, M.; Scala, A. *Tetrahedron Lett*. **2013**, *54*, 4061-4063.
15. (a) Khosravi, K.; Kazemi, S. *Chinese Chem. Lett.* **2012**, *23*, 387-390; (b) Hou, J.; Li, Z.; Jia, X.-D.; Liu, Z.-Q. *Synth. Commun*. **2014**, *44*, 181-187.
16. (a) Shirini, F.; Zolfigol, M. A.; Paktinat, M. *Synthesis* **2006**, 4252-4256; (b) Hojati, S. F.; Zeinali, T.; Nematdoust, Z. *Bull. Korean Chem. Soc.* **2013**, *34*, 117-120.
17. (a) Khazaei, A.; Abbasi, F.; Kianiborazjani, M.; Saednia, S. *J. Brazilian Chem. Soc.* **2014**, *25*, 361-364; (b) Li, Z.; Zhu, W.; Bao, J.; Zou, X. *Synth. Commun*. **2014**, *44*, 1155-1164.
18. Song, S.; Liu, P.; Song, Q. J. *Anal. Sci*. **2007**, *23*, 327-330.
19. Barrett, K. T.; Miller, S. J. *J. Am. Chem. Soc*. **2013**, *135*, 2963-2966.
20. Yin, Q.; You, S.-L. *Org. Lett.* **2012**, *14*, 3526-3529.
21. Cann, R. O.; Waltermire, R. E.; Chung, J.; Oberholzer, M.; Kasparec, J.; Ye, Y. K.; Wethman, R. *Org. Process Res. Dev*. **2010**, *14*, 1147-1152.
22. Radaram, B.; Potvin, J.; Levine, M. *Chem. Commun*. **2013**, *49*, 8259-8261.
23. Ramgren, S. D.; Hie, L.; Ye, Y.; Garg, N. K. *Org. Lett*. **2013**, *15*, 3950-3953.
24. Chassaing, C.; Haudrechy, A.; Langlois, Y. *Tetrahedron Lett.***1997**, *38*, 4415-4416.
25. DBDMH: $0.08/gram; CBr_4: $0.39/gram; NBS: $0.10/gram; Br_2 in AcOH: $0.37/gram.

Electronic Supporting Information for

A Green Bromination Method for the Synthesis of BenzylicDibromides

Bhasker Radaram and Mindy Levine[*]

MATERIALS AND METHODS

All reactions were carried out under a dry nitrogen atmosphere unless otherwise noted. Solvents were dried using an MBraun dual solvent purification system prior to use. Tetrahydrofuran (THF) was dried using sodium/benzophenone and refluxed for 16 hours, followed by distillation to obtain anhydrous THF. Starting materials, reagents and solvents used in this methodology were purchased from Sigma-Aldrich, Acros Organics, TCI America, Matrix Scientific, and Fisher Scientific and were used as received. All reactions were monitored by analytical thin layer chromatography (TLC) technique. Polyester backed-TLC plates were purchased from Sorbent Technologies, GA. Visualization was accomplished with UV light at 254 nm. Column chromatography was performed with silica gel (250-400 mesh) supplied by Silicycle Incorporated.

^{1}H, ^{13}C, and ^{19}F NMR spectra were recorded on a Bruker 300 MHz spectrometer. Multiplicities for ^{1}H NMR spectra were reported as follows: s = singlet, d = doublet, t = triplet, m = multiplet, br = broad singlet.^{1}H NMR chemical shifts were determined relative to residual solvent peaks such as $CDCl_3$ at 7.26 ppm, and DMSO-d_6 at 2.50 ppm. ^{13}C NMR chemical shifts were determined relative to thesolvent, $CDCl_3$ at 77.23 ppm, DMSO-d_6 at 39.52 ppm, and CD_3CN at 118.26 ppm, respectively. High resolution mass spectra were obtained from a BrukerDaltonics APEXIV 4.7 Tesla Fourier Transform Ion Cyclotron Resonance Mass Spectrometer (FT-ICR-MS) at Massachusetts Institute of Technology, in collaboration with Dr. Li Li.

CHART OF COMMERCIALLY AVAILABLE STARTING MATERIALS

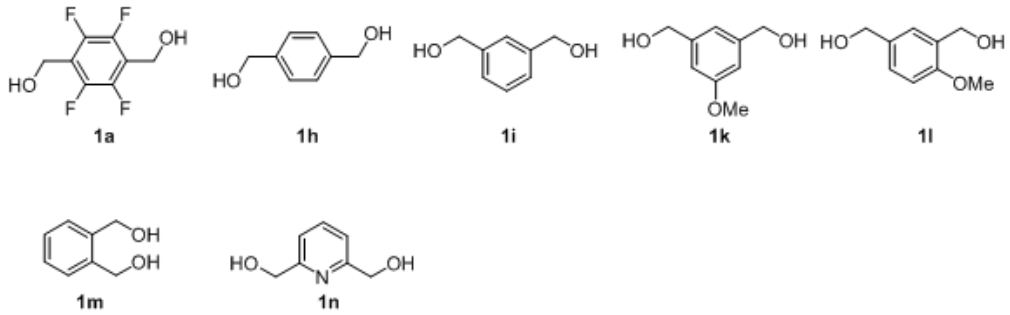

SYNTHETIC DETAILS FOR PREPARATION OF STARTING MATERIALS

Synthesis of 2,6-dinitro-1,4-dihydroxymethylbenzene (1b):

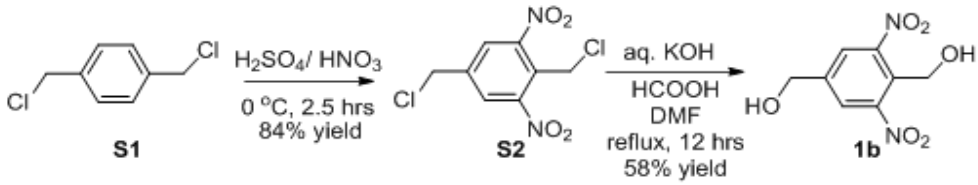

Compound **1b**was prepared according to the reported procedure.[1]

Synthesis of 2,5-bis(hydroxymethyl)bromobenzene (1c):

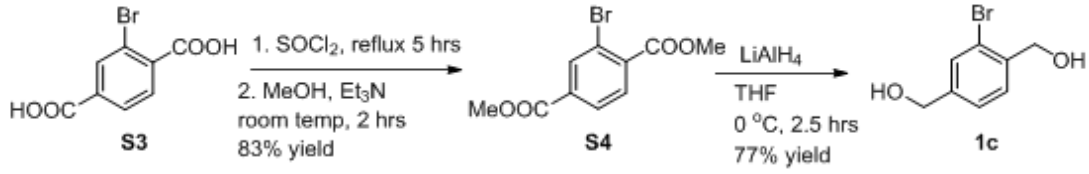

Compound **S4** was prepared according to the reported procedure.[2]

Synthesis of 2,5-bis(hydroxymethyl)bromobenzene (**1c)**: To a stirred solution of **S4**(1.24 g, 4.54mmol, 1.0 eq.)in anhydroustetrahydrofuran (35 mL) at 0 ^{o}C was added lithium aluminum hydride (0.43 g, 11.35 mmol, 2.5 eq.)portion-wise slowly over a period of 5 minutes. After the addition was complete, the reaction mixture was stirred at 0 ^{o}C for 2.5 hours. After the

completion of the reaction, the reaction mixture was quenched by the slow addition of methanol (3 mL), followed by the slow addition of water (5 mL). The reaction mixture was allowed to stir for 15 minutes then filtered through a bed of celite. The filtrate was concentrated under reduced pressure to obtain 2,5-bis(hydroxymethyl)bromobenzene (**1c**) as an off-white solid (0.703 g, 77% yield).^{1}H NMR (300 MHz, DMSO-d_6): δ = 7.48 (m, 2H), 7.28 (m, 1H), 5.40 (s, 1H), 5.29 (s, 1H), 4.49 (br. s, 4H). ^{13}C NMR (75 MHz, DMSO-d_6): δ = 143.38, 139.17, 129.77, 127.95, 125.53, 120.87, 62.51, 61.93.HR-MS (ESI): Calcd for $[M+NH_4^+, C_8H_{13}BrNO_2]^+$ 234.0130, found 234.0131.

Synthesis of 2,5-bis(hydroxymethyl)acetophenone (1d):

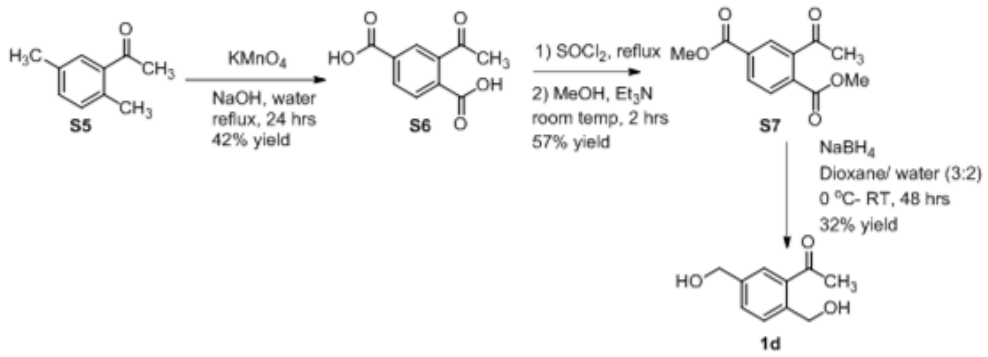

Synthesis of 2-acetyl-1,4-benzenedicarboxylicacid (**S6**):2-acetyl-1,4-benzenedicarboxylic acid was synthesized according to a literature method.[3]A stirred mixture of 2,5-dimethyl acetophenone (**S5**) (3.15 g, 21.25mmol, 1.0 eq.), water (100 mL) and sodium hydroxide (1.27 g, 31.88 mmol, 1.5 eq.) was heated to 95^{o}C, then $KMnO_4$ (13.43 g, 84.98mmol, 4.0 eq.) was added in portions over a period of 2.5 hours. The resulting mixture was refluxed for 24 hours. The reaction mixture was cooled to room temperature and filtered. The filtratewas acidified with concentrated hydrochloric acid (2 mL), and the resulting precipitate was filtered to obtain compound **S6** as a white solid (1.85 g, 42% yield).^{1}H NMR (300 MHz, DMSO-d_6): δ = 13.07

(br, 2H), 8.38 (s, 1H), 7.97 (d, 1H, J = 9.6 Hz), 7.43 (d, 1H, J = 8.1 Hz), 2.58 (s, 3H).^{13}C NMR (75 MHz, DMSO-d_6): δ = 167.94,166.66, 144.38, 132.19, 132.10, 131.22, 130.63, 128.58, 21.43.HR-MS (ESI): Calcd for [M+H^+,$C_{10}H_9O_5$]$^+$209.0450, found 209.0809.

Synthesis of 2-acetyl-1,4-bis(methyl)benzenedicarboxylate (**S7**):A solution of 2-acetyl-1,4-benzenedicarboxylic acid (**S6**) (1.90 g, 9.12 mmol, 1.0 eq.) in thionyl chloride(6.66 mL, 91.27 mmol, 10 eq.) was gradually heated to 100 ^{o}C andstirred for 5 hours at 100 ^{o}C. After 5hours, excess thionyl chloride was evaporated in vacuo. The flask was cooled to 0 ^{o}C, and methanol (10 mL) and triethylamine (5 mL) were added dropwise while stirring. The resulting mixture was stirred at room temperature for 2 hours and the solvent was then evaporated. The residue was dissolved in ethylacetate (15 mL), and washed with 1N HCl(10 mL) followed by 1N $NaHCO_3$(10 mL). The organic layer was further washed with brine and dried over anhydrous sodium sulfate, filtered, and concentrated via rotary evaporation to yield the crude product. The product was purified by washing with hexanes to afford compound **S7** as an off-white solid (0.70 g, 32% yield). ^{1}H NMR (300 MHz, $CDCl_3$): δ = 8.57(s, 1H), 8.04 (d, 1H, J = 9.6 Hz), 7.32 (d, 1H, J = 7.8 Hz), 3.93 (s, 6H),2.66 (s, 3H).^{13}C NMR (75 MHz, DMSO-d_6): δ = 167.37, 166.54, 145.79, 132.84, 132.17, 129.93, 128.15, 52.41, 22.09.HR-MS(ESI): Calcd for [M+H^+,$C_{12}H_{13}O_5$] 237.0763, found 237.0775.

Synthesis of 2-acetyl-1,4-benzenedimethanol (**1d**): 2-acetyl-1,4-benzenedimethanol was synthesized according to a literature procedure.[4]2-acetyl-1,4-bis(methyl)benzenedicarboxylate (**S7**) (0.40 g, 1.69 mmol, 1.0eq.) was dissolved in a 3:2 ratio of 1,4-dioxane:water (25 mL total volume) and cooled to 0 ^{o}C. $NaBH_4$ (0.64 g, 16.92 mmol, 10.0 eq.) was then added slowly. The reaction mixture was stirred at room temperature for 48 hours. Excess $NaBH_4$ was quenched by the addition of 6N HCl (2 mL) dropwise over a period of 30 minutes. The product was extracted with ethyl acetate (3 portions of 10 mL), and the combined organic

extract was washed with brine, dried over anhydrous sodium sulfate, filtered and concentrated via rotary evaporation to yield the crude product as an off-white solid. The crude product was purified by silicagel flash chromatography (6:4 ethylacetate:hexanes as an eluent) to afford the compound **1d** as an off-white solid (0.096 g, 32% yield).^{1}H NMR (300 MHz, DMSO-d_6): δ = 7.31 (s, 1H), 7.06 (s, 2H), 5.06 (m, 2H), 4.45 (t, 4H, J = 6.3 Hz), 2.20 (s, 3H).^{13}C NMR (75 MHz, DMSO-d_6): δ = 139.82, 139.62, 133.14, 129.28, 125.07, 124.71, 62.93, 61.09, 17.92. HR-MS (ESI): Calcd for [M+H+, $C_{10}H_{13}O_3]^+$ 181.0865, found 181.0875.

Synthesis of 2-nitro-1,3-benzenedimethanol (1e):

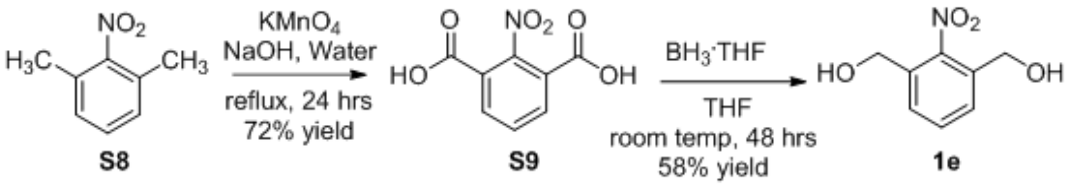

Compound **1e**was prepared according to the reported literature procedure.[3]

Synthesis of 5-nitro-1,3-benzenedimethanol (1g):

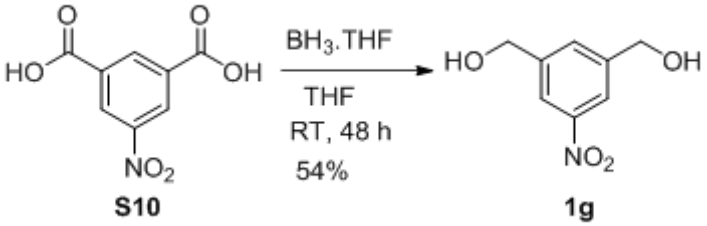

Synthesis of 5-nitro-1,3-benzenedimethanol (**1g**): A solution of 5-nitroisophthalic acid (**S10**) (1.0 g, 4.73mmol, 1.0 eq.) in dry THF (8 mL) was cooled to 0 ^{o}C and was added to a solution of 1.0 M borane-THF (22.66 mL) dropwise over a period of 1 hour. The reaction mixture was allowed to warm slowly to room temperature and stirred for another 48 hours. The reaction

mixture was then quenched with the slow addition of methanol (5 mL) via syringe. The resulting mixture was evaporated and the residue was dissolved in ethyl acetate (25 mL), washed with water (3 portions of 15 mL each), dried over anhydrous sodium sulfate, filtered and concentrated via rotary evaporation to yield the product **1g** as pale yellow solid (0.465 g, 54% yield).^{1}H NMR (300 MHz, DMSO-d_6): δ = 8.04 (s, 2H), 7.70 (s, 1H), 5.53 (t, 2H, J = 5.7 Hz), 4.62(d, 4H, J = 5.7 Hz).^{13}C NMR (75 MHz, DMSO-d_6): δ = 147.84, 144.87, 130.41, 119.00, 61.87. HR-MS (ESI): Calcd for $[M+NH_4^+, C_8H_{13}N_2O_4]^+$201.0875, found 201.0872.

Synthesis of 3,5-bis(hydroxymethyl)phenol (1j):

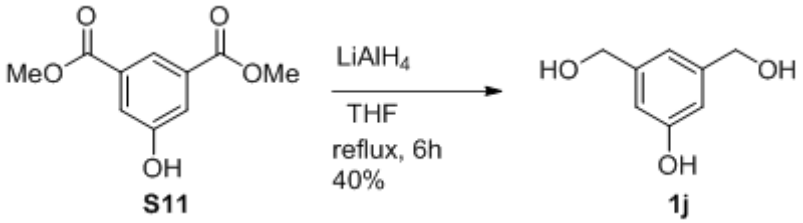

A literature method was used to synthesize 3,5-bis(hydroxymethyl)phenol (**1j**).[5] To a THF (10 mL) suspension of $LiAlH_4$ (0.34 g, 8.88mmol, 3.7 eq.) was added a 5 mL THF solution of dimethyl 5-hydroxyisophthalate (**S11)** (0.50 g, 2.37 mmol, 1.0 eq.) dropwise at 0 ^{o}C. The reaction mixture was then refluxed for 6 hours. After completion of the reaction, a 10% aqueous H_2SO_4 solution (0.5 mL) was carefully added dropwise at 0^{o}C until no more hydrogen evolved. The reaction mixture was filtered, and the filtrate was evaporated via rotary evaporator to obtain the product **1j** as a white solid (147 mg, 40% yield).^{1}H NMR (300 MHz, DMSO-d_6): δ =9.20 (s, 1H), 6.66 (s, 1H), 6.58 (s, 2H), 5.07 (t, 2H, J = 5.7 Hz), 4.38 (d, 4H, J = 5.7 Hz). ^{13}C NMR (75 MHz, CD_3CN): δ =157.16, 143.69, 115.01, 111.56, 62.92.Calcd for $[M+H^+, C_8H_{11}O_3]^+$155.0708, found 155.0709.

SYNTHETIC DETAILS FOR BENZYLIC BROMINATION

General reaction scheme:

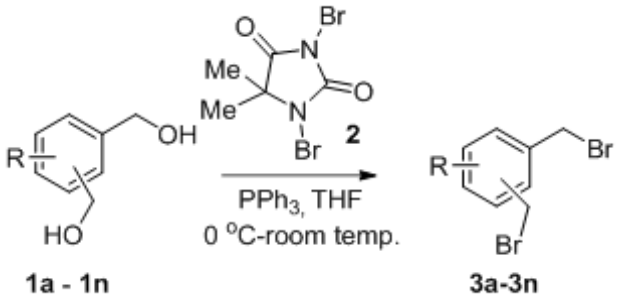

Specific Products:

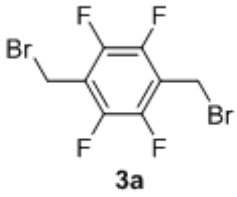

2,3,5,6-tetrafluoro-1,4-bis(bromomethyl)benzene (**3a**): A solution of 2,3,5,6-tetrafluoro-1,4-benzenedimethanol (**1a**) (100 mg, 0.48 mmol, 1.0 eq.) in anhydrous THF (14 mL) was cooled to 0 ^{o}C.1,3-dibromo-5,5-dimethylhydantoin (**2**)(340 mg, 1.19 mmol, 2.5 eq.) was added and allowed to stir for 10 min at 0 ^{o}C. Triphenylphosphine (312 mg, 1.19mmol, 2.5 eq.) was then added and the reaction mixture was warmed to room temperature and stirred for 2 hours. After completion of the reaction, THF was evaporated under reduced pressure to afford the crude product. The crude product was purified by flash chromatography and eluted with 1:9 ethyl acetate: hexanes to obtain compound **3a** as a white crystalline solid (86 mg, 54% yield).^{1}H NMR ($CDCl_3$, 300 MHz): δ = 4.51 (s, 4H).^{13}C NMR (DMSO-d_6, 75 MHz):δ = 145.80, 142.31, 117.83, 17.82. ^{19}F NMR ($CDCl_3$, 300 MHz):δ = -142.32. HR-MS (ESI): Calcd for $[M+H^+, C_8H_5Br_2F_4]^+$ 334.8694, found 334.8689.

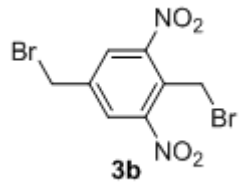

3b

2,6-dinitro-1,4-bis(bromomethyl)benzene (**3b**): A solution of 2,6-dinitro-1,4-bis(hydroxymethyl)benzene (**1b**) (300 mg,1.31mmol, 1.0 eq.) in anhydrous THF (14 mL) was cooled to 0 ^{o}C. 1,3-dibromo-5,5-dimethylhydantoin(**2**) (827 mg, 2.89 mmol, 2.2 eq.) was added and the reaction mixture was allowed to stir for 10 min at 0 ^{o}C. Triphenylphosphine (758 mg, 2.89 mmol, 2.2 eq.) was then added and the reaction mixture was warmed to room temperature and stirred for 2 hours. The reaction progress was monitored by checking TLC. After completion of the reaction, the THF was evaporated under reduced pressure. The crude product was purified by flash chromatography using hexanes:ethylacetate (9:1) to afford compound **3b** as a red liquid (184 mg, 40% yield).^{1}H NMR ($CDCl_3$, 300 MHz): δ = 8.10 (s, 2H), 4.96 (s, 2H), 4.52 (s, 2H). ^{13}C NMR ($CDCl_3$, 75 MHz): δ = 151.15, 140.74, 129.74, 128.52, 57.11, 29.12.HR-MS (ESI): Calcd for $[M\text{-}NO_2^{+}+2H^{+}$, $C_8H_8Br_2NO_2]^{+}$ 307.8960, found 307.9898.

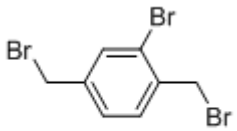

3c

2,5-bis(bromomethyl)bromobenzene (3c): A solution of 2,5-bis(hydroxymethyl)bromobenzene (**1c**) (100 mg, 0.46 mmol, 1.0 eq.) in anhydrous THF (14 mL) was cooled to 0 ^{o}C. 1,3-dibromo-5,5-dimethylhydantoin (**2**) (289 mg, 1.01mmol, 2.2 eq.) was added and the reaction mixture was allowed to stir for 10 minutes at 0

^{o}C.Triphenylphosphine (265 mg, 1.01 mmol, 2.2 eq.) was then added and the reaction mixture was warmed to room temperature and stirred for 2 hours. The reaction progress was monitored by checking TLC. After completion of the reaction, THF was evaporated under reduced pressure. The crude product was purified by flash chromatography using hexanes: ethylacetate (9:1) to afford compound **3c** as yellow solid (80 mg, 51% yield).^{1}H NMR ($CDCl_3$, 300 MHz):δ = 7.61 (s, 1H), 7.43 (d, 1H, J = 7.8 Hz), 7.32 (d, 1H, J = 7.8 Hz), 4.58 (s, 2H), 4.41 (s, 2H).^{13}C NMR ($CDCl_3$, 75 MHz): δ =140.16, 137.35, 133.93, 131.72, 128.78, 124.71, 32.90, 31.52.Calcd for [M-Br^+, $C_8H_7Br_2]^+$ 260.8909, found 260.8926.

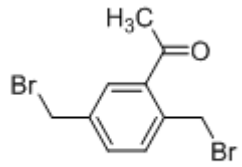

3d

2,5-bis(bromomethyl)acetophenone (3d): A solution of 2,5-bis(hydroxymethyl)acetophenone (**1d**) (100 mg, 0.55 mmol, 1.0 eq.) in anhydrous THF (14 mL) was cooled to 0 ^{o}C. 1,3-dibromo-5,5-dimethylhydantoin (**2**) (349 mg, 1.22 mmol, 2.2 eq.) was added and the reaction mixture was allowed to stir for 10 minutes at 0 ^{o}C. Triphenylphosphine (320 mg, 1.22 mmol, 2.2 eq.) was then added and the reaction mixture was warmed to room temperature and stirred for 2 hours. After completion of the reaction, THF was evaporated under reduced pressure. The crude product was purified by flash chromatography using hexanes: ethylacetate (9:1) to afford compound **3d** as an off-white solid (68 mg, 40% yield).^{1}H NMR ($CDCl_3$, 300 MHz):δ = 7.33 (s, 1H), 7.25 (d, 1H, J = 7.5 Hz), 7.16 (d, 1H, J = 7.8 Hz), 4.49 (s, 2H), 4.46 (s, 2H), 2.40 (s, 3H).^{13}C NMR ($CDCl_3$, 75 MHz): δ = 137.90, 136.45, 136.18, 131.55, 130.72, 129.74, 33.17, 31.89, 18.78.Calcd for [M+H^+, $C_{10}H_{11}Br_2O]^+$ 304.9177, found 304.9194.

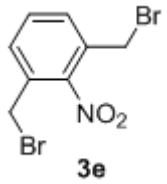

3e

2-nitro-1,3-bis(bromomethyl)benzene (3e): A solution of 2-nitro-1,3-bis(hydroxymethyl)benzene (**1e**) (100 mg, 0.55mmol, 1.0 eq.) in anhydrous THF (14 mL) was cooled to 0 ^{o}C. 1,3-dibromo-5,5-dimethylhydantoin (**2**) (343 mg, 1.20 mmol, 2.2 eq.) was added and the reaction mixture was allowed to stir for 10 min at 0 ^{o}C. Triphenylphosphine (315 mg, 1.20 mmol, 2.2 eq.) was added and the reaction mixture was warmed to room temperature and stirred for 2 hours. After completion of the reaction, THF was evaporated under reduced pressure. The crude product was purified by flash chromatography using hexanes: ethylacetate (9:1) to afford compound **3e** as an off-white solid (100 mg, 58% yield). ^{1}H NMR (DMSO-d_6, 300 MHz): δ = 7.73 (d, 1H, J = 6.9 Hz), 7.66 (d, 1H, J = 6.6 Hz), 7.63 (d, 1H, J = 6.6 Hz), 4.72 (s, 4H). ^{13}C NMR (DMSO-d_6, 75 MHz): δ = 147.38, 134.36, 130.80, 127.55, 59.23. HR-MS (ESI): Calcd for $[M+NH_4^+$, $C_8H_{11}Br_2N_2O_2]^+$324.9187, found 324.9181.

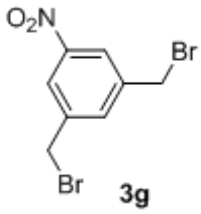

3g

5-nitro-1,3-bis(bromomethyl)benzene (3g): A solution of 5-nitro-1,3-benzenedimethanol (**1g**) (100 mg, 0.55mmol, 1.0 eq.) in anhydrous THF (14 mL) was cooled to 0 ^{o}C. 1,3-dibromo-5,5-dimethylhydantoin (**2**) (343 mg, 1.20 mmol, 2.2 eq.) was added and the reaction mixture was allowed to stir for 10 minutes at 0 ^{o}C. Triphenylphosphine (315 mg, 1.20 mmol, 2.2 eq.) was then added and the reaction mixture was warmed to room temperature and stirred

for 2 hours. After completion of the reaction, THF was evaporated under reduced pressure. The crude product was purified by flash chromatography using hexanes: ethylacetate (9:1) to afford compound **3g** as a pale yellow solid (100 mg, 58% yield). ^{1}H NMR ($CDCl_3$, 300 MHz): δ =8.20 (s, 2H), 7.75 (s, 1H), 4.52 (s, 4H). ^{13}C NMR ($CDCl_3$, 75MHz): δ= 148.78, 140.62, 135.49, 123.93, 30.83.HR-MS (ESI): Calcd for [M+H$^+$, $C_8H_8Br_2NO_2$]$^+$307.8922, found 309.2188.

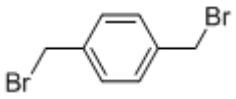

3h

1,4-bis(bromomethyl)benzene (3h): A solution of 1,4-bis(hydroxymethyl)benzene(**1h**) (100 mg, 0.72mmol, 1.0 eq.) in anhydrous THF (14 mL) was cooled to 0 ^{o}C. 1,3-dibromo-5,5-dimethylhydantoin (**2**) (455mg, 1.59 mmol, 2.2 eq.) was added and the reaction mixture was allowed to stir for 10 minutes at 0 ^{o}C. Triphenylphosphine (417 mg, 1.59mmol, 2.2 eq.) was then added and the reaction mixture was warmed to room temperature and stirred for 2 hours. After completion of the reaction, THF was evaporated under reduced pressure. The crude product was purified by flash chromatography using hexanes: ethylacetate (9:1) to afford compound **3h** as an off-white solid (82 mg, 43% yield).^{1}H NMR ($CDCl_3$, 300 MHz): δ = 7.37 (s, 4H), 4.48 (s, 4H). ^{13}C NMR ($CDCl_3$, 75 MHz): δ =138.23, 129.71, 33.01. HR-MS (ESI): Calcd for [M-Br$^+$, C_8H_8Br]$^+$ 182.9804, found 182.9812.

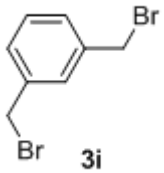

3i

1,3-bis(bromomethyl)benzene (3i): A solution of 1,3-benzenedimethanol (**1i**) (50 mg, 0.36 mmol, 1.0 eq.) in anhydrous THF (8 mL) was cooled to 0 ^{o}C. 1,3-dibromo-5,5-dimethylhydantoin (**2**) (227 mg, 0.79 mmol, 2.2 eq.) was added and the reaction mixture was allowed to stir for 10 minutes at 0 ^{o}C. Triphenylphosphine (208 mg, 0.79 mmol, 2.2 eq.) was then added and the reaction mixture was warmed to room temperature and stirred for 2 hours. After completion of the reaction, THF was evaporated under reduced pressure. The crude product was purified by preparative thin layer chromatography plates using hexanes: ethylacetate (9:1) as an eluent to afford compound **3i** as a pale yellow solid (64 mg, 67% yield),with spectral characterization that matches literature-reported values.[6] ^{1}H NMR ($CDCl_3$, 300 MHz): δ = 7.42 (s, 1H), 7.33 (d, 3H, J = 1.2 Hz), 4.48 (s, 4H). ^{13}C NMR ($CDCl_3$, 75 MHz): δ= 138.62, 129.79, 129.53, 129.29, 33.06.HR-MS (ESI): Calcd for [M-Br^{+}, $C_8H_8Br]^{+}$182.9804, found 182.9813.

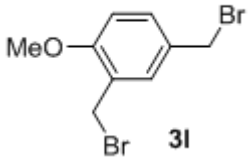

3l

4-methoxy-1,3-bis(bromomethyl)benzene (3l): A solution of 4-methoxy-1,3-benzenedimethanol (**1l**) (100 mg, 0.59 mmol, 1 eq.) in anhydrous THF (14 mL) was cooled to 0 ^{o}C. 1,3-dibromo-5,5-dimethylhydantoin (**2**) (373 mg, 1.30 mmol, 2.2 eq.) was added and the reaction mixture was allowed to stir for 10 minutes at 0 ^{o}C. Triphenylphosphine (343 mg, 1.31mmol, 2.2 eq.) was then added and the reaction mixture was warmed to room temperature and stirred for 2 hours. After completion of the reaction, THF was evaporated under reduced pressure. The crude product was purified by flash chromatography using hexanes: ethylacetate (9:1) to afford compound **3l** as a white solid (120 mg, 69% yield).^{1}H NMR ($CDCl_3$, 300

MHz): δ = 7.37 (s, 1H), 7.33 (d, 1H, J = 8.4 Hz), 6.84 (d, 1H, J = 8.1 Hz), 4.53 (s, 2H), 4.48 (s, 2H),3.90 (s, 3H).^{13}C NMR ($CDCl_3$, 75 MHz): δ = 157.69, 131.88, 131.21, 130.22, 126.74,111.39, 55.99, 33.56, 28.58.HR-MS (ESI): Calcd for $[M+H^+, C_9H_{11}Br_2O]^+$ 292.9177, found 292.9168.

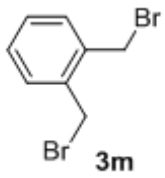

3m

1,2-bis(bromomethyl)benzene (3m): A solution of 1,2-benzenedimethanol (**1m**) (50 mg, 0.36 mmol, 1.0 eq.) in anhydrous THF (8 mL) was cooled to 0 ^oC. 1,3-dibromo-5,5-dimethylhydantoin(**2**) (227 mg, 0.79 mmol, 2.2 eq.) was added and the reaction mixture was allowed to stir for 10 minutes at 0 ^oC.Triphenylphosphine (208 mg, 0.79 mmol, 2.2 eq.) was then added and the reaction mixture was warmed to room temperature and stirred for 2 hours. After completion of the reaction, THF was evaporated under reduced pressure. The crude product was purified by preparative thin layer chromatography using hexanes: ethylacetate (9:1) as an eluent to afford compound **3m** as an off-white solid (60 mg, 63% yield).^{1}H NMR ($CDCl_3$, 300 MHz): δ = 7.38-7.29 (m, 4H), 4.67 (s, 4H). ^{13}C NMR ($CDCl_3$, 75 MHz): δ = 136.78, 131.31, 129.66, 30.21.HR-MS (ESI): Calcd for $[M-Br^+, C_8H_8Br]^+$ 182.9804, found 182.9811.

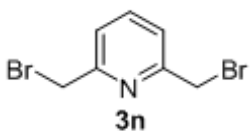

3n

2,6-bis(bromomethyl)pyridine (3n): A solution of 2,6-pyridinedimethanol (**1n**) (100 mg, 0.72 mmol, 1.0 eq.) in anhydrous THF (14 mL) was cooled to 0 ^oC. 1,3-dibromo-5,5-

dimethylhydantoin(**2**) (452 mg, 1.58 mmol, 2.2 eq.) was added and the reaction mixture was allowed to stir for 10 minutes at 0 ^{o}C. Triphenylphosphine (414 mg, 1.58 mmol, 2.2 eq.) was then added and the reaction mixture was warmed to room temperature and stirred for 2 hours. After completion of the reaction, THF was evaporated under reduced pressure and the crude reaction mixture was dissolved in ethylacetate (10 mL) and extracted with 1N HCl (2 x 5 mL).The aqueous HCl layer was basified with 1N NaOH (11 mL to reach pH 8). The product was extracted into ethylacetate (2 x 10 mL). The combined organic layers were washed with brine, dried over anhydrous Na_2SO_4, filtered and concentrated via rotary evaporator. The crude product was purified by flash chromatography using hexanes: ethylacetate (9:1) to afford compound **3n** as a white solid (65 mg, 34% yield). ^{1}H NMR ($CDCl_3$, 300 MHz): δ =7.71 (d, 1H, J = 7.8 Hz), 7.37 (d, 2H, J = 7.5 Hz), 4.54 (s, 4H).^{13}C NMR ($CDCl_3$, 75 MHz): δ = 156.93, 138.32, 123.00, 33.68.HR-MS (ESI): Calcd for [M+H^{+}, $C_7H_8Br_2N]^{+}$ 263.9023, found 263.9029.

SYNTHESIS OF OMEPRAZOLE PRECURSOR

Reaction 1:

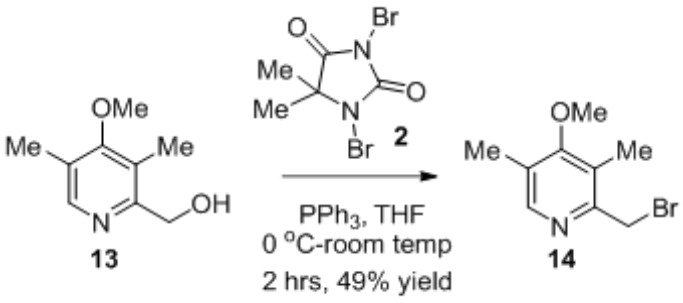

Synthesis of 4-methoxy-3,5-dimethyl-2-bromomethyl pyridine (14): A solution of 4-methoxy-3,5-dimethyl-2-pyridinemethanol (**13**) (100 mg, 0.60 mmol, 1.0 eq.) in anhydrous THF (14 mL) was cooled to 0 ^{o}C. 1,3-dibromo-5,5-dimethylhydantoin (**2**) (376 mg, 1.32

mmol, 2.2 eq.) was added and the reaction mixture was allowed to stir for 10 minutes at 0 ^{o}C.Triphenylphosphine (345 mg, 1.32 mmol, 2.2 eq.) was added and the reaction mixture was warmed to room temperature and stirred for 2 hours. After completion of the reaction, THF was evaporated under reduced pressure and the reaction mixture was dissolved in ethyl acetate (10 mL). The product was extracted into 1N HCl (2 x 10 mL).The aqueous HCl layer was basified with 1N NaOH (23 mL to reach pH 10). The product was extracted into chloroform (2 x 10 mL). The combined organic layers were washed with brine, dried over anhydrous Na_2SO_4, filtered and concentrated via rotary evaporator. The crude product was purified by flash chromatography (neutral alumina)using hexanes: ethylacetate (8.5:1.5) to afford compound **14** as a pale yellow solid (68 mg, 49% yield).^{1}H NMR ($CDCl_3$, 300 MHz): δ = 8.21 (s, 1H), 4.57 (s, 2H), 3.77 (s, 3H), 2.32 (s, 3H), 2.26 (s, 3H).^{13}C NMR ($CDCl_3$, 75 MHz): δ =165.10, 154.45, 149.02, 126.99, 126.37, 60.32, 32.32, 13.75, 11.30. HR-MS (ESI): Calcd for $[M+H^+, C_9H_{13}BrNO]^+$ 230.0181, found 230.0172.

Reaction 2:

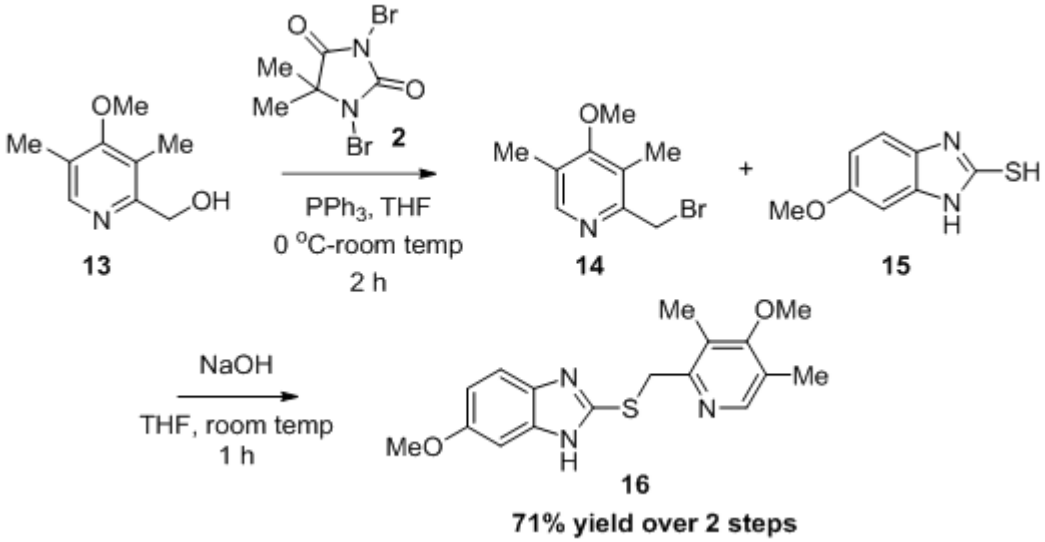

One-pot synthesis of omeprazole precursor (16): A solution of 4-methoxy-3,5-dimethyl-2-pyridinemethanol (**13**) (150 mg, 0.90 mmol, 1.0 eq.) in anhydrous THF (12 mL) was cooled to 0 ^{o}C. 1,3-dibromo-5,5-dimethylhydantoin (**2**) (384 mg, 1.34 mmol, 1.5 eq.) was added and the reaction mixture was allowed to stir for 10 minutes at 0 ^{o}C. Triphenylphosphine (352 mg, 1.34mmol, 1.5 eq.) was added and the reaction mixture was warmed to 40 ^{o}C and stirred for 1 hour under a nitrogen atmosphere. This solution was added to a suspension of 2-mercapto-5-methoxybenzimidazole (**15**) (162 mg, 0.90mmol, 1.0 eq.) in THF (2 mL). The reaction mixture was stirred for 30 minutes at room temperature, followed by the addition of 30% NaOH (0.25 mL, 1.79 mmol, 2.0 eq.) and the stirring was continued for another 30 minutes. Most of the THF was evaporated under reduced pressure. The residue was dissolved in ethyl acetate (10 mL) and extracted into 1N HCl (3 x 10 mL). The aqueous HCl layer was basified with 1N NaOH (30 mL). The product was then extracted into dichloromethane (3 x 10 mL), washed with brine, dried over anhydrous Na_2SO_4, filtered and concentrated via rotary evaporator. The crude product was purified by using a preparative TLC plate with ethyl acetate:hexanes (8:2) to afford compound **16** as a colorless oil (210 mg, 71% yield over two steps).^{1}H NMR ($CDCl_3$, 300 MHz): δ = 12.62 (br, 1H), 8.25 (s, 1H), 7.41 (s, 1H), 7.03 (s,1H), 6.82 (d, 1H, J = 8.7 Hz), 4.35 (s, 2H), 3.84 (s, 3H), 3.78 (s, 3H), 2.32 (s, 3H), 2.28 (s, 3H).^{13}C NMR ($CDCl_3$, 75 MHz): δ =165.31, 156.21, 148.62,126.61, 125.69,111.17,60.31, 56.04, 35.18, 13.63,11.51.HR-MS (ESI): Calcd for $[M+H^+$, $C_{17}H_{20}N_3O_2S]^+$ 330.1276, found 330.1276.

ELUCIDATION OF COMPOUNDS 3JJ AND 3KK:

The reactions of compounds **1j** and **1k** led to a 0% yield of the desired dibrominated products **3j** and **3k**. However, in both cases, a single major product was formed. We undertook a detailed structural elucidation of that product, as shown below:

Elucidation of 3jj:

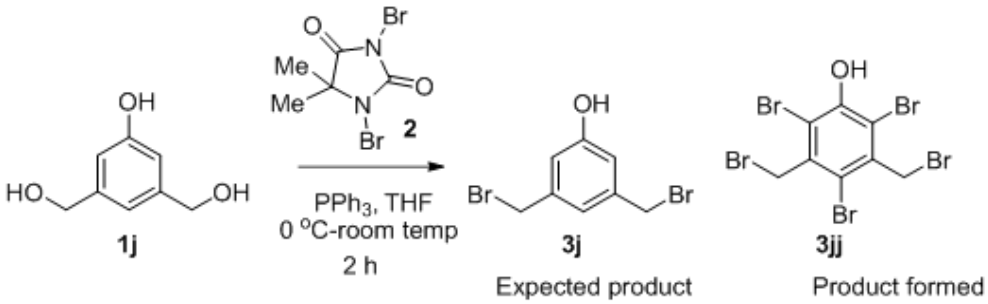

2,4,6-tribromo-3,5-bis(bromomethyl)phenol (**3jj**): A solution of 3,5-bis(hydroxymethyl)phenol (**1j**) (72 mg, 0.47 mmol, 1.0 eq.) in anhydrous THF (10 mL) was cooled to 0 ^{o}C. 1,3-dibromo-5,5-dimethylhydantoin (**2**) (293 mg, 1.03mmol, 2.2 eq.) was added and the reaction mixture was allowed to stir for 10 minutes at 0 ^{o}C. Triphenylphosphine (269 mg, 1.03mmol, 2.2 eq.) was then added and the reaction mixture was warmed to room temperature and stirred for 2 hours. After completion of the reaction, THF was evaporated under reduced pressure. The residue was dissolved in ethyl acetate (15mL) and washed with water twice (10 mL each) followed by brine. The organic layer was dried over anhydrous sodium sulfate, filtered and evaporated to obtain the crude product, which was then purified by column chromatography using hexanes: ethyl acetate (8:2) as an eluent to afford compound **3jj** as a white solid (75 mg, 31% yield).^{1}H NMR (DMSO-d_6, 300 MHz): δ = 10.50 (s, 1H), 4.89 (s, 4H). ^{13}C NMR (DMSO-d_6, 300 MHz): δ = 151.56, 136.62, 117.23, 116.17, 36.66.^{13}C DEPT 45 NMR (DMSO-d_6, 75 MHz): δ = 36.62 (CH_2). ^{13}C DEPT 90 NMR (DMSO-d_6, 75

MHz): no signal found (no CH). ^{13}C DEPT 135 NMR (DMSO-d_6, 75 MHz): δ = 36.62 (CH_2). HR-MS (ESI): Calcd for [M-Br^+, $C_8H_5Br_4O]^+$ 432.7074, found 432.7092.

Elucidation of 3kk:

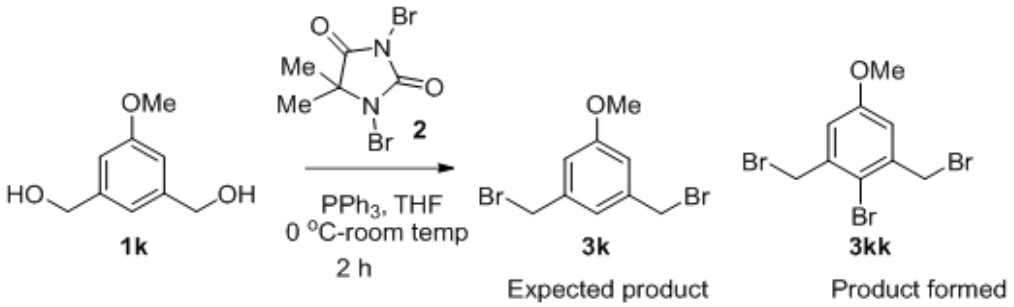

4-bromo-3,5-bis(bromomethyl)anisole (**3kk**): A solution of 3,5-bis(hydroxymethyl)anisole (**1k**) (100 mg, 0.59 mmol, 1.0 eq.) in anhydrous THF (15 mL) was cooled to 0 ^{o}C. 1,3-dibromo-5,5-dimethylhydantoin (**2**) (373 mg, 1.30 mmol, 2.2 eq.) was added and the reaction mixture was allowed to stir for 10 minutes at 0 ^{o}C. Triphenylphosphine (343 mg, 1.30 mmol, 2.2 eq.) was then added and the reaction mixture was warmed to room temperature and stirred for 2 hours. After completion of the reaction, THF was evaporated under reduced pressure. The residue was dissolved in ethyl acetate (15mL) and washed with water twice (10 mL each) followed by brine. The organic layer was dried over anhydrous sodium sulfate, filtered and evaporated to obtain crude product. The crude product was purified by column chromatography using hexanes: ethyl acetate (9:1) as an eluent to afford compound **3kk** as a white solid (138 mg, 63% yield).^{1}H NMR ($CDCl_3$, 300 MHz): δ = 6.97 (s, 2H), 4.60 (s, 4H), 3.82(s, 3H). ^{13}C NMR ($CDCl_3$, 75 MHz): δ = 158.87, 139.28, 117.10, 55.78, 34.01. ^{13}C DEPT 45 NMR ($CDCl_3$, 300 MHz): δ = 117.41 (aryl CH), 55.6 (CH_3), 34.76 (CH_2). ^{13}C DEPT 90 NMR ($CDCl_3$, 75 MHz): δ = 117.41 (CH). ^{13}C DEPT 135 NMR ($CDCl_3$, 75 MHz): δ =

117.41 (negative) (aryl CH), 55.67 (negative) (CH_3), 34.76 (positive)(CH_2).HR-MS (ESI): Calcd for $[M\text{-}Br^+, C_9H_9Br_2O]^+$ 290.9020, found 290.9014.

SPECTRAL CHARACTERIZATION OF ALL COMPOUNDS

^{1}H NMR of **1c**; 300 MHz, DMSO-*d6*:

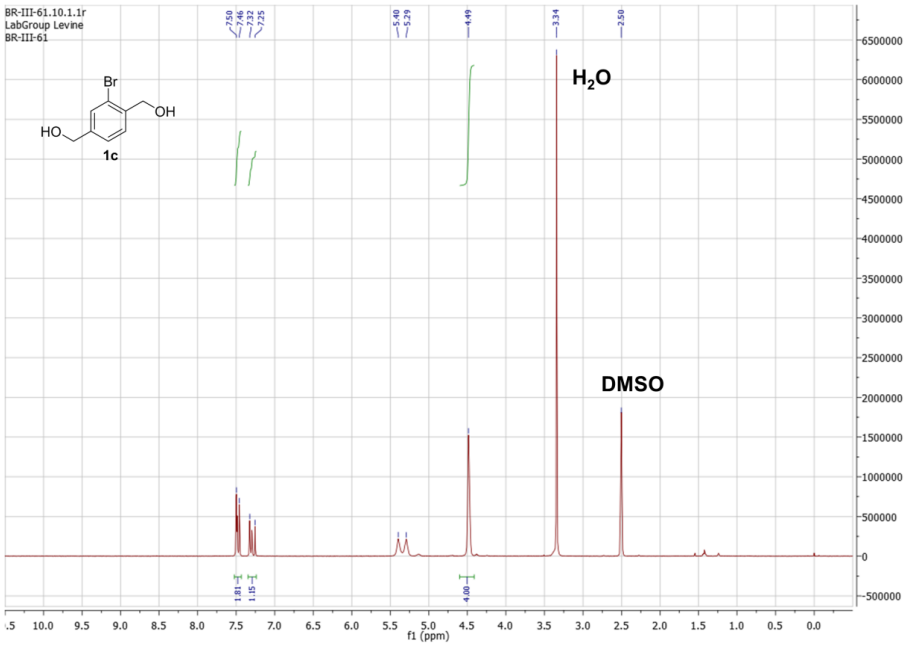

^{13}C NMR of **1c**; 75 MHz, DMSO-*d6*:

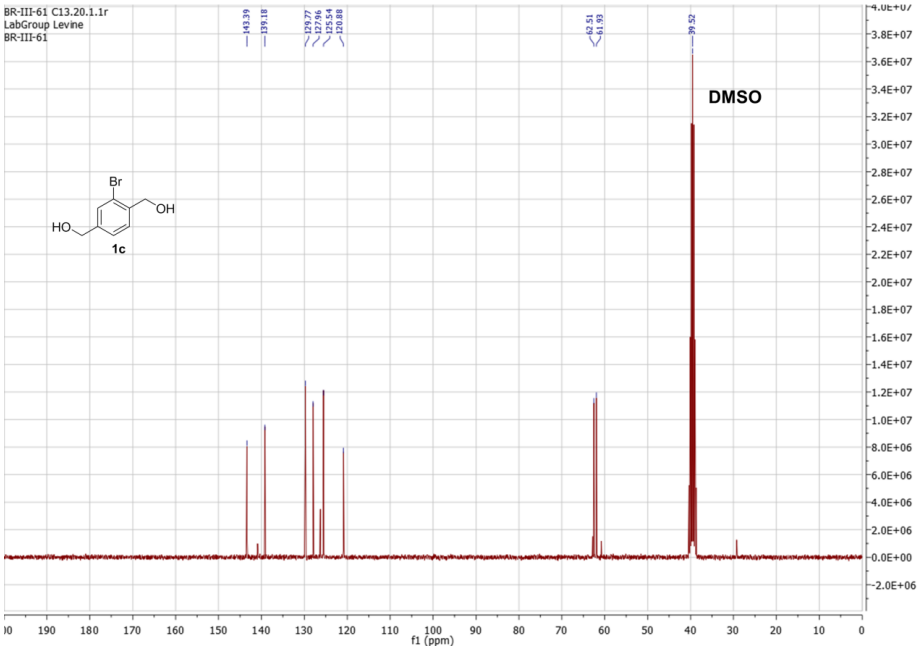

^{1}H NMR of **S6**;300 MHz, DMSO-*d6*:

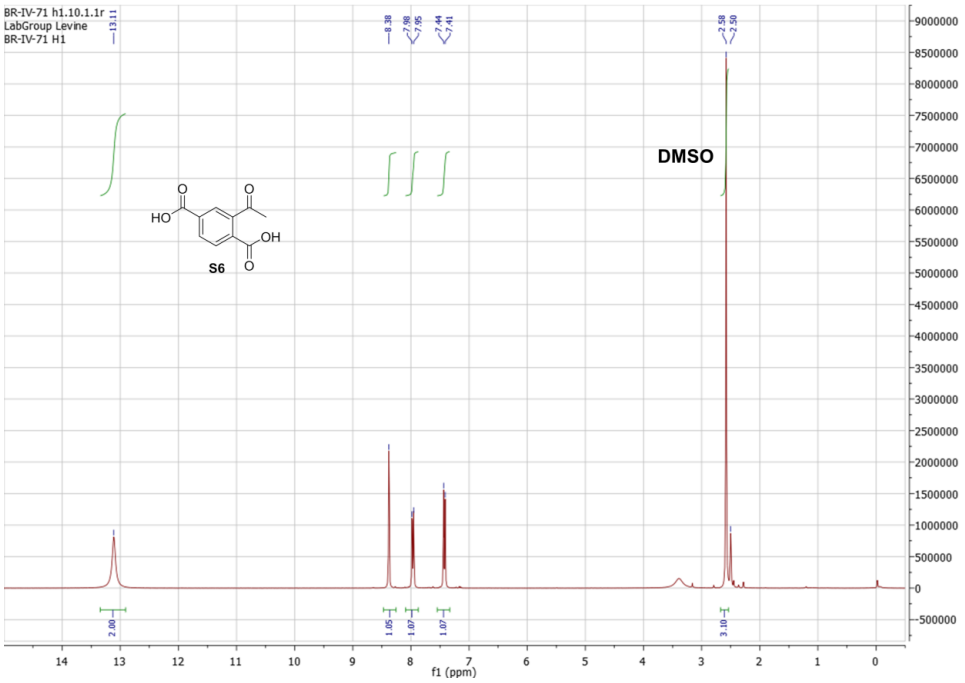

^{13}C NMR of **S6**; 75 MHz, DMSO-*d6*:

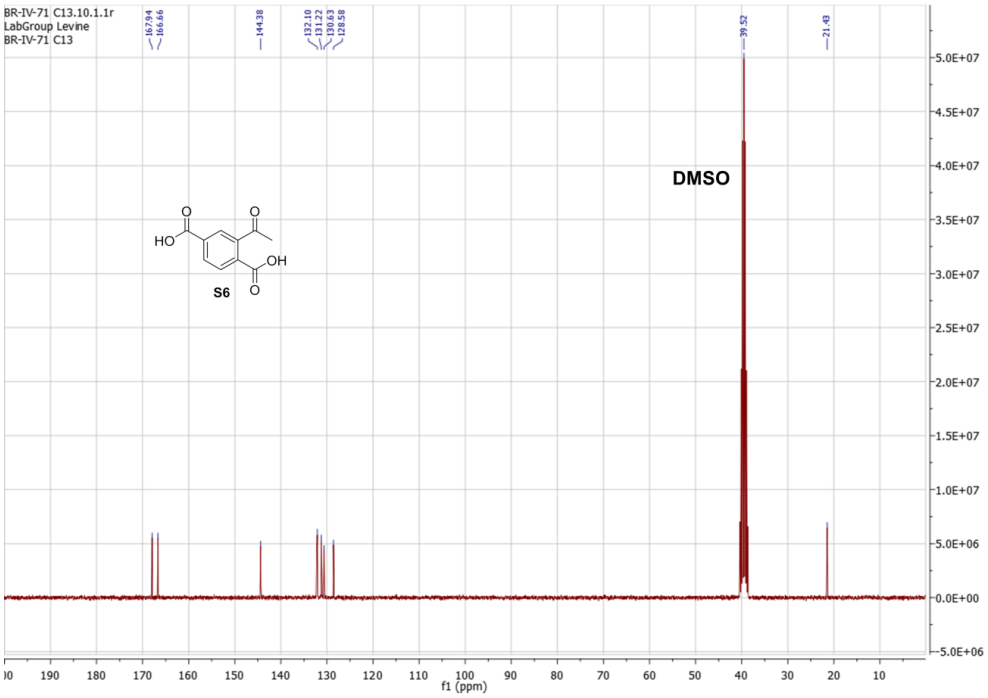

^{1}H NMR of **S7**; 300 MHz, $CDCl_3$:

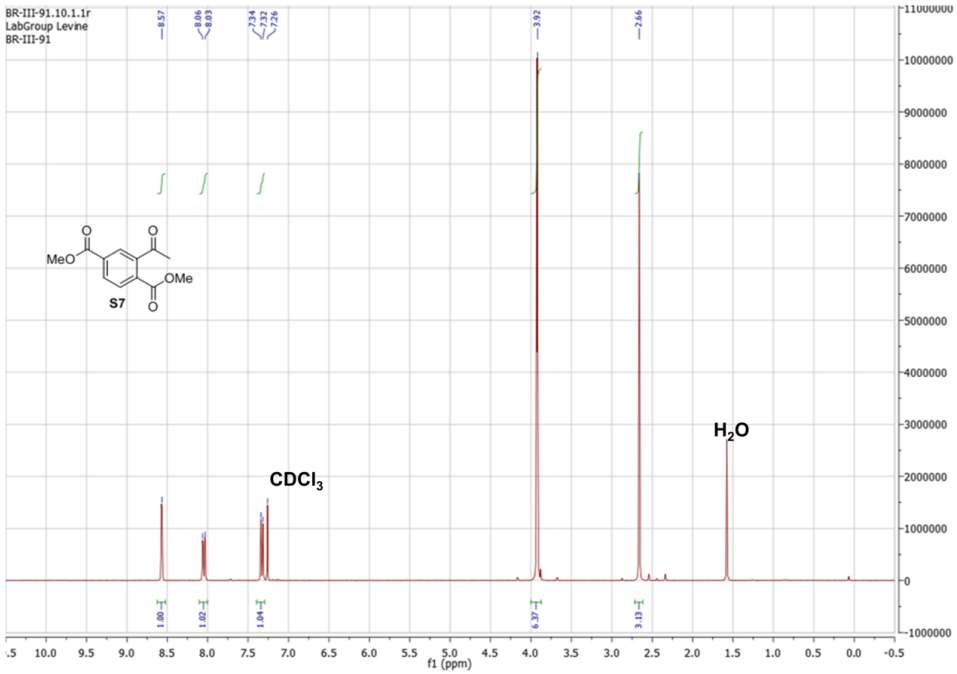

^{13}C NMR of **S7**; 75 MHz, $CDCl_3$:

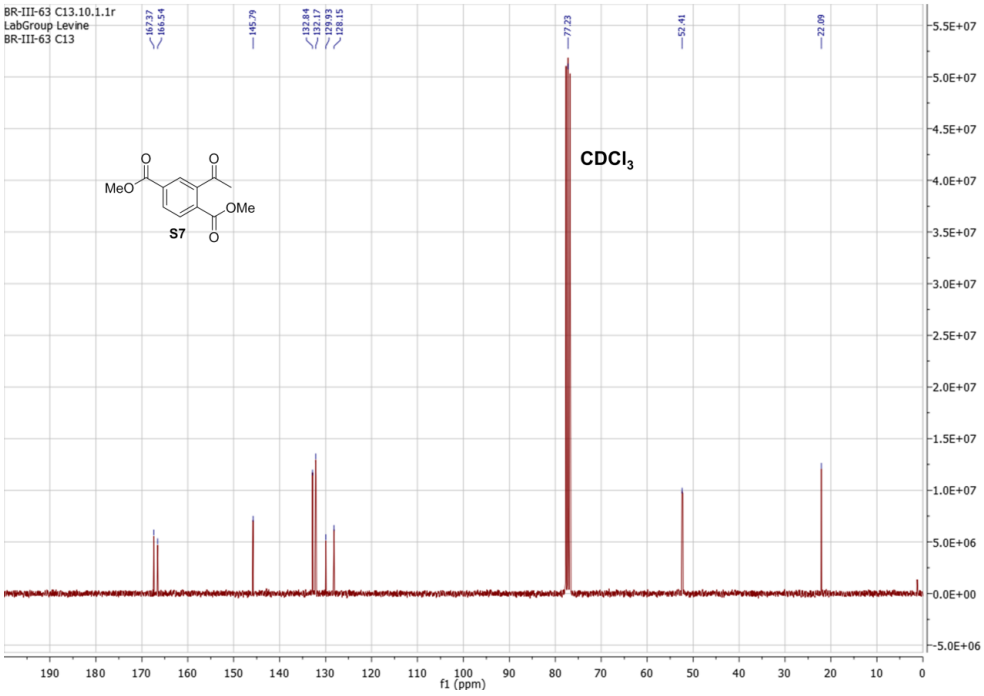

^{1}H NMR of **1d**; 300 MHz, DMSO-*d6*:

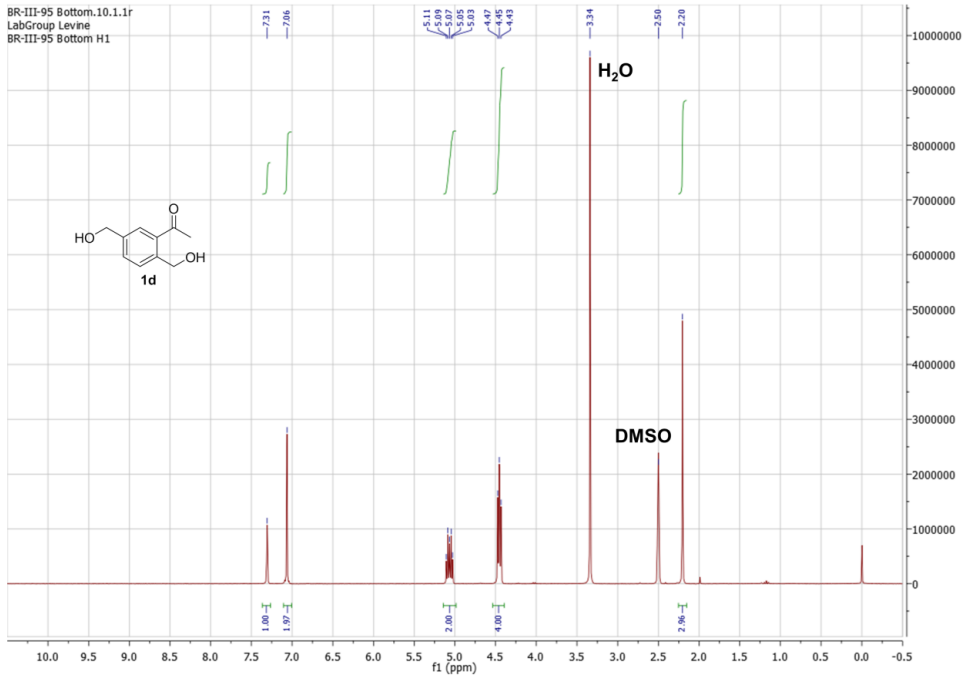

^{13}C NMR of **1d**; 75 MHz, DMSO-*d6*:

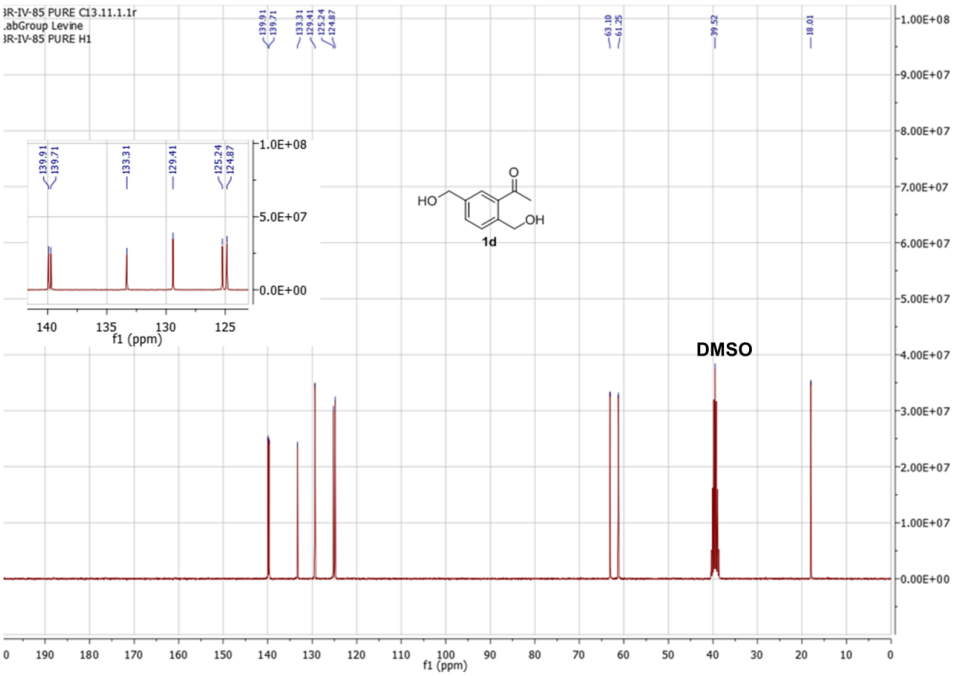

^{1}H NMR of **1g**;300 MHz, DMSO-*d6*:

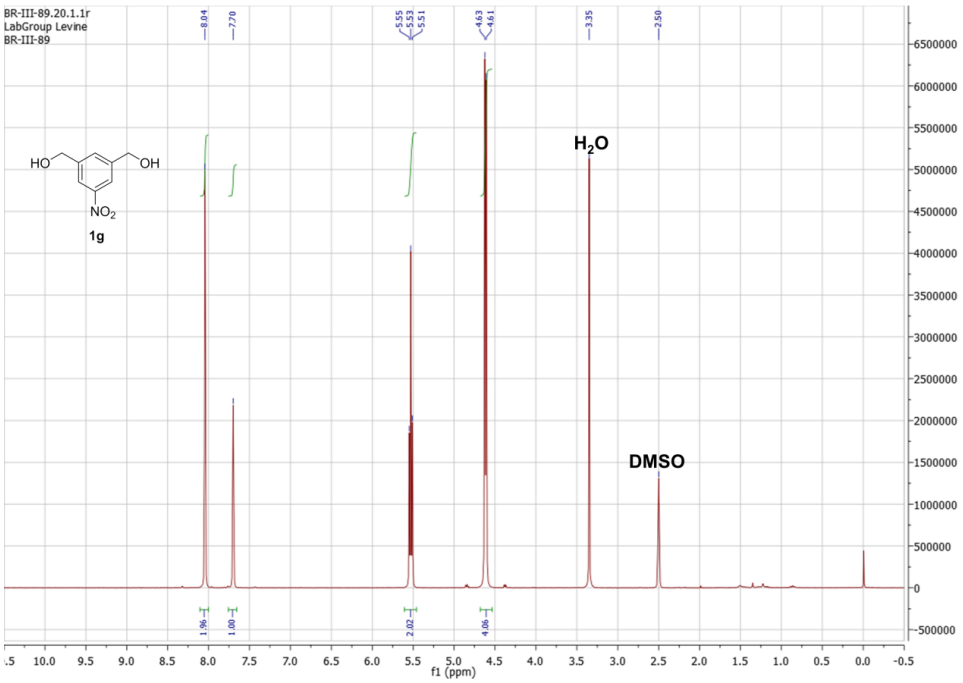

^{13}C NMR of **1g**; 75 MHz, DMSO-*d6*:

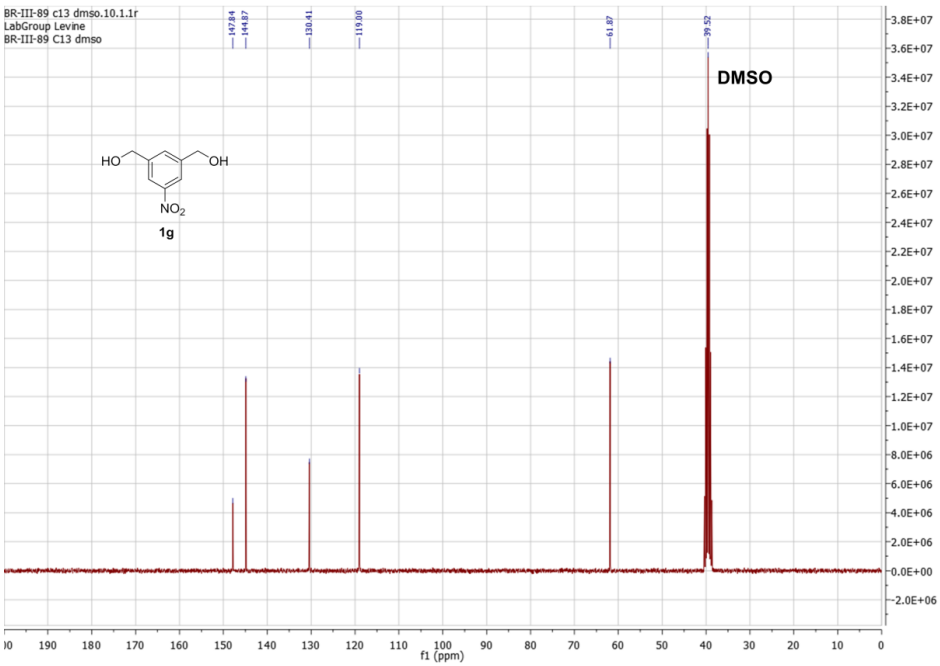

^{1}H NMR of **S11**; 300 MHz, DMSO-*d6*:

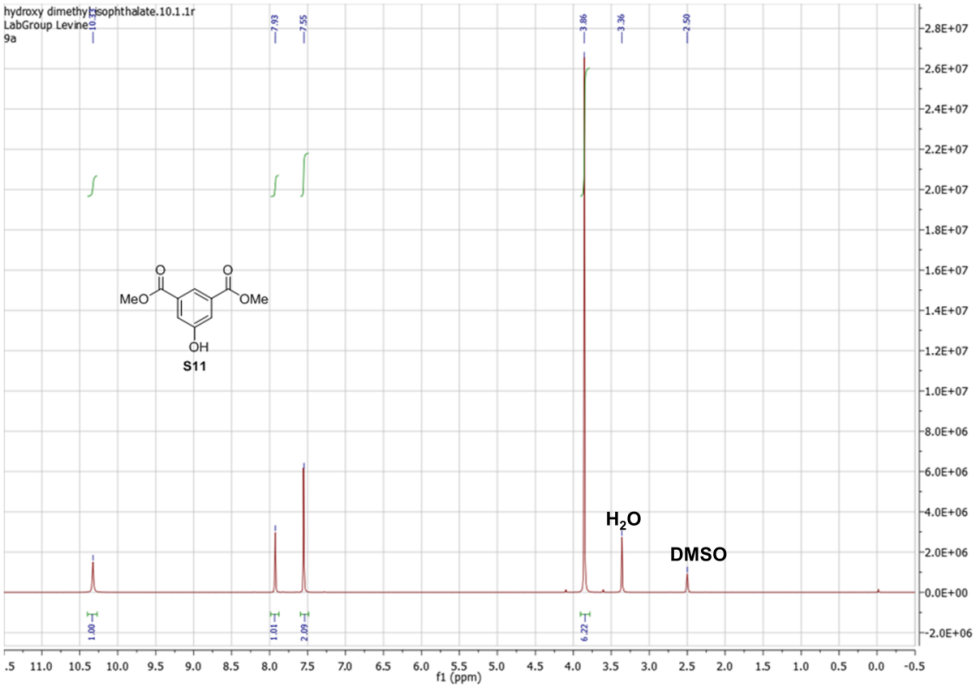

^{1}H NMR of **1j**;300 MHz, DMSO-*d6*:

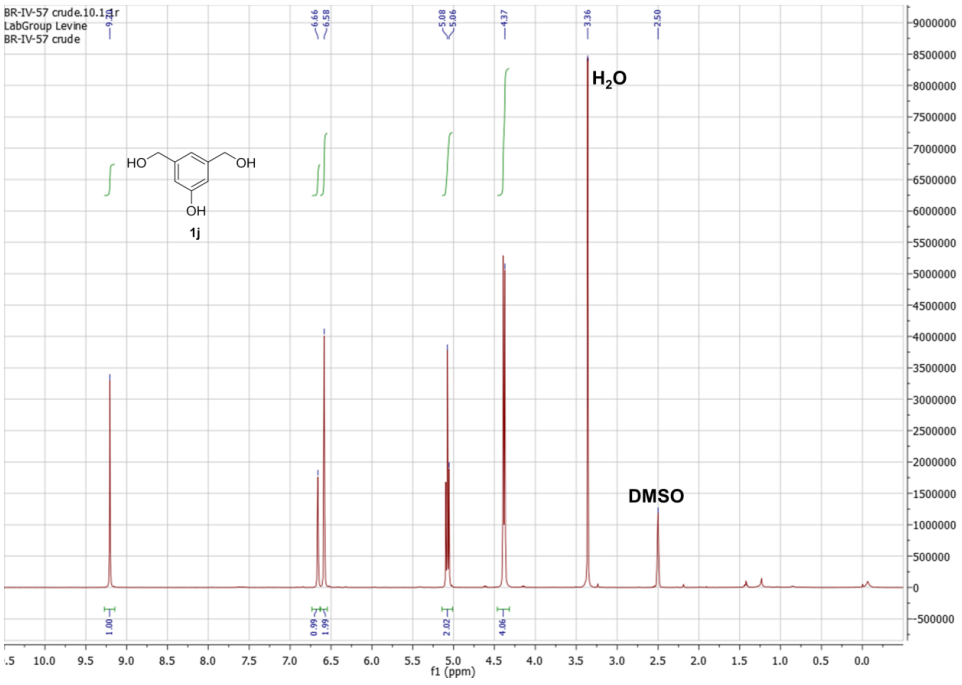

^{13}C NMR of **1j**; 75 MHz, DMSO-*d6*:

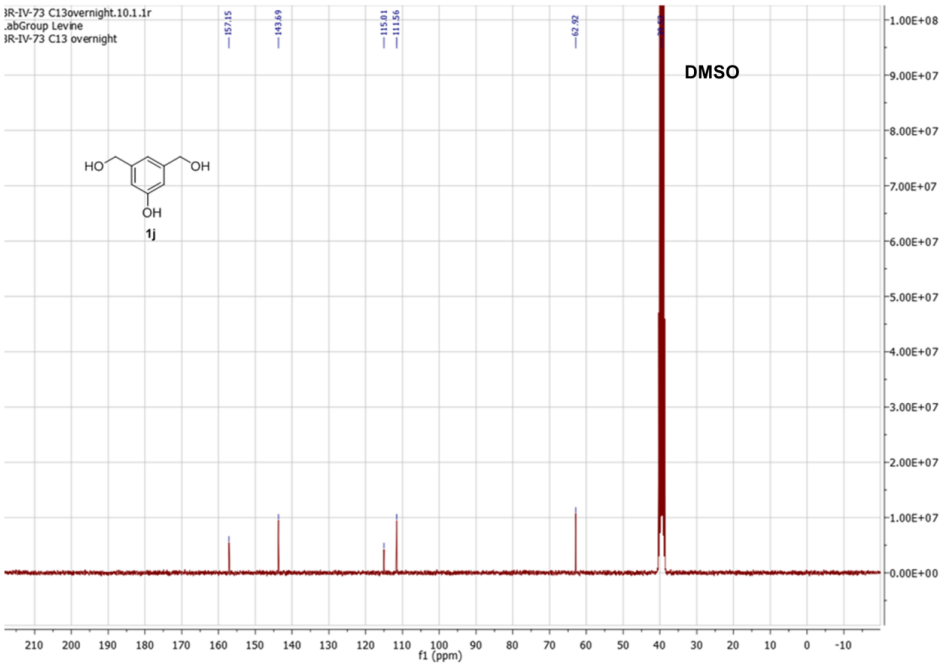

^{1}H NMR of **3a**; 300 MHz, $CDCl_3$:

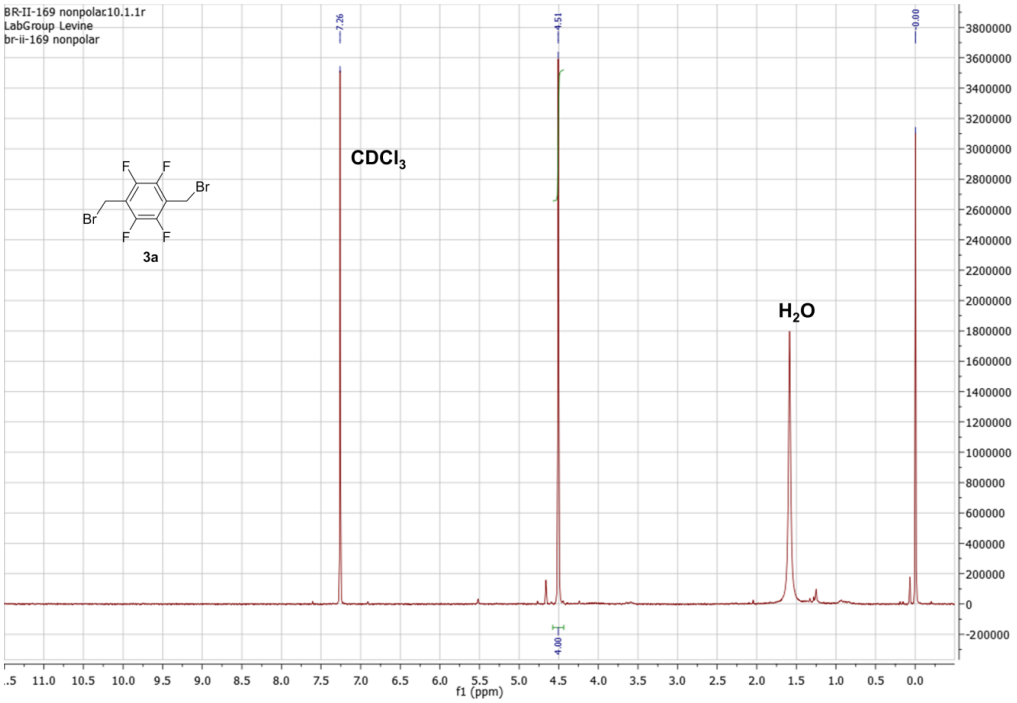

^{13}C NMR of **3a**;75 MHz, $CDCl_3$:

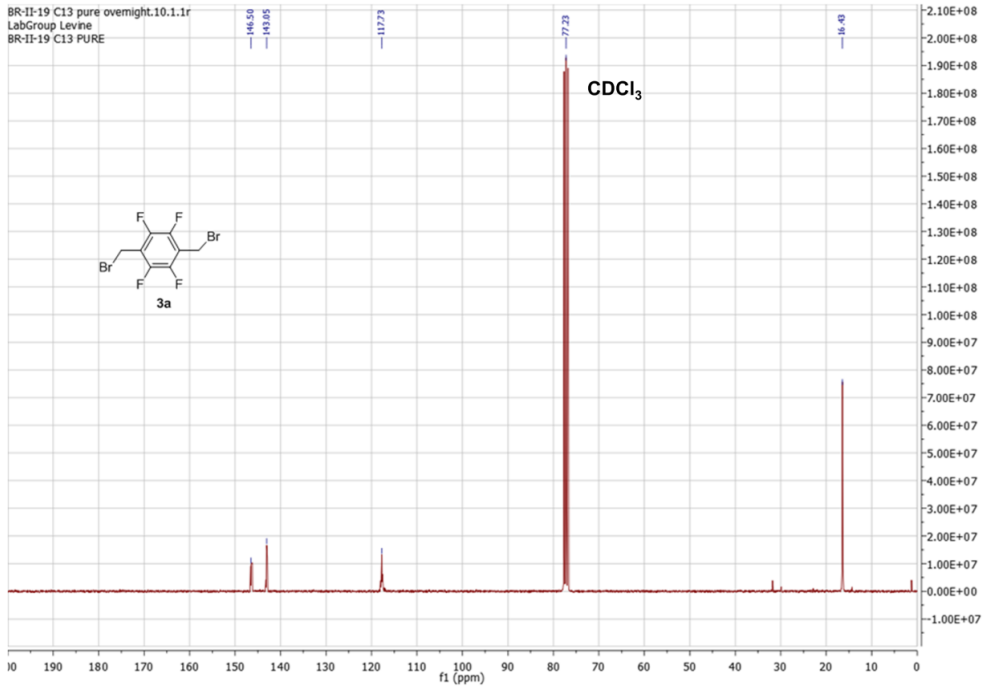

^{19}F NMR of **3a**; 300 MHz, $CDCl_3$:

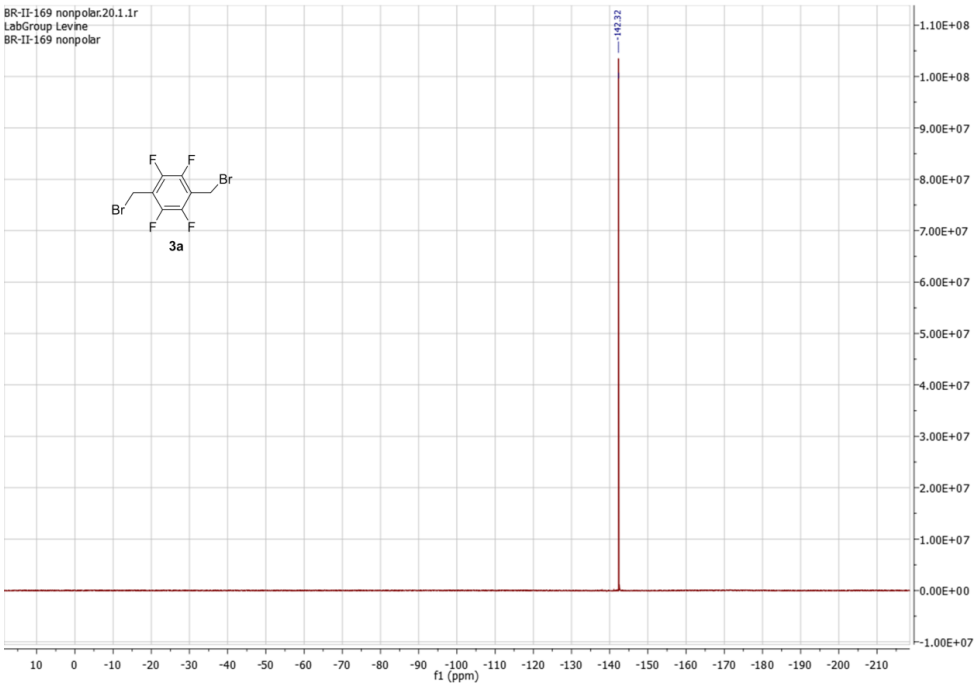

^{1}H NMR of **3b**; 300 MHz, $CDCl_3$:

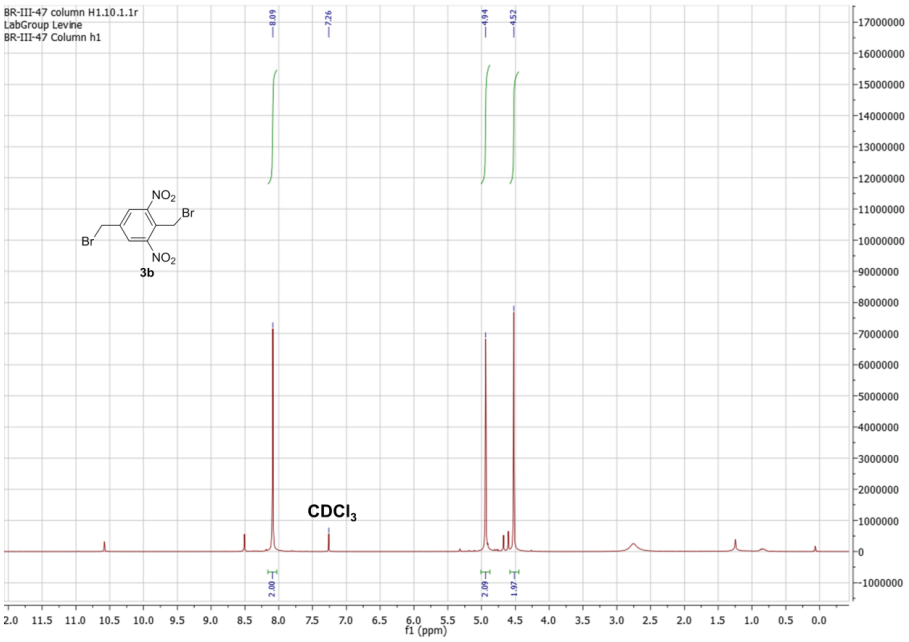

^{13}C NMR of **3b**; 75 MHz, $CDCl_3$:

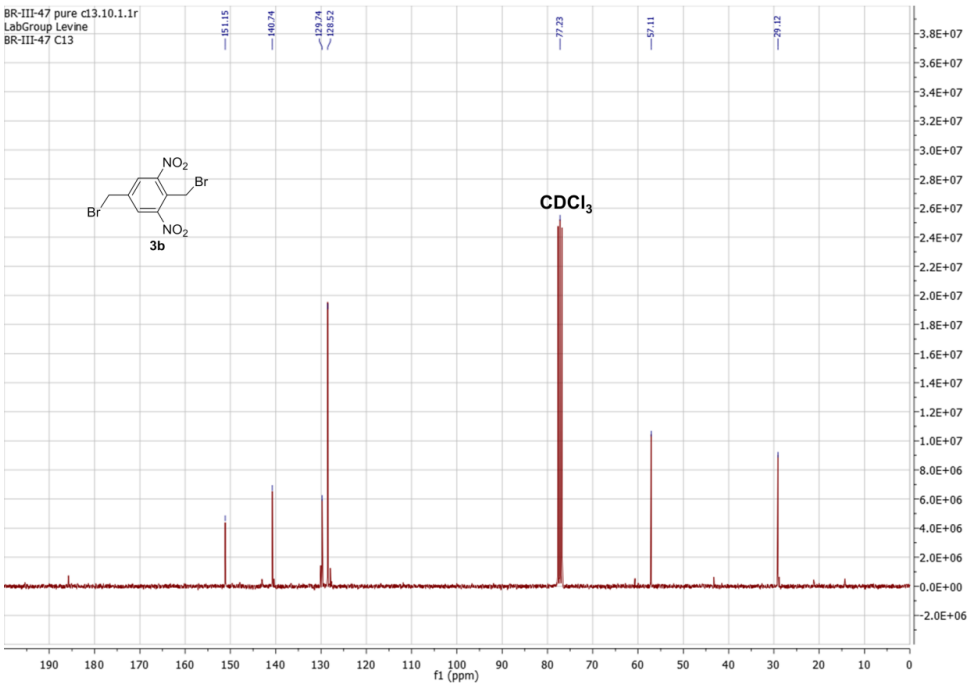

^{1}H NMR of **3c**; 300 MHz, $CDCl_3$:

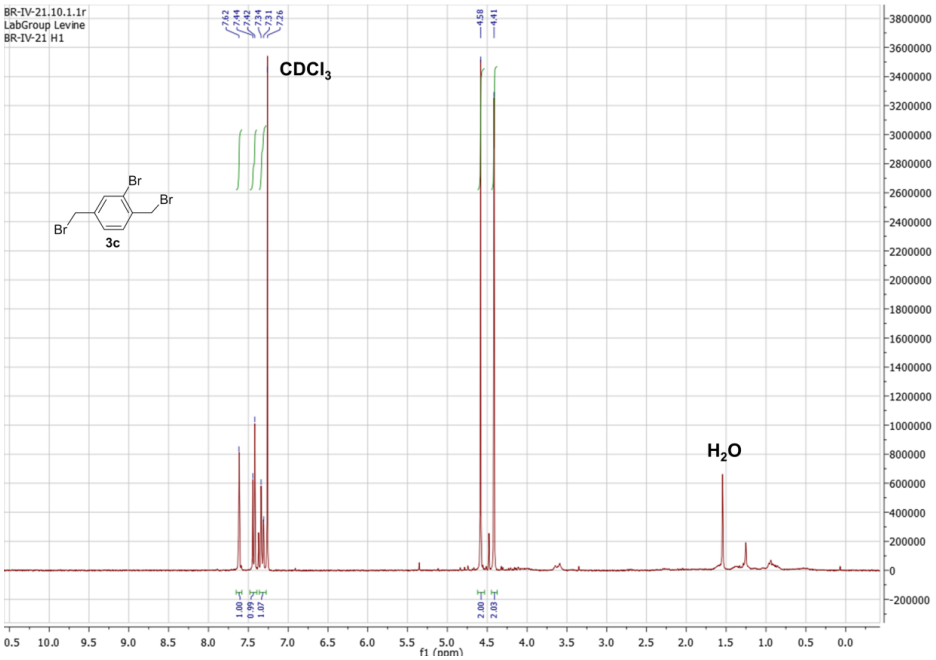

^{13}C NMR of **3c**; 75 MHz, $CDCl_3$:

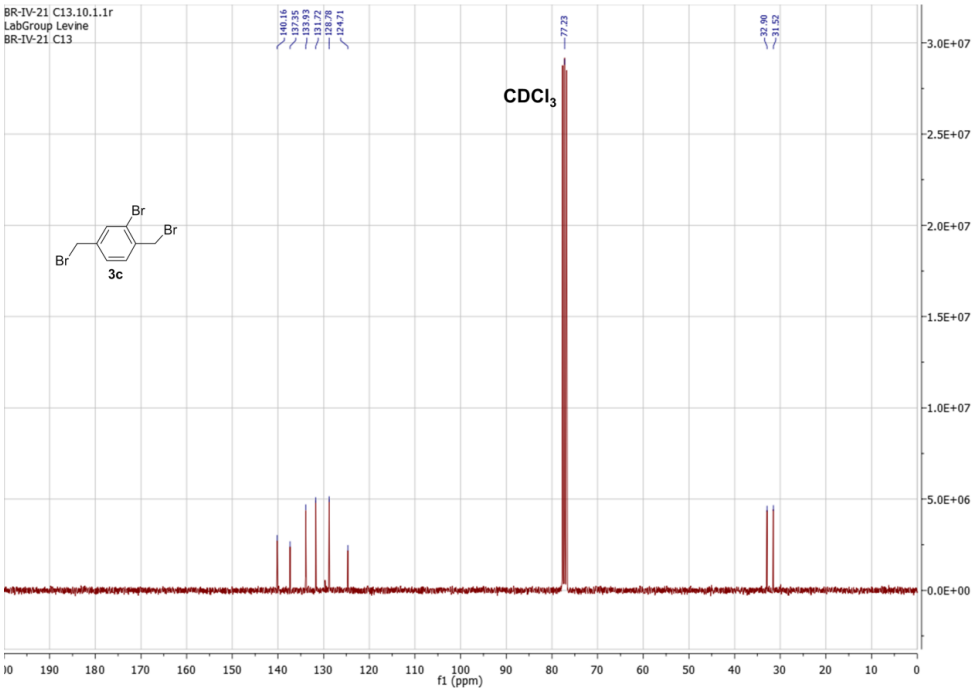

^{1}H NMR of **3d**; 300 MHz, $CDCl_3$:

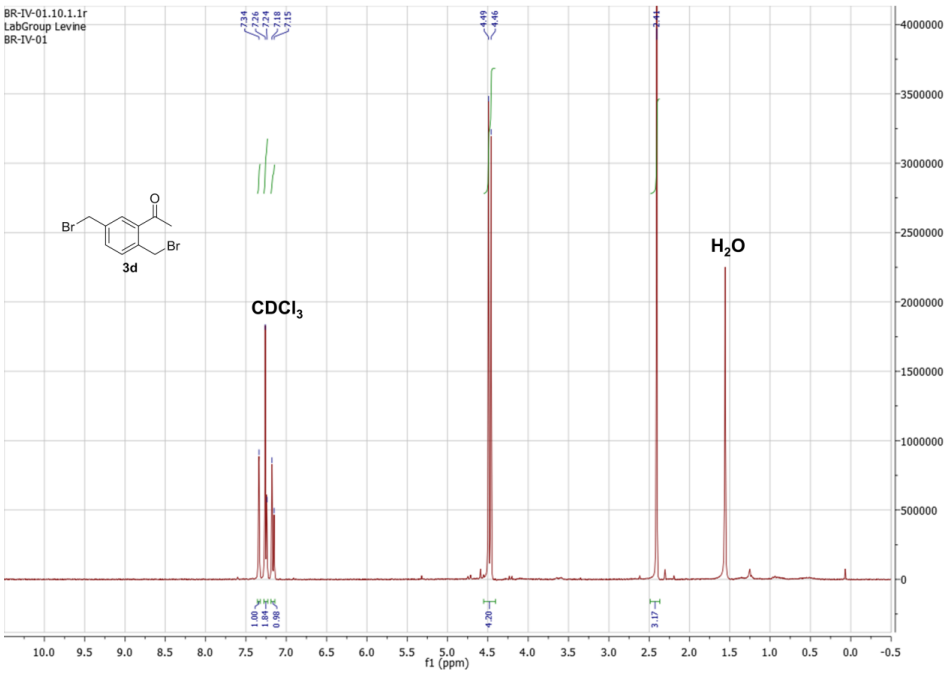

^{13}C NMR of **3d**; 75 MHz, $CDCl_3$:

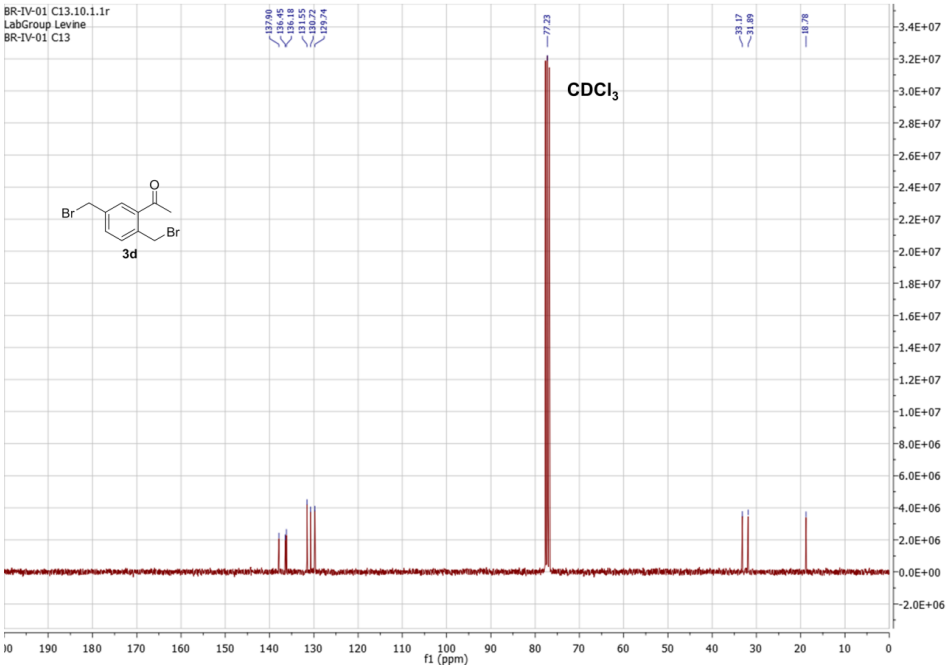

^{1}H NMR of **3e**; 300 MHz, DMSO-*d6*:

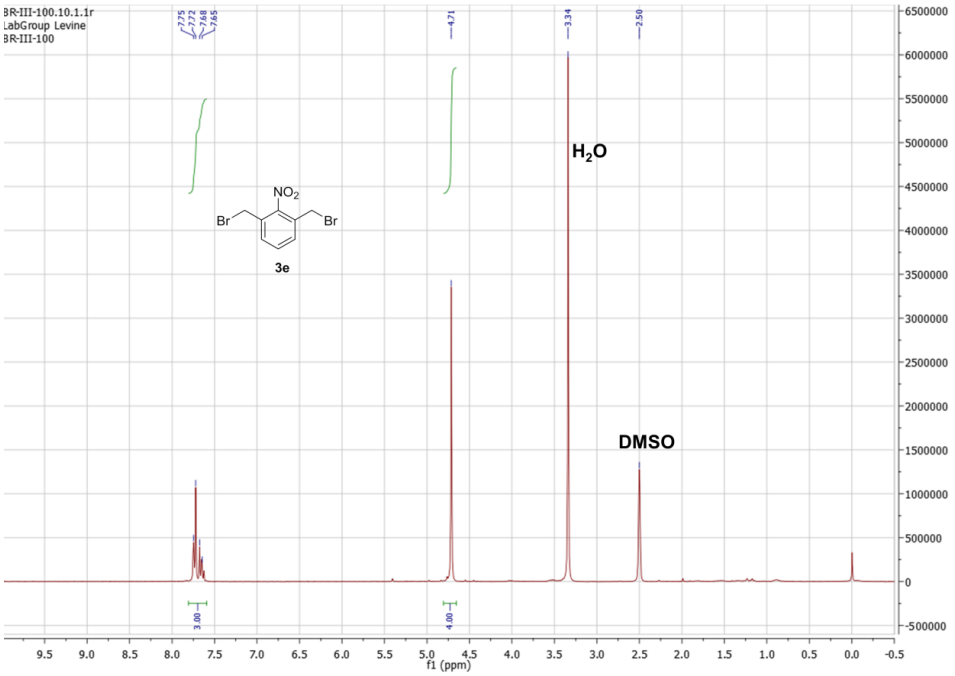

^{13}CNMR of **3e**;75 MHz, DMSO-*d6*:

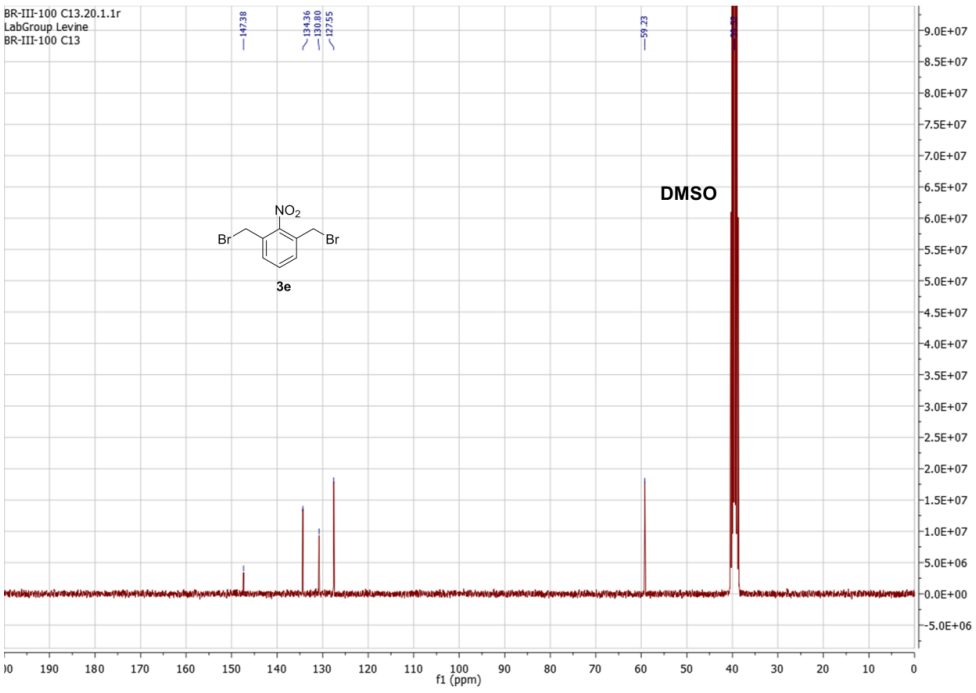

^{1}H NMR of **3g**; 300 MHz, $CDCl_3$:

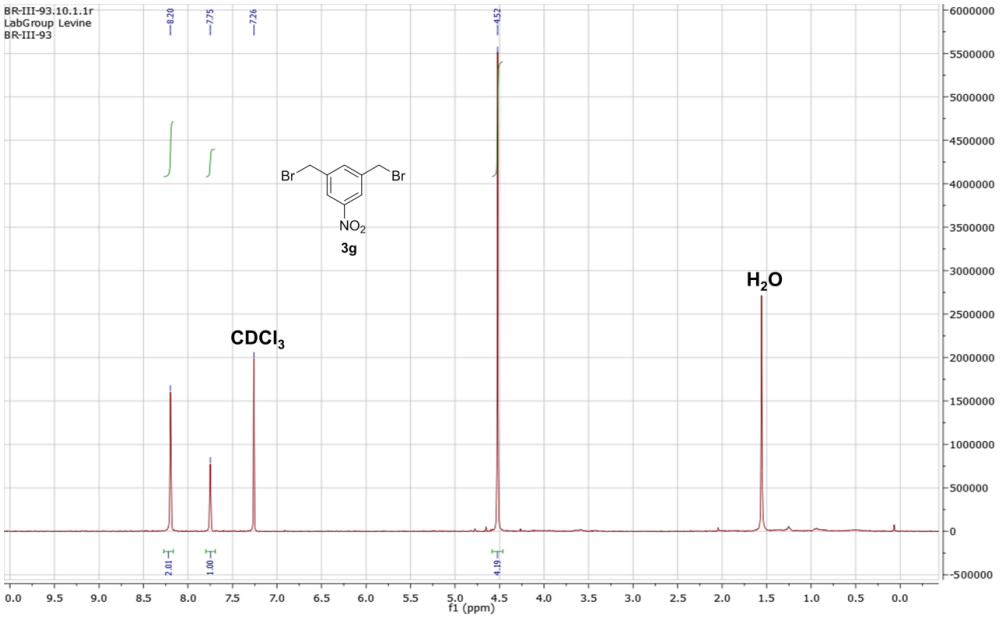

^{13}C NMR of **3g**; 75 MHz, $CDCl_3$:

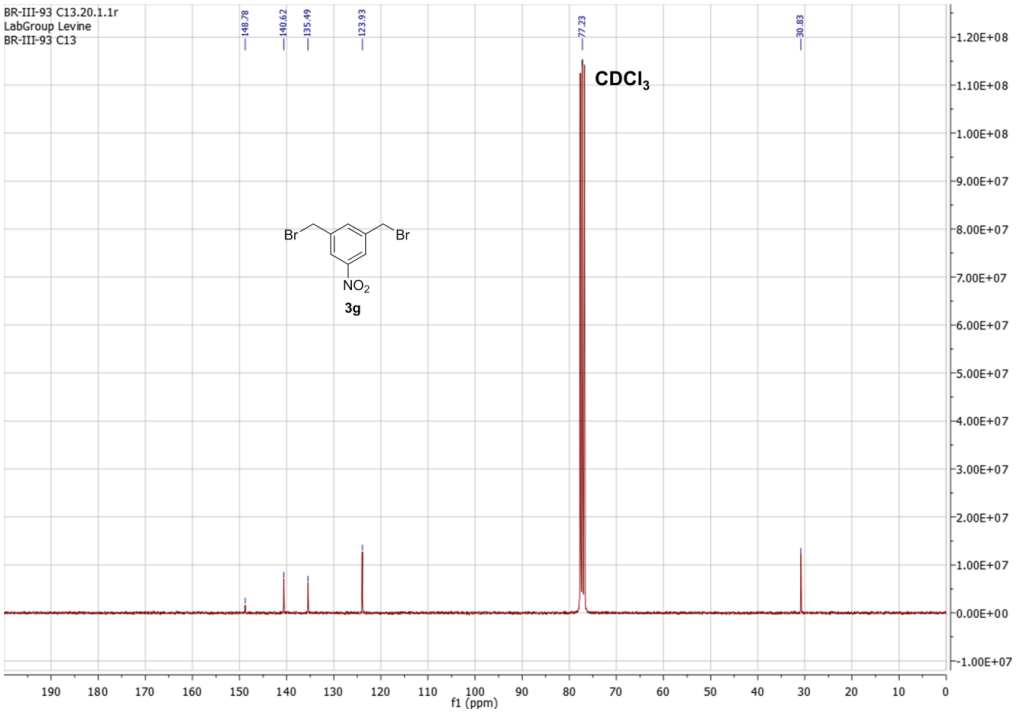

^{1}H NMR of **3h**; 300 MHz, $CDCl_3$:

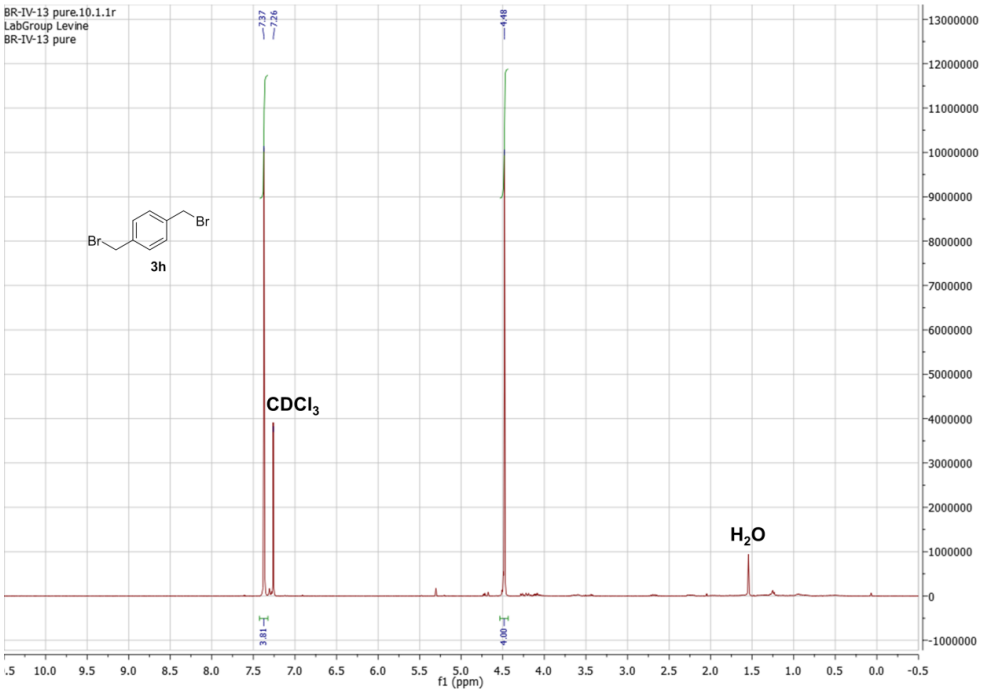

^{13}C NMR of **3h**; 75 MHz, $CDCl_3$:

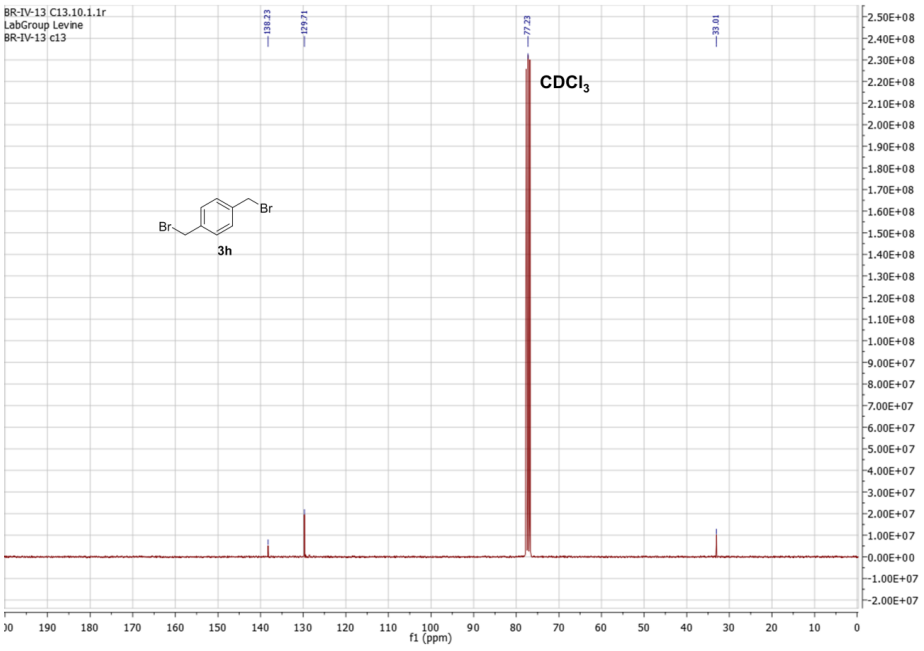

^{1}H NMR of **3i**; 300 MHz, $CDCl_3$:

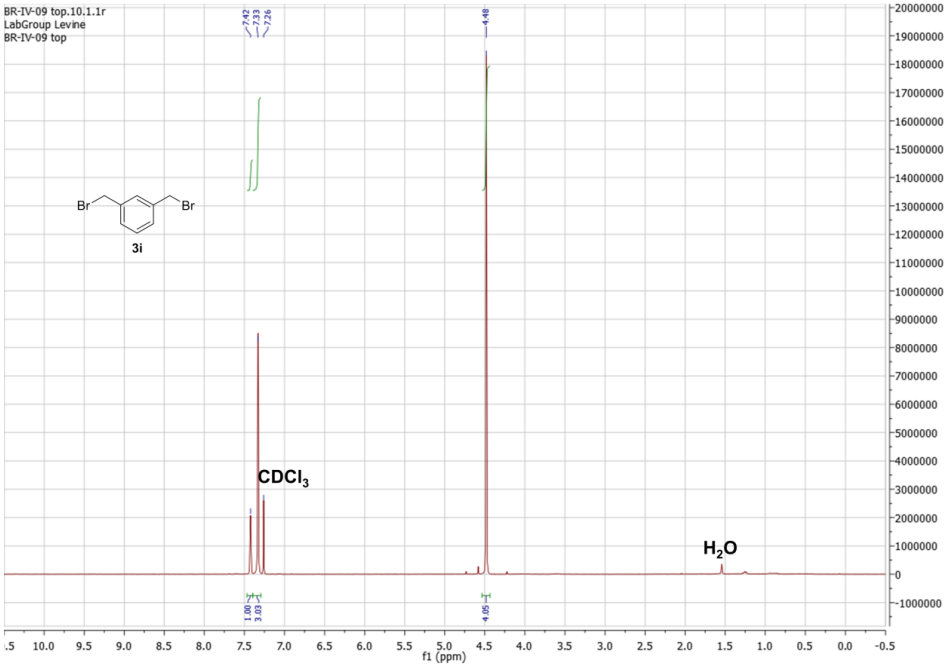

^{13}C NMR of **3i**; 75 MHz, $CDCl_3$:

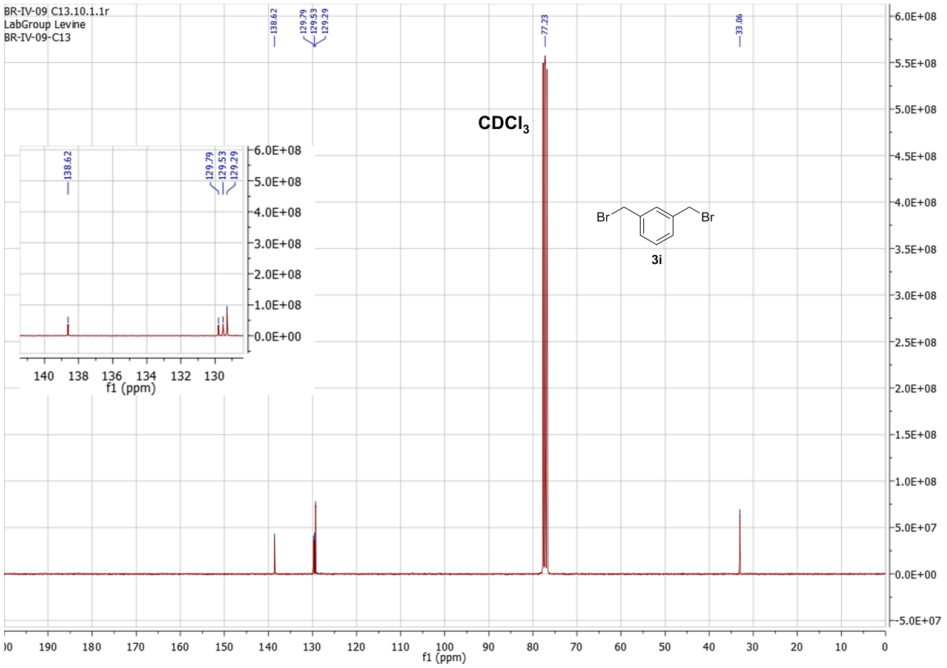

^{1}H NMR of **3l**; 300 MHz, $CDCl_3$:

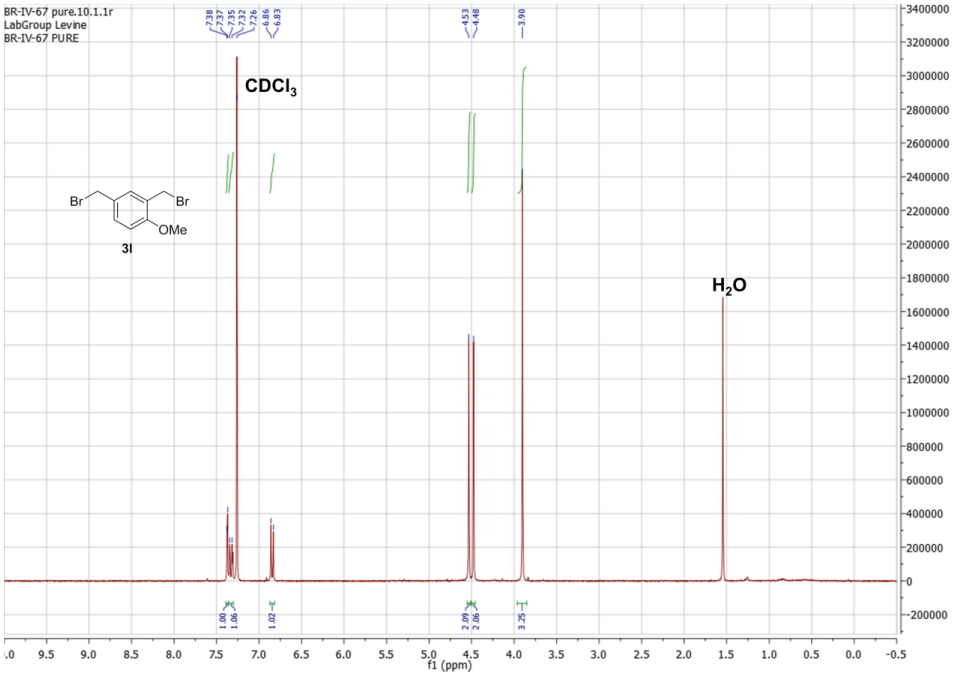

^{13}C NMR of **3l**; 75 MHz, $CDCl_3$:

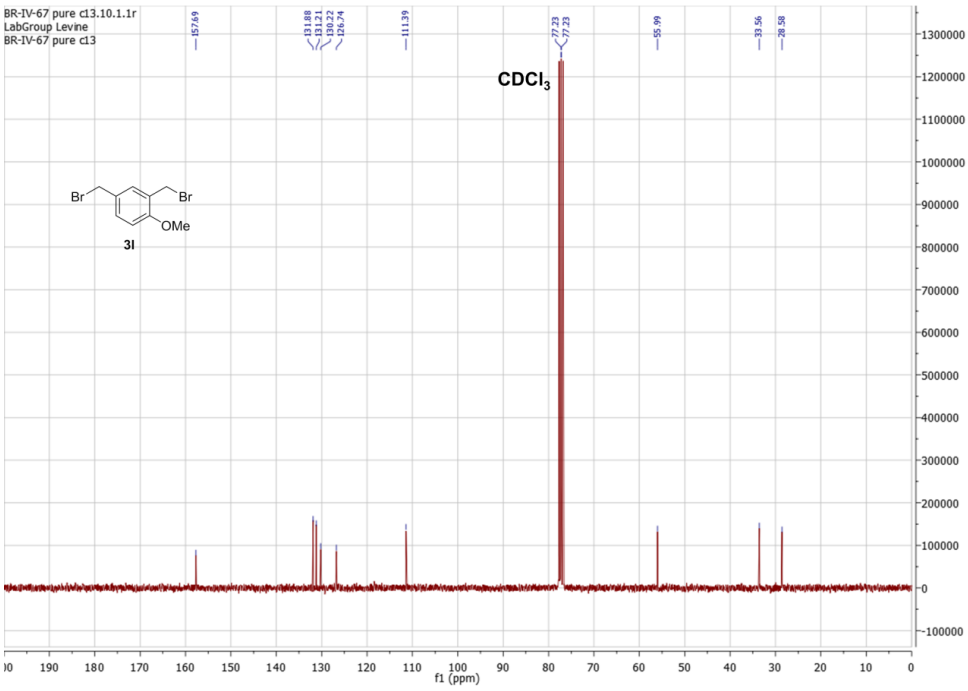

^{1}H NMR of **3m**; 300 MHz, $CDCl_3$:

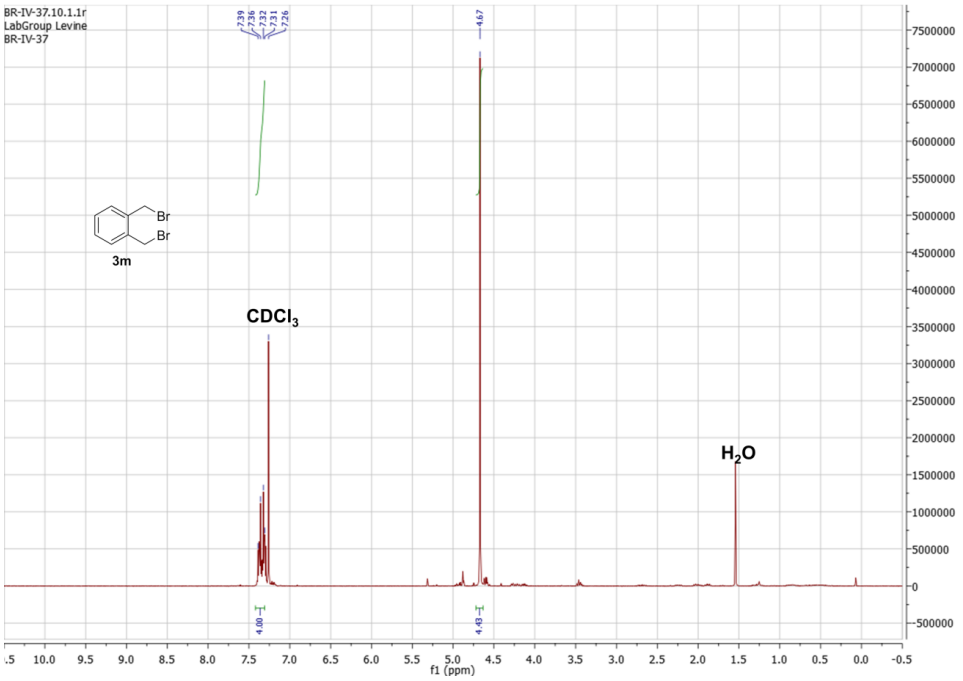

^{13}C NMR of **3m**; 75 MHz, $CDCl_3$:

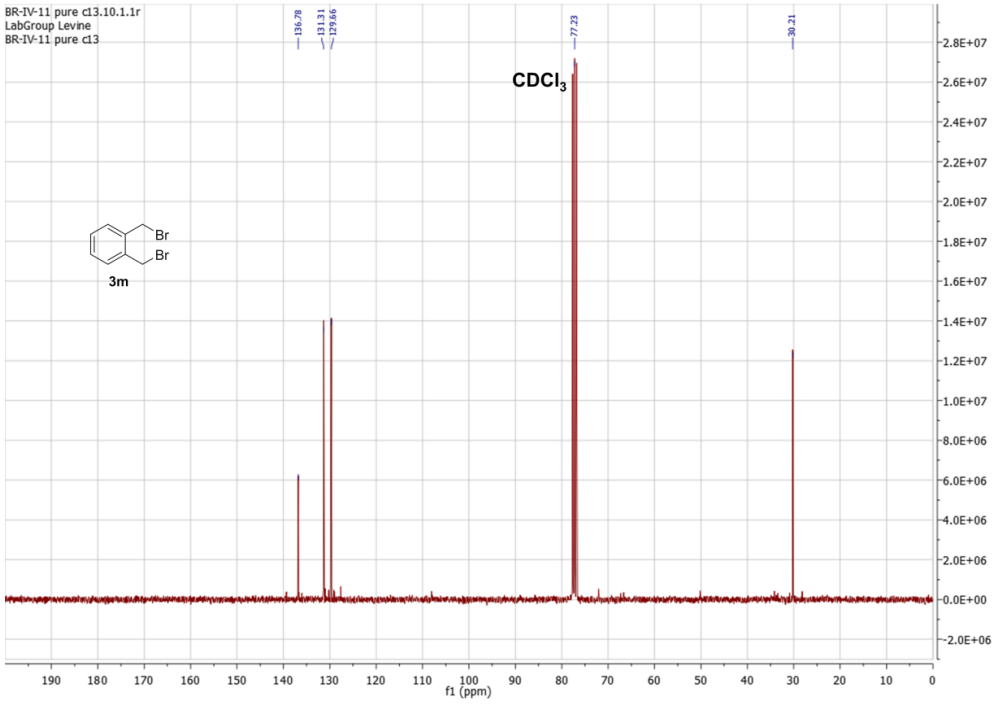

^{1}H NMR of **3n**; 300 MHz, $CDCl_3$:

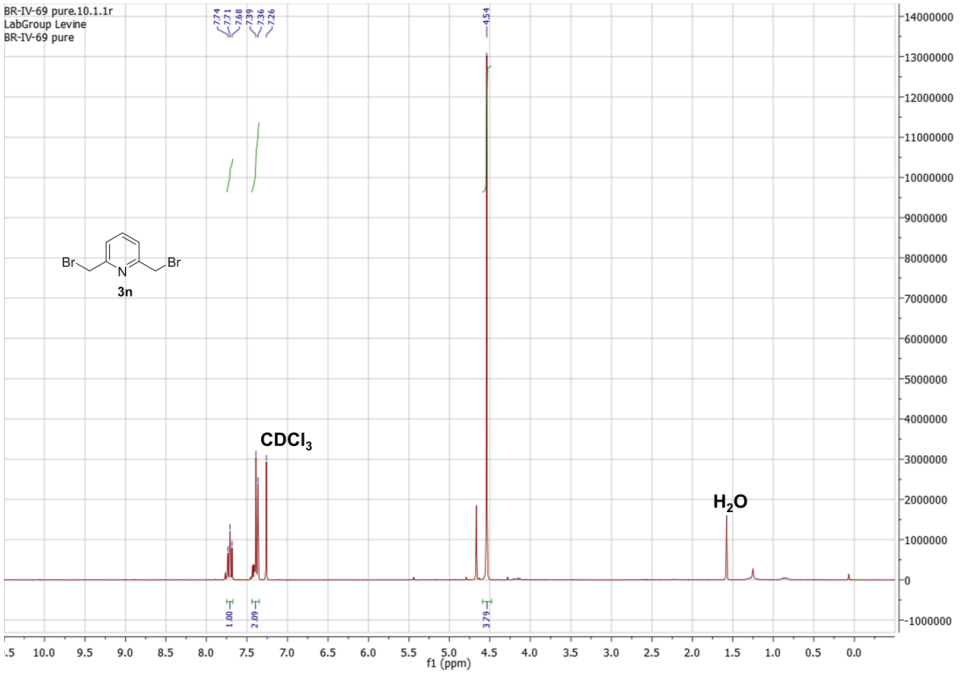

^{13}C NMR of **3n**; 75 MHz, $CDCl_3$:

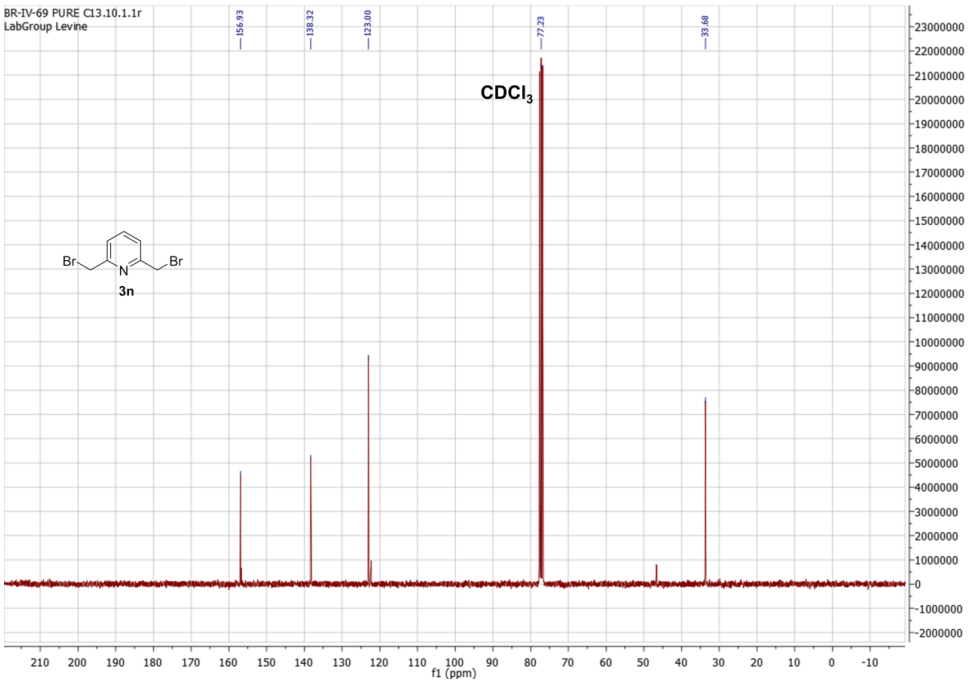

^{1}H NMR of **14**; 300 MHz, $CDCl_3$:

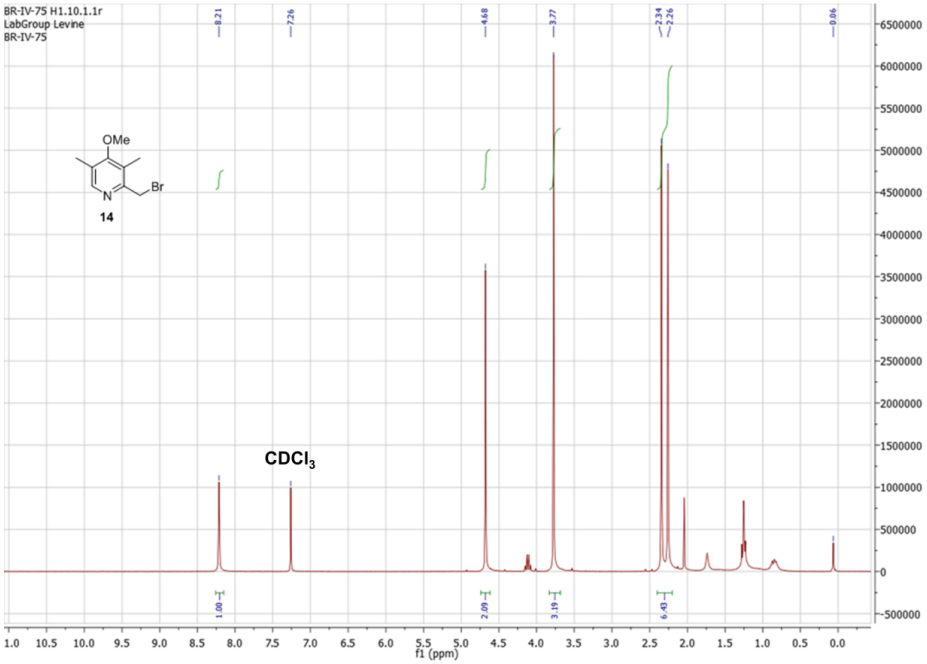

^{13}C NMR of **14**; 75 MHz, $CDCl_3$:

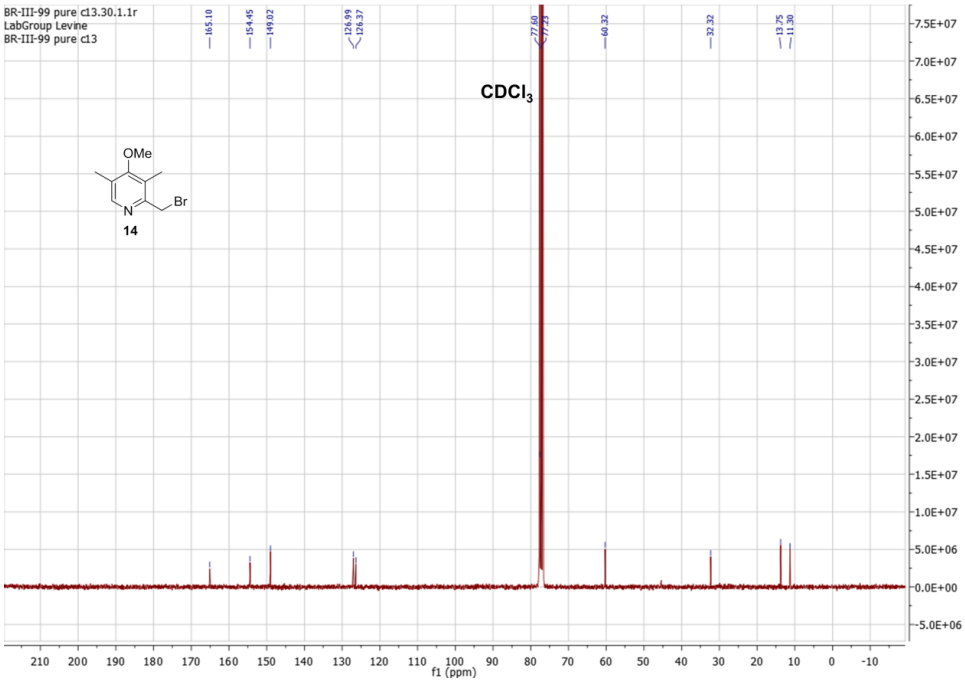

^{1}H NMR of **16**; 300 MHz, $CDCl_3$:

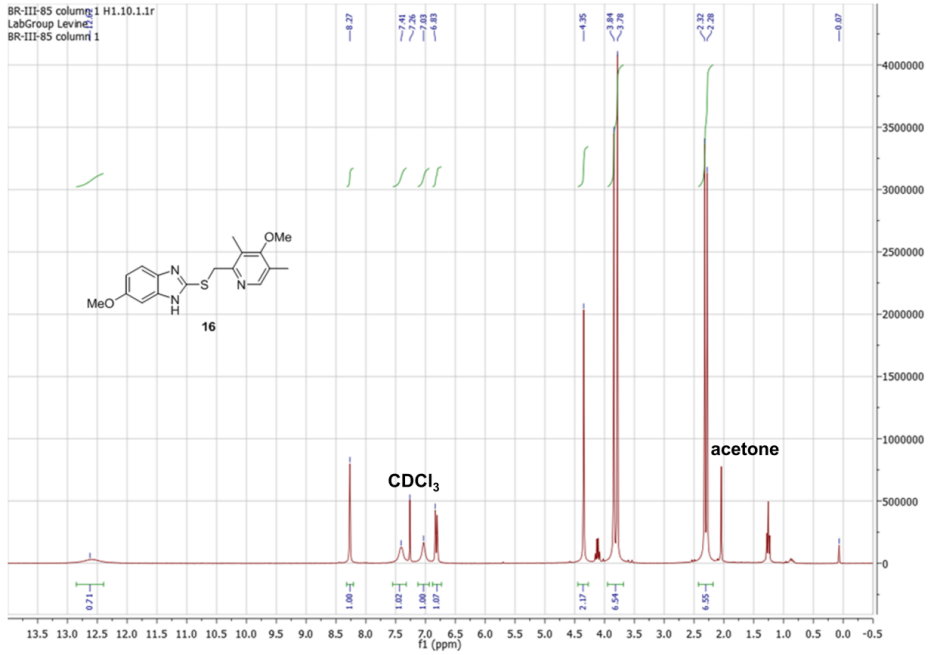

^{13}C NMR of **16**; 75 MHz, $CDCl_3$:

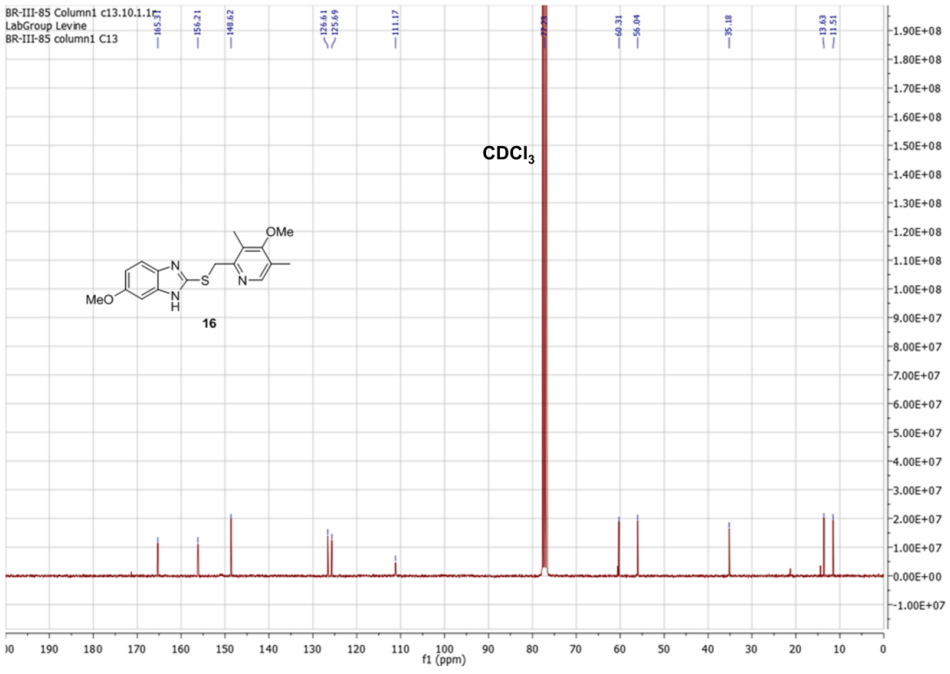

SPECTRAL CHARACTERIZATION OF COMPOUNDS 3jj AND 3kk:

^{1}H NMR of **3jj**; 300 MHz, DMSO-*d6*:

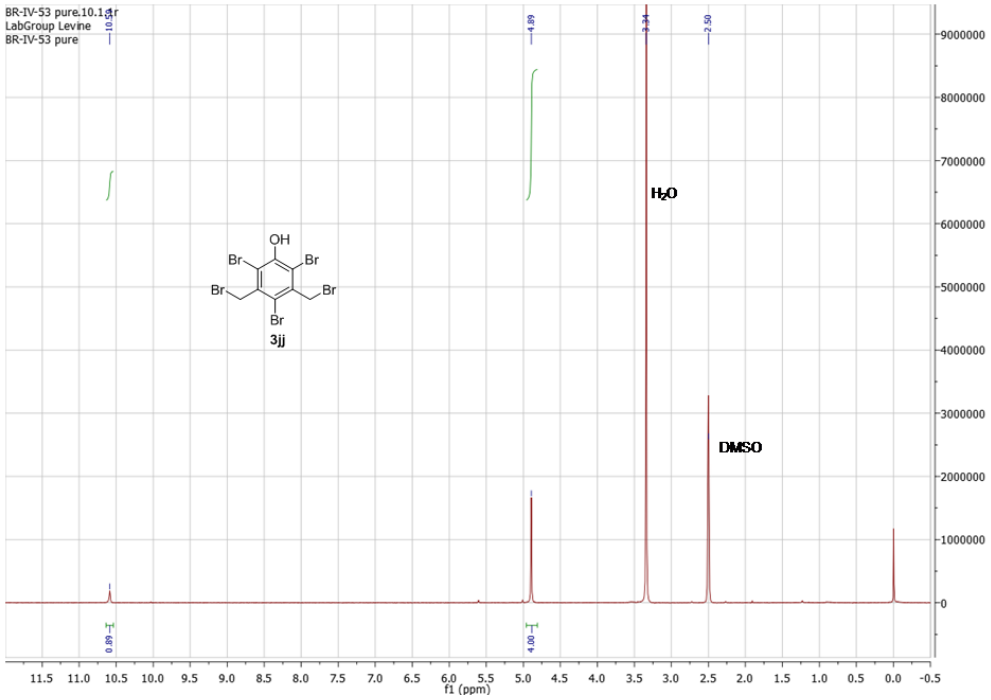

^{13}C NMR of **3jj**; 300 MHz, DMSO-*d6*:

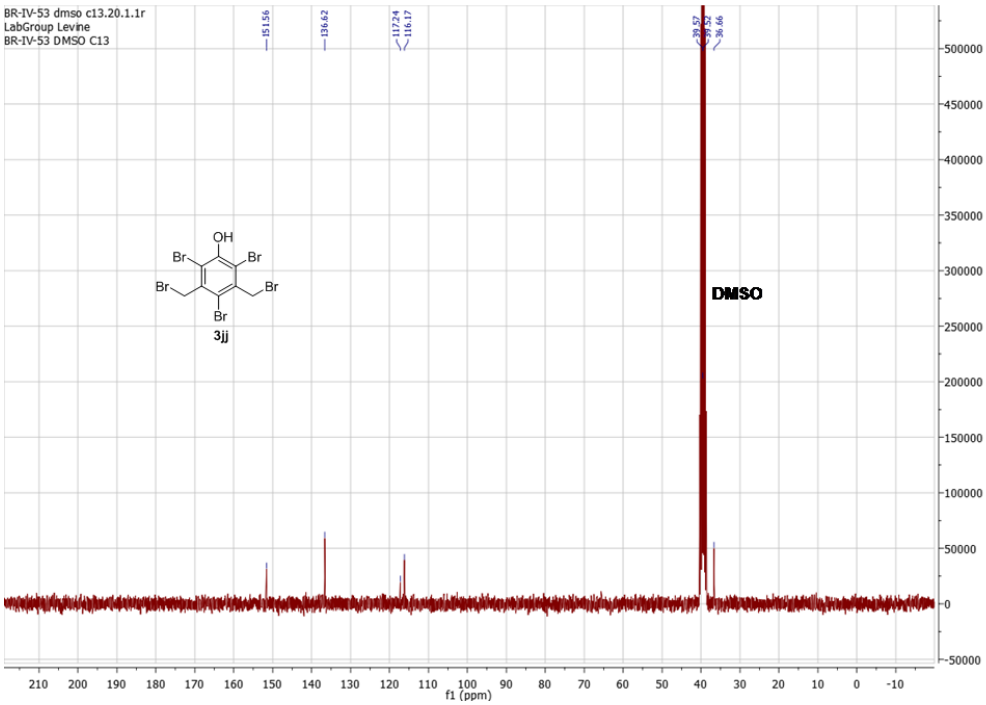

^{13}C DEPT 45 NMR of **3jj**; 75 MHz, DMSO-*d6*:

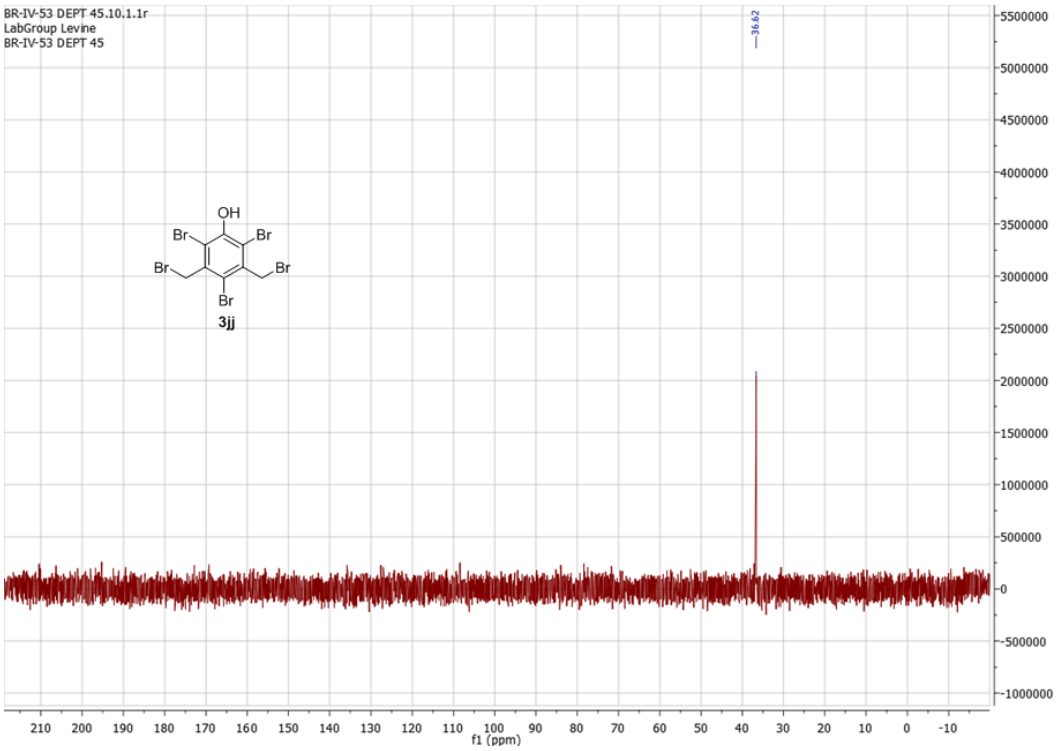

^{13}C DEPT 90 NMR of **3jj**; 75 MHz, DMSO-*d6*:

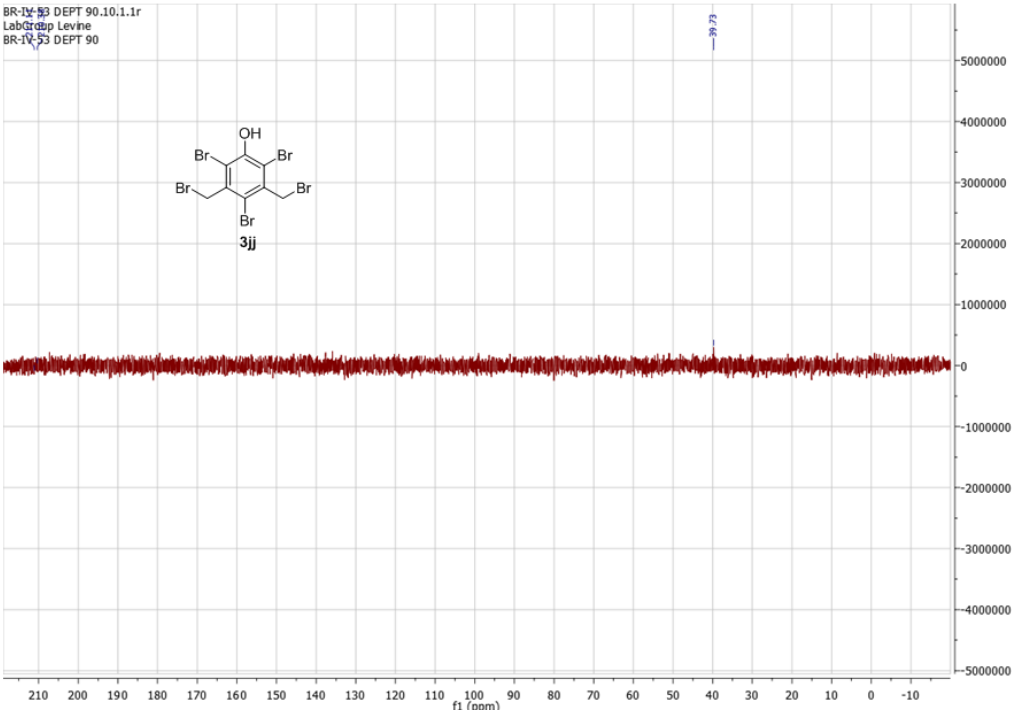

^{13}C DEPT 135 NMR of **3jj**; 75 MHz, DMSO-*d6*:

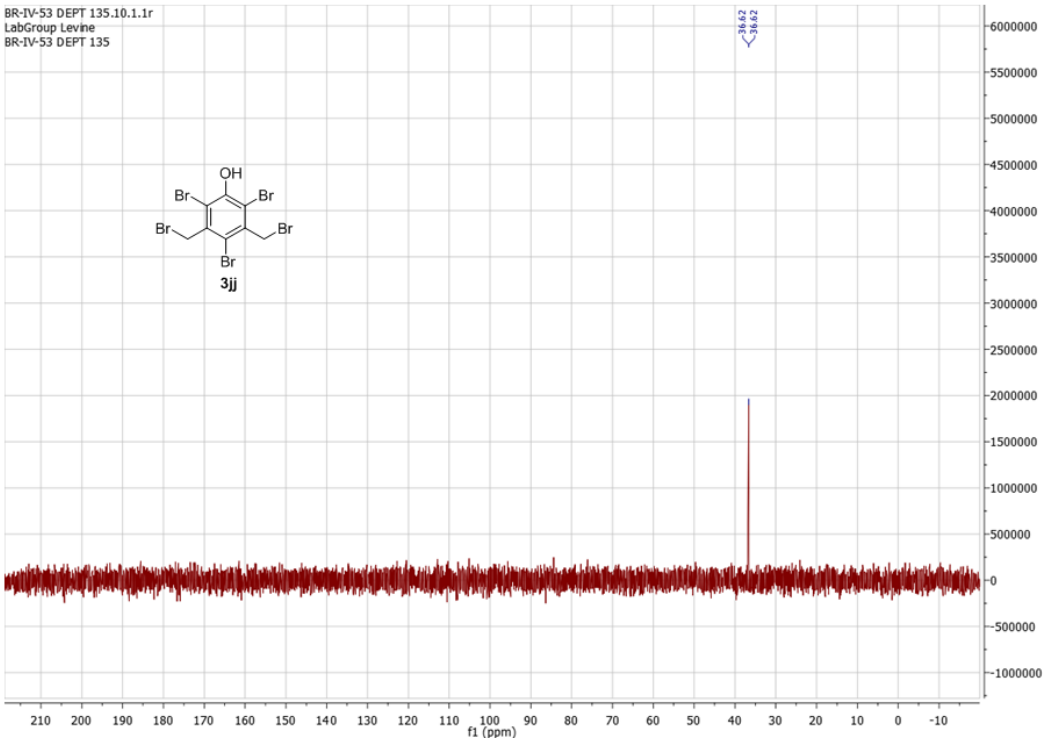

^{1}H NMR of **3kk**; 300 MHz, $CDCl_3$:

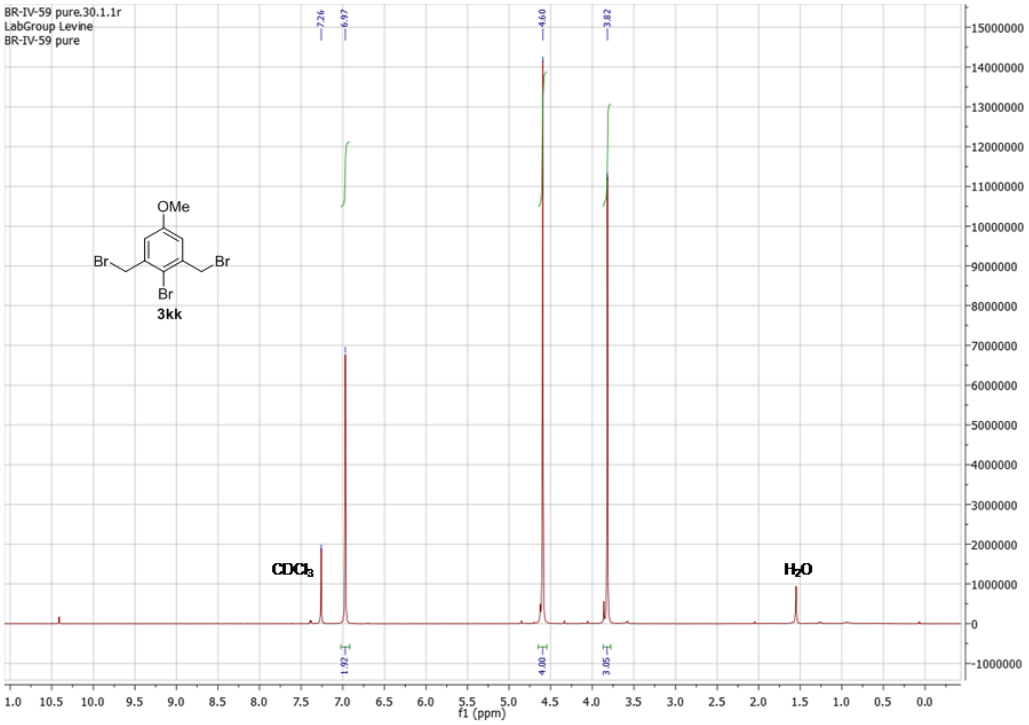

^{13}C NMR of **3kk**; 75 MHz, $CDCl_3$:

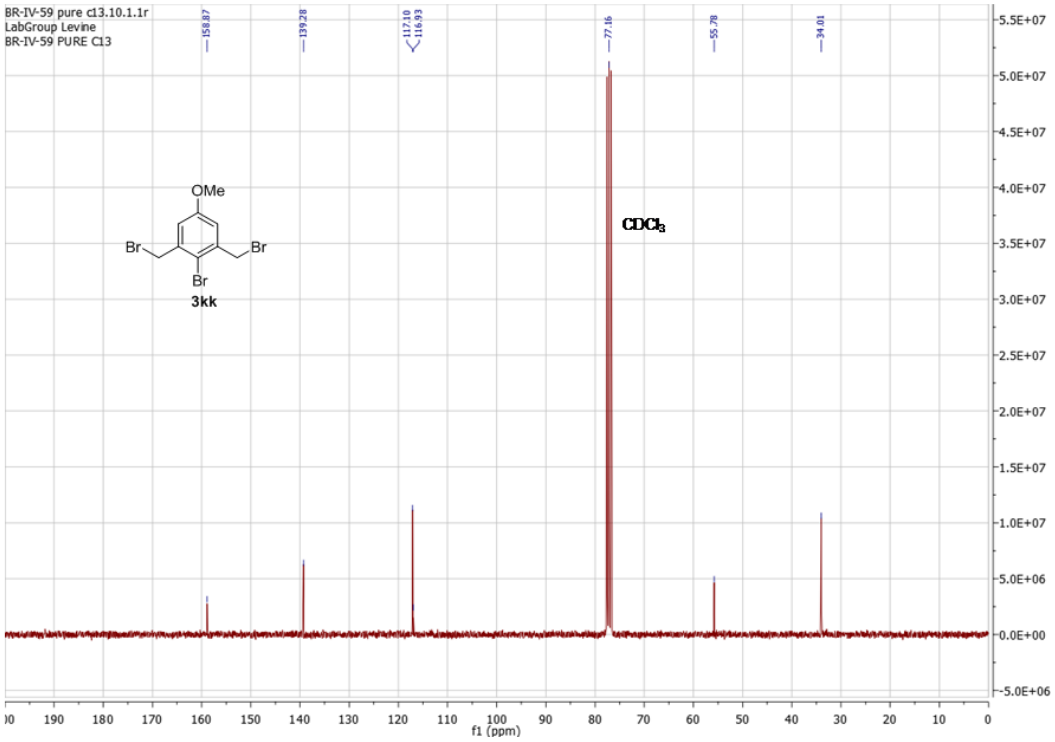

^{13}C DEPT 45 NMR of **3kk**; 75 MHz, $CDCl_3$:

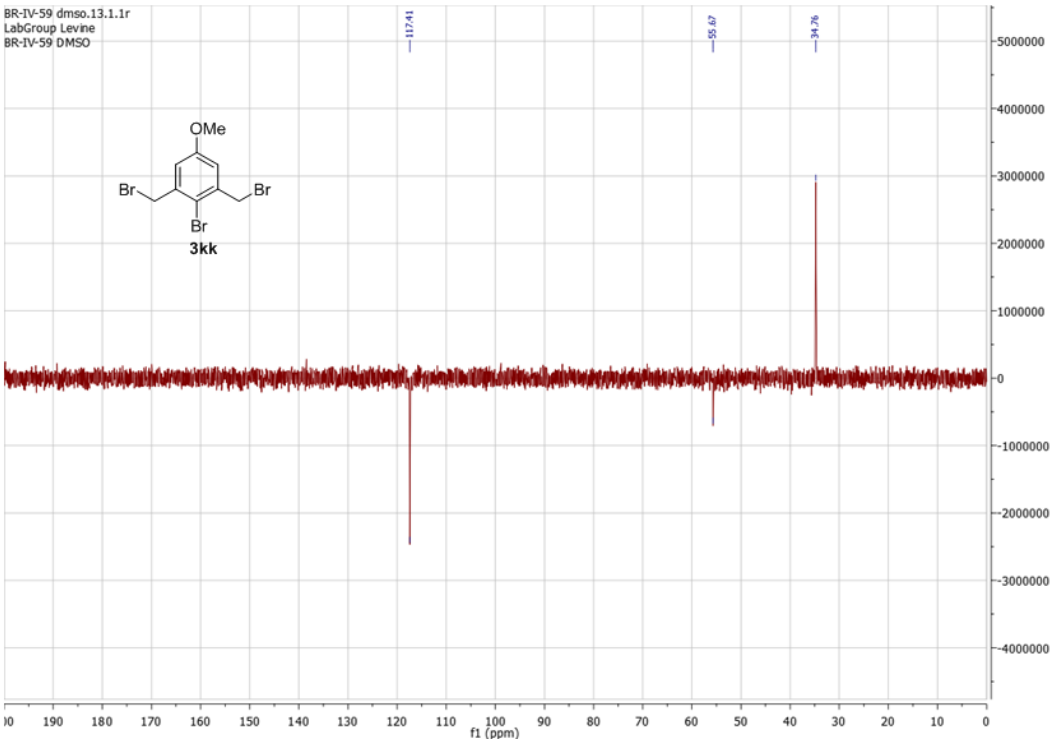

References for Supporting Information

1. Gaud, V.; Rouge, F.; Gnanou, Y.; Desvergne, J.-P.*React.Funct.Polym.* **2012**, *72*, 521-532.
2. Qiao, Z.; Wang, Q.; Zhang, F.; Wang, Z.; Bowling, T.; Nare, B.; Jacobs, R.T.; Zhang, J.; Ding, D.; Liu, Y.; Zhou, H. *J. Med. Chem.* **2012**, *55*, 3553-3557.
3. Han, D.; Tong, X.; Zhao, Y. *Langmuir* **2012**, *28*, 2327-2331.
4. Ye, L.; Ding, D.; Feng, Y.; Xie, D.; Wu, P.; Guo, H.; Meng, Q.; Zhou, H. *Tetrahedron* **2009**, *65*, 8738-8744.
5. Lee, H.J.; Jamison, A.C.; Yuan, Y.; Li, C.-H.; Rittikulsittichai, S.; Rusakova, I.; Lee, T.R. *Langmuir* **2013**, *29*, 10432-10439.
6. Tran, V. M.; Nguyen, T. K. N.; Sorna, V.; Loganathan, D.; Kuberan, B. *ACS Chem. Biol.* **2013**, *8*, 949-957.

MANUSCRIPT 4

This manuscript is published in *Dalton Trans.*, **2013**, *55*, 4905-4908.

Sensitive and selective detection of cesium via fluorescence quenching

Bhasker Radaram, Teresa Mako, and Mindy Levine*

Corresponding author:

Prof. Mindy Levine

Department of Chemistry

University of Rhode Island

Kingston, Rhode Island 02881

mlevine@chm.uri.edu

MANUSCRIPT 4

Sensitive and selective detection of cesium via fluorescence quenching

Abstract: Herein we report a robust and easy method for detecting cesium metal ion (Cs^+) in partially aqueous solutions using the fluorescence quenching of 2,4-bis[4-(*N*,*N*-dihydroxyethylamino)phenyl]squaraine. This squaraine dye was found to be both highly sensitive (low limits of detection) and selective (limited response to other metals) for cesium ion detection. The detection is likely based on the metal complexing to the dihydroxyethanolamine moieties, which disrupts the donor-acceptor-donor architecture and leads to efficient quenching.

Cesium, which is found in industrial,[1] medical[2] and nuclear wastes,[3] can cause a number of negative health effects, including cardiovascular disease and gastrointestinal distress.[4] Current methods for detecting cesium in complex environments include atomic absorption spectroscopy (AAS),[5] inductively coupled plasma mass spectroscopy (ICP-MS),[6] and solid state sensors.[7] While these methods are highly sensitive and selective for cesium detection, they are often expensive and require sample destruction.

Fluorescence-based methods have rarely been used for cesium detection,[8] even though such methods have the potential to be both cheaper and non-destructive,[9] and have been used successfully for the many analytes.[10] In one example of fluorescence-based cesium detection, researchers synthesized a substituted calixarene that bound cesium with high affinities, resulting in a significant fluorescence enhancement and a 0.3 μM detection limit.[11]

Reported herein is a highly sensitive and selective method for cesium detection that relies on the fluorescence quenching of a near-infrared emitting squaraine fluorophore (compound **1**).

Squaraine fluorophores are used extensively in detection schemes due to their narrow absorption and emission bands in the near-infrared spectral region, as well as their marked sensitivity to the surrounding environment.[12] Squaraines have been used to detect metal ions, including mercury, silver, and lead, as well as other transition metals, alkali metals, and lanthanide metals.[13]

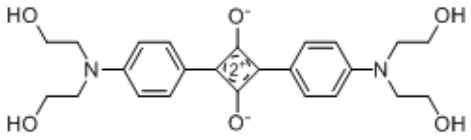

Compound 1

Compound **1** was synthesized following literature-reported procedures.[14] The fluorescence response of the squaraine to various metal ions was tested by mixing a squaraine solution in DMSO with aqueous solutions of metal ions, and comparing the fluorescence spectra of the resulting solutions with the squaraine fluorescence spectra in the absence of any metal ion (but in the same DMSO-water ratio). The squaraine solution was made fresh daily due to partial degradation under the experimental conditions.

The addition of 1.0 mM of cesium carbonate led to a significant quenching of the squaraine fluorescence to 7.6% of its initial value, as well as a complete disappearance of the characteristic squaraine absorption band (Figure 1). Even as little as 0.010 mM of cesium carbonate caused the squaraine fluorescence to decrease to 92% of its initial value (red line, Figure 1). Plotting this fluorescence quenching as a function of cesium carbonate concentration yielded a plot that rapidly approached saturation at high cesium concentrations (Figure 2).

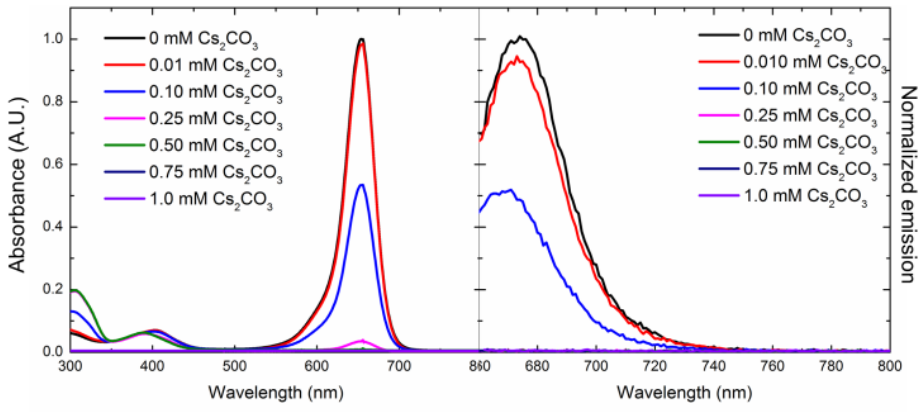

Fig. 1. The absorbance and fluorescence spectra of compound **1** with increasing amounts of cesium carbonate (0.10 mM compound **1**; 650 nm excitation).

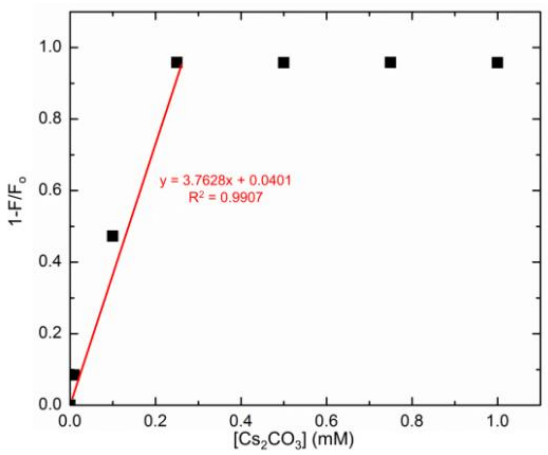

Fig. 2. Illustration of the relationship between cesium concentration and fluorescence quenching.

This complete cesium binding was easily detected by visual inspection of the squaraine solution (Figure 3). The addition of 1.0 mM of cesium carbonate rapidly turned the light blue squaraine solution colorless, whereas other common metal ions displayed no measurable color change.

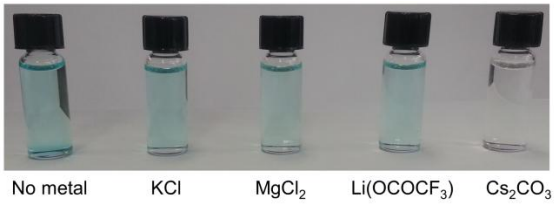

Fig. 3. Visual detection of cesium by color changes of compound **1**

The sensitivity of this method was determined by calculating the limit of detection. Although this limit is typically defined as three times the standard deviation of the background noise (or ten times the standard deviation for quantification limits),[15] in this case that definition led to a value that was effectively zero. Using 30 times the standard deviation of the background noise for these calculations led to a limit of detection of 0.096 μM, which provides an upper boundary for the detection limit. This detection method is more sensitive than previously reported fluorescence-based methods for purely aqueous solutions,[11] as well as for cesium ion detection in mixed solvent systems.[16]

The selectivity of this detection method was determined by screening a wide variety of other metals, including transition metals, alkali metals, and alkali earth metals in a variety of oxidation states. Most of these ions led to no significant changes in the squaraine's fluorescence spectra (Figure 4).

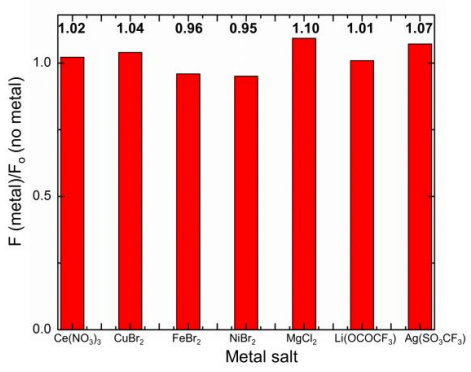

Fig. 4. The effect of metal ion addition on the fluorescence emission spectrum of compound **1** (1.0 mM metal ion; 0.10 mM compound **1**).

Preliminary experiments indicate that both the carbonate anion and cesium cation are necessary for the highly efficient fluorescence quenching, as no fluorescence quenching was observed for the following species: Cs_2SO_4, $CsNO_3$ and CsI. Both K_2CO_3 and Na_2CO_3 induced some degree of squaraine fluorescence quenching, albeit significantly less than the quenching observed for Cs_2CO_3 (at 1.0 mM metal ion: 7.6%, 28% and 29% of initial fluorescence was observed for Cs_2CO_3, K_2CO_3 and Na_2CO_3, respectively).

The squaraine fluorescence was also partially quenched in the presence of palladium chloride, with the addition of 1.0 mM of palladium chloride leading to a 22% decrease in the squaraine emission (Figure 5). In this case, the addition of any amount of palladium led to approximately the same degree of fluorescence quenching (17% quenched at [$PdCl_2$] = 0.010 mM vs. 22% quenched at [$PdCl_2$] = 1.0 mM), indicating a non-specific fluorescence quenching mechanism.

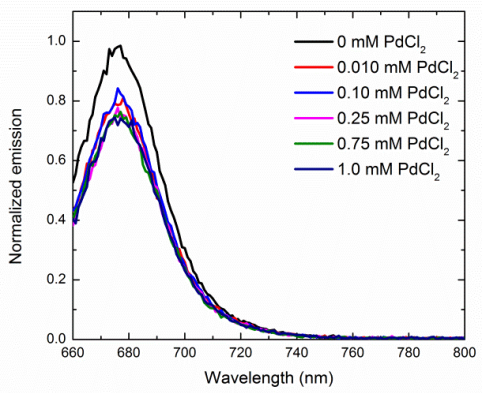

Fig. 5. Partial quenching of compound **1**'s emission in the presence of palladium (II) chloride.

The mechanism of cesium-induced fluorescence quenching is currently under investigation, but the following conclusions can already be drawn: (a) The lack of any bathochromic or hypsochromic shift in the squaraine fluorescence spectra indicates that metal-induced aggregation is unlikely to be a significant contributing factor; (b) the relatively linear

relationship between cesium concentration and fluorescence quenching (for low cesium concentrations) indicates that a well-defined ion-squaraine interaction is occurring; and (c) Job plot experiments do not yield a clear stoichiometry between the metal ion and the squaraine fluorophore.

The observed fluorescence quenching is in line with a literature report of a crown-ether containing squaraine whose fluorescence was quenched in the presence of alkali and alkali earth metals.[17] In that report, the authors concluded that the metal ions caused fluorescence quenching through binding in the crown ether moieties, which disrupted the donor-acceptor-donor nature of the squaraine chromophore.[18] Similarly, in this case we expect that the cesium cation binds strongly to diethanolamine, attenuating its strongly donating character and leading to highly efficient fluorescence quenching.[19]

Conclusions

In conclusion, reported herein is a sensitive and selective method for detecting cesium via fluorescence quenching of a squaraine fluorophore. This detection method has a number of advantages compared to previously-reported systems, including (a) low limits of detection; (b) marked insensitivity to a variety of other common metals; (c) ease of operation; and (d) monitoring of a fluorescent signal in the near-infrared spectral region, which has limited interference from other analytes and will enable detection in complex media. The mechanism of cesium-induced fluorescence quenching and the applicability of this quenching in multiple environments are currently under investigation, and results will be reported in due course.

Notes and references

1. M. V. Chandran, C. V. Ramana, T. B. Reddy and P. V. V. P. Rao, *Int. J. Sci. Nature*, 2012, **3**, 420.

2. A. M. Latifi, S. M. Nabavi, M. Mirzaei, M. Tavalaei, H. Ghafurian, C. Hellio and S. F. Nabavi, *Toxicol. Environ. Chem.*, 2012, **94**, 1670.
3. G. R. Peterson, *Technol. Innovation*, 2011, **13**, 99.
4. (*a*) P. Melnikov and L. Z. Zanoni, *Biol. Trace. Elem. Res.*, 2010, **135**, 1; (*b*) H. Miyazaki, H. Kato, Y. Kato, T. Tsuchiyama and H. Tereda, *J. Food Society Japan*, 2013, **54**, 151.
5. K. Greda, P. Jamroz and P. Pohl, *Talanta*, 2013, **108**, 74.
6. M. Liezers, O. T. Farmer and M. L. Thomas, *J. Radioanal. Nucl. Chem.*, 2009, **282**, 309.
7. E.S. Cho, J. Kim, B. Tejerina, T. M. Hermans, H. Jiang, H. Nakanishi, M. Yu, A. Z. Patashinski, S.C. Glotzer, F.Stellacci and B. A. Grzybowski, *Nature Mater.*, 2012, **11**, 978.
8. I. Leray and B. Valeur, *Eur. J. Inorg. Chem.*, 2009, 3525.
9. (*a*) C. Li and G. Shi, *ACS Appl. Mater. Interfaces*, 2013, **5**, 4503; (*b*) S. W. Thomas, G. D. Joly and T. M. Swager, *Chem. Rev*., 2007, **107**, 1339.
10. (*a*) I. Grabchev, D. Staneva, and R. Betcheva, *Curr. Med. Chem.*, 2012, **19**, 4976; (*b*) R. Rodriguez-Rodriguez and U. Simonsen, *Curr. Anal. Chem.*, 2012, **8**, 485.
11. V. Souchon, I. Leray and B. Valeur, *Chem. Commun.*, 2006, 4224.
12. (*a*) R. R. Avirah, D. T. Jayaram, N. Adarsh and D. Ramaiah, *Org. Biomol. Chem.*, 2012, **10**, 911; (*b*) L. Beverina and P. Salice, *Eur. J. Org. Chem.*, 2010, 1207; (*c*) A. Ajayaghosh, *Acc. Chem. Res.*, 2005, **38**, 449; (*d*) S. Sreejith, P. Carol, P. Chithra and A. Ajayaghosh, *J. Mater. Chem.*, 2008, **18**, 264.

13. (*a*) M. C. Basheer, S. Alex, K. George Thomas, C. H. Suresh and S. Das, *Tetrahedron*, 2006, **62**, 605; (*b*) K. George Thomas, K. J. Thomas, S. Das and M. V. George, *Chem. Commun*., 1997, 597.
14. (*a*) J. V. Ros-Lis, R. Martinez-Manez and J. Soto, *Chem. Commun*., 2002, 2248; (*b*) K. T. Arun and D. Ramaiah, *J. Phys. Chem. A*, 2005, **109**, 5571; (c) H. E. Sprenger and W. Ziegenbein, *Angew. Chem.*, 1966, **78**, 937.
15. B. Saute, R. Premasiri, L. Ziegler and R. Narayanan, *Analyst*, 2012, **137**, 5082.
16. G. G. Talanova, E. D. Roper, N. M. Buie, M. G. Gorbunova, R. A. Bartsch and V. S. Talanov, *Chem. Commun.*, 2005, 5673.
17. U. Oguz and E. U. Akkaya, *Tetrahedron Lett*., 1997, **38**, 4509.
18. W. Shi and H. Ma, *Chem. Commun.*, 2012, **48**, 8732.
19. (*a*) K. Mlinaric-Majerski and T. Sumanovac Ramljak, *Tetrahedron*, 2002, **58**, 4893; (*b*) M. Tanaka, M. Nakamura, T. Ikeda, K. Ikeda, H. Ando, Y. Shibutani, S. Yajima and K. Kimura, *J. Org. Chem.*, 2001, **66**, 7008.

Electronic Supplementary Information for

Sensitive and selective detection of cesium via fluorescence quenching

Bhasker Radaram, Teresa Mako, and Mindy Levine[*]

Materials and Methods

All reagents and solvents were purchased from Sigma Aldrich and were used as received without further purification. ^{1}H NMR spectra were recorded on a Bruker 300 MHz spectrometer. Fluorescence measurements were recorded on Shimadzu RF 5301 spectrophotometer with a 3 nm excitation slit width and a 3 nm emission slit width. All spectra were integrated vs. wavenumber using OriginPro software.

Synthesis of Compound 1

Compound **1** was synthesized following literature-reported procedures for analogous compounds (see for example *J. Am. Chem. Soc.* **2006**, *128*, 13320).

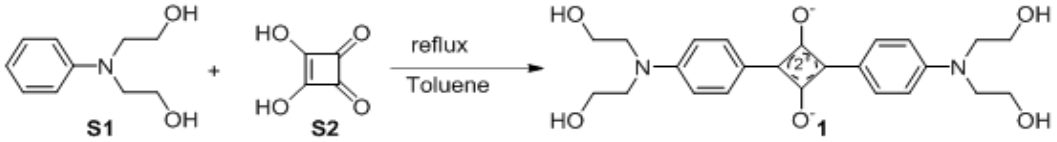

Phenyldiethanolamine **S1** (0.88 mmol, 160 mg, 2.0 eq.) and squaric acid **S2** (0.44 mmol, 50 mg, 1.0 eq.) were dissolved in a 1:1 mixture of toluene and *n*-butanol. The reaction mixture was equipped with a Dean-Stark trap and condenser, and the reaction mixture was stirred in the dark at reflux overnight. The reaction mixture was cooled to room temperature and then to 0 ^{o}C. The precipitate was collected by vacuum filtration and thoroughly dried to yield 19 mg of compound **1** (12.5% yield).

Screen of Other Metals

All non-interacting metals were screened using the following procedure:

All metal salts were dissolved in distilled water to a final concentration of 10 mM. Compound **1** was dissolved in DMSO to a final concentration of 1.0 mM.

The following solutions were added to a quartz cuvette: 20 µL of the aqueous solution, 980 µL of distilled water, 20 µL of the compound **1** solution, and 980 µL of DMSO. This created a 1:1 water: DMSO solution with final concentrations of [metal] = 0.1 mM and [compound **1**] = 0.01 mM.

After thorough mixing, the fluorescence spectra were recorded from 650 nm excitation with 3 nm excitation slit width and 3 nm emission slit width.

Counterion Effect

The following additional metal salts were screened to probe the effect of the counterion: Cs_2SO_4, $CsNO_3$, CsI, K_2CO_3, and Na_2CO_3. None of the cesium salts showed a significant quenching of the squaraine's fluorescence; however, both K_2CO_3 and Na_2CO_3 induced some fluorescence quenching.

Summary figures for all the salts:

Cesium Iodide:

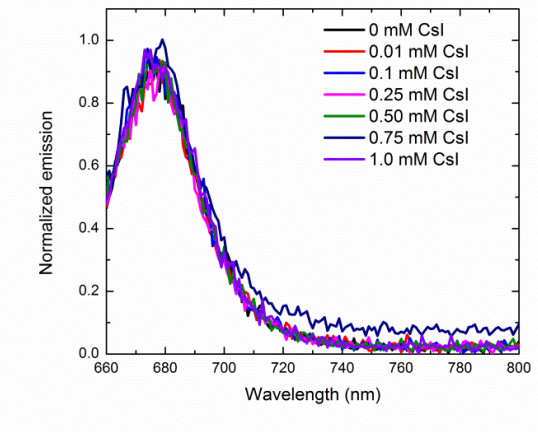

Cesium Nitrate:

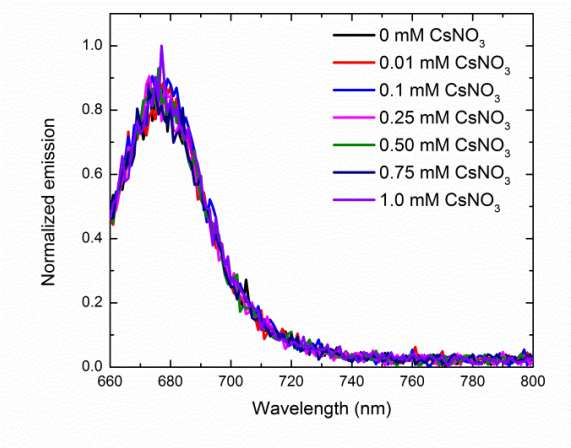

Cesium Sulfate:

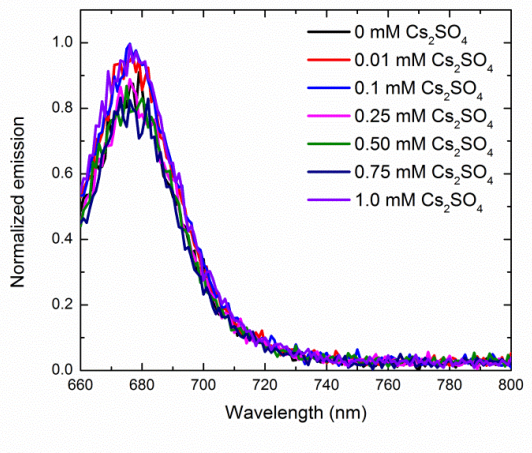

Potassium Carbonate:

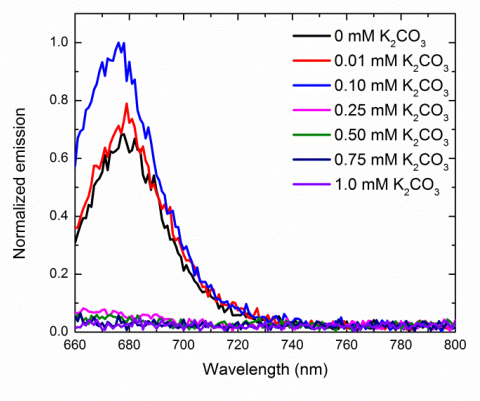

Sodium Carbonate:

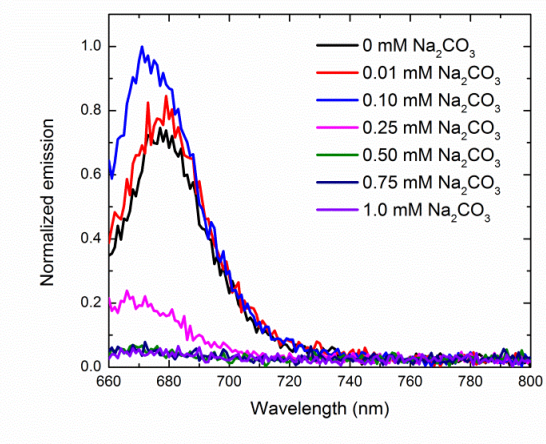

Job Plot Data

Job plot experiments were conducted as follows:

1. A stock solution of the squaraine (0.01 mg/ mL) in DMSO was formed.

2. 1.25 mL of the stock solution of squaraine was mixed with 1.25 mL of pure water. The absorbance of the solution was measured.

3. 1.25 mL of the stock solution of squaraine was mixed with 1.25 mL of cesium solution A and the absorbance was measured.

4. 1.25 mL of the stock solution of squaraine was mixed with 1.25 mL of cesium solution B and the absorbance was measured.

5. 1.25 mL of the stock solution of squaraine was mixed with 1.25 mL of cesium solution C and the absorbance was measured.

6. 1.25 mL of the stock solution of squaraine was mixed with 1.25 mL of cesium solution D and the absorbance was measured.

7. 1.25 mL of the stock solution of squaraine was mixed with 1.25 mL of cesium solution E and the absorbance was measured.

8. 1.25 mL of the stock solution of squaraine was mixed with 1.25 mL of cesium solution F and the absorbance was measured.

9. 1.25 mL of the stock solution of squaraine was mixed with 1.25 mL of cesium solution G and the absorbance was measured.

Table S1: Prepared Cesium solutions A-G

	initial conc (M)	initial conc (mM)	final mols delivered	molar ratio
solution A	0.0001	0.1	1.25E-05	4.432624113
solution B	0.00001	0.01	1.25E-06	0.443262411
solution C	0.000001	0.001	1.25E-07	0.044326241
solution D	0.000005	0.005	0.000000625	0.221631206
solution E	0.0000025	0.0025	3.125E-07	0.110815603
solution F	0.00002	0.02	0.0000025	0.886524823
solution G	0.000015	0.015	0.000001875	0.664893617

The results of these experiments were plotted with the [moles of squaraine]/ [moles of squaraine + moles of Cesium] on the X-axis, and the absorbance at 656 nm (the absorption maximum of the squaraine) on the Y-axis:

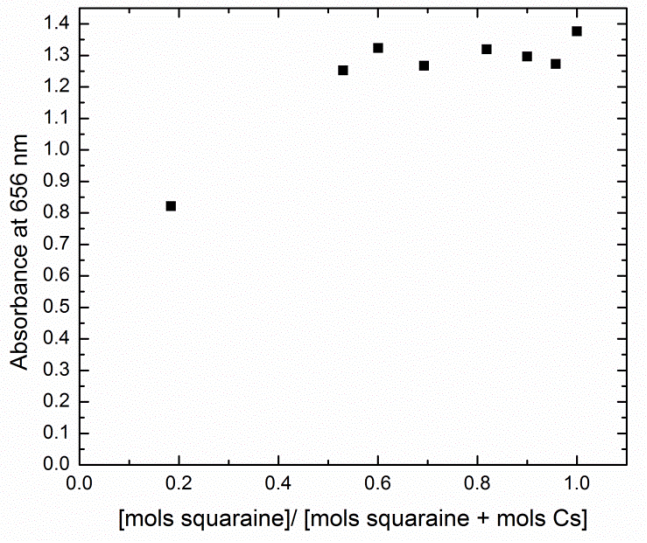

Details for Limit of Detection Experiments

The limit of detection (LOD) is defined as the lowest concentration of analyte at which a signal can be detected. To determine the limit of detection, the following experiments were conducted:

1. Dilutions of the cesium carbonate stock solution were made to yield the following seven solutions:
2. Solution 1 was prepared to make a final concentration of 0 mM.
3. Solution 2 was prepared to make a final concentration of 0.010 mM.
4. Solution 3 was prepared to make a final concentration of 0.1 mM.
5. Solution 4 was prepared to make a final concentration of 0.25 mM.
6. Solution 5 was prepared to make a final concentration of 0.5 mM.
7. Solution 6 was prepared to make a final concentration of 0.75 mM.
8. Solution 7 was prepared to make a final concentration of 1.0 mM.
9. 20 µL of each solution was combined with 980 µL of distilled water, 20 µL of the squaraine solution, and 980 µL of DMSO. The solutions were excited at 650 nm and the emission spectra were recorded 6 times for each cesium concentration.

Table S2: Series of dilutions of cesium carbonate

Solution number	Initial concentration	Final concentration in squaraine solution
1	0 mM	0 mM
2	1 mM	0.010 mM
3	10 mM	0.10 mM
4	25 mM	0.25 mM
5	50 mM	0.50 mM
6	75 mM	0.75 mM
7	100 mM	1.0 mM

All fluorescence emission spectra of the fluorophore were integrated vs. wavenumber, and calibration curves were generated, with the analyte concentration on the X-axis (in mM) and $1\text{-}F/F_o$ on the Y-axis, where F = the integrated fluorophore emission at a particular cesium concentration and F_o = the integrated fluorophore emission in the absence of cesium. The lower cesium concentrations yielded a linear relationship, and the equation for the line was determined.

The limit of the blank was taken to be the average of the blank (squaraine emission without cesium) + 30 times the standard deviation of the blank.

This value was entered into the equation determined in step 3 (for the Y value), and the corresponding X value was determined. This value provided the LOD in mM.

MANUSCRIPT 5

This manuscript is published in *Chem. Commun.*, **2015**, *51*, 7061-7064.

Highly efficient detection of hydrogen peroxide in solution and in the vapor phase via fluorescence quenching

Patrick Marks, Bhasker Radaram, Mindy Levine*, and Igor A. Levitsky*

Corresponding authors:

Prof. Mindy Levine

Department of Chemistry

University of Rhode Island

Kingston, Rhode Island 02881

mlevine@chm.uri.edu

Dr. Igor A. Levitsky

Principal Scientist

Emitech, Inc.,

Fall River, MA 02720

ilevitsky@chm.uri.edu; ilevitsky@emitechinc.com

MANUSCRIPT 5

Highly efficient detection of hydrogen peroxide in solution and in the vapor phase via fluorescence quenching

Abstract: Herein we report the highly efficient and sensitive detection of hydrogen peroxide in both aqueous solution and in the vapor phase via fluorescence quenching (turn-off mechanism) of the amplified fluorescent conjugated polymer-titanium complex induced by hydrogen peroxide. Inter and intra-polymer energy migration leads to extremely high sensitivity.

The detection of hydrogen peroxide (HP) remains a crucial research objective, as hydrogen peroxide has been used in the manufacture of homemade explosives,[1] and has caused significant accidental explosions, even at low concentrations.[2] The presence of elevated levels of hydrogen peroxide in biofluids indicates significant oxidative stress;[3] such stress can cause long-term oxidative damage to cells and organs.[4]

Despite the importance of detecting hydrogen peroxide in multiple environments, the reactive and transient nature of hydrogen peroxide means that it is difficult to develop direct detection methods. Most detection methods for hydrogen peroxide react the hydrogen peroxide with a substrate, and monitor the conversion of that substrate to product using a variety of analytical techniques,[5] including electrochemistry,[6]chemiluminescence,[7] and fluorescence spectroscopy.[8,9] Such indirect methods have been used successfully in a number of cases, including the hydrogen peroxide-induced hydrolysis of boronate esters, which often correlates with a detectable fluorescence change.[8] Colorimetric-based methods have also been

developed, wherein the introduction of hydrogen peroxide leads to a visible change in the color of the sensor that can be quantified to measure hydrogen peroxide concentrations.[10] In one reported example, titanium-oxo complex **1** was adsorbed on paper towels.[11] Upon exposure to the vapor of a 35 weight% solution of hydrogen peroxide, the paper towel turned from colorless to yellow due to the formation of titanium-oxo complex **2** (Scheme 1).[12]

Most literature reports about liquid phase hydrogen peroxide detection via fluorescence enhancement as the basis for detection ("turn-on mechanism");[8] meanwhile, there are a few studies where fluorescence quenching ("turn-off mechanism") has been employed as a transducer signal.[9] It was demonstrated in pioneering works by Swager's group that the fluorescence quenching of sensory conjugated polymers results in amplification of the responsive signal due to the energy migration effect.[13] The exciton energy migration along the polymer chain provides effective trapping and quenching of excitations generated by light, which is much greater than the quenching observed for isolated molecules (*i.e.* the concept of "amplifying polymers" (AMP) used in chemosensing).[14] He et al[9] reported hydrogen peroxide and glucose sensing in aqueous media via the AMP effect. The detection of HP vapors has been studied by fluorescence turn-on[8] and colorometric[10,11] methods, neither of which can provide the same high sensitivity as the AMP approach.

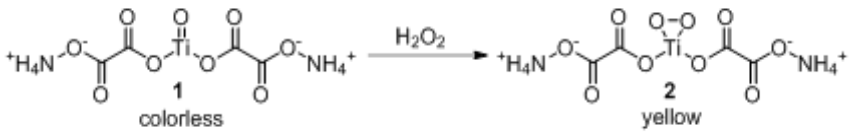

Scheme 1 Literature-reported colorimetric sensor for hydrogen peroxide.

Reported herein is the detection of hydrogen peroxide in both solution and in the vapor phase, using a combination of titanium complex **1**, fluorescent conjugated polymer **3**, and inert polymer **4**(Chart 1).

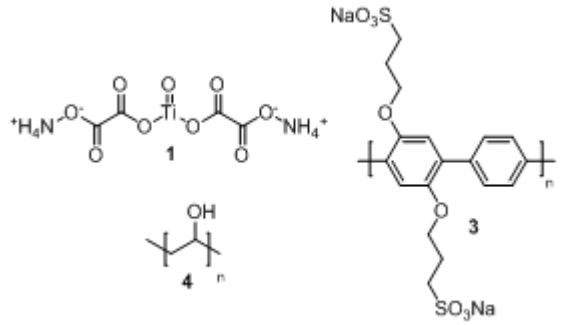

Chart 1 Structures of compounds used for hydrogen peroxide detection

The introduction of hydrogen peroxide led to the highly efficient fluorescence quenching of polymer **3** in these complex mixtures, through energy migration along the polymer backbone. The critical feature of this research is the application of AMPs to the design of an HP detection system, resulting in extraordinary sensitivity to HP vapors in the solid state (detection limit is ~ 200 ppt), which significantly exceeds previously reported results.[8-11] Fluorescence quenching-based detection methods have a number of advantages compared to other methods,[15] including the potential for high sensitivities,[16] rapid response times,[17] and straightforward experimental design and set-up. We have previously reported the use of fluorescence quenching for the detection of electron-deficient nitroaromatic compounds[18] and cesium carbonate.[19] The system reported herein has a number of notable advantages, including the use of a solid-state fluorescent film to detect extremely low vapor concentrations of hydrogen peroxide via highly efficient fluorescence quenching.

Polymer **3** was mixed with titanium complex **1** in two ways: by mixing the two compounds in an aqueous solution, and by co-depositing the two compounds on spin-cast thin films. In neither case were the polymer and titanium complex covalently linked; however, the electrostatic complementarity between the negatively charged polymer and positively charged

titanium complex enabled such association. This close association meant that the hydrogen peroxide-induced conversion of compound **1** to compound **2** directly influenced the fluorescence emission spectra of polymer **3**, leading to highly efficient fluorescence quenching. The association between polymer **3** and complex **1**can be confirmed by the fact that the absorption spectrum of solution of **3** and **1** is different from a sum of spectrum **1** and spectrum **3** (Figure 1A).

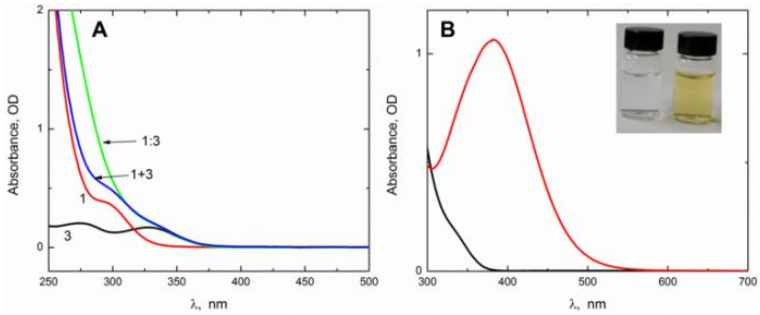

Fig. 1 (A) Absorption spectra of polymer **3** ([**3**] = 6.25E-3 M, black line), titanium complex **1** ([**1**] = 1.7 mM, red line), solution of **1** and **3** (polymer:titanium complex **1**:**3**, green line), and the sum of spectrum of titanium complex **1** and spectrum of polymer **3** (**1+3**,blue line); (B) Absorption spectra of polymer:titanium complex in the absence (black line) and the presence (red line) of hydrogen peroxide at concentration of 0.83 mM. Inset shows the color change at addition of hydrogen peroxide.

Upon introduction of hydrogen peroxide (up to 0.83 mM) to the polymer-titanium solution ([**3**] = 6.25E-3 mg/mL; [**1**] = 1.7 mM), the absorbance spectrum changed dramatically to show a broad absorption peak at 381 nm (Figure 1B). This result, and the concomitant color change of the solution (see inset), is in line with the literature-reported conversion of compound **1** to compound **2**.[11]

Concurrently with this change in the solution absorption spectrum was a dramatic quenching of the solution's fluorescence (Figure 2). Interestingly, the quenching efficiencies depended strongly on the fluorescence excitation wavelength, with the longer wavelength excitation

leading to more efficient fluorescence quenching. Such dependency on excitation wavelength could be related to the inner filter effect[20] masking the energy transfer mechanism. The most efficient quenching was observed with 370 nm excitation, where the addition of 0.83 mM of hydrogen peroxide led to an 80% decrease in the solution's fluorescence emission. Control experiments indicate that hydrogen peroxide has a limited effect on the photophysical properties of polymer **3** directly, causing a slight increase and red-shift in the fluorescence emission spectrum (see ESI for more details).

Because of the close proximity of complex **2** to polymer **3**, and significant overlap between the absorption band of **2** and the fluorescence emission band of **3**, energy transfer from donor **3** to acceptor **2** is highly likely. We believe that the salt bridges between Ti complex and water soluble polymer strongly affects the quenching process providing the trapping of excitations (energy or/and electron transfer). In this context, it is noteworthy that photoinduced charge transfer or Dexter energy transfer mechanisms could also contribute to fluorescence quenching in parallel with Forster energy transfer. However in our case, energy transfer could coexist with a trivial "inner filter" effect[20] when excitation light and the fluorescence of polymer **3** are partially absorbed by compound **2** (λ_{max} abs = 381 nm).

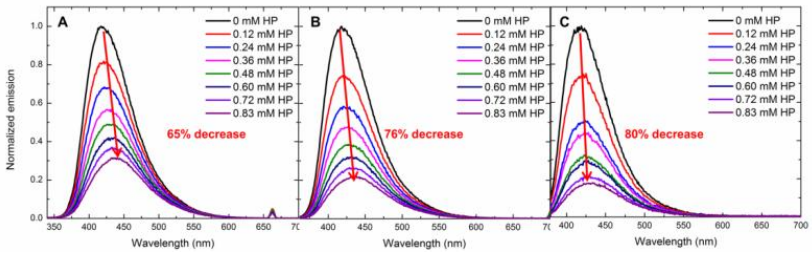

Fig. 2 Fluorescence quenching of the polymer-titanium solution from (A) 330 nm excitation; (B) 350 nm excitation; (C) 370 nm excitation**.**

Such an inner filter effect consists of two mechanisms: primary screening, wherein absorptive species reduce the intensity of excitation light, and secondary screening (or reabsorption),

when fluorescence intensity is absorbed due to overlapping of absorbance and fluorescence spectra. The clear indication of reabsorption is a red shift of the quenched fluorescence band with increasing concentrations of hydrogen peroxide (Figure 2). In order to avoid reabsorption, the Stern-Volmer plots shown in Figure 3 were calculated taking into account only the fraction of fluorescence band where overlap between the absorption band of **2** and the fluorescence band of **3** is minimal (integrated area from 475 to 600 nm).

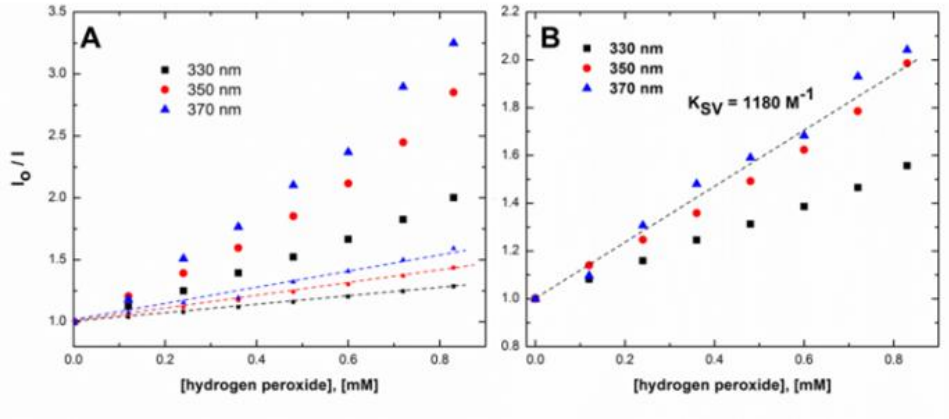

Fig. 3 (A) Stern–Volmer plots for excitation wavelengths of 330nm, 350nm and 370 nm as measured (large dots) and calculated SV plots according to Eq. 1 without accounting for energy transfer (small dots/dash lines), presenting a contribution of the primary screening effect; (B) Stern–Volmer plots corrected on primary screening effect. Stern-Volmer constant (K_{SV} = 1180 M^{-1}) was determined from the slope of the dashedline.

Next, we corrected Stern-Volmer (SV) plots on the primary screening effect taking into account the optical densities of **2** and **3** for the three excitation wavelengths at increasing concentrations of compound **2** (see ESI). The dashed lines in Figure 3A show the calculated plots (eqn S5 in ESI) with the absence of the energy transfer (K_{ET} = 0) and presents the contribution of the primary screening effect for each excitation wavelength (330 nm, 350 nm, and 370 nm). The slopes of these dependencies are significantly smaller than the slope of the

measured SV plots, which indicates an existence of the energy transfer effect. Figure 3B demonstrates the corrected SV plots obtained by dividing the measured SV plots by the calculated contributions of the primary screening effects for the three excitation wavelengths.

As it is expected after this correction, the SV plots at 350 and 370 nm excitation are almost identical, however they are slightly distinctive from the SV plot at 330 nm excitation. The latter fact can be associated with additional absorption of hydrogen peroxide itself at 330 nm (Fig. 1A), which affects the correction term in Equation S5 (ESI). Considering the linear SV plots at 350 and 370 nm only, an energy transfer constant of K_{ET} = 1180 M^{-1} can be deduced.

The most interesting results were obtained using thin films for the detection of HP vapors via fluorescence quenching. Attempts to directly spin-coat aqueous solutions of polymer **3** on thin films were unsuccessful, likely due to difficulties in fully evaporating water from the film[21] However, the addition of inert polymer **4** to the solution prior to thin film formation enabled the successful spin-coating of fluorescent thin films, by providing a hydrogen-bonding matrix for polymer **3**.[22] The films were spun-coat from hot aqueous solutions of compounds **1**, **3**, and **4** ([**1**] = 50 g/L; [**3**] = 0.10 g/L; [**4**] = 23 g/L), and were suspended in a cuvette saturated with vapors from a hydrogen peroxide solution, while ensuring no direct contact between the film and the solution (see ESI).

Under these experimental conditions, efficient fluorescence quenching was observed upon exposure of the thin films to vapors from a 30 and 300 ppm hydrogen peroxide solution (Figure 4C and 4D), with the degree of fluorescence quenching correlating with the concentration of hydrogen peroxide. No significant changes in the fluorescence spectra were observed in the absence of hydrogen peroxide or with 3 ppm of hydrogen peroxide solution (Figure 4A and B). The degree of fluorescence quenching for the 30 and 300 ppm hydrogen peroxide solutions is particularly noteworthy given the low concentration of hydrogen

peroxide in the vapor phase (approximately 0.27 ppb and 2.7 ppb for the 30 ppm and 300 ppm solutions, respectively).[23] Thus, the detection limit (DL) for HP vapors can be estimated as low as ~ 200 ppt, which is significantly lower than limits reported by Sanchez et al (300 ppb)[8] and by Xu et al (400 ppb).[11] Such substantial improvements in the system's sensitivity to HP vapors is related to an amplifying polymers effect (turn-off mechanism), which outperforms colorimetric chemosensing or fluorescent sensory polymers with turn-on mechanisms.[8,10,11] We already noted that AMP provides an extremely high sensitivity due to energy migration along the polymer backbone, resulting in effective fluorescence quenching ("turn-off") when multiple excitations (excitons) can be quenched by a single analyte. Meanwhile, energy migration through the polymer chain resulting in fluorescence enhancement ("turn-on" mechanism) is not so obvious as no direct evidence of the amplification effect has been presented in most studies,[24] (with few exceptions).[25] Turn-off AMPs, in contrast, have been confirmed by the comparison of the responsive signal between the monomer and polymer species.[13] Furthermore, films of amplifying polymers demonstrate increased sensitivity due to inter-polymer energy migration[26] compared to isolated polymer chains in solution or films composed from highly diluted polymers by inert matrix. We have found the same trends in quenching efficiencies for our system, with substantially increased sensitivity in thin films compared to in the solution state.

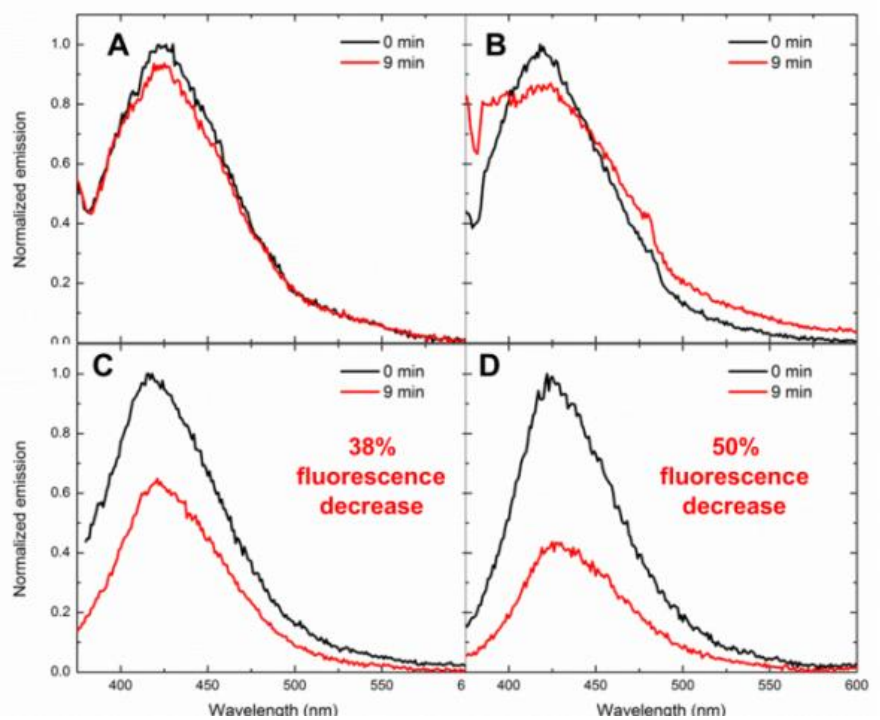

Fig. 4 Fluorescence quenching of hybrid thin films upon exposure to (A) 0 ppm hydrogen peroxide; (B) 3 ppm hydrogen peroxide; (C) 30 ppm hydrogen peroxide; and (D) 300 ppm hydrogen peroxide.

Table 1 shows how the fluorescence quenching (I_o/I ratio after 9 min exposure to HP vapors) depends on varying concentration of polymer **4** (at constant concentration of **3** and **1**) in the solutions prepared for spin coating (the inner filter effect is negligible because of the film's small thickness). As it can be seen, there is a clear trend of more efficient quenching with decreasing fractions of inert polymer **4**, strongly implying the presence of inter-polymer energy migration between chains of polymer **3**. Thus, the detection limit can be further reduced by approximately 40% using lower concentrations of polymer **4** ([**4**]=10g/L). It is noteworthy that optimization of the preparation methods for thin films (*i.e*. using dip coating or Langmuir-Blodgett techniques) could additionally improve the film sensitivity to the low

parts per trillion range, due to more equilibrium deposition and improved polymer chains alignment.

Table 1. Fluorescence quenching (I_0/I) after 9 min of exposure to HP vapors for films spin coated from a solution with [**3**] = 0.1 g/L; [**1**] = 50 g/L; and varying concentration of **4.**

[HP]	**[4] = 10 g/L**	**[4] = 23 g/L**	**[4] = 55 g/L**
0.27 ppb HP	2.0	1.6	1.1
2.7 ppb HP	5.1	2.1	1.2

The proposed mechanism of fluorescence quenching likely involves the hydrogen peroxide-induced conversion of compound **1** to compound **2** (Scheme 1). Whereas the presence of compound **1** has no effect on the fluorescence of polymer **3**, compound **2** acts as a strong fluorescence quencher using amplified fluorescence quenching. Figure 5shows a schematic illustration of possible mechanisms of fluorescence quenching upon HP exposure for isolated polymer chains (solution, highly diluted films) and for a polymer network (low diluted films). Here the intra- and inter- energy migration mechanisms are presented by small blue arrows (exciton hopping between adjacent conjugated segments along the polymer chain) and green small arrows (exciton hopping between polymer chains in the junction area), respectively. Red arrows represent direct energy transfer from polymer **3** to complex **2**. It is expected that at the limit of no dilution of polymer **3**, that the sensitivity should be maximal and controlled by inter- and intra- 3D energy migration through the densely packed chains of polymer **3** only. Efforts to fully understand this quenching mechanism and to use these results to develop practical hydrogen peroxide sensors are in progress.

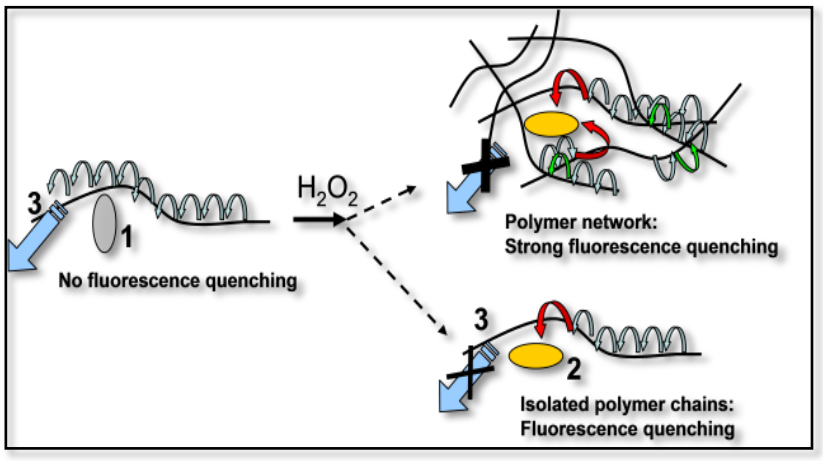

Fig. 5. Schematic illustration of mechanisms of HP-induced fluorescence quenching of conjugated polymer **3**.

In conclusion, reported herein is the fluorescence quenching of a polymer **3**-titanium **1** mixture in the presence of extremely low concentrations of hydrogen peroxide. To our knowledge, this is a first report describing a fluorescence-based sensor for hydrogen peroxide vapors with extremely high sensitivity (detection level of approximately 200 ppt). Such high sensitivity is a result of the amplified fluorescence quenching enabled by conjugated polymers, and can be further improved by the use of rational design of donor-acceptor pairs and polymer morphology in solid films. This system, which relies on the hydrogen peroxide induced conversion of compound **1** to compound **2**, has a number of operational advantages, including: (a) high sensitivity to low concentrations of hydrogen peroxide; (b) straightforward, rapid readout, and (c) the ability to detect hydrogen peroxide in both concentrated solutions and in highly dilute vapor phases. This approach has substantial potential applications in the development of practical sensors for hydrogen peroxide detection in biological systems, environmental monitoring and public safety. The results of these and other investigations will be reported in due course.

Notes and references

1. E. A. Espinosa-Fuentes, A. J. Pena-Quevedo, L. C. Pacheco-Londono, R.Infante-Castillo and S. P. Hernandez-Rivera, *Explosive Materials*, 2011, 259; S. Lee, J. Oh, R. S. Ruoff and S. Park, *Carbon*, 2012, **50**, 1442.
2. J. C. Oxley, J. Brady, S. A. Wilson and J. L. Smith, *J. Chem. Health Safety*, 2012, **19**, 27.
3. E. Schroeder and P. Eaton, *Curr. Opinion Pharmacol.*, 2008, **8**, 153; M. Rojkind, J.-A. Dominguez-Rosales, N. Nieto and P.Greenwel, *Cellular Molec. Life Sci.*, 2002, **59**, 1872.
4. A. Spector, *FASEB J.*,1995, **9**, 1173; M. Karin and E. Shaulian, *IUBMB Life*, 2001, **52**, 17; A. Quincozes-Santos, A. C. Andreazza, P.Nardin, C.Funchal, C.-A. Goncalvesand C. Gottfried, *Neurotoxicology*, 2007, **28**, 886.
5. Q. Yin, C. Huang, C. Zhang, W. Zhu, Y. Xu, X. Qian and Y. Yang, *Org. Biomol. Chem.*, 2013, **11**, 7566; P. Singh, A. A.Prabhune, S. B. Ogale and D. Guin, *J. Mater. Chem. B*, 2013, **1**, 6538.
6. S. Gaspar, *ACS Symposium Series*, 2011, **1083**, 289.
7. Z. Wang, Y. Tang, H. Hu, L. Xing, G. Zhang and R. Gao, *J. Lumin.*, 2014, **145**, 818; S. Parajuli and W. Miao, *Anal. Chem.*, 2013, **85**, 8008.
8. W. Sun, J. Wu, J. Li, H. Fang, L. Du and M. Li, *Curr. Med. Chem.*, 2012, **19**, 3622; A. R. Lippert, G. C. Van de Bittner and C. J. Chang, *Acc. Chem. Res.*, 2011, **44**, 793; X. Sun, S.-Y. Xu, S. E. Flower, J. F. Fossey, X. Qian andT. D. James, *Chem. Commun.*, 2013, **49**, 8311; D. Srikun, E. W. Miller, D. W. Domaille and C. J. Chang, *J. Am. Chem. Soc.*, 2008, **130**, 4596; J. C. Sanchez and W. C. Trogler, *J. Mater. Chem.*, 2008, **18**, 5134.
9. F. He, Y. Tang, M. Yu, S. Wang, Y. Li and D. Zhu, *Adv. Funct. Mater.*, 2006, **16**, 91.
10. M. Kaur, D. S. Yang, K. Choi, M. J. Cho and D. H. Choi, *Dyes Pigm.*, 2013, **100**, 118; M. Liu, B. Li and X. Cui, *Talanta*, 2013, **115**, 837.

11. M. Xu, B.R. Bunes, and L. Zang, *ACS Appl. Mater. Interfaces* 2011, **3**, 642.

12. G. M. H. Van de Velde, S. Harkema and P.J. Gellings, *Inorg. Chim. Acta*, 1974, **11**, 243.

13. Q. Zhou, T.M. Swager, *J. Am. Chem. Soc.* 1995, **117,** 12593; J.-S. Yang, T.M. Swager, *J. Am. Chem. Soc*. 1998, **120**, 11864.

14. T.M. Swager, *Acc. Chem. Res.* 1998, **31**, 201.

15. S. W.Thomas III; G.D. Joly, T.M. Swager, *Chem. Rev.* 2007, **107**, 1339.

16. D. Gopalakrishnan, W.R. Dichtel, *J. Am. Chem. Soc.* 2013, **135**, 8357.

17. S.H. Lee, A. Parthasarathy, K.S. Schanze, *Macromol. Rapid Commun.* 2013, **34**, 791.

18. I.A. Levitsky, W.B. Euler, N.Tokranova, A. Rose, *Appl. Phys. Lett.* 2007, **90**, 041904/1; P. Marks, S. Cohen, M. Levine, *J. Polym. Sci. A Polym. Chem.* 2013, **51**, 4150; N. Tokranova, S. W. Novak, J. Castracane, I.A. Levitsky, *J. Phys. Chem. C.,* 2013,**117**, 22667.

19. B. Radaram, T. Mako, M. Levine, *Dalton Trans.*, 2013, **42**, 16276.

20. J.R. Lakowicz**,** *Principles of Fluorescence Spectroscopy*, 3rd edn. Springer 2006.

21. P.Shi, C.M. Amb, A.L. Dyer, J. R. Reynolds, *ACS Appl. Mater. Interfaces* 2012, **4**, 6512; X.-T. Hao, N.Y. Chan, C. Heck, N.Tanigaki, M.F. Paige, D.E. Dunstan, T.A.Smith, *Macromolecules.,* 2010, **43**, 10475; C.-J. Qin, X.-F. Wu; H. Tong, L.-X. Wang, *J. Mater. Chem.*, 2010, **20**, 7957.

22. H.A. Al Attar, A.P. Monkman, *Phys. Rev. B*2012, **86**, 235420/1.

23. G.F. Simmons, J.L. Smilanick, S. John, D.A. Margosan, *J. Food Prot.*,1997, **60**, 188.

24. X. Zhao, Y. Liu and K. S. Schanze, *Chem. Commun.*, 2007, 2914; K.Y. Pu and B. Liu, *Adv. Funct. Mater*., 2009, **19**, 277; S. Wang, B. S. Gaylord and G. C. Bazan, *J. Am. Chem. Soc.*, 2004, **126**, 5446; B. Liu and G. C. Bazan, *J. Am. Chem. Soc*., 2004, **126**, 1942; Y.-H. Kim and T. M. Swager, *Angew. Chem. Int. Ed.*, 2003, **43**, 4803.

25. S. W. Thomas III and T. M. Swager, *Adv. Mater.*, 2006,**18**, 1047.

26. I. A. Levitsky, J. Kim, T.M. Swager, *J. Am. Chem. Soc.*,1999, **121**, 1466; D. Zhao, T.M. Swager, *Macromolecules.*, 2005, **38**, 9377.

Electronic Supplementary Information for

Highly efficient detection of hydrogen peroxide in solution and in the vapor phase via fluorescence quenching

Patrick Marks, Bhasker Radaram, Mindy Levine, and Igor A. Levitsky**

MATERIALS AND METHODS

Polymer **3** (part number: 659223), ammonium titanyl oxalate monohydrate **1** (part number: 229989), and poly(vinyl alcohol) **4** (part number: 341584) were purchased from Sigma Aldrich Chemical Company and used as received. Hydrogen peroxide was purchased as a 30% solution in water from Fisher Scientific (part number: H325) and used as received. All fluorescence spectra were recorded on a Shimadzu RF 5301 spectrophotometer, and all absorbance measurements were recorded on an Agilent 8453 UV-visible spectrophotometer. Thin films were spun using a Laurell Technologies Spin Processor.

SOLUTION QUENCHING EXPERIMENTS

Experimental procedure: Two solutions were made: Solution A contained polymer **3** (6.25E-3 mg/mL) and titanium complex **1** (1.70E-3 M), and Solution B contained polymer **3** (6.25E-3 mg/mL), titanium complex **1** (1.70E-3 M), and hydrogen peroxide (0.0306 M).

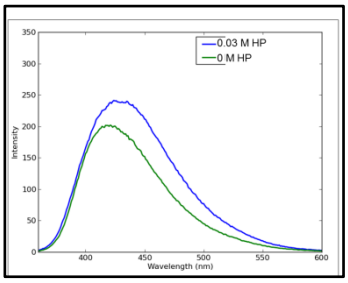

The effect of hydrogen peroxide addition on the fluorescence of polymer **3** is shown in the figure above, and shows a slight increase and red-shift in the fluorescence spectra of polymer

3 upon addition of hydrogen peroxide ([**3**] = 6.25 mg/L; [hydrogen peroxide] = 0 M and 0.03 M.)

10 µL aliquots of Solution B were added to Solution A (so that the concentration of polymer **3** and titanium complex **2** were kept constant, and the only changing variable was the concentration of hydrogen peroxide), and the fluorescence spectra were recorded after each addition. The solution was excited at 330 nm, 350 nm, and 370 nm, and the results of these experiments are discussed below.

With 330 nm excitation:

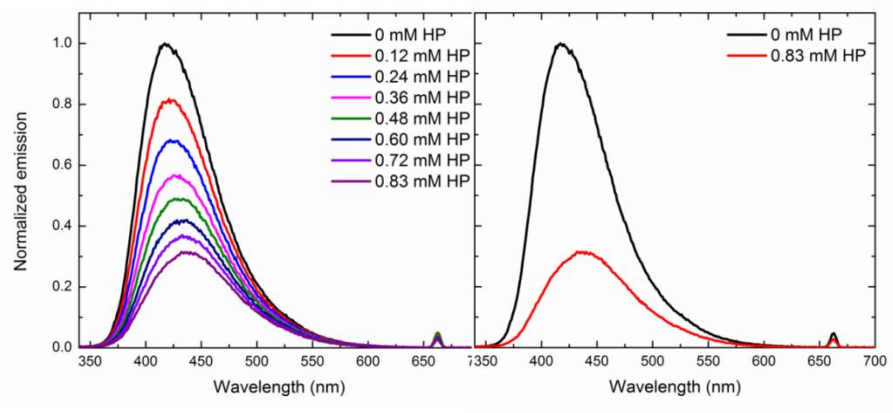

The fluorescence of the solution in the presence of 0.83 mM of hydrogen peroxide decreased to 35% of its initial value; even with as little as 0.12 mM of hydrogen peroxide, the fluorescence decreased by 16%, to 84% of its initial value.

With 350 nm excitation:

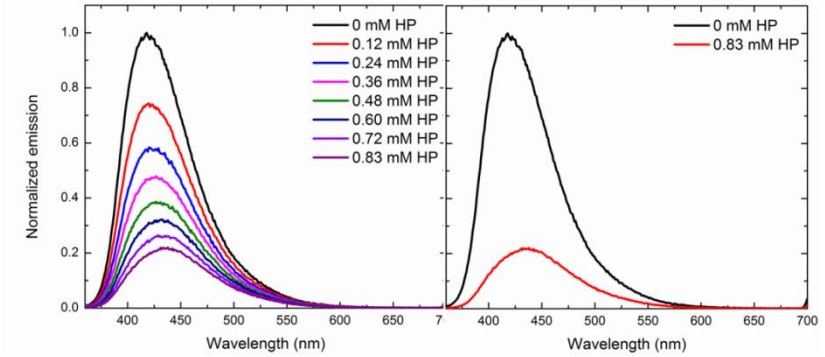

The fluorescence of the solution in the presence of 0.83 mM of hydrogen peroxide decreased to 24% of its initial value; even with as little as 0.12 mM of hydrogen peroxide, the fluorescence decreased by 22%, to 78% of its initial value.

With 370 nm excitation:

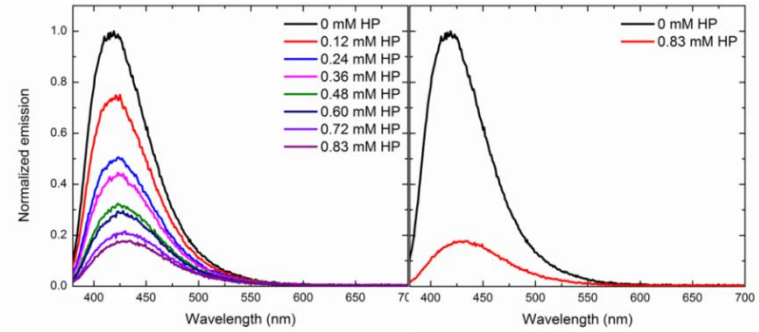

The fluorescence of the solution in the presence of 0.83 mM of hydrogen peroxide decreased to 20% of its initial value; even with as little as 0.12 mM of hydrogen peroxide, the fluorescence decreased by 24%, to 76% of its initial value.

A direct comparison of the solutions' fluorescence from 330 nm, 350 nm, and 370 nm excitation is shown below (0.83 mM hydrogen peroxide;6.25E-3 mg/mL polymer **3**, and 1.70E-3 M compound **1**), and indicates that the quenching efficiency strongly depends on the excitation wavelength:

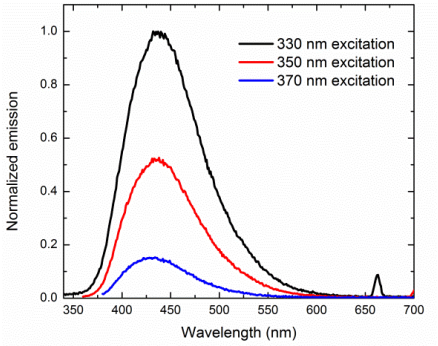

This dependence of fluorescence quenching on the excitation wavelength was quantified by constructing Stern-Volmer plots for each excitation wavelength, where the I_o/I ratios were calculated using the integrated fluorescence emissions vs. wavenumbers on the X-axis:

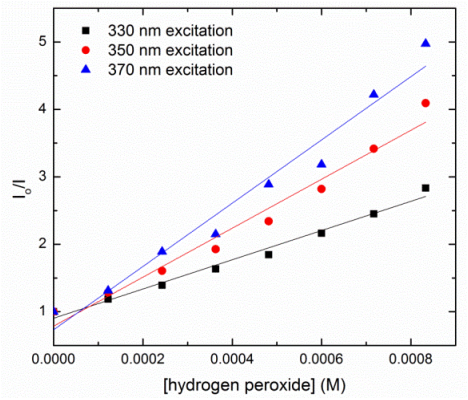

330 nm: y = 2167.1x + 0.904; R^2 = 0.9852; K_{SV} =2167 M^{-1}

350 nm: y = 3630.6x + 0.7865; R^2 = 0.9725; K_{SV} =3631 M^{-1}

370 nm: y = 4691.5x + 0.7325; R^2 = 0.9689; K_{SV} =4692 M^{-1}

MODIFICATIONS TO STERN-VOLMER EXPRESSION TO ACCOUNT FOR PRIMARY SCREENING EFFECT

The initial intensity of polymer **3**'s fluorescence in the absence of complex **2** can be expressed as:

$$I_0 = \frac{K_r J_0 (1 - \exp(-\varepsilon_3))}{K_r + K_d} \qquad \text{(Eq. S1)}$$

where K_r and K_d are radiative and radiativeless rate constants, respectively, ε_3 is the optical density of polymer **3,** and J_0 is the intensity of the incident light. The fluorescence intensity of **3** in the presence of **2,** taking into account both energy transfer and the primary screening effect, can be expressed as:

$$I = \frac{K_r A(C)}{K_r + K_d + K_{ET}(C)} \qquad \text{(Eq. S2)}$$

where $K_{ET}(C)$ is the energy transfer constant, $A(C)$ is the light energy absorbed by **3** in the presence of **2**,and C is the complex **2** concentration. A light absorbed by polymer **3**, dA ,in the slab of the thickness dx is proportional to the extinction coefficient of **3** and intensity of the light $J(x)$ at the distance x from the surface, as shown in Equation S3:

$dA = -e_3 J(x)dx$, with $J(x)=J_0 exp(-(e_2(C) +e_3)x)$ (Eq. S3)

where e_3 and $e_2(C)$ represent the extinction coefficients of **3** and **2,** respectively. The integration of Equation S3 over optical path d yields :

$$A(C) = \frac{\varepsilon_3(1-\exp(-(\varepsilon_2(C)+\varepsilon_3))}{\varepsilon_2(C)+\varepsilon_3} \qquad \text{(Eq. S4)}$$

whereε_2 (C) = $de_2(C)$ and $\varepsilon_3 = de_3$. Substitution of Equation S4 in Equation S2, followed by dividing Equation S1 by Equation S2, results in Equation S5 :

$$\frac{I_0}{I} = \frac{(K_r + K_d + K_{ET}(C))(\varepsilon_2(C)+\varepsilon_3)(1-\exp(-\varepsilon_3))}{(K_r + K_d)\varepsilon_3(1-\exp(-(\varepsilon_2(C)+\varepsilon_3))} \qquad \text{(Eq.S5)}$$

where K_r and K_d are radiative and radiativeless rate constants, $K_{ET}(C)$ is the energy transfer constant, ε_2(C) and ε_3 are optical densities of complex **2** and polymer **3**, and C is the concentration of complex **2**. Equation S5 is transformed to a standard Stern-Volmer expression in the case that ε_2=0.

THIN FILM QUENCHING EXPERIMENTS

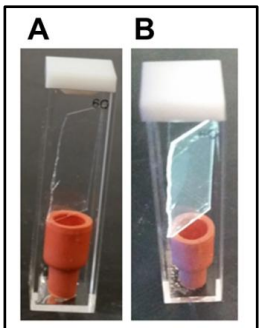

Figure S1: Photograph of (A) initial thin film; and (B) the fluorescent thin film after 3 minutes of exposure to HP

Thin films were fabricated using the following procedure: an aqueous solution of polymer **3** (0.10 g/L) was warmed to 90 ^{o}C, and polymer **4** (55 g/L) was added to the solution while stirring. After polymer **4** dissolved, the solution was heated to 110 ^{o}C and complex **1** (variable amounts) was added. The solution was briefly sonicated to ensure thorough mixing, then spun-coat on a 2x2 cm glass cover slip at 7000 rpm for 1 minute. Films were dried in open air for at least 2 days before running fluorescence experiments.

The thin films were then cut in half and placed on a rubber septa that was inserted into a 1 cm^2 quartz cuvette (Figure S1). The film's fluorescence was recorded for approximately 1 minute, and then an aqueous hydrogen peroxide solution was added to the cuvette via pipette, with the rubber septa ensuring that the thin film did not directly contact the hydrogen peroxide solution. The fluorescence spectra of the solution were recorded for several minutes after the hydrogen peroxide addition, to observe the solid-state fluorescence quenching in the presence of hydrogen peroxide vapors. All films were excited at 350 nm.

The following variables were tested: concentration of titanium complex **1**, concentration of polymer **4**, and amount of hydrogen peroxide added. The results of these experiments are discussed below.

DIFFERENT CONCENTRATIONS OF TITANIUM COMPLEX 1 ([3] = 0.10 g/L; [4] = 55 g/L):

1. 0.05 g/L of titanium complex

A. A 30% hydrogen peroxide solution was added after 1 minute:

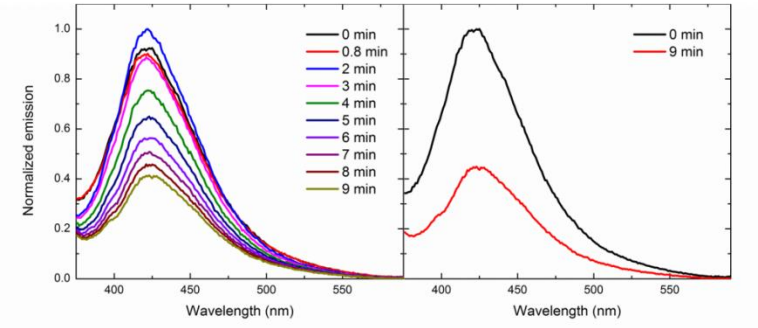

The fluorescence declined to 48% of its initial value after 9 minutes.

Plotting this data as the change in I_o/I over time:

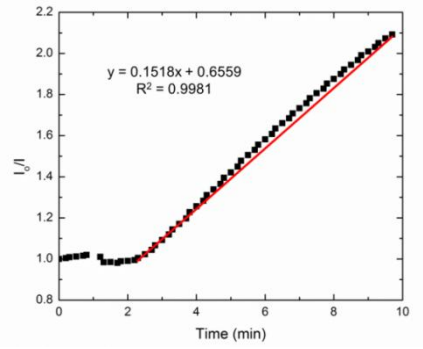

2. 5.0 g/L of titanium complex 2:

A. The 30% hydrogen peroxide solution was added after 1 minute:

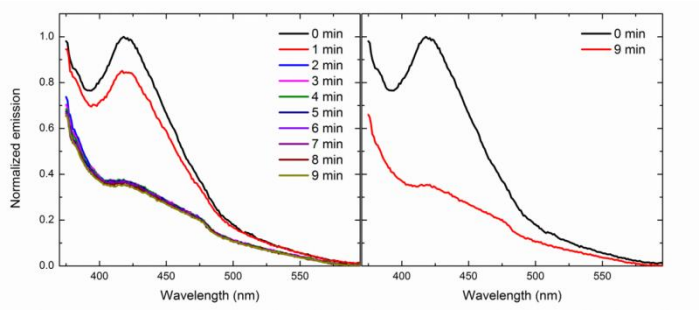

After the addition of hydrogen peroxide, a significant fluorescence quenching was observed, to 60% of its initial value after 2 minutes. After that initial quench, the fluorescence remains fairly constant for the rest of the 9 minutes (57% of the initial value after 9 minutes).A plot of I_0/I vs. time:

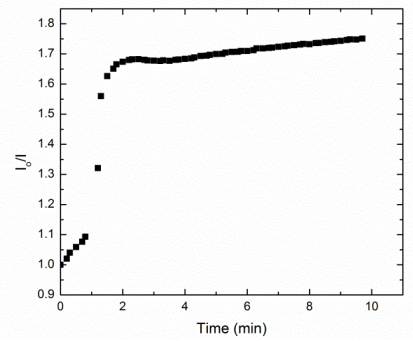

3. 50 g/L of titanium complex 2:

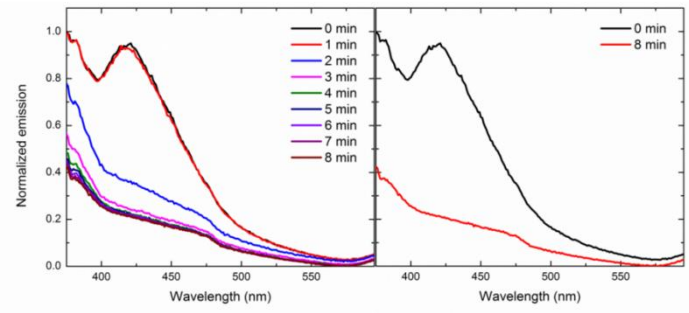

The fluorescence was quenched to 44% of its initial value after 3 minutes and 38% after 8.5 minutes. The plot of I_o/I vs. time is shown below:

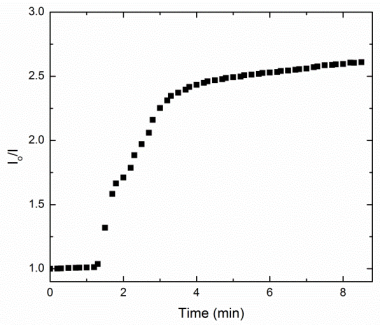

DIFFERENT CONCENTRATIONS OF POLYMER 4 ([3] = 0.10 g/L; [1] = 50 g/L):

1. 10 g/L PVA:

A. 3 ppm hydrogen peroxide:

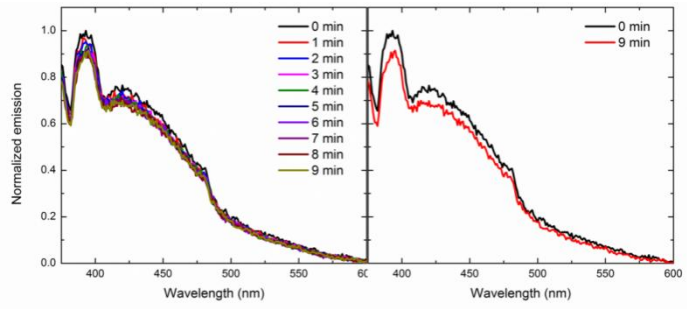

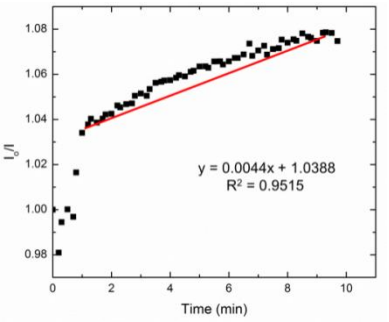

A slight fluorescence quench was observed after 9 minutes, to 93% of the initial value.

B. 30 ppm hydrogen peroxide:

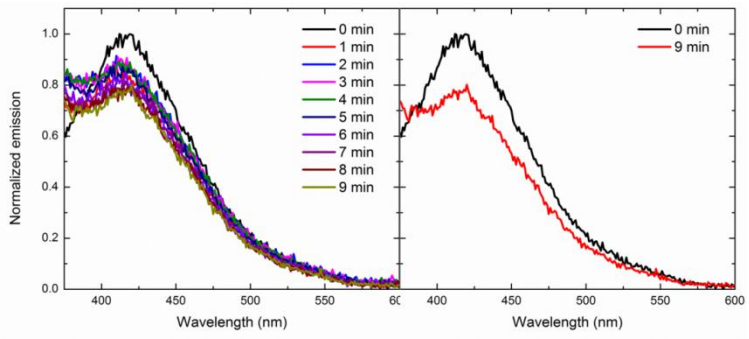

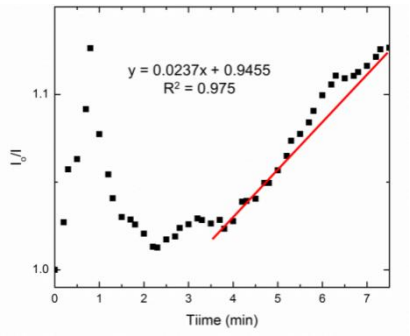

Fluorescence quench to 86% after 9.7 minutes.

C. 300 ppm hydrogen peroxide:

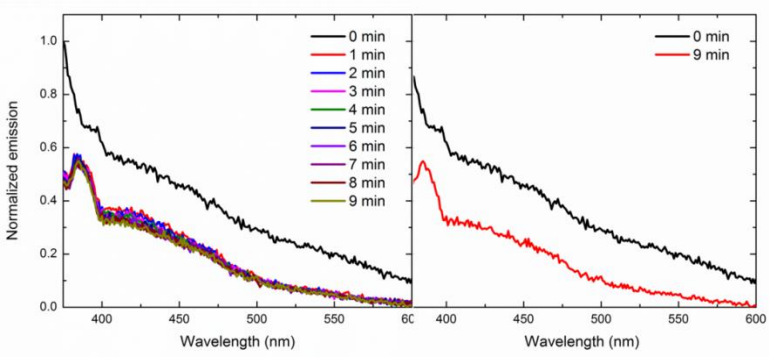

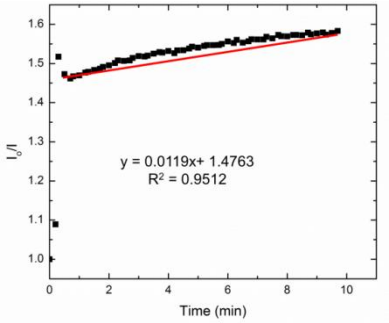

Fluorescence quench to 63% after 9.7 minutes.

D. No hydrogen peroxide:

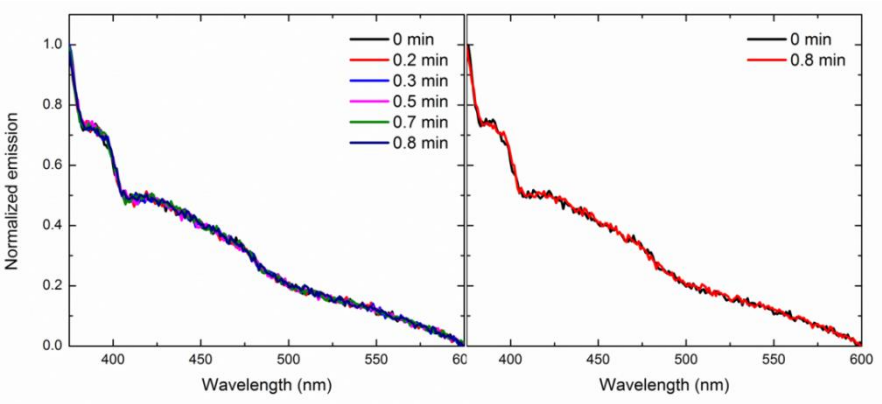

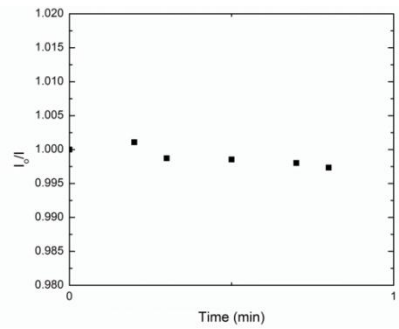

100% of initial fluorescence remains after 1 minute.

2. 23 g/L of polymer 4:

A: 3 ppm hydrogen peroxide:

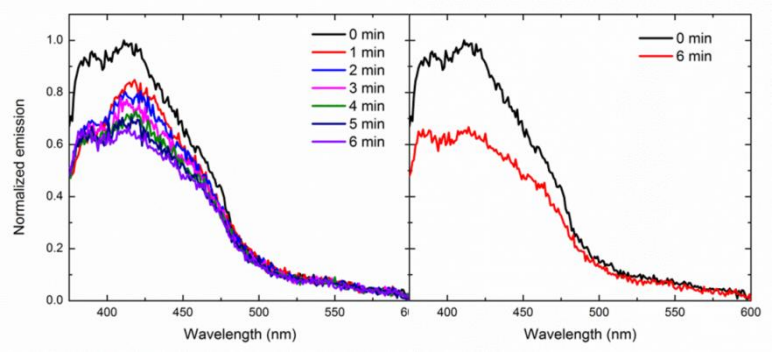

77% of initial fluorescence remaining after 6 minutes.

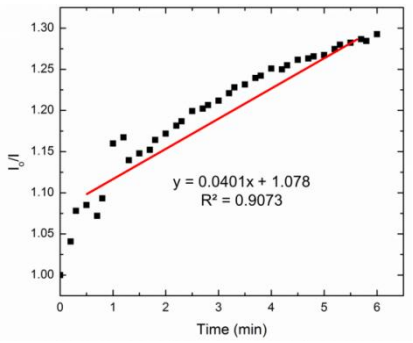

B. 30 ppm hydrogen peroxide:

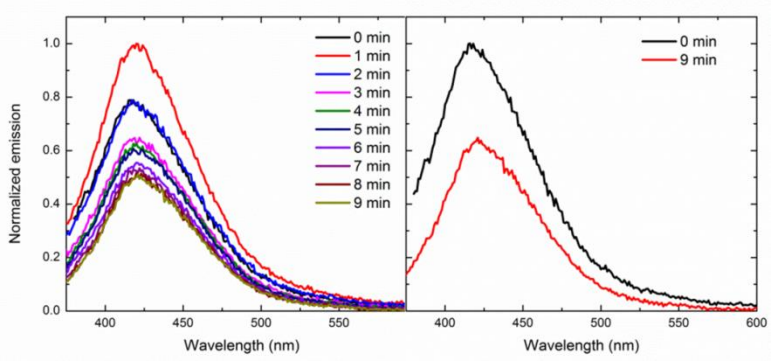

62% of fluorescence remaining after 9.7 minutes.

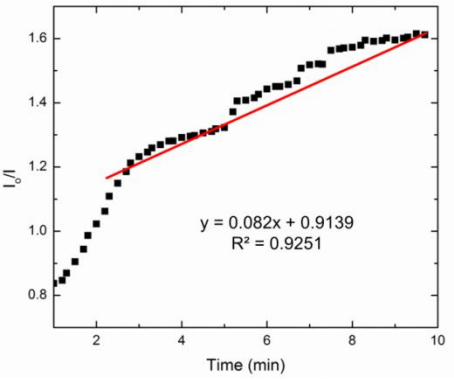

C. 300 ppm hydrogen peroxide:

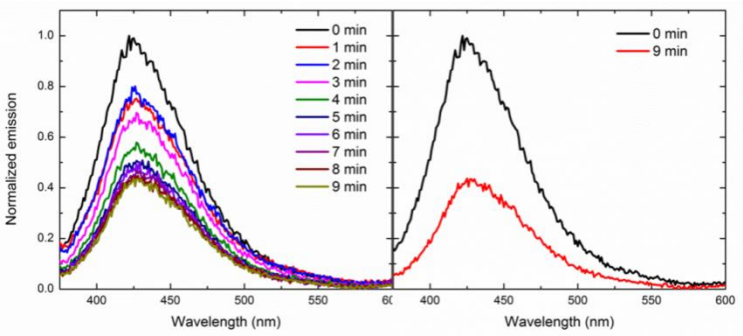

50% of the fluorescence was remaining after 9.7 minutes.

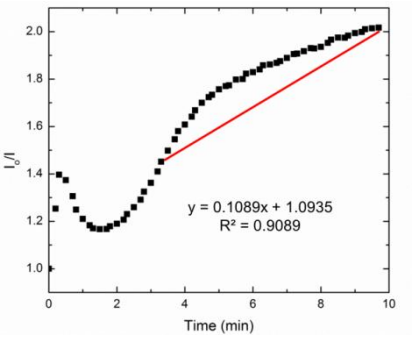

D. No hydrogen peroxide:

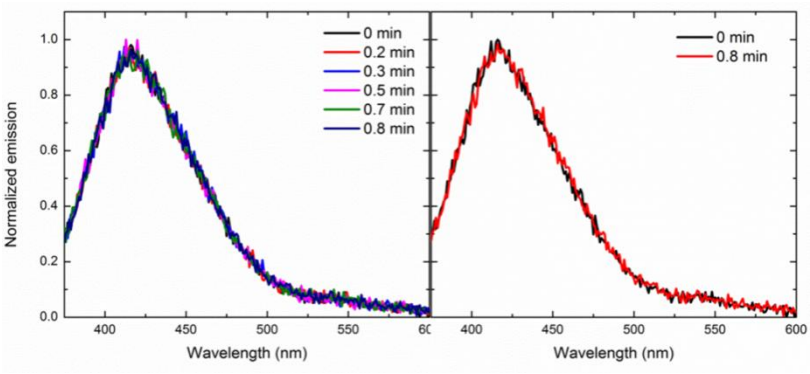

100% of the fluorescence remained after 1 minute.

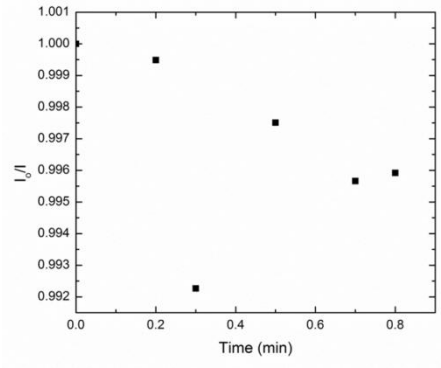

3. 55g/L polymer 4:

A. 3 ppm HP:

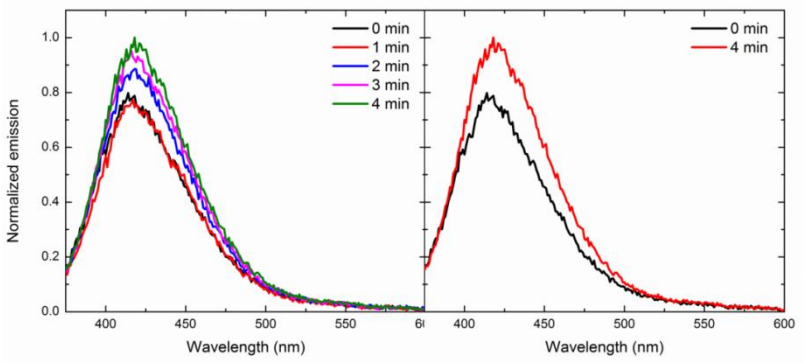

Slight increase in fluorescence to 120% of its initial value after 4.3 minutes.

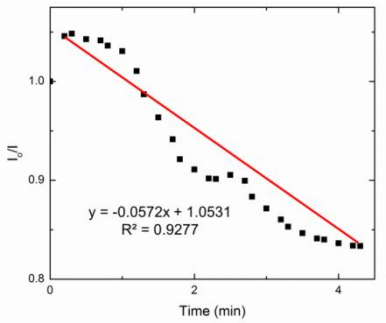

B. 30 ppm HP:

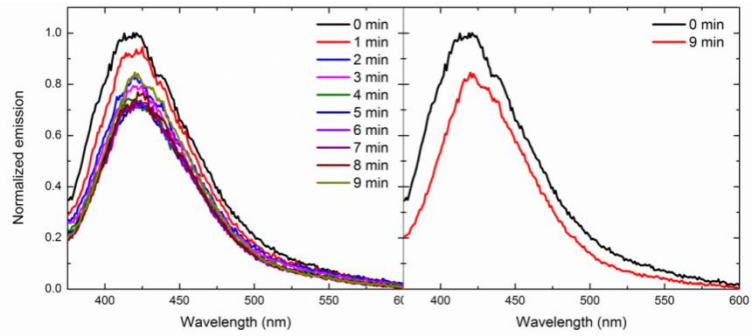

Decrease in fluorescence to 80% of its initial value.

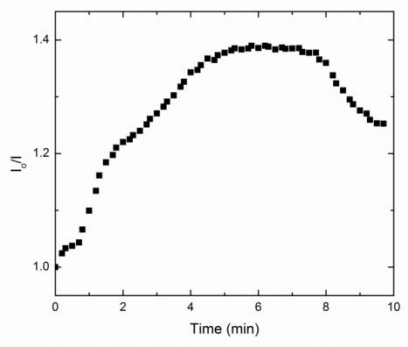

C. 300 ppm HP:

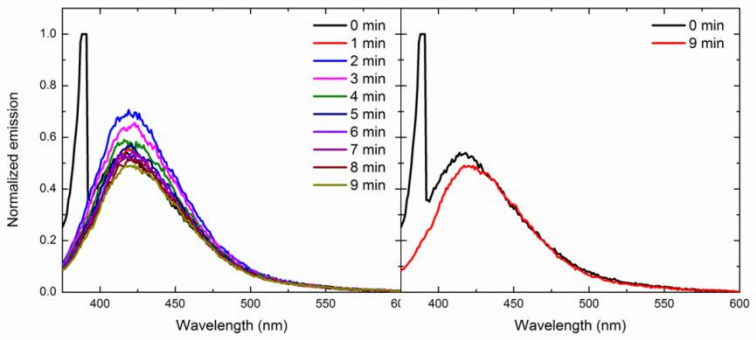

Decrease in fluorescence to 75% of its initial value.

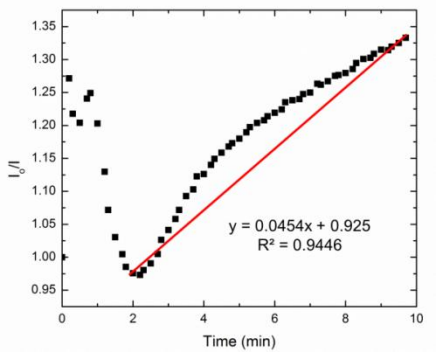

D. No Hydrogen Peroxide:

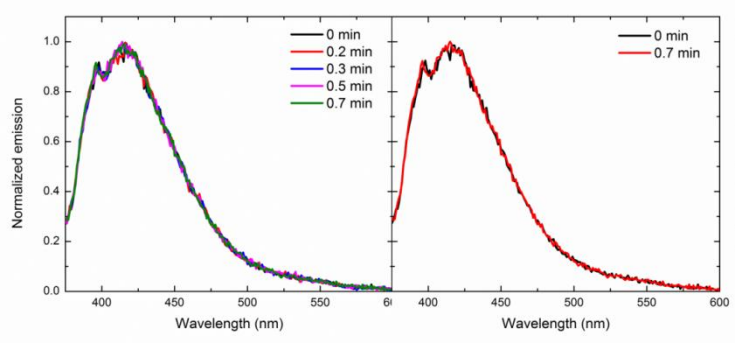

100% of the initial fluorescence was maintained after 0.7 minutes.

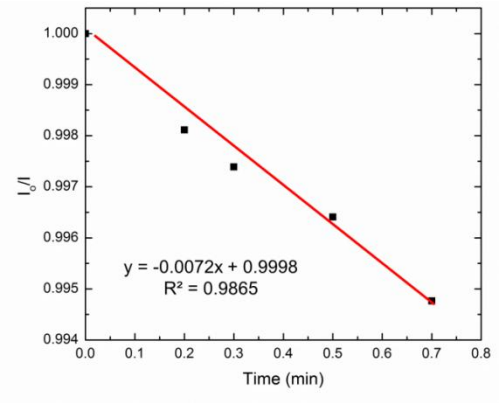

SUMMARY TABLES OF THIN FILM QUENCHING EXPERIMENTS

[3]	[4]	[1]	HP	Remaining fluorescence
0.10 g/L	55 g/L	0.05 g/L	30% HP solution	62%
0.10 g/L	55 g/L	5 g/L	30% HP solution	46%
0.10 g/L	55 g/L	50 g/L	30% HP solution	38%
0.10 g/L	10 g/L	50 g/L	3 ppm	92%
0.10 g/L	10 g/L	50 g/L	30 ppm	86%
0.10 g/L	10 g/L	50 g/L	300 ppm	67%
0.10 g/L	10 g/L	50 g/L	0 ppm	100%
0.10 g/L	23 g/L	50 g/L	3 ppm	96%
0.10 g/L	23 g/L	50 g/L	30 ppm	62%
0.10 g/L	23 g/L	50 g/L	300 ppm	50%
0.10 g/L	23 g/L	50 g/L	0 ppm	98%
0.10 g/L	55 g/L	50 g/L	3 ppm	133%
0.10 g/L	55 g/L	50 g/L	30 ppm	80%
0.10 g/L	55 g/L	50 g/L	300 ppm	75%
0.10 g/L	55 g/L	50 g/L	0 ppm	92%

SUMMARY FIGURES FOR THIN FILM QUENCHING EXPERIMENTS:

Varying the concentration of titanium complex 1:

Change in I_o/I vs. time:

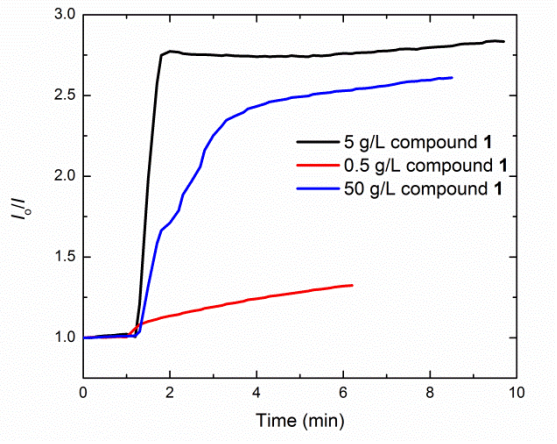

Initial fluorescence spectra:

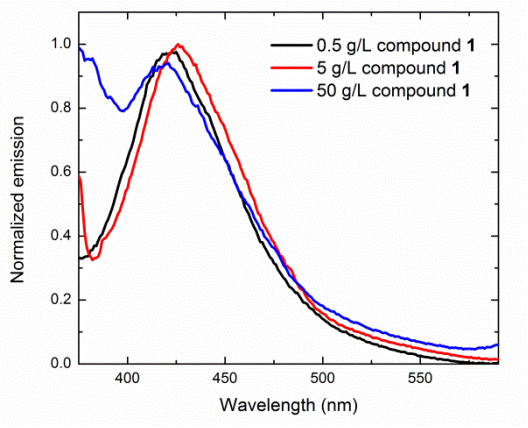

Final fluorescence spectra after addition of 30% aqueous hydrogen peroxide solution:

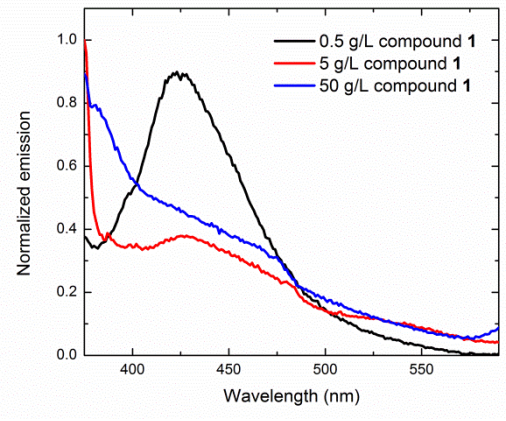

Varying the concentration of polymer 4:

10 g/L polymer 4:

Change in I_o/I vs. time:

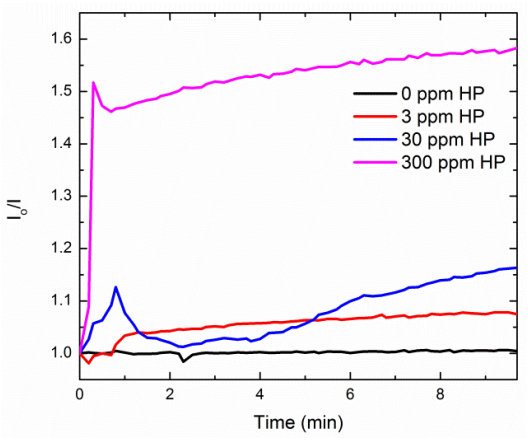

Initial fluorescence spectra:

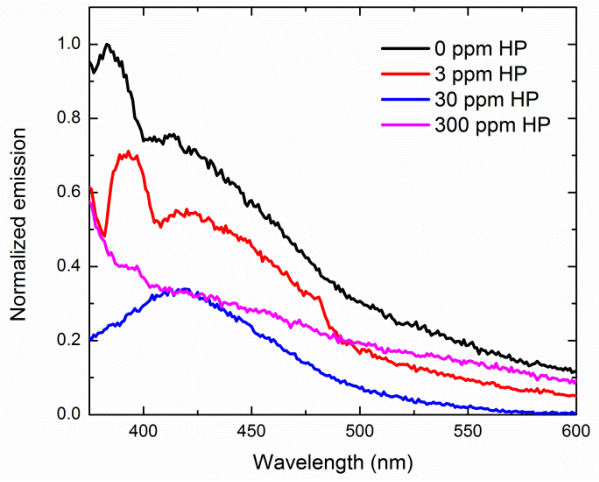

Final fluorescence spectra:

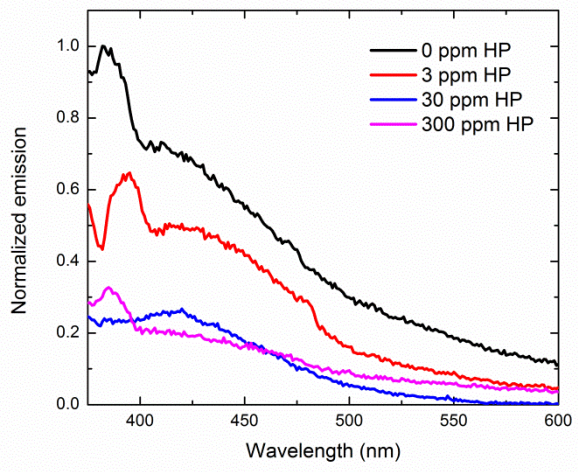

23 g/L polymer 4:

Change in I_o/I vs. time:

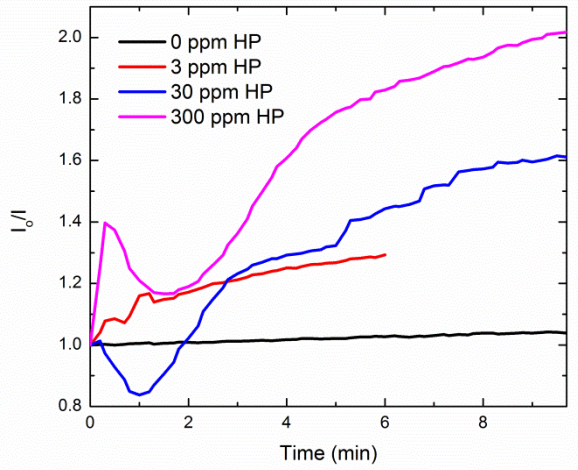

Initial fluorescence spectra:

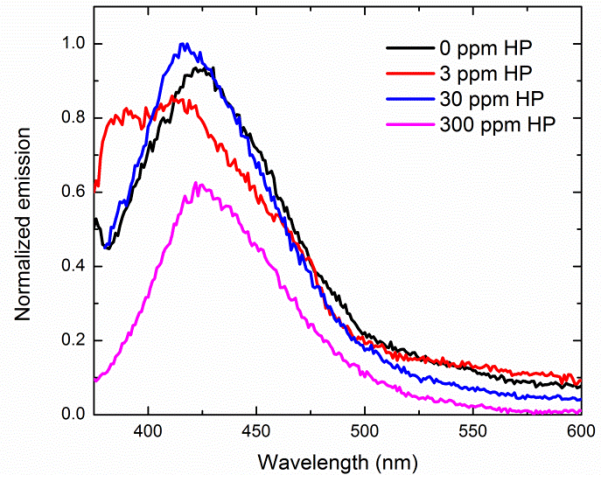

Final fluorescence spectra:

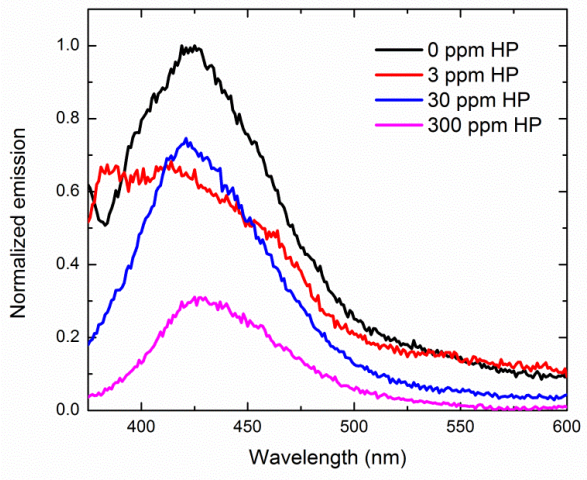

55 g/L polymer 4:

Change in I_o/I vs. time:

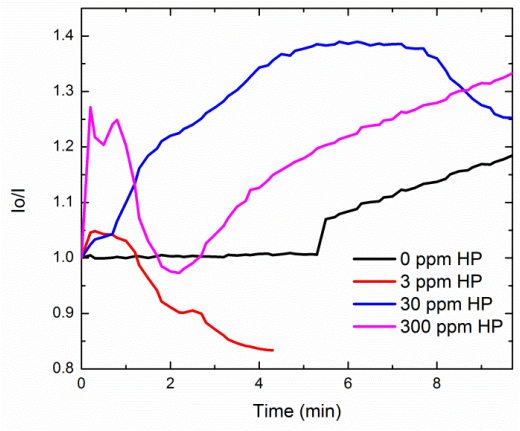

Initial fluorescence spectra:

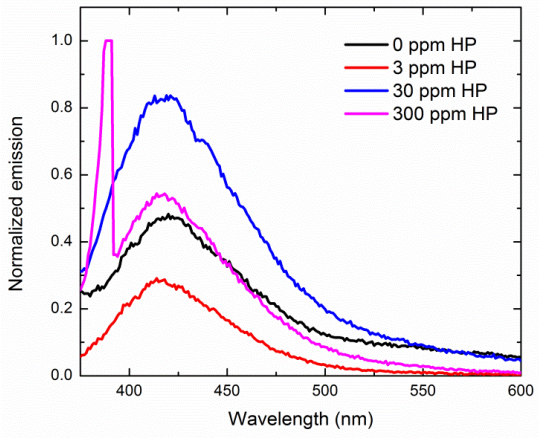

Final fluorescence spectra: